INVESTIGATIONS ON AGGREGATION OF SOFT SYSTEMS

THESIS SUBMITTED IN FULFILLMENT OF REQUIREMENTS

FOR THE DEGREE OF

DOCTOR OF PHILOSOPHY (SCIENCE)

OF

JADAVPUR UNIVERSITY, INDIA

by

RAJESH BANIK, M.Sc.

2024

Department of Chemistry

Jadavpur University

Kolkata-700032

India

Prof. Soumen Ghosh, M. Sc., Ph. D.
Professor of Chemistry & Co-ordinator,
Centre for Surface Science
Department of Chemistry, **Jadavpur University**
Kolkata – 700 032, West Bengal, India
Awards of Prof. B. N. Ghosh from ICS, Dr. B. C. Deb
from ISCA & Visiting Chair Professor of St. F. X. University, Canada

Phone : +91-33-2414 6411
Fax : 91-33-2414 4266
Mob - 9432 075 363
E-Mail – gsoumen17@yahoo.co.in/
soumen.ghosh@jadavpuruniversity.in

CERTIFICATE FROM THE SUPERVISOR

This is to certify that the thesis entitled **"INVESTIGATIONS ON AGGREGATION OF SOFT SYSTEMS"** submitted by **Sri. RajeshBanik,** who got his name registered on 06.03.2018 for the award of **Ph.D. (Science) degree** of **Jadavpur University**, is absolutely based upon his own work under the supervision of **Prof. Soumen Ghosh** and that neither this thesis nor any part of it has been submitted for any degree/diploma or any other academic award anywhere before.

Soumen Ghosh. 19.07.24

Soumen Ghosh
Centre for Surface Science
Department of Chemistry
Jadavpur University
Kolkata- 700032

Prof. Soumen Ghosh
Department of Chemistry
Jadavpur University
Kolkata-700 032, W.B., India

"Success can only be achieved through repeated failure and introspection."

Acharya Prafulla Chandra Ray (1861 - 1944)

Dedicated To

My Beloved Parents

DECLARATION

I hereby declared that the work incorporated in the present dissertation was carried out by me at the centre for surface science, Department of Chemistry, Jadavpur University, Kolkata-700032, India. The entire work or any part of it has never been submitted before for any prize or degree anywhere.

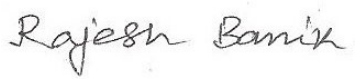

(RAJESH BANIK)

ACKNOWLEDGEMENT

I am profoundly grateful to the individuals whose unwavering support and contributions have been involved in the completion of this dissertation, entitled *"**Investigations on Aggregation of Soft Systems**,"* conducted at the Centre for Surface Science, Department of Chemistry, Jadavpur University, Kolkata, India.

First and foremost, I extend my heartfelt thanks to Prof. Dr. Soumen Ghosh, Department of Chemistry, Jadavpur University, for his exceptional mentorship, scholarly guidance, and unwavering support throughout this research endeavor. His insightful advice and encouragement have been pivotal in shaping the direction and outcomes of this study.

I am deeply grateful to Dr. Asitanga Ghosh for his invaluable insight, scholarly discussions, and constructive feedback that significantly enriched the research process.

Special appreciation goes to Prof. Dr. Kajal Krishna Rajak, Head of the Department of Chemistry, Jadavpur University, for facilitating access to essential research facilities and resources, which were crucial for the successful completion of this work.

I would like to thank the entire faculty of the Department of Chemistry at Jadavpur University for their academic support and guidance, as well as the university administration for their administrative assistance.

I also wish to acknowledge my colleagues, Mr. Bipin Bihari Mandal, Mr. Sumanta Bandyopadhyay, Ms. Tanaya Saha, Mrs. Sudipta Chakraborty, Ms. Ankita Saha, Mr. Raju Sardar, Mr. Rabindranath Pal, Dr. Sourav Das, Dr. Nitai Patra, Dr. Arpan Mal, Dr. Jayabrata Maity, Dr. Gulmi Chakraborty, Dr. Apensu Dey, and Dr. Sonali Mandal for their collaborative spirit, technical expertise, and unwavering encouragement throughout this research journey.

My sincere gratitude extends to my friend Dr. Swagatam Barman for his valuable assistance and insightful discussions that enhanced the quality of this research.

Special thanks are due to the Central Instrumentation Facility at IACS, DBT-IPLS, and CRNN, University of Calcutta, for their technical support and provision of necessary instrumentation.

I gratefully acknowledge the financial support provided by the Council of Scientific and Industrial Research (CSIR), Government of India, which enabled the successful execution of this research.

Finally, I express my deepest appreciation to my parents and family members for their unwavering love, encouragement, and sacrifices throughout my academic journey.

Centre for Surface Science
Department of Chemistry
Jadavpur University
Kolkata – 700032
India

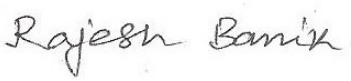

(Rajesh Banik)

PREFACE

Mixed surfactants, combining cationic, anionic, gemini, zwitterionic, and non-ionic forms, have become increasingly important. This interest is driven by their ability to form 'mixed micelles' in aqueous solutions, which enhances our understanding of biological supramolecular assemblies, ion transfer, drug delivery, and the creation of biomimetic systems. Technologically, mixed surfactants are pivotal in pharmaceuticals, detergents, food, cosmetics, drug solubilization, and enhanced oil recovery, showcasing their versatility and critical role in modern applications.

Alcohols can act as cosurfactants or cosolvents, altering the critical micelle concentration (CMC) during amphiphile self-assembly. 2,2,2-trifluoroethanol (TFE), a fluorinated alcohol, due to its demand in molecular biology for protein denaturation and its properties attributed to the trifluoromethyl (CF_3) group is a very unique solvent to discuss about. Despite its hydrophobic $-CF_3$ terminal, TFE is highly water-soluble, though surfactant aggregation in TFE has been underexplored. The facilitating solubilization and hydrogen bonding capabilities of alcohols set them out as preferred solvents.

Chlorpromazine (CPZ), known as Thorazine or Largactil, treats schizophrenia, anxiety, nausea, bipolar disorder, and pre-surgery anxiety, but can cause phospholipidosis and cardiovascular, antihistamine, and anticholinergic side effects. To reduce these side effects, CPZ is often combined with surfactants.

Supramolecular chemistry has focused on cyclodextrin (CD)-based molecular recognition due to its strong binding to various substrates. CDs can form nanostructures like catenanes, rotaxanes, supramolecular polymers, and functionalized nanoparticles. Triton X, a widely used detergent in industry and research, lyses cells to extract organelles and proteins and is found in influenza vaccines. It solubilizes proteins and retrieves membrane components under mild conditions. The interaction of various surfactants and CD could help us to explore several biological processes, drug delivery and other biochemical applications.

Bile acids play roles in supramolecular synthesis and in developing photorheological fluids. Most research on mixed micelle formation in pharmaceutical applications focuses on phospholipids and bile salts, often using organic systems in manufacturing. Investigating the impact of bile salts on the structural transformation of non-ionic micelles can enhance our comprehension of the molecular interactions that significantly influence the process of fat digestion and other biologically significant processes.

INTRODUCTION

Introduction:

The term **'SURFACTANTS'** is derived from SURFace ACTive ageNTS.[1] These are the main ingredients found in soaps and detergents used in laundry and domestic places. Since it was initial formulation[2] as a "self-activated" cleaning agent in 1907 by a German business company, this detergent has been used commercially as a laundry detergent known as **'PERSIL'**. In the past, sodium PERborate, which was utilized as a bleaching agent, and sodium SILicate, which served as a basic washing agent, were combined to create **'PERSIL'**, but none of these ingredients are typical surfactants that we often use as flexible washing agents. Surfactant molecules tend to approach the interface (either interfaces of air-liquid, solid-liquid, or interfaces of two immiscible liquids; Fig. 1) with their polar heads, and as a consequence, the interfacial free energy decreases. Surfactants are used in a wide range of day-to-day products (toothpaste, shampoo, conditioner, shaving foam, facewash, toilet cleaner, adhesive, hair gel, ink, etc.) as emulsifiers, dispersants, wetting agents, foaming agents and stabilizing agents. They also possess rich detergency properties.

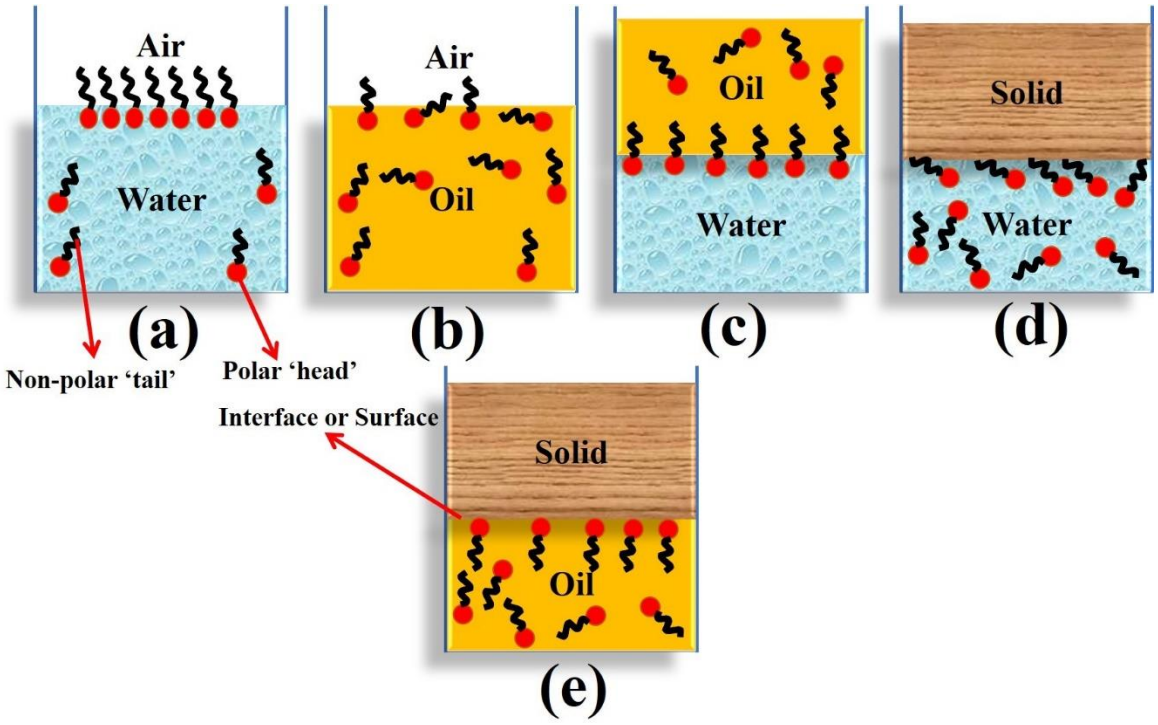

Fig. 1. Adsorption patterns of surfactants at various interfaces: (a) air-water interface, (b) air-oil interface, (c) oil-water interface, (d) solid-water interface, and (e) solid-oil interface.

As a result of their dual solubility, surfactants are often referred to as amphiphiles. The hydrophobic tail of a surfactant is usually made up of long chains of alkyl hydrocarbons (8-22 carbon atoms),[3] and the hydrophilic head group is usually either cationic,[4-13] anionic,[14-20] nonionic,[21-24] or zwitterionic.[25-27] In contrast to normal soaps, which are prepared by saponifying naturally occurring fatty acids (triglycerides) from vegetable and animal sources, surfactants are made from petroleum products whose structures can be modulated in various ways.[4-26] The majority of the 10–20 different components found in a modern detergent are the salts of surfactants and fatty acids (sodium and potassium salts of $C_{12–18}$ long alkyl chain,[3, 28, 29]), which are extracted from animal fats, palm oil, soy bean oil, and coconut oil through the process of saponification. Compared to soaps, surfactants are more interesting to use since they can clean a surface more thoroughly, even at low temperatures and in the presence of hard water.

Surfactants are also important components of our biological system. Amphiphile-like molecules called phospholipids[30] are found in biological cell membranes (lipid bilayers), and they facilitate the selective movement of ions, proteins, and other molecules both inside and outside of cells. A significant organic solute in bile juice, bile salt (steroidal anionic surfactants) aids in the intestine's absorption of dietary lipids.[31] The pulmonary surfactant, sometimes referred to as pulmonary epithelial lining fluid (ELF), is produced by the human lungs and aids in raising lung compliance and total lung capacity. In order to reduce surface tension at the air-liquid boundary in the lung, lipoprotein type surfactant, which is released from lung epithelial type II cells and delivered to the alveolar space, is present in ELF.[32]

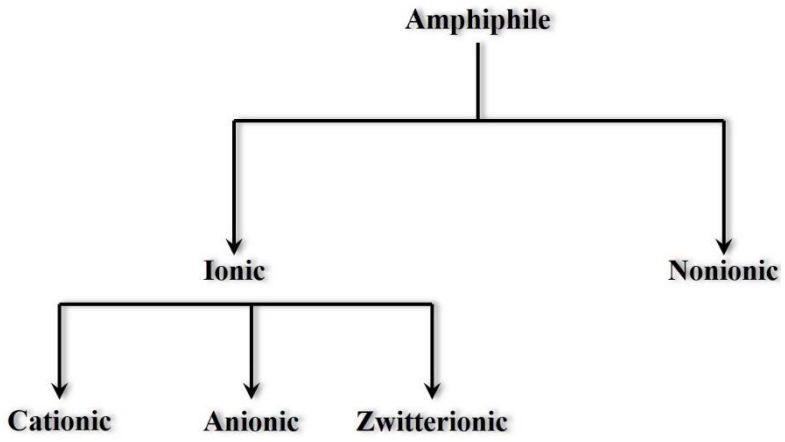

Fig. 2. Schematic representation of classification of amphiphiles/surfactants.

Classification of surfactants:

In aqueous solutions, surfactants are often arranged based on the charge of their head groups. The following section lists a few surfactants that are frequently utilized:

Cationic Surfactant:

These surfactants have positive charged head groups (phosphonium salts, alkyl quaternary ammonium salts, amine salts, amine oxides, etc.) along with negatively charged counterions (mainly chlorides and bromides). Preparations of these types of surfactants are expensive, so their use is limited.

Example:

Dodecyltrimethylammonium chloride (DTAC), 1-hexadecyltriphenylphosphonium bromide (C_{16}TPB).

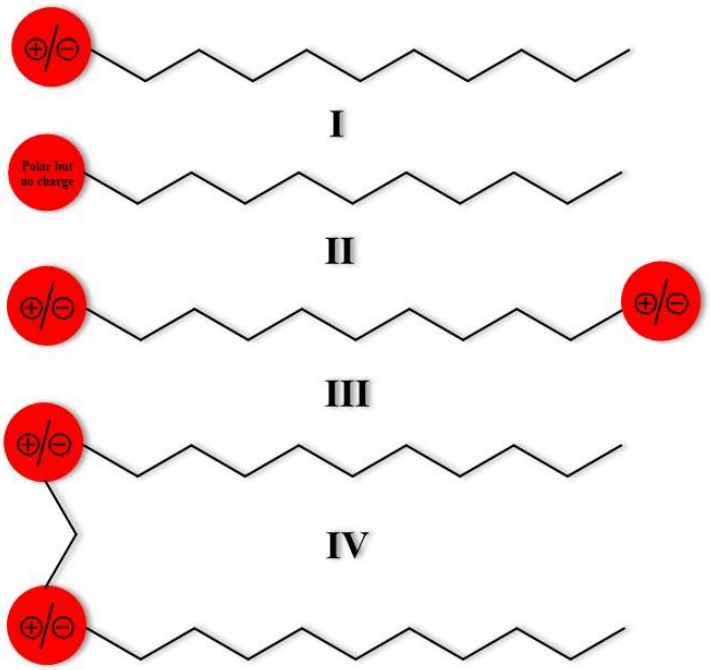

Fig. 3. Schematic representation of (I) ionic (cationic/anionic) (II) nonionic (III) zwitterionic (bola electrolyte type) (IV) gemini type amphiphiles/surfactants.

Anionic Surfactant:

This type of surfactant has negatively charged head groups with positively charged counterions. Head groups may be sulfonates, alkyl-sulfates, carboxylates, sulfosuccinates, N-acyl amino acids, etc. Quaternary ammonium cations and positively charged alkali metal ions (Na^+/K^+) may be present as counterions. Anionic surfactants have been used mostly in daily products. Anionic surfactants are almost always used in household products.

Example:

Sodium lauryl sulphate (SLS/SDS), Sodium laureth sulfate (SLES), Sodium lauryl sarcosinate (SDDS).

Nonionic Surfactant:

These types of surfactants have no electrical charges. These compounds are miscible in water due to the presence of polar functionality in their structures. Alkylpolyglucosides, polyoxyethylenes, N-based glucamine, polyglycidols surfactants belong to this class. They are hugely produced industrially after anionic surfactants.

Example:

(1,1,3,3-Tetramethylbutyl) phenyl-polyethylene glycol (Triton X-114), Polyoxyethylene (20) sorbitan monolaurate (Tween-20), N-decanoyl-N-methylglucamine (MEGA-10).

Zwitterionic Surfactants:

These surfactants contain both negative and positive charged centres and can be used either as anionic or cationic surfactants with variation of pH. Imidazole derivatives, phosphatides, betaines etc. belong to this class. The source of positive charge is contributed by normally ammonium ions and negative charge by carboxylates, sulfates, or sulfonate ions. These surfactants have excellent dermatological properties. Zwitterionic surfactants are frequently used in cosmetic products, hand and dishwashing liquids, shampoos because of their high frothing properties and less sensitive to skin.

Example:

Lauramidopropyl betaine, 3-[(3-cholamidopropyl) dimethylammonio]-1-propanesulfonate (CHAPS).

Surfactants are further categorized into a few unique classes in addition to their general classification. Over the last twenty years, these types of surfactants have been the focus of substantial attention and research.

Gemini Surfactant:

Gemini surfactants are a unique class of surfactants (Fig. 4) that have richer surface activity than traditional surfactants. They are composed of an extended hydrocarbon chain that is attached to a polar head group, a rigid or non-rigid spacer, and another hydrocarbon chain that is arranged sequentially with another polar head group. The nature of these polar head groups can be classified as nonionic (based on carbohydrates),[33] negative (sulphates, carboxylate, etc.),[34] and positive

(ammonium).[35] Spacer lengths can range from two to twelve methylene groups, and they can be stiff (stilbene) or flexible (saturated hydrocarbon chain). Bunton et al. produced gemini surfactants for the first time in 1971.[36] In 1991, Menger et al.[37] initially used the word "Gemini." Spacers have two possible connections: either to the middle of the long hydrocarbon tails, or to both of the same head groups.

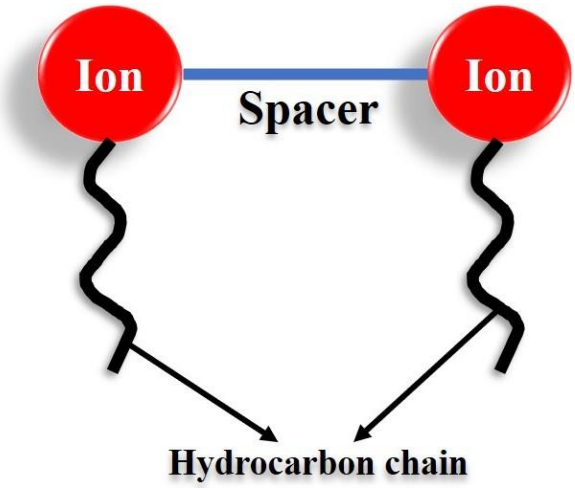

Fig. 4. Schematic representation of gemini surfactants.

Fluorosurfactants:

These belong to the distant class of surfactants in which an F-atom replaces at least one hydrogen in the alkyne chain. Fluorosurfactants find extensive usage in numerous applications, including adhesives, cosmetics, biomedicines, and firefighting.[38-40] The amount of fluorine atoms that replace the alkyne hydrogens in these surfactants has been used to measure their surface activity. Compared to conventional organic surfactants, fluorosurfactants have higher surface activity.

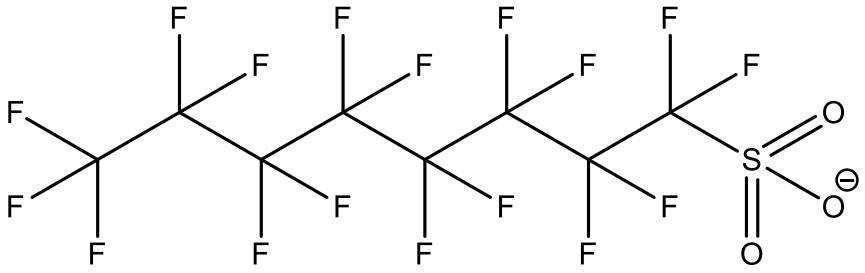

Fig. 5. Perfluorooctane sulfonate (PFOS) generally used in firefighting foam.

SILICONE surfactants:

Silicone surfactants, also known as siloxane-polyoxyalkylene copolymers, are a unique type of surfactants that have one or more hydrophilic polar groups that can be anionic, cationic, non-ionic, or zwitterionic, together with permethylated siloxane hydrophobic groups. The most prevalent types of non-ionic groups are those that are composed of polyoxyethylene (PEO) or polyoxypropylene (PPO) in nature. Compared to normal hydrocarbon surfactants, silicon surfactants successfully reduce surface tension to 15-20 $mN.m^{-1}$ in both aqueous and non-aqueous solvents.[41] Due to their distinctive spreading qualities, these surfactants are frequently utilized as emulsifiers in the cosmetics industry, conditioners in textiles, additives in ink, and stabilizers in polyurethane foams.[42]

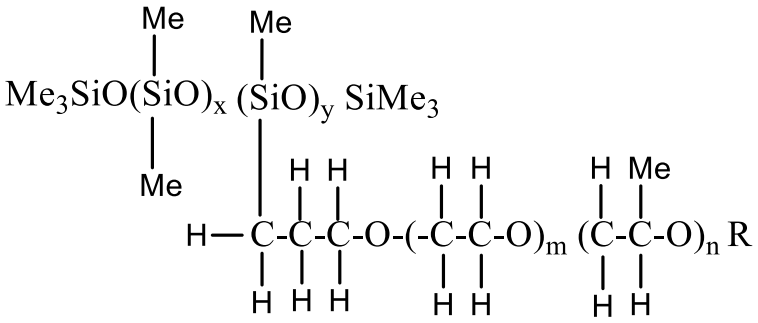

Fig. 6. General structure of silicone surfactants; x = 7 to 10, y = 2 to 5, m = 5 to 15, n = 0 to 5 and R is the alkyl group which has been selected for the compatibility of surfactants in special purpose.

Different amphiphilic compounds have varying degrees of hydrophilicity and lipophilicity based on their structural makeup. The process known as hydrophilic lipophilic balance, or HLB, is crucial for classifying surfactants as either water soluble or oil soluble based on their relative solubility.

Aggregation of Surfactants:

The ability of surfactants to self-aggregate in solution is their most important characteristic. In order to prevent an unfavourable interaction with polar solvents, hydrophobic parts of surfactants can form favourable contacts with one another at bulk. This leads to the formation of arrangements at bulk where hydrophobic tails (Fig. 7A) attract one another into an oil-like core while simultaneously exposing hydrophilic heads to the polar environment. A micelle is a type of self-assembly of surfactants, which can be small or large in size (Fig. 7B). The concentration of surfactants above which micelles form is known as the Critical Micelle Concentration (CMC). In the dynamic process of micellization, free surfactant molecules and micelles are in balance.

Micelles are dimensions of colloids. McBain predicted the possibility of surfactants self-assembling in solution for the first time in 1913.[43] Even though at the time he was roundly criticized by a group of scientists at a Royal Society meeting in London, it was subsequently established by science that surfactants can practically aggregate in solution, as demonstrated by their superior detergency properties, which allow them to dissolve dirt to its hydrophobic core with ease. In addition, electrostatic and van der Waals forces have been important in the formation of ionic surfactants by binding counterions to the oppositely charged micellar heads in order to neutralize the charge and simultaneously cause repulsion between head groups. The majority of the driving force behind micelle formation is hydrophobic in nature, generated between the hydrophobic tails.

The micellization process is largely influenced by positive entropy contribution, since the gain in entropy from the free water molecules that were "trapped" in the solvation cage around the surfactant monomers due to their H-bonding interaction overshadows the entropy lost from the aggregate of the surfactant monomers.[44] In essence, a limited range of surfactant concentrations rather than a specific surfactant concentration is called CMC—which addresses "inexact" but "convenient"—refers to.[45] Micelles can be formed in a variety of morphologies that have been explored elsewhere, depending on the surfactant composition and microenvironments.

Similar to water droplets in an oil system, reverse micelles form in a solution where the concentration of a non-polar solvent (such as alkanes, haloalkanes, aromatic solvents, etc.) is greater than the polar one. Surfactants are used to stabilize the solution's constituents while the amphiphiles form aggregates. One sort of microemulsion was formed using this technique.[46] In the reverse micelle (Fig. 7C), the hydrophobic portions are exposed outside the non-polar solvents, and the polar head groups are aligned with the inner micellar core (referred to as the "Water pool," labelled "W" in Fig. 7C) surrounding the water molecules. Reverse micelles have nanoscale dimensions, and adding more water to a solution will make them bigger. These reverse micelle water pools are employed in the solubilization of proteins[47] and the creation of nanomaterials.[48]

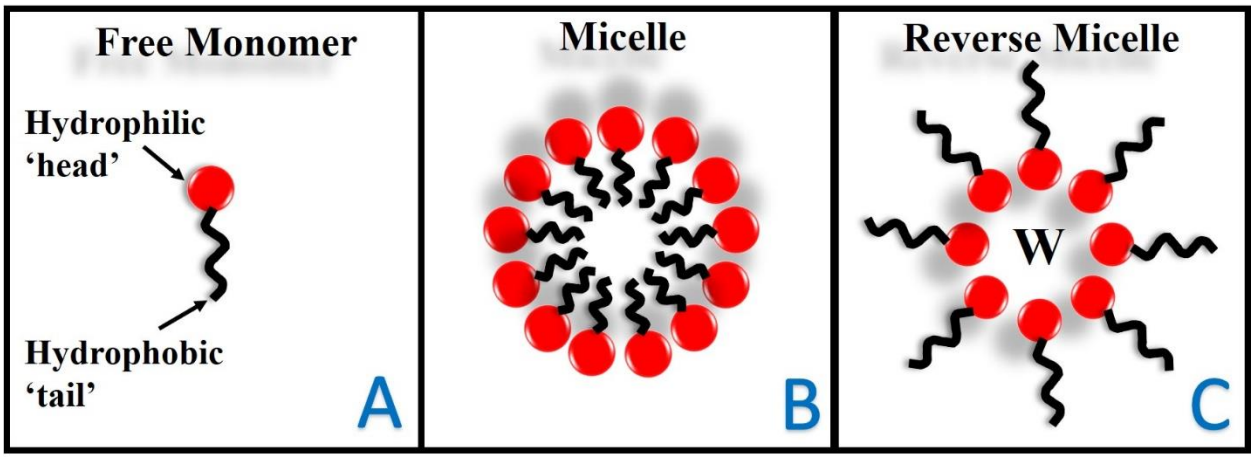

Fig. 7. Aggregates of surfactants in solution: (A) free monomer, (B) normal micelle (spherical structure), (C) reverse micelle.

Determination of CMC:

The most basic characteristic of surfactants is their CMC. There are quantitative techniques for calculating CMC that can be found in literature. For example, Mukerjee and Mysels[49] state that there are 71 potential approaches that they have identified through literature review, and they have addressed each approach critically. The right approach, however, will rely on a number of factors, including the investigator's preferences, the instruments that are available, and how the methodology will ultimately be used. Conductometry, tensiometry, viscometry, vapour pressure osmometry, turbidimetry, light scattering, fluorimetry (steady state, steady state anisotropy, and

time resolved fluorimetry), calorimetry, spectrophotometry, magnetic resonance, and other useful techniques can all be used to determine CMC. The techniques that are most frequently employed among them are conductometry, fluorimetry, and tensiometry. Conductometry techniques are limited to using with ionic surfactants. Different approaches are used to measure the physical properties of surfactants in solution, and variations in surfactant concentration result in diverse features in the appearance of different plots in different ways (Fig. 8).

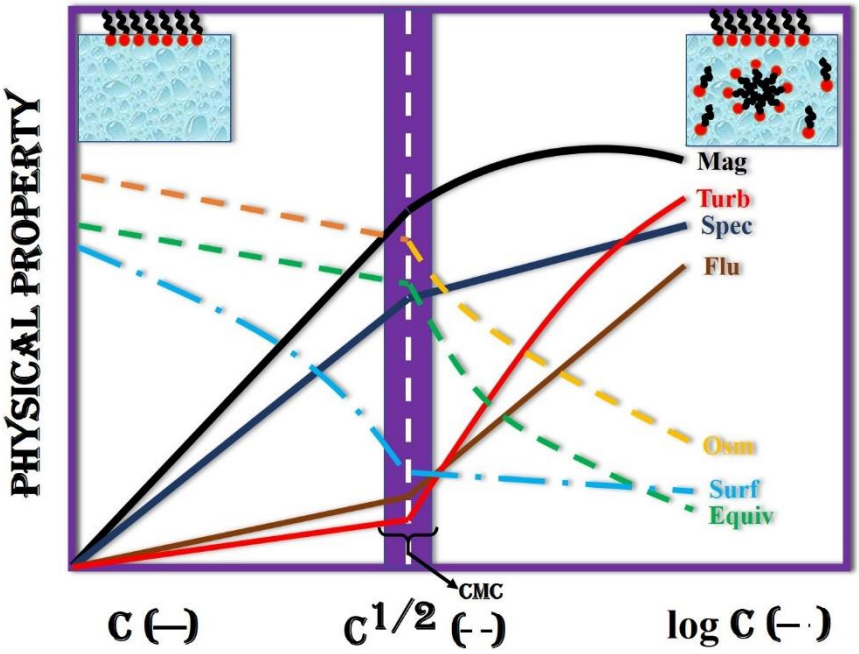

Fig. 8. Evaluation of CMC of a surfactant with variation of surfactant concentration (C) by different methods: viz., Mag: magnetic resonance; Turb: turbidimetry; Flu: Fluorimetry; Spec: spectrophotometry (plotted against C); Surf: surface tension (against log C); Equiv: equivalent conductance; Osm: osmotic coefficient (against $C^{1/2}$).

Every physical property exhibits clear breaks that are identified as CMC and are represented by the dotted white line. Because CMC varies depending on the approach, it should be emphasized that it is not simply a point but rather a narrow range (represented by a narrow bar indicated by a second bracket). Large assemblies after CMC are directly demonstrated by a significant increase in scattering radiation above CMC using light scattering method,[50] since this scattering phenomenon is dependent on the size of scattering units in solution. After concentrating on the

self-diffusion of monomers following CMC by nuclear magnetic resonance (NMR) analysis, another significant demonstration of the compactness of surfactant monomers in micelles has been made.[51]

Micellar characteristics:

Structures, Shapes, Microenvironment and properties of micelles:

Hartley[52] (1936) postulated that micelles are fundamentally spherical. This plan concurs with McBain's 1920 publication, concept.[53] According to Hartley's spherical micelle model, micelles should consist of 50–100 monomers that are grouped together in a relatively small concentration range. The diameter of this group of monomers is roughly twice the length of the hydrocarbon chain. As previously mentioned, the inside of micelles is essentially hydrophobic, but their head groups connect with some counterions to prevent them from coming into close contact because of their repulsive interaction. A single surfactant system with ionic properties could have numerous characteristics that the classical Hartley model successfully characterized.

Because of their surface charge and zeta potential, ionic micelles create an electrical double layer structure[54] that displays electrophoresis in an electric field. Ionic micelles in the immediate vicinity of head groups and oppositely charged counter ions create a "stern layer" when they interact electrostatically. Conversely, the contents of the "Stern layer" are surrounded by the "Gouy Chapman layer," which is generated around them. Both layers have the ability to unbind free monomers, counterions, and free water molecules, which solvate micelles through ion-dipole interaction. Electrical double layer is the collective term for the "Stern layer" and the "Gouy Chapman layer" (Fig. 9). Within the "Stern layer" there is a hydrophobic micelle core.

The micellar kinetic portion is comprised of the core and the Stern layer together. Another name for the Gouy Chapman layer is the diffuse layer. A shear or slipping plane, which is able to move with the micelle in solution, is another term for the diffuse layer's boundary. Zeta potential (μ), which is commonly utilized to indicate the stability of colloidal dispersions, is the slipping plane potential (Fig. 9). A stable micellar solution is one where the magnitude of the zeta potential values is more than ± 30 mV. When it comes to non-ionic micelles, a few water molecules stop inside the core due to an H-bonding contact with polyethylene oxide groups that occurs very next to head groups (palisade layer).

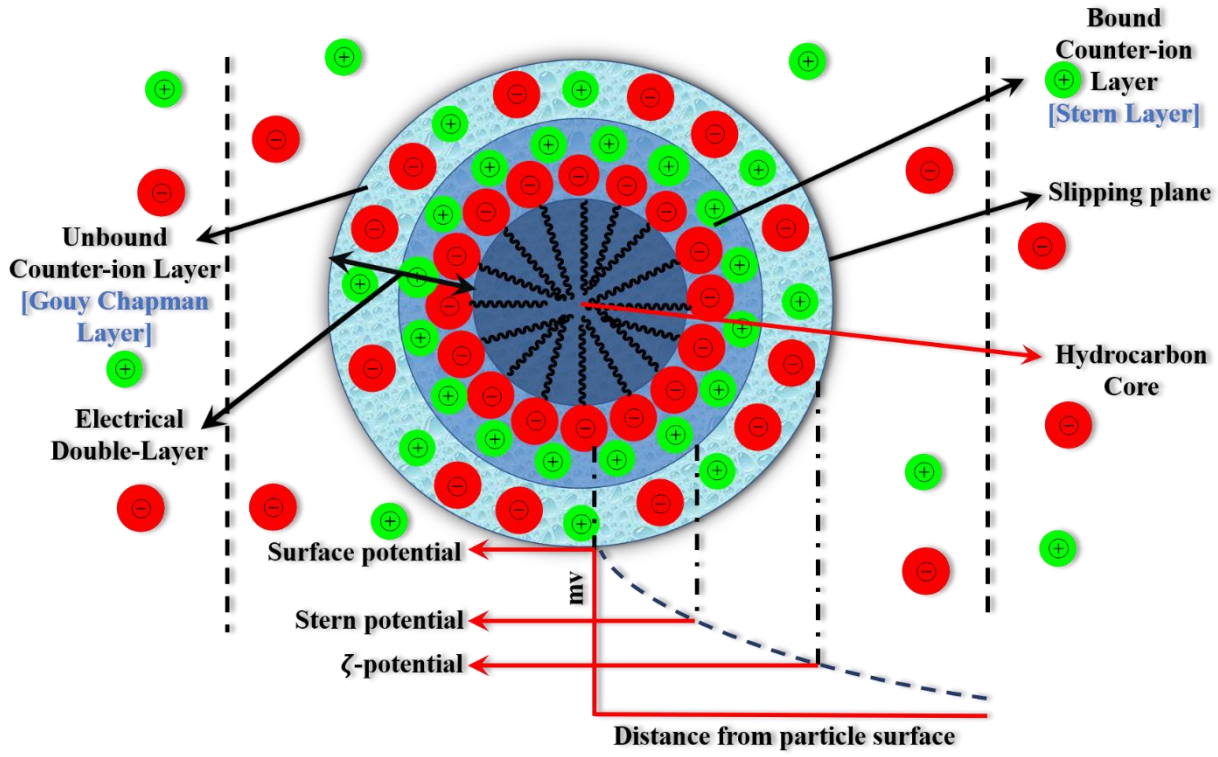

Fig. 9. Schematic representation of ionic micelles demonstrating counter ion binding, charge neutralization, micellar core and electrical double layer assuming spherical symmetry of micelle.

Modern science has created a more convenient microscopic image of micelles by starting with Hartley's concept. The result is that micelles are, of course, dynamic. Molecules can move quickly between solution phase and micelle phase. Micelles can be observed as irregular molecular clusters instead of smooth, perfectly uniform molecules if a high-resolution camera is designed or if the motion of molecules is frozen. Hartley's straightforward "two-states" spherical micellar model has drawn criticism since it is unable to account for a number of experimental observations. In terms of the solubilization of non-polar compounds into micelles, Menger[55] has provided a molecular model that is significantly different from Hartley.[52] According to Menger's "porous cluster" model,[55] water molecules can enter a micelle up to a certain distance (3–4 methylene carbon atoms after the head group); this indicates that the micelle has a relatively smaller interior or core and is easier to enter, as shown by NMR and fluorescence measurements. Other suggested geometries include the rod-like micelle of Debye,[56] the spherical bilayer (vesicle)[57] structure, the worm-like

structure,[58] the ellipsoid shape,[59] the disk or cylindrical structure,[60] and the lamellar type of Philippoff.[61] In order to discriminate between the many supramolecular assemblages that form in solution, Israelachvili et al.[62, 63] introduced the idea of packing parameter. The following formula can be used to get the micelle's amphiphile packing parameter (P):

$$P = \frac{v}{A_{min} \times l_c} \quad (1)$$

l_c is the maximum effective length of a hydrophobic chain of an amphiphile (nm), and v is the volume of hydrophobic chain (nm^3) assuming it is incompressible. A_{min} is the headgroup's surface area (nm^2/molecule) at the micellar-solution interface. Tanford's formula is used to determine the effective length and volume of the hydrophobic chain in pure amphiphiles.[64, 65] The number of carbon atoms in the hydrophobic chain is denoted by n_c.

$l_c \leq l_{max} \approx (0.154 + 0.126\, n_c)$ nm and $v = (0.0274 + 0.0269 n_c)$ nm^3 (2)

where, l_{max} is the maximum length of the monomer chain.

Packing parameter values for different aggregates are tabulated as follows:

Aggregates	P
Micelles	< 1/3
Non-spherical aggregates	1/3 < P < 1/2
Bilayers and vesicles	1/2 < P <1
Inverted aggregates	>1

Some aggregated molecular geometries have been seen in Fig. 10.

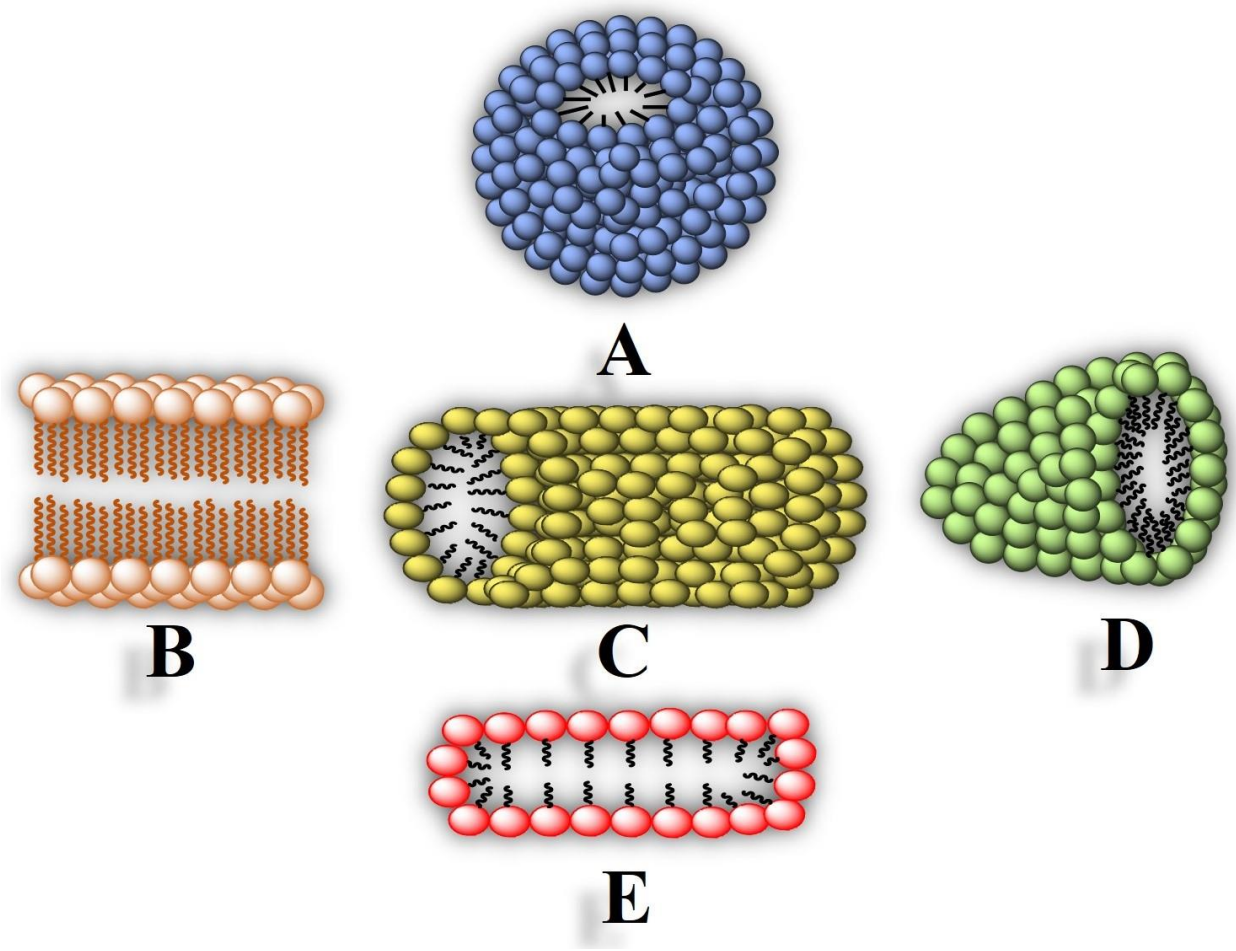

Fig. 10. Schematic representation of geometrical forms of aggregates. A: spherical micelle; B. lamellar or bilayer arrangement; C: rodlike micelle, D: oblate ellipsoid (bisected) micelle, and E: wormlike or cylindrical micelle.

Current technological advancements enable us to collect experimental evidence and photos of many micelle kinds. By assuming spherical micelles[66] and taking into account of the size distribution, the dynamic light scattering (DLS) method allows us to directly see micellar size (average hydrodynamic diameter) and diffusivity without revealing the true form of the micelle. Static light scattering (SLS), small angle neutron scattering (SANS), small angle X-ray scattering (SAXS), cryo-transmission electron microscopy (cryo-TEM), and atomic force microscopy (AFM) techniques can all be used to estimate the size and form of a microcollar sample.[67-70] The sole method that can differentiate between branching and linear micelles is cryo-TEM. Micelles' shapes change when different inorganic and organic salts are present.

A few examples supporting the transitions from spherical to cylindrical, as well as from spherical to wormlike or rod-like, have been given here: In the presence of concentrated NaCl solution, sodium dodecyl sulfate micelles change from spherical to cylindrical conformation;[71] sodium alkylbenzenesulfonate micelles change from spherical to cylindrical and, at high salt concentrations, to multilamellar vesicles;[72] cetyl trimethyl ammonium bromide, cetyl pyridinium chloride micelles become wormlike micelles;[73, 74] etc.

Aggregation number:

The number of molecules that aggregate during micellar assembly is known as the aggregation number (n). Debye[75] introduced a classical method for determining aggregation number that used elastic light scattering. The intensity of scattered radiation at different angles below and above CMC was measured to determine the average aggregation number and molecular weight (MW) of the aggregates. Another approach used to determine aggregation number and hydrodynamic diameter is laser light scattering.[76-78] Another essential technique, which is still widely used today, is fluorescence quenching of a luminous probe using a hydrophobic quencher.[79, 80]

The distribution of probe and quencher among micelles follows Poisson statistics; describe one probe that lives in a micelle and is primarily quenched by a quencher. Surfactant solutions were generated above their CMC, and probe concentrations were fixed in both quencher and micellar solution. The [probe] to [micelles] and [quencher] to [micelles] ratios were kept low enough to assure Poisson distributions. Both the probe and the quencher should be chosen so that they are both located on the micellar interiors or at the surface. The fluorescence technique uses probes to not only interact with the micellar system, which provides information regarding aggregation quantity, but also to identify the polarity of the micellar core, its immediate surroundings, and the balance of substrate-micelle interaction.

Pyrene, anthracene sulphonate, safranine-T, fluorescein, and other probes are often employed to determine mean aggregation number; on the other hand, quenchers such as cetylpyridinium chloride, dodecyl pyridinium chloride, thiourea, inorganic complexes of Ru^{2+}, Cu^{2+}, and Ni^{2+} have been utilized. The mean aggregation number can be determined using both steady state and time resolved fluorescence approaches, depending on whether the quenching is static or dynamic. The static quenching approach is widely employed (in which it is considered that increasing quencher

concentration may lower the emission of probe situated on micelle, but does not change its life time), utilizing the following relation.

$$ln\frac{F}{F_0} = \frac{n[Q]}{[Surfactant]-CMC} \quad (3)$$

where F and F_0 are the fluorescence intensities in presence and absence of quencher, [Surfactant] is the total concentration of surfactant, [Q] is the quencher concentration, n is the average aggregation number at CMC. Plot of ln(F/F$_0$) vs. [Q] readily yields the value of n from the slope.

When quenching occurs dynamically—that is, when a probe's lifetime is altered by an increase in quencher concentration in tandem with a drop in fluorescence intensity—the aforementioned equation produces an incorrect answer in terms of amalgamation number values. Particularly, for the system with relatively large micro viscosity and smaller aggregation number, it is observed that the mean aggregation number identified by steady state measurement is found to be lower than those predicted in time resolved technique.[81] In contrast to the free probe situated on the same micelle, the fluorescence decay curve of the micelle-soluble probe in the presence of the "immobile" quencher demonstrates a distinct form. Following equation[79, 82, 83] can be used to fit the fluorescence decay curve in the presence of a quencher in such a scenario.

$$I_t = I_0 exp\left\{-\frac{t}{\tau_0} - R[1-\exp(-k_Q t)]\right\} \quad (4)$$

I_t and I_0 are the fluorescence intensities at time t and zero respectively. k_Q is the first order quenching rate constant. τ_0 is the lifetime of a probe in absence of quencher. R can be written as, $R = \frac{[Q]}{[Micelle]}$; [*Micelle*] is the concentration of micelle. R values are adjusted close to 1 and not exceeded to 2 for theoretical consideration.[84] Taking the value of R, average no of aggregation number (n) can be calculated at a particular quencher concentration [Q] using the following relation:

$$n = R\frac{([Surf]-CMC)}{[Q]} \quad (5)$$

Due to solvation and counter-ion binding to the micelles, the light scattering experiment overestimates the mass and thus, the volume of the micelles. It is feasible to determine solvation

and counterion binding by comparing light scattering and fluorescence studies. Numerous internal and external factors can influence the size and dispersity of micelles.

Internal factors:

A homologous series of surfactants with longer hydrocarbon chains will have more aggregation numbers. A new study[85] assesses that when every carbon atom is converted to an alkyl group, the number of micelle aggregation increases linearly by around 16 monomers per micelle. Conversely, a decrease in the hydrophilicity of the head group—that is, a higher degree of ion binding, a shorter polyoxyethylene group, etc.—causes the aggregation number (n) to increase. For spherical and ellipsoid structures across a specific ellipticity range, Tanford[86] was projected to raise micellar aggregation number to maximum for a given alkyne chain length.

In an aqueous solution at 298.15K, it is observed that[87] increase in the spacer length of gemini surfactants from 2 to 12 reduces the aggregation number from roughly 48 to 11. It follows that a drop in the aggregation number occurs with an increase in the effective head group size (i.e., relatively bulky head groups). Bile salt micelles may aggregate with a lower aggregation number[88, 89] of 4–10. In an aqueous solution, cationic surfactants have aggregation numbers that range from 20 to 100.

External factors:

Aggregation number falls with increasing salinity of the medium; yet, micellar aggregation number is greater than that measured in pure aqueous solution when salt concentration is increased or pH is raised, because these conditions screen the head group charges of surfactant monomers living at the Stern layer.[81, 90] While the aggregation number of ionic surfactants reduces little with temperature, the "cloud point" phenomenon is responsible for the considerable increase in aggregation number of non-ionic surfactants.[91] Micellar size appears to rise when small amounts of poorly soluble non-amphiphilic organic compounds are added; however, this may be more the result of solubilization than of an increase in the quantity of surfactant molecules in the micelle.

Degree of counterion binding: The essential component of the micelles,[92, 93] to the stern layer of the micelle, are counterions. The electrical double layer and the determination of thermodynamic parameters for the micellization process both depend on the degree of counterion binding. The degree of counterion binding varies from 20 to 80%, based on a variety of factors, such as,

amphiphiles, solution media, and additives. A number of techniques exist for determining counterion binding, the most widely used being conductometry measurement.

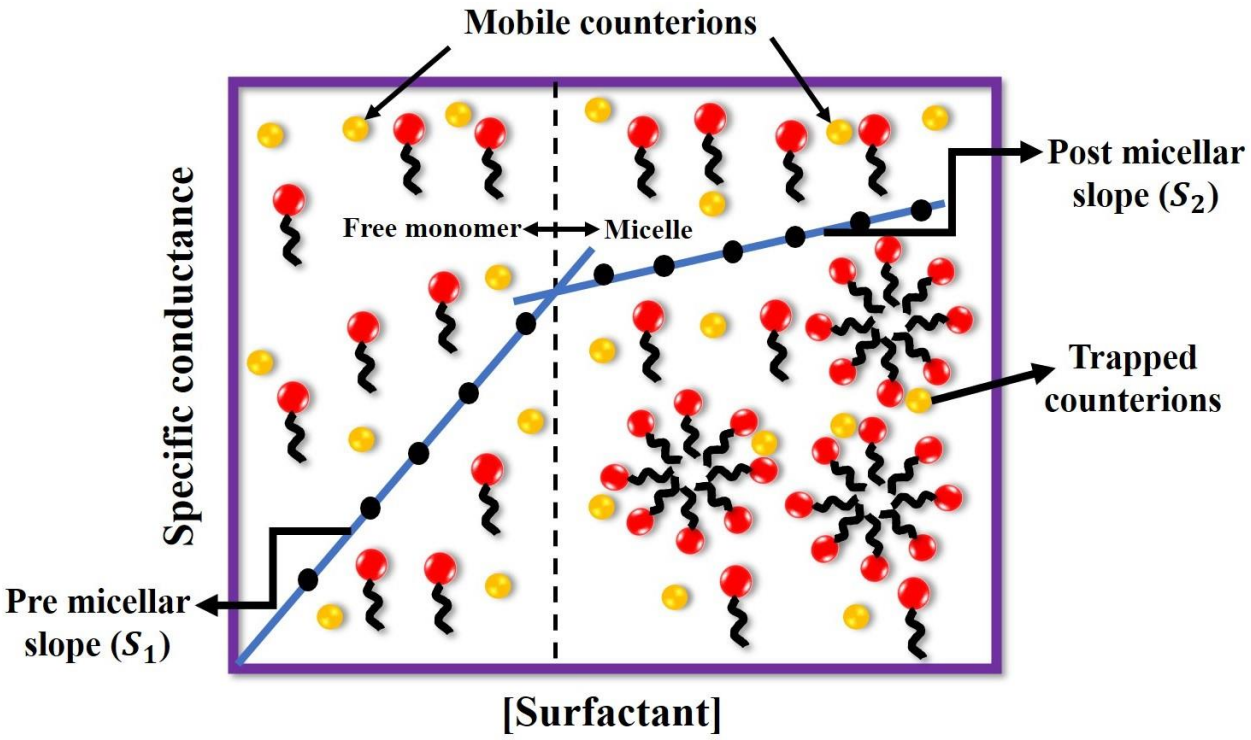

Fig. 11. Specific conductance vs. [Surfactant] profile for determination of CMC and degree of counterion binding using pre (S_1) and post micellar (S_2) slopes.

Initially, free surfactant monomers and counterions both contribute to a specific conductance value at low surfactant concentrations. The specific conductance value increases monotonically with increasing surfactant concentrations due to the rising fraction of both monomer and counterions (Fig. 11). But following micellization, some counterions attach themselves to the produced micelles, making them bigger and less movable. A reduced quantity of free monomers and unbound counterions is the single factor that contributes to specific conductance values (Fig. 11), which causes specific conductance values to be offset. Two unique slopes (S_1 and S_2) of separate magnitude are identified as a result of this conductometric phenomena, and these are employed in a straightforward relation to determine the degree of counterion binding (g), as follows:

$$g = 1 - \frac{S_2}{S_1} \qquad (6)$$

Despite some assumptions, this method works quite well, and the allowable error range (about 2-3%) covers the uncertainty of the degree of counterion binding.

Thermodynamics of micellization:

The micellization process is energetically governed by thermodynamic considerations. During surfactant micellization, the so-called 'iceberg' structure around the surfactant monomer breaks down, resulting in an increase in entropy.[94, 95]

Two approaches have been widely utilized in classical literature and are recognized as useful micellization models: (i) the mass action model, and (ii) the phase separation model, sometimes known as the pseudo phase model.[96, 97]

According to the mass action model, after CMC, monomer and micelles are interdependent, as increasing monomer concentration causes an increase in micelle concentration, and vice versa, as seen in the following equilibrium:

$$nS \overset{K_M}{\leftrightarrow} S_n \text{ or } M \quad (7a)$$

for a nonionic surfactant, S, S_n, n and K_M denote surfactant monomers, micelles, aggregation number and equilibrium micellization constant respectively.

In case of ionic surfactants, while studying micellization, the above equilibrium takes the new equilibrium incorporating the charges and counterions:

$$nS^{\pm} + mZ^{\mp} \underset{K_M}{\leftrightarrow} (S_n Z_m)^{\pm(n-m)} \text{ or } M^{\pm(n-m)} \quad (7b)$$

for an ionic surfactant, where $Z^{\pm}$ and m denote counterions and no of counterions are attached to the micelle in the above equilibrium process.

Hence, it is written as, for nonionics, neglecting activity effect,

$$K_M = \frac{a_M}{a_S^n} \approx \frac{C_M}{C_S^n} \quad (7c)$$

where, a is the activity coefficient and C is the concentration.

For ionic surfactants,

$$K_M = \frac{a_M^{\pm(n-m)}}{a_{S^\pm}^n a_{Z^\mp}^m} \approx \frac{C_M^{\pm(n-m)}}{C_{S^\pm}^n C_{Z^\mp}^m} \quad (7d)$$

For nonionic surfactants, standard Gibbs free energy of micellization can be given by the following relation:

$$\Delta G_M^0 = -RT\ln K_M = -RT\ln C_M + nRT\ln C_S \quad (8)$$

Change of standard Gibbs free energy of micellization per monomeric unit (n) can be presented as:

$$\frac{\Delta G_M^0}{n} = \Delta G_{mic}^0 = -\frac{RT}{n}\ln C_M + RT\ln C_S \quad (9)$$

At CMC, percentage of monomers forms micelles which are very small. Hence, the eq. 9 can be approximated as:

$$\Delta G_M^0 = RT\ln C_S = RT\ln CMC \quad (10)$$

For ionic surfactants,

$$\Delta G_M^0 = -RT\ln K_M = -RT\ln C_M^{\pm(n-m)} + nRT\ln C_S^\pm + mRT\ln C_Z^\mp \quad (11)$$

Therefore, it can be written as standard Gibbs free energy change per monomeric unit in the following form:

$$\frac{\Delta G_M^0}{n} = \Delta G_{mic}^0 = -\frac{RT}{n}\ln C_M^{\pm(n-m)} + RT\ln C_S^\pm + \frac{m}{n}RT\ln C_Z^\mp \quad (12)$$

Again, as the percentage of monomers is very small and usually n is large, the eq. 12 is transformed as

$$\Delta G_{mic}^0 = RT\ln C_S^\pm + \frac{m}{n}RT\ln C_Z^\mp \quad (13)$$

For normal ionizable surfactants, it can be written as

$$C_S^\pm = C_Z^\mp \quad (14)$$

Hence, at CMC, it is obvious, $C_S^\pm = C_Z^\mp = CMC$ (15)

so that, $\Delta G_{mic}^{0} = \left(1 + \frac{m}{n}\right) RT \ln CMC = (1 + g)\, RT \ln CMC$ (16)

where, g is the fraction or degree of counterion binding.

If g = 0, there is no counterion binding in case of nonionic surfactant,

$$\Delta G_{mic}^{0} = RT \ln CMC \quad (17)$$

On the other hand, if 100% counterions are bound, g = 1 and the Eq. 16 takes the form:

$$\Delta G_{mic}^{0} = 2RT \ln CMC \quad (18)$$

The above relation is based on constant condition of aggregation number (n) and several valid approximations.

Pseudophase model is based on the assumption that, micelles are considered to constitute a new phase at or above CMC and concentration of monomers remains invariant at or above CMC.

According to Pseudophase model, the following equilibrium can be conferred based on phase equilibrium: $\boldsymbol{monomer} \leftrightarrow \boldsymbol{micelle}\ (\boldsymbol{Pseudophase})$ (19)

At a constant temperature, chemical potential of free surfactant monomers (μ_S) in solution is equal to chemical potential of surfactant monomers in pseudo micellar phase ($\mu_S^{micelle}$).

Thus, for nonionic surfactant,

$$\mu_S = \mu_S^{micelle} \text{ or } \mu_M \quad (20)$$

The eq. 20 can be written for nonionic surfactant,

$$\mu_S^{0} + RT \ln a_S = \mu_M^{0} + RT \ln a_M \quad (21)$$

or, $\Delta G_m^{0} = \mu_M^{0} - \mu_S^{0} = RT \ln a_S \approx RT \ln CMC$ (22)

Since, a_M (activity of micelle considering it as a separate pure phase or pseudo phase) = 1,

in case of ionic surfactant,

$$\mu_S^{\pm} + \frac{m}{n}\, \mu_Z^{\mp} = \mu_M^{\pm} \quad (23)$$

as, $\mu_S = \mu_M$

Therefore, the eq. 23 is transformed to

$$\mu^0_{S^\pm} + RT \ln a_S^\pm + \frac{m}{n}\mu^0_{Z^\mp} + \frac{m}{n} RT \ln a_Z^\mp = \mu^0_{M^\pm} + RT \ln a_M^\pm \quad (24)$$

Or, $\left[\mu^0_{M^\pm} - (\mu^0_{S^\pm} + \frac{m}{n}\mu^0_{Z^\mp})\right] = RT \ln a_S^\pm + \frac{m}{n} RT \ln a_Z^\mp - RT \ln a_M^\pm \quad (25)$

hence, $\Delta G^0_m = RT \ln a_S^\pm + \frac{m}{n} RT \ln a_Z^\mp - RT \ln a_M^\pm \quad (26)$

Since, $a_M^\pm = 1$, $\Delta G^0_m = RT \ln a_S^\pm + \frac{m}{n} RT \ln a_Z^\mp = \left(1 + \frac{m}{n}\right) RT \ln CMC \quad (27)$

Or, $\Delta G^0_m = (1 + g)\, RT \ln CMC \quad (28)$

In the equations [23] to [27], $\mu_M^\pm$ is actually $\mu_M^{\pm(n-m)}$; the factor (n-m) has been neglected for simplicity.

We get the same equation for ΔG^0_m from pseudophase model that we get from mass action model. μ^0_S and μ^0_M are the standard chemical potentials of monomer and micelle respectively, and, a_S and a_M are the activities for the same respectively. Here, it is noted that, for the above two methods, equilibrium concentration of free monomer (C_S) is considered to be equivalent to CMC.

In case of mass action model, including the contribution of aggregation number (n),[98] standard Gibbs free energy of micellization (ΔG^0_{mic}) and standard enthalpy of micellization (ΔH^0_{mic}) can be expressed by,

$$\Delta G^0_{mic} = (1 + g)\, RT \ln X_{CMC} + \frac{RT}{n} \ln[2n(n + m)] \quad (29)$$

and, $\Delta H^0_{mic} = -RT^2 \left[(1 + g)\frac{d \ln X_{CMC}}{dT} + \ln X_{CMC} \frac{dg}{dT} + \frac{d\left[\left(\frac{1}{n}\right) \ln\{2n(n+m)\}\right]}{dT}\right] \quad (30)$

CMC has been expressed in mole fraction (X_{CMC}) unit in the above two equations. Here, g is the number of counterion binding and n is the aggregation number. Usually, the second and third terms

of equations [29] and [30] are small. In the pseudophase model, the terms can be conceptually avoided.

Thus, for ionic micelles,

$$\Delta H_{mic}^{0} = -RT^{2}\left[(1+g)\frac{d\ln X_{CMC}}{dT} + \ln X_{CMC}\frac{dg}{dT}\right] \quad (31)$$

and for nonionic micelles,

$$\Delta H_{mic}^{0} = -RT^{2}\frac{d\ln X_{CMC}}{dT} \quad (32)$$

Entropy of micellization (ΔS_{mic}^{0}) can be calculated from Gibbs- Helmholtz equation,

$$\Delta S_{mic}^{0} = \frac{\Delta H_{mic}^{0} - \Delta G_{mic}^{0}}{T} \quad (33)$$

CMC should be measured at different temperatures in order to evaluate ΔH_{mic}^{0} and ΔS_{mic}^{0} using equations 29 to 33, whichever is applicable for different systems. ΔS_{mic}^{0} values are normally positive. Negative entropy contribution due to amphiphilic association in micelle or the solvation of monomers are overshadowed by the disruption of iceberg structure around the monomers to take them into micelle, this process in terms increases the overall entropy.

It may be mentioned that for calculation of thermodynamic parameters, CMC should be converted in mole fraction unit (stated earlier). The van't Hoff method is used to calculate standard enthalpy of micellization (ΔH_{mic}^{0}) by measuring the CMC values at different temperatures using the equation 32. By using ITC (isothermal titration calorimetry), both CMC and ΔH_{mic}^{0} can be measured directly. Determination of ΔH_{mic}^{0} using calorimetry method gives the exact value with high precision of accuracy.[99-102] The enthalpies determined by van't Hoff method (by determining CMC at different temperatures) are generally found dissimilar with those calculated by direct method, especially for ionic surfactants.[103-106]

Neither the mass action nor the pseudophase models for surfactant micellization are entirely correct. Both approaches assume that the equilibrium free monomer concentration throughout the micellization process is equal to CMC. It is also convenient to presume that the aggregation number and degree of counterion binding are temperature independent, or at least within the

investigated temperature range. Despite these drawbacks, these two models are the simplest ways to determine thermodynamic characteristics.

Besides, the two models mentioned above, there are various alternative ways. Hill created a thermodynamic model for small systems,[107] which Hall and Pethica adapted to nonionized and noninteracting systems.[97] Hall has produced a detailed treatment of a multicomponent system with interacting aggregates.[108-110] Corkill and associates[111-113] presented another thermodynamic strategy for non-ionic surfactant systems. Tanford[114] offered an intriguing concept for micelle production based on micelle structure. This geometrical technique is expanded by Israelachvili et al.[62] and further explored by Ruckenstein and Nagarajan.[115]

It is difficult to determine thermodynamic parameters with absolute precession due to a number of factors, including changes in aggregation number, micellar shape and size, counter ion condensation, micellar solvation with temperature variation, and other environmental changes. For these reasons, this topic merits more research.

Theory of mixed micelles:

When combined with one another, two or more surfactants show extensive interfacial properties in an aqueous solution, such as a drop in CMC, an increase in surface activity, a rise in the intensity of scattered radiation, etc. As a result of the active involvement of both surfactants, mixed micelles are generated in solution (Fig. 12) and remain in equilibrium with individual monomeric species following CMC.[9] It has been approved to treat possible skin irritation with a low concentration of mixed surfactant mixture.[116] It is also better for the environment because less surfactant is needed to generate mixed micelles and less surfactant is released.[117]

The human body's ability to absorb hydrophobic medicines has been significantly improved by mixed micelles.[118, 119] It is noteworthy to note that an equimolar mixture of anionic and cationic surfactants can produce an insoluble ion pair; nevertheless, if one component's percentage in solution is noticeably higher than the other, the insoluble ion pair will become soluble.

The conjugation of catanionic surfactants has also been described in literature to exhibit vesicle-like structure.[120-122] A washing product that reduces water hardness can be made by combining cationic and anionic surfactants.[123] There have been reports in the literature of mixed micelles of ionic-ionic,[124-133] ionic-nonionic,[134-140] and nonionic-nonionic[141-143] combinations; nonionic-nonionic and cationic-cationic combinations are uncommon among them. Surface active ionic liquid (SAIL), mixed micelle formation in conjunction with anionic,[144-150] amphiphilic drugs,[151-155] cationic[9, 156-163] and nonionic surfactants[24, 164-169] have also been extensively researched.

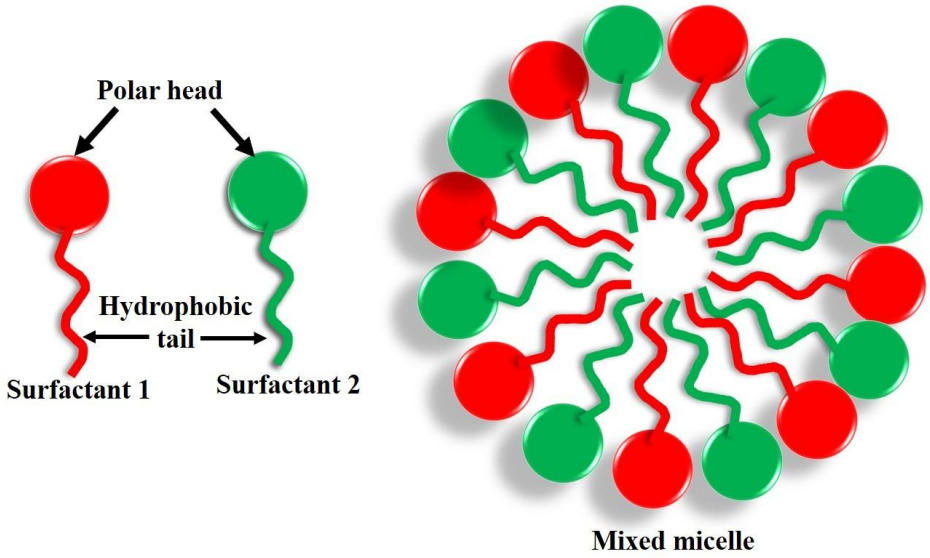

Fig. 12. Schematic representation of a mixed micelle formed by two ionic surfactants (Surfactant 1 (green) and Surfactant 2 (red)).

A simple theory is proposed by Clint[170] to determine CMC assuming the ideal mixing by the monomeric amphiphiles during mixed micelle formation. The proposed relation made by Clint's[170] assumption is given here:

$$\frac{1}{(CMC)_{max}} = \sum_i \frac{\alpha_i}{(CMC)_i} \tag{34}$$

where, α_i and $(CMC)_i$ are the stoichiometric mole fraction and CMC of i^{th} component respectively. If the mixing of surfactant components forming mixed micelle is not ideal, eq. [34] takes the form:

$$\frac{1}{(CMC)_i} = \sum_i \frac{\alpha_i}{f_i\,(CMC)_i} \tag{35}$$

where, f_i is the activity coefficient of the i^{th} species.

Clint's[170] theory, which describes homologous surfactant series with similar head groups where nearly ideal mixing might be expected, is sufficient in these situations. However, it is unable to predict $(CMC)_{max}$ or the monomeric compositions in the mixed micelle formed by surfactants with different head groups. Regarding this, it has been shown that a theory grounded in Regular Solution Theory (RST) offers a means of addressing both enthalpic and entropic variables in the mixed micelle formation. With the experimental CMCs ($(CMC)_{max}$) on the compositions of ionic-nonionic or nonionic-nonionic mixed micelles, the prediction of this theory yields a satisfactory outcome.

For binary mixtures of nonionics, Lange[171] developed an equation that, under the assumption of ideal mixing—the entropy changes that results from the mixing of two amphiphilic species within the micelle which is the only source of contribution to the free energy of mixing—that accurately reflected the dependence of CMC on bulk composition. Assuming perfect mixing for a homologous pair of ionic surfactants, Lange[172] and Shinoda[173] also separately developed a comparable method. Afterwards, the Lange-Shinoda method synthesizing ionic and non-ionic surfactants was expanded by Moroi and associates.[174] In the middle to late 1970s, theories were created[174, 175] to explain the micellar mole fraction, activity coefficient, and degree of surfactant interaction in mixed micelles.

A theoretical method was developed by Rubingh[175] to connect surfactant micellar mole fraction to monomer concentration. Despite the fact that a micellar system could be satisfactorily explained,[176, 177] Rubingh's idea[175] was questioned due to thermodynamic concerns. Motomura et al.[178] put up a mixed micellar theory where they provided a more accurate explanation of mixed surfactant solutions. Sarmoria et al.[179] and Puvvada et al.[180] created the Molecular Thermodynamic Model (SPB model) for mixed surfactant systems in the early 1990s. The Rubingh[175] theory, which contains a unique interaction parameter (β) assessing the interaction with surfactants—whether synergistic or antagonistic—has been as the foundation for the majority of research that have described mixed micellar systems so far. The SPB model is more complex than the Rubingh treatment.

Rubingh's treatment on binary mixtures:

If two amphiphiles 1 and 2 produce mixed micelle, the mole fraction of surfactant 1 can be estimated from the known values of CMC of individual surfactants, C_1 and C_2 and the CMC of mixed micelle, C^* and stoichiometric mole fraction of surfactant 1 (α) in the total mixed solute.

List of symbols:

μ_1 = chemical potential of monomeric surfactant 1

μ_1^0 = standard chemical potential of monomeric surfactant 1

μ_{1M} = chemical potential of 1 in micelle

μ_{1M0} = chemical potential of 1 in pure micelle

$C_1^m \; and \; C_2^m$ = concentration of monomeric surfactants 1 and 2

$f_1 \; and \; f_2$ = activity coefficient of surfactants 1 and 2 in mixed micelle

x = mole fraction of surfactant 1 in mixed micelle.

The chemical potential of monomeric component 1in mixed micelle solution can be written as:

$$\mu_1 = \mu_1^0 + RT \ln C_1^m \tag{36}$$

and chemical potential of component 1 in mixed micelle is

$$\mu_{1M} = \mu_{1M0} + RT \ln f_1 x \tag{37}$$

By using a phase separation model of micellization, we can write for component 1 in the pure micelle,

$$\mu_{1M0} = \mu_1^0 + RT \ln C_1 \tag{38}$$

As, at equilibrium since $\mu_1 = \mu_{1M}$, we obtain from Eq. [36], [37] and [38] that for component 1,

$$C_1^m = x f_1 C_1 \tag{39}$$

Similarly, for component 2, we may write,

$$C_2^m = (1-x) f_2 C_2 \tag{40}$$

Below *C**, the concentration of component 1 is given by,

$$C_1^m = \alpha C \tag{41}$$

here, C is total surfactant concentration of surfactants 1 and 2 in solution.

Similarly, for component 2, we can write,

$$C_2^m = (1-\alpha) C \tag{42}$$

At the mixed CMC (*C**), by considering the Eqs. [39]-[42], it can be written

$$\alpha C^* = x f_1 C_1 \tag{43}$$

$$(1-\alpha)\, C^* = (1-x) f_2 C_2 \tag{44}$$

Eliminating x from the equations [43] and [44], we can write,

$$\frac{1}{C^*} = \frac{\alpha}{f_1 C_1} + \frac{1-\alpha}{f_2 C_2} \tag{45}$$

Since, $f_1 = f_2$ (ideal approximation), then Eq. [45] reduces to,

$$\frac{1}{C^*} = \frac{\alpha}{C_1} + \frac{1-\alpha}{C_2} \tag{46}$$

Equation [46] is derived by Lange, Beck and Clint.

On the other hand, we can eliminate C^* between the two equations ([43] and [44]) to get the mole fraction of component 1 at CMC (Eq. [47]),

$$x = \frac{\alpha f_2 C_2}{\alpha f_2 C_2 + (1-\alpha) f_1 C_1} \tag{47}$$

Relationships of monomer concentrations valid above CMC can be developed from the following relation:

$$x = \frac{\alpha C - C_1^m}{C - C_1^m - C_2^m} \tag{48}$$

Substituting C_1^m and C_2^m from the Eqs. [39] and [40] to Eq. [48], one can get a quadratic expression of x; upon solving yields the following value of x.

$$x = \frac{-(C-\Delta)+\sqrt{(C-\Delta)^2+4\alpha C\Delta}}{2\Delta} \quad (49)$$

where, $\Delta = f_2C_2 - f_1C_1$

Finally, using the equation [39] again, the monomer concentration of component 1 can be written explicitly,

$$C_1^m = \frac{-(C-\Delta)+\sqrt{(C-\Delta)^2+4\alpha C\Delta}}{\left(\frac{f_2C_2}{f_1C_1}\right)-1} \quad (50)$$

and, $C_2^m = \left(1 - \frac{C_1^m}{f_1C_1}\right) f_2C_2$ (51)

Although, the eqs. [50] and [51] correct the expression for micellar composition and monomer concentrations, remain incomplete without some relation between activity coefficients in micelle and micellar composition. Regular solution approximation can be used to determine activity coefficient of monomers in mixed micellar state.

$$f_1 = \exp \beta\ (1-x)^2 \quad (52)$$

and, $f_2 = \exp \beta x^2$ (53)

This parameter β (stated earlier) is also molecular interaction in mixed micelle,

$$\beta = \frac{N\ (W_{11}+W_{22}-2W_{12})}{RT} \quad (54)$$

where, W_{11} and W_{22} are the energies of interaction between surfactant molecules in pure micelles and W_{12} is the interaction between two species in mixed aggregate. *N* is Avogadro number. It can be demonstrated within regular solution context, the excess enthalpy (H_E) is given by,

$$H_E = \beta\ RT\ x\ (1-x) \quad (55)$$

Since, β cannot be 0, this model considers both enthalpy and entropy (for ideal mixing) contribution in mixed micelle formation. If β is negative, then it can be said that the interaction

between surfactants is synergistic in mixed micelle and reverse is true for antagonistic type interaction. β can be calculated using the following relationships in terms of C_1, C_2, α and C^*,

$$\frac{x^2 \ln\left(\frac{C^*\alpha}{C_1\alpha}\right)}{(1-x)^2 \ln\left(\frac{C^*(1-\alpha)}{(1-x)}\right)} = 1 \quad (56)$$

Eq. [56] is solved iteratively for x, and substitution of x into equation [57] yields the immediate solution of β.

$$\beta = \ln\left[\frac{\left(\frac{C^*\alpha}{C_1\alpha}\right)}{(1-x)^2}\right] \quad (57)$$

Numerous researchers have made detailed attempts at mixed micellization investigations.[172, 181-185] The CMC values of combinations containing alkyl sulphate anions[172, 186] and quaternary ammonium cations[187] have been examined. In order to assess CMC, combinations of ionic and nonionic surfactants have been examined by Moroi et al.[174] and others.[188-190] While it has been observed that the CMCs of mixed surfactant systems fall between those of pure surfactants, other studies indicate that the CMCs of mixed surfactant systems surpass those of their pure parent components.[191-193]

Drugs:

Drug compounds are often amphiphilic, with the hydrophobic portion being the aromatic ring. Two intriguing features of their hydrophobicity group have been noted: first, the hydrophobic ring portion exhibits a high degree of flexibility; hence, the association behaviour of these medications may be similar to that of normal surfactants. However, unlike dye molecules, which delocalize inside the ring system, the ring hydrophobic component bearing rigidity can maintain their charge at the terminal position of the rather long connected hydrocarbon chain of the ring group. Drug molecules are typically only categorized in current research based on their biological and pharmacological implications; but in this case, we attempted to categorize various drug kinds with colloidal behavior based on their medicinal implications, which are uncommon.

1. Antihistamine:

Two types of antihistamine drugs exhibit colloidal behaviour which are (a) diphenylmethane derivatives and (b) pyridine derivatives.

(a) *Diphenylmethane derivatives*:

Antihistamine diphenylmethane derivatives' light-scattering studies (Fig. 13) verify how similar they are to conventional surfactants because of the presence of a distinct infection in their plot, which identifies their CMC.[194] While the number of monomers aggregating is low, ranging from 9 to 12, it is possible that affiliations are not entirely synchronous and that micelle formation is the cause of CMC. Anyhow, Mukerjee insisted that this was just an oversimplification of the situation.[195]

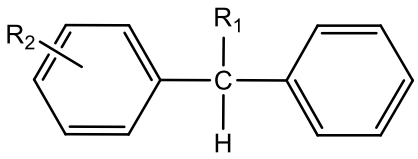

Diphenylhydramine HCl, R_1 = -$OCH_2CH_2N(CH_3)_2$,
R_2 = H
Bromodiphenylhydramine HCl, R_1 = -$OCH_2CH_2N(CH_3)_2$,
R_2 = p-Br
Medrylamine maleate, R_1 = -OCH_2CH_2 $N(CH_3)_2$,
R_2 = p-OCH_3
Phenyltoloxamine citrate, R_1 = H, R_2 = o-OCH_2CH_2 $N(CH_3)_2$

Fig. 13. Structures of some anti histaminic drugs of diphenylmethane derivatives.

(b) *Pyridine derivatives:*

Pyridine compounds with antihistaminic properties are shown in Fig. 14. For these kinds of medications, small associations happen at very high concentrations.[196] There is a continuous aggregation that seems to have no clear CMC.[196, 197]

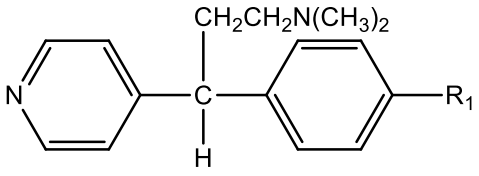

Pheniramine R_1 = H
Chlorpheniramine R_1 = Cl
Brompheniramine R_1 = Cl

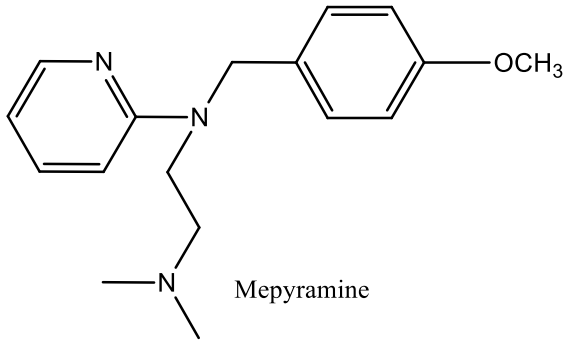

Mepyramine

Fig. 14. Molecular structures of few pyridine ring containing anti histaminic drugs.

2. Antiacetylcholine drugs:

Several antiacetylcholine medications are made up of diphenyl methane moiety structures; some of these are depicted in Fig. 15. Their nature is essentially amphiphilic.[198] These kinds of drugs have higher CMC values and lower aggregation numbers. They function as an antidepressant medication in terms of physiology.

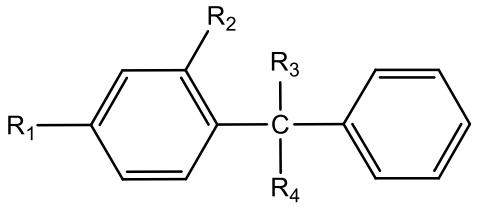

Adiphenine HCl, R_1 = H, R_2 = H, R_3 = H, R_4 = $COO(CH_2)_2N(C_2H_5)_2$
Orphenadrine HCl, R_1 = H, R_2 = CH_3, R_3 = H, R_4 = $O(CH_2)_2N(CH_3)_2$
Chlorphenoxamine HCl, R_1 = Cl, R_2 = H, R_3 = CH_3, R_4 = $O(CH_2)_2N(CH_3)_2$
Lachesine CI, R_1 = H, R_2 = H, R_3 = OH, R_4 = $COO(CH_2)_2N^+(CH_3)_2C_2H_5$

Fig. 15. Structures of some Antiacetylcholine drugs.

3. Phenothiazine and thioxanthene tranquillizers:

Antipsychotics with phenothiazine derivatives are used to treat psychotic illnesses and schizophrenia. A carbon atom replaces the nitrogen in the middle ring to generate thioxanthene, also known as thiothixene, which is closely linked to phenothiazines (Fig. 16). A thorough surface analysis of these two drug kinds reveals that their association process is micellar in nature.[199] CMCs are obtained for these kinds of medicines using several approaches that accord rather well. For such compounds, a straight chain substituent has a greater effect on hydrophobicity than a branched chain with the same number of carbons. The presence of organic cations, such as tetra-alkylammonium ions, was discovered to have a notable inhibitory impact, which grows as chain length does.

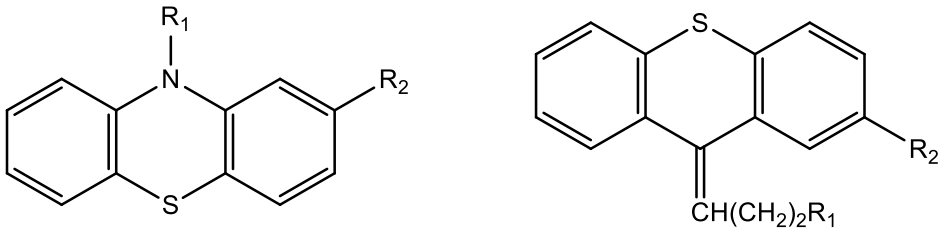

Phenothiazine tranquilizers Thioxanthene tranquilizers

Fig. 16. Structures of Phenothiazine tranquillizers and Thioxanthene tranquillizers moieties.

4. Tricyclic antidepressants:

For a number of tricyclic antidepressant drugs, light-scattering experiments and many other methods validate their micellar characteristics in solution.[200] For such medications, the tricyclic system exhibits the least amount of flexibility, indicating the direct need for additional structural requirements for their solution connection. It has been observed that substituents have a significant impact on the characteristics of such medications' solutions, altering the hydrophobic moiety entirely. Since these medications are mostly hydrochloride salts, the influence of counterions is disregarded while examining their solution association characteristics (Fig. 17). Such medications are more hydrophobic when -Cl similar substituent groups are present on the phenyl position. The surface activity of several antidepressant solutions at pH 6 has been determined by Nambu et al.[201]

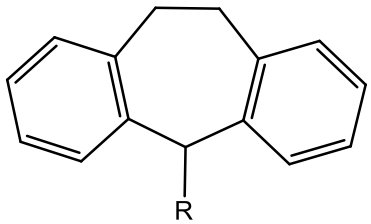

Amitriptyline HCl, R = $-CH(CH_2)_2N(CH_3)_2$
Nortriptyline HCl, R = $-CH(CH_2)_2NHCH_3$
Noxiptioryline HCl, R = $-NO(CH_2)_2N(CH_3)_2$
Butriptioryline HCl, R = $-CH_2{\cdot}CH(CH_3)CH_2N(CH_3)_2$

Fig. 17. Examples of some tricyclic antidepressant drugs with their structures.

5. Antihypertensives:

Only propanolol hydrochloride (Fig. 18) exhibits certain association qualities in the absence of any electrolyte among these medication groups that block the β-adrenoceptor. A limited amount of success was achieved in correlating the efficacy of these medications for local anaesthesia with the β-adrenoceptor blocking compounds derived from the research of surface activity.[202, 203]

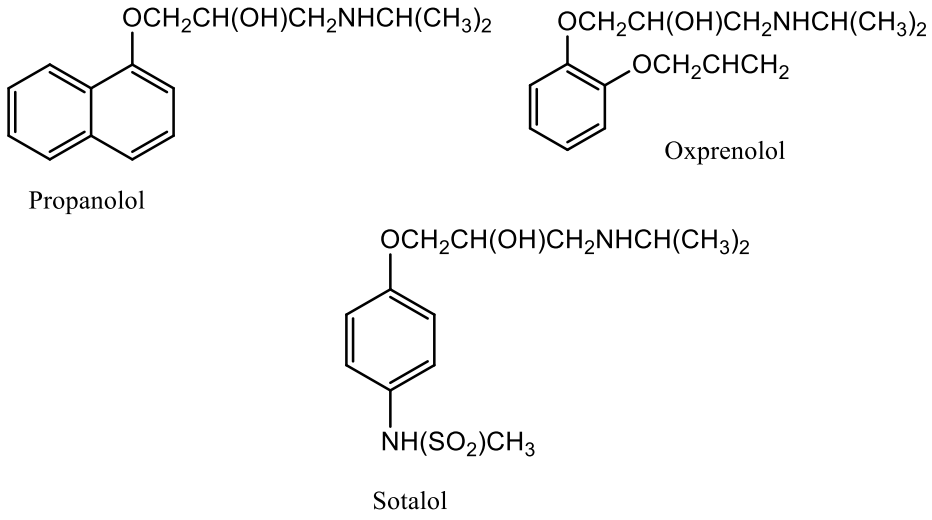

Fig. 18. Structures of some antihypertensive drugs.

6. Local anaesthetics:

The colloidal characteristics of local anaesthetics such as cinchocaine, tetracaine and its higher homologues, and stadacaine have been the subject of several investigations.[204-206] Micellar in nature, the association process is measured by aggregation numbers, which are established through a variety of methods that are correlated with one another. It has been attempted to correlate surface characteristics with local anesthetic effect by measuring the surface activity of local anesthetics. Fig. 19 lists some of their structural details.

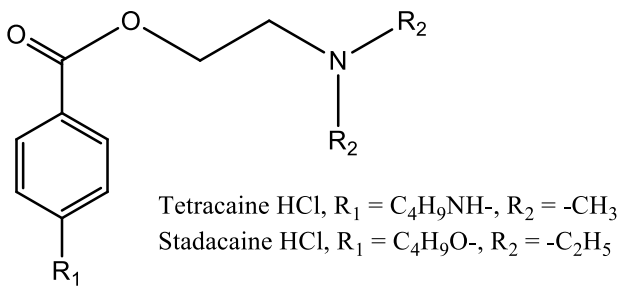

Fig. 19. Some structures of local anesthetic drugs.

7. Antibiotics:

The analysis of the colloidal characteristics of antibiotics (Fig. 20) reveals a complicated outcome because to inaccuracy. This mistake is primarily caused by surface-active contaminants when the drug concentration is lower (below the critical mass concentration). Although quantitative data is not available, Penicillin G (sodium benzyl-penicillin) aggregates very little in aqueous solution, yet their CMC is relatively high.[207, 208] These findings were first derived from surface tension and conductance, and then from the chemical shift of the aromatic Hs by NMR analysis.[209] A conflicting view was discovered between Hauser and Marlowe[210] and Kumler and Alpen,[211] who reported only modest surface activity in the sodium and potassium salts of Penicillin G. In certain samples,[212] which exhibit minimal surface activity, a better purification procedure eliminates highly surface-active impurities of the sodium salt, with the exception of pH values below 4.1.

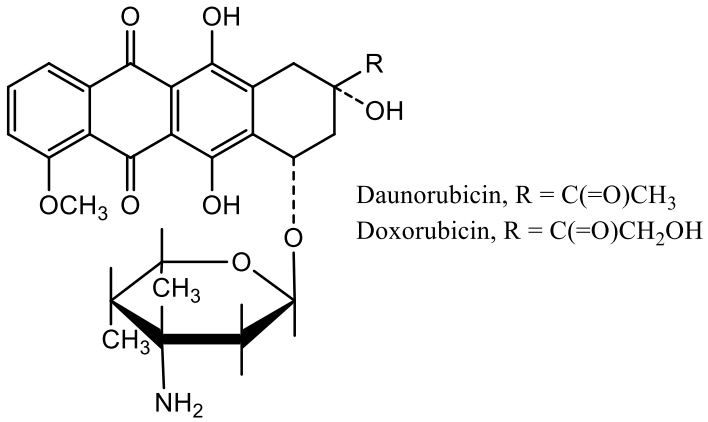

Fig. 20. Some structures of antibiotics.

8. Antibacterials:

Antibacterial drugs have colloidal characteristics, typically attributed to a high concentration of pyridinium or quaternary ammonium cationic surfactants. These chemicals' micelle qualities have been extensively researched, with the goal of establishing a link between surface activity and antibacterial activity. As antibacterials, nonionic surfactants have no effect on bacteria. Cationic dyes, such as methylene blue, proflavine, and acriflavine (Fig. 21), are used as bactericides; Duff and Giles investigated the colloidal characteristics of these dyes.[213]

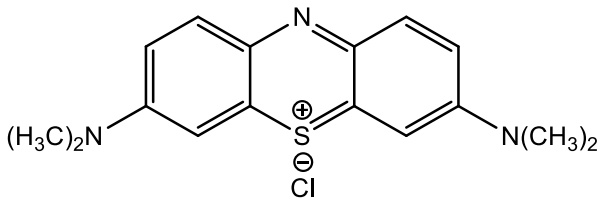

Fig. 21. Methylene blue, a cationic dye having antibacterial activities.

9. Analgesics:

Analgesics are classified according to their colloidal features, which include diphenylmethane or a moiety that is comparable, like methadone and dextropropoxyphene (Fig. 22). The NMR technique is utilized to investigate the hydrophobic interaction in an aqueous solution of these medicines at high concentrations. CMC values range around ~ 0.10 millimole and aggregation number around to 7.[214, 215] Conine provided evidence of their capacity to solubilize organic acids that are only weakly soluble.[216]

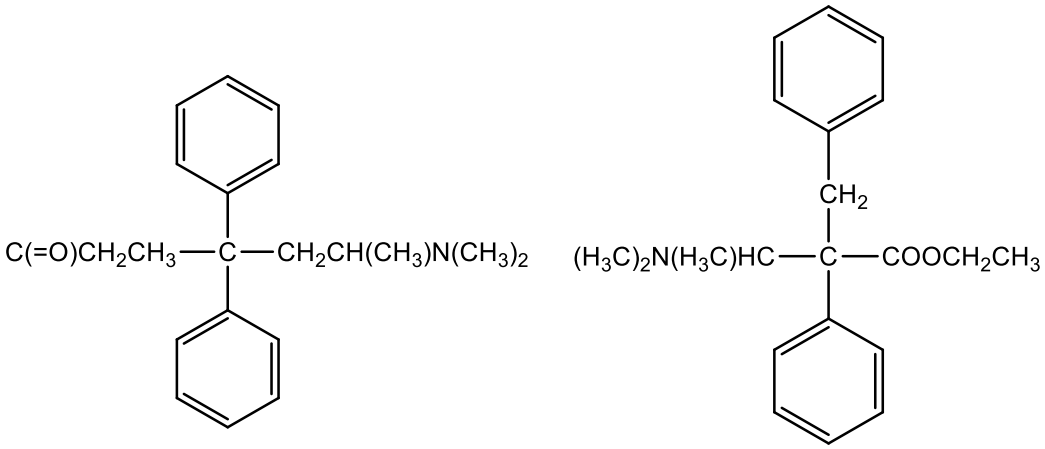

Fig. 22. Structure of methadone and dextropropoxyphene.

10. Xanthones and thioxanthones:

Scholtan studied the colloidal characteristics of 23 derivatives of xanthone and thioxanthone together.[217] They can be distinguished not only by the alkyl chain R, but also by the tricyclic ring substituent (Fig. 23). Generally speaking, thioxanthones have a greater aggregation number than xanthones. Scholtan and Gonnert have demonstrated a correlation between micellar mass and activity of numerous xanthones in the treatment of schistosomiasis.[218]

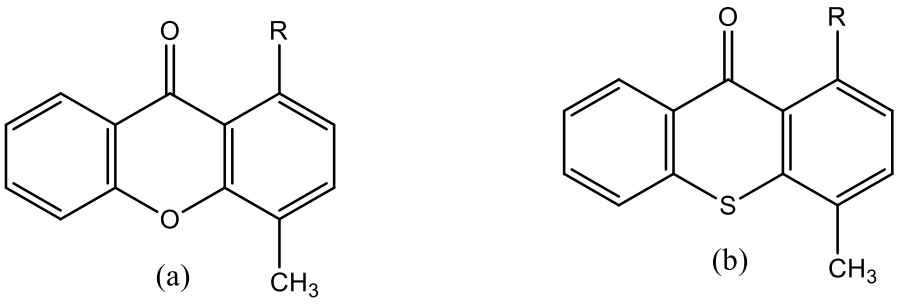

Fig. 23. Structures of (a) Xanthones (b) thioxanthones derivatives.

11. Xanthine derivatives:

Guttman and Higuchi investigated the self-association of various xanthine stimulants, such as ethyl theobromine and many theophylline derivatives (Fig. 24).[219] The results of the NMR analysis indicate that the structurally identical purines, which include the vertical stacking of the monomers, are responsible for the comparable aggregation of the xanthine derivatives.[220] The NMR data has also indicated that the hydrophobic interaction plays a role in self-association.[221] When hydrogen makes bonds with theophylline in non-aqueous (deuterochloroform) solutions, self-association occurred.[222]

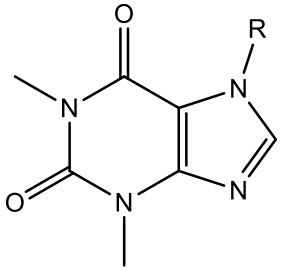

Fig. 24. Structure of theophylline and derivative.

Effect of cosolvent on micellization:

Nonaqueous solvents (e.g., alcohol) have been studied extensively in amphiphile-water-solvent ternary systems, both theoretically and experimentally.[223-231] Alcohols are preferred solvents owing to their high solubility and hydrogen bonding potential.[232] Furthermore, alcohols have the dual property of acting as cosurfactants or cosolvents to affect the critical micelle concentration (CMC) in the self-assembly of amphiphilic systems.[233] Such alcohols operate as cosurfactants at low concentrations, lowering CMC, and as cosolvents at greater concentrations, raising CMC.[234] Increasing the CMC breaks down the water structure in the medium, improving its hydrophobicity. Because of this, it is imperative that attention be paid to two things: the structural characteristics of the aggregates are generated in these media and the requirement for a solvent for amphiphilic assembly. One often used method to overcome these problems is to gradually substitute other polar solvents for water, which exposes a wide variety of polarities. Numerous researches have been conducted using this methodology.

The solvophobic effect controls a solvent's propensity to induce amphiphile self-assembly and may be related to solvent cohesiveness, which may be measured using the Gordon parameter.[235, 236] For binary mixtures, it can be calculated using experimental surface tension data from various homogeneous mixtures. The equation yielded the following Gordon parameters:

$$G = \frac{\gamma_{sol}}{V_m^{\frac{1}{3}}} \qquad (58)$$

where γ_{sol} denotes the combined solvent's surface tension and V_m represents its molar volume. Moyá et al.[237] found that G was linearly dependent on ΔG_m^0, which is consistent with the current experimental findings.

Drug-Surfactant Interaction:

In the pharmaceutical industry, mixed micelle systems have been proven to improve the absorption of different water-insoluble medications in the human body, making them useful drug carriers.[118, 238-241] The majority of medications used as antidepressants, sedatives, local anesthetics, and antibiotics are amphiphilic, like conventional surfactants, and can produce micellar aggregates in water with aggregation numbers ranging from 8 to 10.[242] Pharmacological activity of such medicines demands a concentration far below their CMCs,[243] which are determined in vitro with a small number of drug monomers in aggregated units. Amphiphilic medicines are not advised as

self-carriers because they require a greater drug concentration to form micelle-like aggregates. Sometimes, these amphiphilic medicines are not lipophilic enough to create micelle-like aggregates.[244] Because of their nanosized aggregates, mixed micelles serve as an ideal drug carrier in aqueous medium for directing the medication to specific spots inside tissue, decreasing unwanted drug binding to other locations during drug delivery and eliminating a variety of adverse effects.[245]

Many tricyclic amphiphilic compound with a hydrophobic part as an amino group (e.g., CPZ), has several side effects including antihistamine, cardiovascular, and anticholinergic side effects.[246-248] It also causes phospholipidosis (a physiological disorder of gathering unnecessary intracellular phospholipids)[249] by interacting with the negative phosphate oxygen of the phospholipids found in the body. To mitigate these side effects, phenothiazine medications are frequently combined with a carrier.[250]

Scope and Objective of the present work:

The physicochemical modification of surface-active compounds has gathered significant attention from the surface chemist community in order to improve the effectiveness of surfactant formulations. In this context, various additives have been introduced into the micellar environment of amphiphilic systems to achieve the desired properties with varying industrial importance in food products, cosmetics, enhanced oil recovery, pharmaceuticals, and other fields. These additives include salts, solvents, polymers, drugs, and so on. Using both theoretical and practical methods, nonaqueous alcohol solvents have been the most studied additives in ternary amphiphile-water-solvent systems. The facilitating solubilization and hydrogen bonding capabilities of alcohols set them out as preferred solvents.

Additionally, alcohols have the ability to function as cosurfactants or cosolvents, which can be used as a motif to alter the CMC during the self-assembly of amphiphilic entities. 2,2,2-trifluoroethanol (TFE), a fluorinated alcohol, has been chosen for use in this work because of its high demand as a co-solvent for use in molecular biology, especially during the denaturation of proteins. More significantly, TFE has been well documented in the literature as a means of clarifying the secondary structures of biological macromolecules, such as proteins and polypeptides. The trifluoromethyl (CF_3) group, which withholds electrons, gives TFE its distinct properties as a solvent when compared to other traditional alcohols.

Despite having a hydrophobic $-CF_3$ terminal, TFE has the benefit of being very soluble in water. However, the aggregation of surfactants in TFE solvent has not received much attention.

This dissertation presents a comparative analysis of micellization behavior between nonionic Triton X-114 and traditional cationic sodium dodecyl sulfate (SDS), alongside N-lauroylsarcosine sodium salt (SDDS) surfactants, as well as anionic hexadecyl trimethylammonium bromide (CTAB) and hexadecyl trimethylammonium p-toluenesulfonate (CTAT). The analysis was conducted using a variety of techniques, including tensiometry, steady state and time-resolved fluorimetry, conductometry, and microcalorimetry.

Chlorpromazine (CPZ) is a medicine belonging to the amphiphilic phenothiazine class. It is available under several trade names, such as Thorazine or occasionally, Largactil. Many psychotic diseases, including schizophrenia, are treated with this medication. Before surgery, it is also used to treat anxiety, nausea, vomiting, and bipolar disorder. Phospholipidosis, a physiological condition characterized by the accumulation of excess intracellular phospholipids, is caused by the interaction between the protonated amine group of CPZ and the negative phosphate oxygen of phospholipids found in the body. This tricyclic amphiphilic compound, which has a hydrophobic part as an amino group has a number of side effects, including cardiovascular, antihistamine, and anticholinergic side effects.

Phenothiazine medications are frequently used in conjunction with a carrier (surfactants, polymers, block co-polymers, etc.) to lessen these side effects.

This study focuses on the aggregation behavior of two types of zwitterionic surfactants in the presence of CPZ: a gemini surfactant and a single chain surfactant with the same head group and roughly the same number of carbon atoms in the alkyl. The two surfactants were produced in a lab (refer to the section on the synthesis and characterization of zwitterionic surfactants). A non-spherical structure was seen to develop by zwitterionic gemini surfactant at the ideal concentration of CPZ. Several physicochemical techniques, including tensiometry, steady-state anisotropy, steady-state and time-resolved fluorescence spectroscopy, dynamic light scattering (DLS), confocal microscopy, and transmission electron microscopy (TEM), were used in this study to investigate the micellar aggregates formed by zwitterionic surfactants and CPZ across various stoichiometric mole fractions. Additionally, a number of theoretical models were utilized, such as SPB, Clint, and Rubingh. Here, the parameters have been assessed in light of the properties of the

gemini-drug mixed micelles. They could be useful in comprehending different physicochemical features of drug distribution, solubilization, and other relevant fields.

Cyclodextrins (CDs) are macrocyclic oligosaccharides with α-1,4-glucosidic linkages. In 1891, French scientist Antoine Villiers discovered it as a fermented by-product of potato starch production. Truncated conelike oligosaccharides are classified as α-, β-, or γ-CDs based on the number of D-glucose units. Each has six, seven, or eight α-(1,4) D-glucopyranose units. The oligosaccharide β-cyclodextrin (β-CD) consists of seven glucose units and has a toroidal structure with a hydrophilic outer side. Because of these fascinating features, they can selectively bind some organic molecules into their cavities forming stable host-guest inclusion complexes with exceptional chemical selectivity and enantioselectivity.

Over the past few decades, supramolecular chemistry has focused on CD-based molecular recognition and assembly, primarily because of its exceptional molecular binding capabilities to a wide range of organic and bioactive substrates, both in aqueous solutions and solids. Moreover, other molecular-level nanostructures with unique topological properties, such as catenanes, (pseudo)rotaxanes, supramolecular polymers, crosslinked hydrogels and networks, functionalized nanoparticles, etc., can be formed as a result of CDs self-assembling.

Triton X is a detergent that is widely utilized in enterprises, laboratories, and for research purposes. It can also be used to lyse cells, extracting the organelles and proteins. It is among the components of influenza vaccines that are often utilized. In biochemical applications, Triton X is widely used for solubilizing proteins and retrieving membrane components in mildly nondenaturing conditions. The aggregation behavior of inclusion complexes formed by nonionic Triton X-114 and Triton X-100 with β-CD is compared in this dissertation which can provide an insight into the effect of ethylene oxide (EO) chain length in the process of complex formation.

Bile salts play an important role in the process of fat solubilization during digestion. However, there is one major distinction. The hydrophilic component (concave side) of bile salts is made up of carboxylate ions (-COO) and hydroxyl (-OH) groups, in addition to the steroid ring. According to, there is no clear distinction between their hydrophilic and hydrophobic sections, and their micelles are formed through a process that begins with hydrophobic contact and progresses to hydrogen bonding. When compared to sodium deoxycholate (NaDC), sodium cholate (NaC) possesses an additional -OH group, increasing its water solubility and CMC. The solubilization of

fat-soluble vitamin E is related to the creation of mixed micelles including bile salt, fatty acids, cholesterol, and monoglycerides.

Bile acids have also found applications in supramolecular synthesis and have contributed to the development of photorheological fluids. During the review of the literature, it was observed that the majority of studies investigating the formation of mixed micelles and their subsequent applications in pharmaceuticals concentrate on phospholipids and bile salts. These investigations frequently necessitate the use of organic systems throughout the manufacturing procedure.

So, in this study, the characteristics and aggregation properties of mixed micelles, which are made up of sodium deoxycholate (NaDC)/sodium cholate (NaC) and the conventional non-ionic surfactant Brij-30 were explored. Furthermore, no attempts have been made so far to explore how various stimuli impact the alteration of microstructure in Brij-30 micelles when bile salts are present. Taking into account all these factors, the current study aimed to investigate how bile salts affect the dimensions and structure of Brij-30 micelles under different solution conditions. Interesting results could be obtained by conducting a comprehensive investigation into the micellization and transition of Brij-30 micelles when exposed to two bile salts (NaDC and NaC) and external triggers. This study seeks to conduct thorough examinations of the behavior of mixed micelles composed of aqueous Brij-30 and bile salts. By doing so, it was attempted to enhance comprehension of the molecular interactions that significantly influence the process of fat absorption and other biologically significant processes.

REFERENCES:

1. Rosen, M. J.; Kunjappu, J. T., *Surfactants and interfacial phenomena*. John Wiley & Sons: 2012.
2. Morwind, K.; Koppenhöfer, J. P.; Nüßler, P., Markenführung im Spannungsfeld zwischen Tradition und Innovation: Persil — Da weiß man, was man hat. In *Markenmanagement: Grundfragen der identitätsorientierten Markenführung*, Meffert, H.; Burmann, C.; Koers, M., Eds. Gabler Verlag: Wiesbaden, 2002; pp 477-505.
3. Sakamoto, K.; Lochhead, R. Y.; Maibach, H. I.; Yamashita, Y., *Cosmetic science and technology: theoretical principles and applications*. Elsevier: 2017.
4. Kaczerewska, O.; Martins, R.; Figueiredo, J.; Loureiro, S.; Tedim, J., Environmental behaviour and ecotoxicity of cationic surfactants towards marine organisms. *Journal of Hazardous Materials* **2020,** *392*, 122299.

5. Ali, A.; Farooq, U.; Uzair, S.; Patel, R., Conductometric and tensiometric studies on the mixed micellar systems of surface-active ionic liquid and cationic surfactants in aqueous medium. *Journal of Molecular Liquids* **2016,** *223*, 589-602.
6. Vyas, B.; Pillai, S. A.; Ray, D.; Aswal, V. K.; Wang, M.-R.; Chen, L.-J.; Bahadur, P., Interactions of alkyltriphenyl phosphonium based ionic liquids with block copolymer microstructures: A multitechnique study. *Journal of Molecular Liquids* **2020,** *300*, 112341.
7. Pal, N.; Saxena, N.; Mandal, A., Synthesis, characterization, and physicochemical properties of a series of quaternary gemini surfactants with different spacer lengths. *Colloid and Polymer Science* **2017,** *295* (12), 2261-2277.
8. Saha, A.; Mal, A.; Ghosh, S., An elaborate investigation on the transition of rod-like micelle of cetyltrimethylammonium p-toluenesulfonate in presence of different additives. *Journal of Molecular Liquids* **2020,** *309*, 113084.
9. Das, S.; Ghosh, S.; Das, B., Formation of Mixed Micelle in an Aqueous Mixture of a Surface Active Ionic Liquid and a Conventional Surfactant: Experiment and Modeling. *Journal of Chemical & Engineering Data* **2018,** *63* (10), 3784-3800.
10. Mondal, S.; Pan, A.; Patra, A.; Mitra, R. K.; Ghosh, S., Ionic liquid mediated micelle to vesicle transition of a cationic gemini surfactant: a spectroscopic investigation. *Soft Matter* **2018,** *14* (20), 4185-4193.
11. Kumar, V.; Pal, N.; Jangir, A. K.; Manyala, D. L.; Varade, D.; Mandal, A.; Kuperkar, K., Dynamic interfacial properties and tuning aqueous foamability stabilized by cationic surfactants in terms of their structural hydrophobicity, free drainage and bubble extent. *Colloids and Surfaces A: Physicochemical and Engineering Aspects* **2020,** *588*, 124362.
12. Hossain, K. M. Z.; Calabrese, V.; da Silva, M. A.; Bryant, S. J.; Schmitt, J.; Scott, J. L.; Edler, K. J., Cationic surfactants as a non-covalent linker for oxidised cellulose nanofibrils and starch-based hydrogels. *Carbohydrate Polymers* **2020,** *233*, 115816.
13. Ivanova, A. A.; Cheremisin, A. N.; Barifcani, A.; Iglauer, S.; Phan, C., Molecular insights in the temperature effect on adsorption of cationic surfactants at liquid/liquid interfaces. *Journal of Molecular Liquids* **2020,** *299*, 112104.
14. Kumar, K.; Patial, B. S.; Chauhan, S., Conductivity and fluorescence studies on the micellization properties of sodium cholate and sodium deoxycholate in aqueous medium at different temperatures: Effect of selected amino acids. *The Journal of Chemical Thermodynamics* **2015,** *82*, 25-33.
15. Bordes, R.; Holmberg, K., Amino acid-based surfactants – do they deserve more attention? *Advances in Colloid and Interface Science* **2015,** *222*, 79-91.
16. Mondal, S.; Ghosh, S., Spectroscopic study on the interaction of curcumin with single chain and gemini surfactants. *Chemical Physics Letters* **2021,** *762*, 138144.
17. Hu, R.; Tang, S.; Mpelwa, M.; Jin, L.; Jiang, Z.; Feng, S.; Zheng, Y., Study on the structure–activity relationship between the molecular structure of anionic Gemini surfactants and the rheological properties of their micelle solutions. *Journal of Dispersion Science and Technology* **2022,** *43* (4), 490-500.
18. Singh, V.; Tyagi, R., Physicochemical properties and effect of organic and inorganic electrolytes on surface properties of C12 and C16 alcohol-based bis-sulfosuccinate anionic gemini surfactants. *Colloid and Polymer Science* **2017,** *295* (4), 601-611.
19. Patra, N.; Ray, D.; Aswal, V. K.; Ghosh, S., Exploring Physicochemical Interactions of Different Salts with Sodium N-Dodecanoyl Sarcosinate in Aqueous Solution. *ACS Omega* **2018,** *3* (8), 9256-9266.

20. Saha, P.; Pyne, D. K.; Ghosh, S.; Banerjee, S.; Das, S.; Ghosh, S.; Dutta, P.; Halder, A., Effect of an anionic surfactant (SDS) on the photoluminescence of graphene oxide (GO) in acidic and alkaline medium. *RSC Advances* **2018,** *8* (1), 584-595.
21. Patist, A.; Bhagwat, S. S.; Penfield, K. W.; Aikens, P.; Shah, D. O., On the measurement of critical micelle concentrations of pure and technical-grade nonionic surfactants. *Journal of Surfactants and Detergents* **2000,** *3* (1), 53-58.
22. Pan, A.; Mati, S. S.; Naskar, B.; Bhattacharya, S. C.; Moulik, S. P., Self-Aggregation of MEGA-9 (N-Nonanoyl-N-methyl-d-glucamine) in Aqueous Medium: Physicochemistry of Interfacial and Solution Behaviors with Special Reference to Formation Energetics and Micelle Microenvironment. *The Journal of Physical Chemistry B* **2013,** *117* (25), 7578-7592.
23. Abe, M.; Uchiyama, H.; Yamaguchi, T.; Suzuki, T.; Ogino, K.; Scamehorn, J. F.; Christian, S. D., Micelle formation of pure nonionic surfactants and their mixtures. *Langmuir* **1992,** *8* (9), 2147-2151.
24. Inoue, T.; Yamakawa, H., Micelle formation of nonionic surfactants in a room temperature ionic liquid, 1-butyl-3-methylimidazolium tetrafluoroborate: Surfactant chain length dependence of the critical micelle concentration. *Journal of Colloid and Interface Science* **2011,** *356* (2), 798-802.
25. Yoshimura, T.; Ichinokawa, T.; Kaji, M.; Esumi, K., Synthesis and surface-active properties of sulfobetaine-type zwitterionic gemini surfactants. *Colloids and Surfaces A: Physicochemical and Engineering Aspects* **2006,** *273* (1), 208-212.
26. Kroflič, A.; Šarac, B.; Bešter-Rogač, M., Thermodynamic Characterization of 3-[(3-Cholamidopropyl)-dimethylammonium]-1-propanesulfonate (CHAPS) Micellization Using Isothermal Titration Calorimetry: Temperature, Salt, and pH Dependence. *Langmuir* **2012,** *28* (28), 10363-10371.
27. Banik, R.; Das, S.; Ghosh, A.; Ghosh, S., Comparative studies on the aggregate formation of synthesized zwitterionic gemini and monomeric surfactants in the presence of the amphiphilic antipsychotic drug chlorpromazine hydrochloride in aqueous solution: an experimental and theoretical approach. *Soft Matter* **2023,** *19* (41), 7995-8010.
28. Showell, M., *Handbook of detergents, part D: formulation*. CRC Press: 2016.
29. Kent, J. A., *Riegel's handbook of industrial chemistry*. Springer Science & Business Media: **2012**.
30. Alberts, B.; Johnson, A.; Lewis, J.; Raff, M.; Roberts, K.; Walter, P., The shape and structure of proteins. In *Molecular Biology of the Cell. 4th edition*, Garland Science: **2002**.
31. Maldonado-Valderrama, J.; Wilde, P.; Macierzanka, A.; Mackie, A., The role of bile salts in digestion. *Advances in Colloid and Interface Science* **2011,** *165* (1), 36-46.
32. Veldhuizen, E. J. A.; Haagsman, H. P., Role of pulmonary surfactant components in surface film formation and dynamics. *Biochimica et Biophysica Acta (BBA) - Biomembranes* **2000,** *1467* (2), 255-270.
33. Lin, L.-H.; Lai, Y.-C., Synthesis and physicochemical properties of nonionic gemini surfactants with a sulfonate spacer. *Colloids and Surfaces A: Physicochemical and Engineering Aspects* **2011,** *386* (1), 65-70.
34. Yoshimura, T.; Esumi, K., Synthesis and surface properties of anionic gemini surfactants with amide groups. *Journal of Colloid and Interface Science* **2004,** *276* (1), 231-238.
35. Menger, F. M.; Keiper, J. S.; Azov, V., Gemini Surfactants with Acetylenic Spacers. *Langmuir* **2000,** *16* (5), 2062-2067.

36. Bunton, C. A.; Robinson, L. B.; Schaak, J.; Stam, M. F., Catalysis of nucleophilic substitutions by micelles of dicationic detergents. *The Journal of Organic Chemistry* **1971,** *36* (16), 2346-2350.
37. Menger, F. M.; Keiper, J. S., Gemini Surfactants. *Angewandte Chemie International Edition* **2000,** *39* (11), 1906-1920.
38. Sontake, A. R.; Wagh, S. M., The phase-out of perfluorooctane sulfonate (PFOS) and the global future of aqueous film forming foam (AFFF), innovations in fire fighting foam. *Fire Engineer* **2014,** *39* (3), 19-23.
39. Porter, M. R., *Handbook of surfactants*. Springer: **2013**.
40. Renner, R., The long and the short of perfluorinated replacements. ACS Publications: **2006**.
41. Li, X.; Washenberger, R. M.; Scriven, L. E.; Davis, H. T.; Hill, R. M., Phase Behavior and Microstructure of Water/Trisiloxane E6 and E10 Polyoxyethylene Surfactant/Silicone Oil Systems. *Langmuir* **1999,** *15* (7), 2278-2289.
42. Hill, R. M., *Silicone surfactants*. CRC Press: **1999**; Vol. 86.
43. McBain, J. W., Micellar formation of aqueous solution. *Trans. Faraday Soc* **1913,** *9*, 99-112.
44. Schmid, R., Recent Advances in the Description of the Structure of Water, the Hydrophobic Effect, and the Like-Dissolves-Like Rule. *Monatshefte für Chemie / Chemical Monthly* **2001,** *132* (11), 1295-1326.
45. Sheng, J. J., *Modern chemical enhanced oil recovery: theory and practice*. Gulf Professional Publishing: **2010**.
46. Ray, S.; Moulik, S. P., Dynamics and thermodynamics of aerosol OT-aided nonaqueous microemulsions. *Langmuir* **1994,** *10* (8), 2511-2515.
47. Melo, E. P.; Aires-Barros, M. R.; Cabral, J. M. S., Reverse micelles and protein biotechnology. In *Biotechnology Annual Review*, Elsevier: **2001**; Vol. 7, pp 87-129.
48. Chaurasiya, R. S.; Hebbar, H. U., Reverse Micelles for Nanoparticle Synthesis and Biomolecule Separation. In *Nanoscience in Food and Agriculture 4*, Ranjan, S.; Dasgupta, N.; Lichtfouse, E., Eds. Springer International Publishing: Cham, **2017**; pp 181-211.
49. Mukerjee, P.; Mysels, K. J., *Critical micelle concentrations of aqueous surfactant systems*. US National Bureau of Standards Washington, DC: **1971**; Vol. 36.
50. Anacker, E. W.; Ghose, H. M., Counterions and micelle size. II. Light scattering by solutions of cetylpyridinium salts. *Journal of the American Chemical Society* **1968,** *90* (12), 3161-3166.
51. Lindman, B.; Puyal, M. C.; Kamenka, N.; Brun, B.; Gunnarsson, G., Micelle formation of ionic surfactants. Tracer self-diffusion studies and theoretical calculations for sodium p-octylbenzenesulfonate. *The Journal of Physical Chemistry* **1982,** *86* (9), 1702-1711.
52. Hartley, G. S.; Donnan, F. G., Aqueous solutions of paraffin-chain salts: a study in micelle formation. *(No Title)* **1936**.
53. McBain, J. W.; Salmon, C. S., Colloidal Electrolytes. Soap solutions and their constitution. 2. *Journal of the American Chemical Society* **1920,** *42* (3), 426-460.
54. Shaw, D. J., Introduction to colloid and surface chemistry. **1970**.
55. Menger, F. M., The structure of micelles. *Accounts of Chemical Research* **1979,** *12* (4), 111-117.
56. Debye, P.; Anacker, E. W., Micelle shape from dissymmetry measurements. *The Journal of Physical Chemistry* **1951,** *55* (5), 644-655.
57. Walker, S. A.; Kennedy, M. T.; Zasadzinski, J. A., Encapsulation of bilayer vesicles by self-assembly. *Nature* **1997,** *387* (6628), 61-64.

58. Rothstein, J. P.; Mohammadigoushki, H., Complex flows of viscoelastic wormlike micelle solutions. *Journal of Non-Newtonian Fluid Mechanics* **2020,** *285*, 104382.
59. Tchakalova, V.; Oliveira, C. L. P.; Figueiredo Neto, A. M., New Lyotropic Complex Fluid Structured in Sheets of Ellipsoidal Micelles Solubilizing Fragrance Oils. *ACS Omega* **2023,** *8* (32), 29568-29584.
60. Harkins, W. D.; Mittelmann, R., X-ray investigations of the structure of colloidal electrolytes. IV. A new type of micelle formed by film penetration. *Journal of Colloid Science* **1949,** *4* (4), 367-381.
61. Philippoff, W., Micelles and X-rays. *Journal of Colloid Science* **1950,** *5* (2), 169-191.
62. Israelachvili, J. N.; Mitchell, D. J.; Ninham, B. W., Theory of self-assembly of hydrocarbon amphiphiles into micelles and bilayers. *Journal of the Chemical Society, Faraday Transactions 2: Molecular and Chemical Physics* **1976,** *72* (0), 1525-1568.
63. Israelachvili, J., *Intermolecular and Surface Forces, 3rd Edition*. 2011.
64. Tanford, C., *The hydrophobic effect: formation of micelles and biological membranes 2d ed*. J. Wiley.: 1980.
65. Ghosh, S.; Ray, G. B.; Mondal, S., Physicochemical investigation on the bulk and surface properties of the binary mixtures of N-methyl-N-dodecanoyl sodium glycinate (SDDS) and N-methyl-N-decanoyl glucamine (MEGA 10) in aqueous medium. *Fluid Phase Equilibria* **2015,** *405*, 46-54.
66. Sutherland, E.; Mercer, S. M.; Everist, M.; Leaist, D. G., Diffusion in Solutions of Micelles. What Does Dynamic Light Scattering Measure? *Journal of Chemical & Engineering Data* **2009,** *54* (2), 272-278.
67. Gustafsson, J.; Nylander, T.; Almgren, M.; Ljusberg-Wahren, H., Phase Behavior and Aggregate Structure in Aqueous Mixtures of Sodium Cholate and Glycerol Monooleate. *Journal of Colloid and Interface Science* **1999,** *211* (2), 326-335.
68. Berclaz, N.; Müller, M.; Walde, P.; Luisi, P. L., Growth and Transformation of Vesicles Studied by Ferritin Labeling and Cryotransmission Electron Microscopy. *The Journal of Physical Chemistry B* **2001,** *105* (5), 1056-1064.
69. Tavernier, S. M. F.; Vonk, C. G.; Gijbels, R., Inverted micellar structure determination of zinc di-isohexadecyl zinc sulfonate in isododecane by small-angle X-ray scattering and vapor pressure lowering. *Journal of Colloid and Interface Science* **1981,** *81* (2), 341-353.
70. Pérez, L.; Pinazo, A.; Infante, M. R.; Pons, R., Investigation of the Micellization Process of Single and Gemini Surfactants from Arginine by SAXS, NMR Self-Diffusion, and Light Scattering. *The Journal of Physical Chemistry B* **2007,** *111* (39), 11379-11387.
71. Hayashi, S.; Ikeda, S., Micelle size and shape of sodium dodecyl sulfate in concentrated sodium chloride solutions. *The Journal of Physical Chemistry* **1980,** *84* (7), 744-751.
72. Rafique, A. S.; Khodaparast, S.; Poulos, A. S.; Sharratt, W. N.; Robles, E. S. J.; Cabral, J. T., Micellar structure and transformations in sodium alkylbenzenesulfonate (NaLAS) aqueous solutions: effects of concentration, temperature, and salt. *Soft Matter* **2020,** *16* (33), 7835-7844.
73. Varade, D.; Joshi, T.; Aswal, V. K.; Goyal, P. S.; Hassan, P. A.; Bahadur, P., Effect of salt on the micelles of cetyl pyridinium chloride. *Colloids and Surfaces A: Physicochemical and Engineering Aspects* **2005,** *259* (1), 95-101.
74. Hoffmann, H.; Platz, G.; Rehage, H.; Schorr, W., The influence of the salt concentration on the aggregation behavior of viscoelastic detergents. *Advances in Colloid and Interface Science* **1982,** *17* (1), 275-298.

75. Schmitz, K. S., *Introduction to dynamic light scattering by macromolecules*. Elsevier: 2012.
76. Stetefeld, J.; McKenna, S. A.; Patel, T. R., Dynamic light scattering: a practical guide and applications in biomedical sciences. *Biophysical Reviews* **2016,** *8* (4), 409-427.
77. Pike, E. R., Photon Correlation Velocimetry. In *Photon Correlation Spectroscopy and Velocimetry*, Cummins, H. Z.; Pike, E. R., Eds. Springer US: Boston, MA, 1977; pp 246-343.
78. Chu, B., Laser light scattering. *NASA STI/Recon Technical Report A* **1974,** *75*, 12150.
79. Infelta, P. P., Fluorescence quenching in micellar solutions and its application to the determination of aggregation numbers. *Chemical Physics Letters* **1979,** *61* (1), 88-91.
80. Turro, N. J.; Yekta, A., Luminescent probes for detergent solutions. A simple procedure for determination of the mean aggregation number of micelles. *Journal of the American Chemical Society* **1978,** *100* (18), 5951-5952.
81. Alargova, R. G.; Kochijashky, I. I.; Sierra, M. L.; Zana, R., Micelle Aggregation Numbers of Surfactants in Aqueous Solutions: A Comparison between the Results from Steady-State and Time-Resolved Fluorescence Quenching. *Langmuir* **1998,** *14* (19), 5412-5418.
82. Almgren, M., Diffusion-influenced deactivation processes in the study of surfactant aggregates. *Advances in Colloid and Interface Science* **1992,** *41*, 9-32.
83. Yekta, A.; Aikawa, M.; Turro, N. J., Photoluminescence methods for evaluation of solubilization parameters and dynamics or micellar aggregates. Limiting cases which allow estimation of partition coefficients, aggregation numbers, entrance and exit rates. *Chemical Physics Letters* **1979,** *63* (3), 543-548.
84. Almgren, M.; Leofroth, J. E.; Van Stam, J., Fluorescence decay kinetics in monodisperse confinements with exchange of probes and quenchers. *The Journal of Physical Chemistry* **1986,** *90* (18), 4431-4437.
85. Oliver, R. C.; Lipfert, J.; Fox, D. A.; Lo, R. H.; Doniach, S.; Columbus, L., Dependence of Micelle Size and Shape on Detergent Alkyl Chain Length and Head Group. *PLOS ONE* **2013,** *8* (5), e62488.
86. Tanford, C., Micelle shape and size. *The Journal of Physical Chemistry* **1972,** *76* (21), 3020-3024.
87. Nakahara, H.; Nishino, A.; Tanaka, A.; Fujita, Y.; Shibata, O., Interfacial behavior of gemini surfactants with different spacer lengths in aqueous medium. *Colloid and Polymer Science* **2019,** *297* (2), 183-189.
88. Madenci, D.; Egelhaaf, S. U., Self-assembly in aqueous bile salt solutions. *Current Opinion in Colloid & Interface Science* **2010,** *15* (1), 109-115.
89. Small, D. M., The Physical Chemistry of Cholanic Acids. In *The Bile Acids Chemistry, Physiology, and Metabolism: Volume 1: Chemistry*, Nair, P. P.; Kritchevsky, D., Eds. Springer US: Boston, MA, 1971; pp 249-356.
90. Lianos, P.; Zana, R., Fluorescence probe studies of the effect of concentration on the state of aggregation of surfactants in aqueous solution. *Journal of Colloid and Interface Science* **1981,** *84* (1), 100-107.
91. Zana, R.; Weill, C., Effect of temperature on the aggregation behaviour of nonionic surfactants in aqueous solutions. *J. Physique Lett.* **1985,** *46* (20), 953-960.
92. Evans, H. C., 117. Alkyl sulphates. Part I. Critical micelle concentrations of the sodium salts. *Journal of the Chemical Society (Resumed)* **1956,** (0), 579-586.
93. Scamehorn, J. F., Phenomena in mixed surfactant systems. **1986**.
94. Kavanau, J. L., Structure and Functions of Biological Membranes. *Nature* **1963,** *198* (4880), 525-530.

95. Némethy, G.; Scheraga, H. A., Structure of Water and Hydrophobic Bonding in Proteins. II. Model for the Thermodynamic Properties of Aqueous Solutions of Hydrocarbons. *The Journal of Chemical Physics* **1962,** *36* (12), 3401-3417.
96. Hall, D. G., Thermodynamics of micelle formation. *Nonionic surfactants: physical chemistry, surfactant science series* **1987,** *23*, 233-96.
97. Schick, M. J., *Nonionic surfactants: physical chemistry*. CRC Press: 1987.
98. Moroi, Y., *Micelles: theoretical and applied aspects*. Springer Science & Business Media: 2013.
99. Kresheck, G. C., Comparison of the Calorimetric and van't Hoff Enthalpy of Micelle Formation for a Nonionic Surfactant in H_2O and D_2O Solutions from 15 to 40 °C. *The Journal of Physical Chemistry B* **1998,** *102* (34), 6596-6600.
100. Lah, J.; Pohar, C.; Vesnaver, G., Calorimetric Study of the Micellization of Alkylpyridinium and Alkyltrimethylammonium Bromides in Water. *The Journal of Physical Chemistry B* **2000,** *104* (11), 2522-2526.
101. Majhi, P. R.; Moulik, S. P., Microcalorimetric Investigation of AOT Self-Association in Oil and the State of Pool Water in Water/Oil Microemulsions. *The Journal of Physical Chemistry B* **1999,** *103* (29), 5977-5983.
102. Olofsson, G.; Loh, W., On the use of titration calorimetry to study the association of surfactants in aqueous solutions. *Journal of the Brazilian Chemical Society* **2009,** *20*.
103. Chatterjee, A.; Moulik, S. P.; Sanyal, S. K.; Mishra, B. K.; Puri, P. M., Thermodynamics of Micelle Formation of Ionic Surfactants: A Critical Assessment for Sodium Dodecyl Sulfate, Cetyl Pyridinium Chloride and Dioctyl Sulfosuccinate (Na Salt) by Microcalorimetric, Conductometric, and Tensiometric Measurements. *The Journal of Physical Chemistry B* **2001,** *105* (51), 12823-12831.
104. Moulik, S. P.; Mitra, D., Energetics of Micelle Formation: Non Agreement between the Enthalpy Change Measured by the Direct Method of Calorimetry and the Indirect Method of van't Hoff. In *Recent Trends in Surface and Colloid Science*, WORLD SCIENTIFIC: 2011; Vol. Volume 12, pp 51-68.
105. Enderby, J. E.; Neilson, G. W., Water, a comprehensive treatise. *by F. Franks, Plenum Press, New York* **1979,** *6*, 1.
106. Hait, S. K.; Majhi, P. R.; Blume, A.; Moulik, S. P., A Critical Assessment of Micellization of Sodium Dodecyl Benzene Sulfonate (SDBS) and Its Interaction with Poly(vinyl pyrrolidone) and Hydrophobically Modified Polymers, JR 400 and LM 200. *The Journal of Physical Chemistry B* **2003,** *107* (15), 3650-3658.
107. Hill, T. L., *Thermodynamics of small systems*. Courier Corporation: 1994.
108. Hall, D. G., Thermodynamics of solutions of interacting aggregates by methods similar to surface thermodynamics. Part 3.—Solutions of ionic surfactants in the absence and presence of electrolyte with a common counterion. *Journal of the Chemical Society, Faraday Transactions 2: Molecular and Chemical Physics* **1977,** *73* (7), 897-910.
109. Hall, D. G., Thermodynamics of solutions of interacting aggregates by methods similar to surface thermodynamics. Part 1.—General equations for multi-component systems. *Journal of the Chemical Society, Faraday Transactions 2: Molecular and Chemical Physics* **1972,** *68* (0), 1439-1447.
110. Hall, D. G., Thermodynamics of solutions of ideal multi-component micelles. Part 1. *Transactions of the Faraday Society* **1970,** *66* (0), 1351-1358.

111. Corkill, J. M.; Herrmann, K. W., Solution structure in concentrated non-ionic surfactant systems. *The Journal of Physical Chemistry* **1963,** *67* (4), 934-937.
112. Corhill, J. M.; Goodman, J. F., The interaction of non-ionic surface-active agents with water. *Advances in Colloid and Interface Science* **1969,** *2* (3), 298-330.
113. Corkill, J. M.; Goodman, J. F.; Walker, T.; Wyer, J.; Tabor, D., The multiple equilibrium model of micelle formation. *Proceedings of the Royal Society of London. A. Mathematical and Physical Sciences* **1997,** *312* (1509), 243-255.
114. Tanford, C., Theory of micelle formation in aqueous solutions. *The Journal of Physical Chemistry* **1974,** *78* (24), 2469-2479.
115. Nagarajan, R.; Ruckenstein, E., Critical micelle concentration: A transition point for micellar size distribution: A statistical thermodynamical approach. *Journal of Colloid and Interface Science* **1977,** *60* (2), 221-231.
116. García, M. T.; Ribosa, I.; Sanchez Leal, J.; Comelles, F., Monomer-micelle equilibrium in the diffusion of surfactants in binary systems through collagen films. *Journal of the American Oil Chemists Society* **1992,** *69* (1), 25-29.
117. Kibbey, T. C. G.; Hayes, K. F., A Multicomponent Analysis of the Sorption of Polydisperse Ethoxylated Nonionic Surfactants to Aquifer Materials: Equilibrium Sorption Behavior. *Environmental Science & Technology* **1997,** *31* (4), 1171-1177.
118. Aungst, B. J.; Phang, S., Metabolism of a neurotensin (8–13) analog by intestinal and nasal enzymes, and approaches to stabilize this peptide at these absorption sites. *International Journal of Pharmaceutics* **1995,** *117* (1), 95-100.
119. Noriyuki, M.; Yasuko, N.; Mariko, K.; Shozo, M.; Hitoshi, S., Mechanism for the inducement of the intestinal absorption of poorly absorbed drugs by mixed micelles II. Effect of the incorporation of various lipids on the permeability of liposomal membranes. *International Journal of Pharmaceutics* **1980,** *4* (4), 281-290.
120. Dutta, R.; Ghosh, S.; Banerjee, P.; Kundu, S.; Sarkar, N., Micelle-vesicle-micelle transition in aqueous solution of anionic surfactant and cationic imidazolium surfactants: Alteration of the location of different fluorophores. *Journal of Colloid and Interface Science* **2017,** *490*, 762-773.
121. Mal, A.; Bag, S.; Ghosh, S.; Moulik, S. P., Physicochemistry of CTAB-SDS interacted catanionic micelle-vesicle forming system: An extended exploration. *Colloids and Surfaces A: Physicochemical and Engineering Aspects* **2018,** *553*, 633-644.
122. Bergström, M., Thermodynamics of Vesicle Formation from a Mixture of Anionic and Cationic Surfactants. *Langmuir* **1996,** *12* (10), 2454-2463.
123. Hill, R. M.; Ogino, K.; Abe, M., Mixed surfactant systems. *Surfactant science series* **1993,** *46*, 317.
124. Azum, N.; Rub, M. A.; Asiri, A. M., Bile salt–bile salt interaction in mixed monolayer and mixed micelle formation. *The Journal of Chemical Thermodynamics* **2019,** *128*, 406-414.
125. Azum, N.; Abdul Rub, M.; Asiri, A. M.; Marwani, H. M.; Akram, M., Synergistic interaction between anti-allergic drug and cationic/anionic surfactants–Experimental and theoretical analysis. *Journal of Saudi Chemical Society* **2020,** *24* (9), 683-692.
126. George, A.; Vora, S.; Dogra, A.; Desai, H.; Bahadur, P., Mixed micelles of cationic surfactants and bile acid salts in aqueous media. *Journal of Surfactants and Detergents* **1998,** *1* (4), 507-514.

127. Das, C.; Chakraborty, T.; Ghosh, S.; Das, B., Physicochemistry of mixed micellization: Binary and ternary mixtures of cationic surfactants in aqueous medium. *Colloid Journal* **2010,** *72* (6), 788-798.
128. Mahbub, S.; Rana, S.; Abdul Rub, M.; Hoque, M. A.; Kabir, S. E.; Asiri, A. M., Influence of Alcohol/Temperature on the Interaction of Sodium Dodecyl Sulfate with Cetyltrimethylammonium Bromide: Experimental and Theoretical Study. *Journal of Chemical & Engineering Data* **2019,** *64* (10), 4376-4389.
129. Gandhi, H.; Varade, D.; Bahadur, P., Mixed Micelles of Anionic and Cationic Surfactants in Aqueous Solutions. **2002,** *39* (3), 16-19.
130. Parekh, P.; Varade, D.; Parikh, J.; Bahadur, P., Anionic–cationic mixed surfactant systems: Micellar interaction of sodium dodecyl trioxyethylene sulfate with cationic gemini surfactants. *Colloids and Surfaces A: Physicochemical and Engineering Aspects* **2011,** *385* (1), 111-120.
131. Azum, N.; Naqvi, A. Z.; Akram, M.; Kabir-ud-Din, Studies of mixed micelle formation between cationic gemini and cationic conventional surfactants. *Journal of Colloid and Interface Science* **2008,** *328* (2), 429-435.
132. Moulik, S. P.; Haque, M. E.; Jana, P. K.; Das, A. R., Micellar Properties of Cationic Surfactants in Pure and Mixed States. *The Journal of Physical Chemistry* **1996,** *100* (2), 701-708.
133. Blandamer, M. J.; Briggs, B.; Cullis, P. M.; Engberts, J. B. F. N., Titration microcalorimetry of mixed alkyltrimethylammonium bromide surfactant aqueous solutions. *Physical Chemistry Chemical Physics* **2000,** *2* (22), 5146-5153.
134. Sharma, K. S.; Rodgers, C.; Palepu, R. M.; Rakshit, A. K., Studies of mixed surfactant solutions of cationic dimeric (gemini) surfactant with nonionic surfactant C12E6 in aqueous medium. *Journal of Colloid and Interface Science* **2003,** *268* (2), 482-488.
135. Joshi, T.; Mata, J.; Bahadur, P., Micellization and interaction of anionic and nonionic mixed surfactant systems in water. *Colloids and Surfaces A: Physicochemical and Engineering Aspects* **2005,** *260* (1), 209-215.
136. Ogino, K.; Tsubaki, N.; Abe, M., Solution properties of mixed surfactant system (II): Electric properties of anionic-nonionic surfactants in aqueous solutions. *Journal of Colloid and Interface Science* **1984,** *98* (1), 78-83.
137. Sahu, A.; Choudhury, S.; Bera, A.; Kar, S.; Kumar, S.; Mandal, A., Anionic–Nonionic Mixed Surfactant Systems: Micellar Interaction and Thermodynamic Behavior. *Journal of Dispersion Science and Technology* **2015,** *36* (8), 1156-1169.
138. Mahajan, R. K.; Kaur, N.; Bakshi, M. S., Cyclic voltammetry investigation of the mixed micelles of cationic surfactants with pluronic F68 and TritonX-100. *Colloids and Surfaces A: Physicochemical and Engineering Aspects* **2005,** *255* (1), 33-39.
139. Mandal, A. B.; Ray, S.; Biswas, A. M.; Moulik, S. P., Physicochemical studies on the characterization of Triton X 100 micelles in an aqueous environment and in the presence of additives. *The Journal of Physical Chemistry* **1980,** *84* (8), 856-859.
140. Ćirin, D. M.; Poša, M. M.; Krstonošić, V. S., Interactions between selected bile salts and Triton X-100 or sodium lauryl ether sulfate. *Chemistry Central Journal* **2011,** *5* (1), 89.
141. Thomas, H. G.; Lomakin, A.; Blankschtein, D.; Benedek, G. B., Growth of Mixed Nonionic Micelles. *Langmuir* **1997,** *13* (2), 209-218.
142. Guo, L.; Colby, R. H.; Lin, M. Y.; Dado, G. P., Micellar structure changes in aqueous mixtures of nonionic surfactants. *Journal of Rheology* **2001,** *45* (5), 1223-1243.

143. Ghosh, S.; Chakraborty, T., Mixed Micelle Formation among Anionic Gemini Surfactant (212) and Its Monomer (SDMA) with Conventional Surfactants (C12E5 and C12E8) in Brine Solution at pH 11. *The Journal of Physical Chemistry B* **2007,** *111* (28), 8080-8088.
144. Vashishat, R.; Sanan, R.; Mahajan, R. K., Bile salt-surface active ionic liquid mixtures: mixed micellization and solubilization of phenothiazine. *RSC Advances* **2015,** *5* (88), 72132-72141.
145. Comelles, F.; Ribosa, I.; González, J. J.; Garcia, M. T., Micellization of sodium laurylethoxysulfate (SLES) and short chain imidazolium ionic liquids in aqueous solution. *Journal of Colloid and Interface Science* **2014,** *425*, 44-51.
146. Wang, X.; Wang, R.; Zheng, Y.; Sun, L.; Yu, L.; Jiao, J.; Wang, R., Interaction between Zwitterionic Surface Activity Ionic Liquid and Anionic Surfactant: Na+-Driven Wormlike Micelles. *The Journal of Physical Chemistry B* **2013,** *117* (6), 1886-1895.
147. Kumar, H.; Kaur, G., Effect of changing alkyl chain in imidazolium based ionic liquid on the micellization behavior of anionic surfactant sodium hexadecyl sulfate in aqueous media. *Journal of Dispersion Science and Technology* **2021,** *42* (7), 970-983.
148. Smirnova, N. A.; Vanin, A. A.; Safonova, E. A.; Pukinsky, I. B.; Anufrikov, Y. A.; Makarov, A. L., Self-assembly in aqueous solutions of imidazolium ionic liquids and their mixtures with an anionic surfactant. *Journal of Colloid and Interface Science* **2009,** *336* (2), 793-802.
149. Gu, X.-f.; Huo, J.; Wang, R.-t.; Wu, D.-c.; Yan, Y.-l., Synergism in Mixed Zwitterionic Surface Activity Ionic Liquid and Anionic Surfactant Solution: Analysis of Interfacial and Micellar Behavior. *Journal of Dispersion Science and Technology* **2015,** *36* (3), 334-342.
150. Jafari-Chashmi, P.; Bagheri, A., The strong synergistic interaction between surface active ionic liquid and anionic surfactant in the mixed micelle using the spectrophotometric method. *Journal of Molecular Liquids* **2018,** *269*, 816-823.
151. Saha, U.; Banerjee, A.; Das, B., Drug-surfactant comicellization: Propranolol hydrochloride-surface active ionic liquid systems in aqueous medium. *Journal of Molecular Liquids* **2020,** *309*, 113164.
152. Khan, A. B.; Ali, M.; Malik, N. A.; Ali, A.; Patel, R., Role of 1-methyl-3-octylimidazolium chloride in the micellization behavior of amphiphilic drug amitriptyline hydrochloride. *Colloids and Surfaces B: Biointerfaces* **2013,** *112*, 460-465.
153. Farooq, U.; Patel, R.; Ali, A., Interaction of a Surface-Active Ionic Liquid with an Antidepressant Drug: Micellization and Spectroscopic Studies. *Journal of Solution Chemistry* **2018,** *47* (3), 568-585.
154. Pal, A.; Yadav, A., Mixed micellization of a trisubstituted surface active ionic liquid 1-dodecyl-2,3-dimethylimidazolium chloride [C12bmim][Cl] with an amphiphilic drug amitriptyline hydrochloride AMT: A detailed insights from conductance and surface tension measurements. *Journal of Molecular Liquids* **2019,** *279*, 43-50.
155. Patel, R.; Khan, A. B.; Dohare, N.; Maroof Ali, M.; Rajor, H. K., Mixed Micellization and Interfacial Properties of Ionic Liquid-Type Imidazolium Gemini Surfactant with Amphiphilic Drug Amitriptyline Hydrochloride and its Thermodynamics. *Journal of Surfactants and Detergents* **2015,** *18* (5), 719-728.
156. Qin, L.; Wang, X.-H., Surface adsorption and thermodynamic properties of mixed system of ionic liquid surfactants with cetyltrimethyl ammonium bromide. *RSC Advances* **2017,** *7* (81), 51426-51435.

157. Tiwari, A. K.; Sonu; Saha, S. K., Aggregation behaviour and thermodynamics of mixed micellization of gemini surfactants with a room temperature ionic liquid in water and water-organic solvent mixed media. *The Journal of Chemical Thermodynamics* **2013,** *60*, 29-40.
158. Pal, A.; Punia, R., Effect of chain length and counter-ion on interaction study of mixed micellar system of isoquinoline-based surface active ionic liquid and cationic surfactants in aqueous medium. *Colloid and Polymer Science* **2019,** *297* (11), 1541-1557.
159. Qi, X.; Zhang, X.; Luo, G.; Han, C.; Liu, C.; Zhang, S., Mixing Behavior of Conventional Cationic Surfactants and Ionic Liquid Surfactant 1-Tetradecyl-3-methylimidazolium Bromide ([C14mim]Br) in Aqueous Medium. *Journal of Dispersion Science and Technology* **2013,** *34* (1), 125-133.
160. Pal, A.; Punia, R., Mixed micellization behaviour of tri-substituted surface active ionic liquid and cationic surfactant in aqueous medium and salt solution: Experimental and theoretical study. *Journal of Molecular Liquids* **2019,** *296*, 111831.
161. Luo, G.; Qi, X.; Han, C.; Liu, C.; Gui, J., Salt Effect on Mixed Micelle and Interfacial Properties of Conventional Cationic Surfactants and the Ionic Liquid Surfactant 1-Tetradecyl-3-methylimidazolium Bromide ([C14mim]Br). *Journal of Surfactants and Detergents* **2013,** *16* (4), 531-538.
162. Sharma, R.; Mahajan, S.; Mahajan, R. K., Surface adsorption and mixed micelle formation of surface active ionic liquid in cationic surfactants: Conductivity, surface tension, fluorescence and NMR studies. *Colloids and Surfaces A: Physicochemical and Engineering Aspects* **2013,** *427*, 62-75.
163. Farooq, U.; Ali, A.; Patel, R.; Malik, N. A., Self-aggregation of ionic liquid-cationic surfactant mixed micelles in water and in diethylene glycol–water mixtures: Conductometric, tensiometric, and spectroscopic studies. *Journal of Molecular Liquids* **2017,** *234*, 452-462.
164. Li, N.; Zhang, S.; Ma, H.; Zheng, L., Role of Solubilized Water in Micelles Formed by Triton X-100 in 1-Butyl-3-methylimidazolium Ionic Liquids. *Langmuir* **2010,** *26* (12), 9315-9320.
165. Misono, T.; Okada, K.; Sakai, K.; Abe, M.; Sakai, H., Surface adsorption and micelle formation of polyoxyethylene-type nonionic surfactants in mixtures of water and hydrophilic imidazolium-type ionic liquid. *Journal of oleo science* **2016,** *65* (6), 499-506.
166. Misono, T.; Sakai, H.; Sakai, K.; Abe, M.; Inoue, T., Surface adsorption and aggregate formation of nonionic surfactants in a room temperature ionic liquid, 1-butyl-3-methylimidazolium hexafluorophosphate (bmimPF6). *Journal of Colloid and Interface Science* **2011,** *358* (2), 527-533.
167. Comelles, F.; Ribosa, I.; González, J. J.; Garcia, M. T., Interaction of Nonionic Surfactants and Hydrophilic Ionic Liquids in Aqueous Solutions: Can Short Ionic Liquids Be More Than a Solvent? *Langmuir* **2012,** *28* (41), 14522-14530.
168. Pathan, H.; Patil, R.; Ray, D.; Aswal, V. K.; Bahadur, P.; Tiwari, S., Structural changes in non-ionic surfactant micelles induced by ionic liquids and application thereof for improved solubilization of quercetin. *Journal of Molecular Liquids* **2019,** *290*, 111235.
169. Bhatt, D.; Maheria, K.; Parikh, J., Mixed system of ionic liquid and non-ionic surfactants in aqueous media: Surface and thermodynamic properties. *The Journal of Chemical Thermodynamics* **2014,** *74*, 184-192.
170. Clint, J. H., Micellization of mixed nonionic surface active agents. *Journal of the Chemical Society, Faraday Transactions 1: Physical Chemistry in Condensed Phases* **1975,** *71* (0), 1327-1334.

171. Lange, H.; Beck, K. H., Zur Mizellbildung in Mischlösungen homologer und nichthomologer Tenside. *Kolloid-Zeitschrift und Zeitschrift für Polymere* **1973,** *251* (6), 424-431.
172. Lange, H., Über die Mizellenbildung in Mischlösungen homologer Paraffinkettensalze. *Kolloid-Zeitschrift* **1953,** *131* (2), 96-103.
173. Shinoda, K., The critical micelle concentration of soap mixtures (two-component mixture). *The Journal of Physical Chemistry* **1954,** *58* (7), 541-544.
174. Moroi, Y.; Nishikido, N.; Saito, M.; Matuura, R., The critical micelle concentration of ionic-nonionic detergent mixtures in aqueous solutions. III. *Journal of Colloid and Interface Science* **1975,** *52* (2), 356-363.
175. Rubingh, D. N.; Mittal, K. L., Solution chemistry of surfactants. *vol* **1979,** *1*, 337-354.
176. Rosen, M. J.; Zhao, F., Binary mixtures of surfactants. The effect of structural and microenvironmental factors on molecular interaction at the aqueous solution/air interface. *Journal of Colloid and Interface Science* **1983,** *95* (2), 443-452.
177. Turro, N. J.; Kuo, P. L.; Somasundaran, P.; Wong, K., Surface and bulk interactions of ionic and nonionic surfactants. *The Journal of Physical Chemistry* **1986,** *90* (2), 288-291.
178. Motomura, K.; Yamanaka, M.; Aratono, M., Thermodynamic consideration of the mixed micelle of surfactants. *Colloid and Polymer Science* **1984,** *262* (12), 948-955.
179. Sarmoria, C.; Puvvada, S.; Blankschtein, D., Prediction of critical micelle concentrations of nonideal binary surfactant mixtures. *Langmuir* **1992,** *8* (11), 2690-2697.
180. Puvvada, S.; Blankschtein, D., Thermodynamic description of micellization, phase behavior, and phase separation of aqueous solutions of surfactant mixtures. *The Journal of Physical Chemistry* **1992,** *96* (13), 5567-5579.
181. Desai, T. R.; Dixit, S. G., Interaction and Viscous Properties of Aqueous Solutions of Mixed Cationic and Nonionic Surfactants. *Journal of Colloid and Interface Science* **1996,** *177* (2), 471-477.
182. Makayssi, A.; Bury, R.; Treiner, C., Thermodynamics of micellar solubilization for 1-pentanol in weakly interacting binary cationic surfactant mixtures of 25. degree. C. *Langmuir* **1994,** *10* (5), 1359-1365.
183. Kato, T.; Takeuchi, H.; Seimiya, T., Change in size and composition of mixed micelles with concentration in anionic/cationic surfactant solutions. *Journal of colloid and interface science* **1990,** *140* (1), 253-257.
184. Tokiwa, F., Solubilization behavior of mixed surfactant micelles in connection with their zeta potentials. *Journal of Colloid and Interface Science* **1968,** *28* (1), 145-148.
185. Shinoda, K., The effect of alcohols on the critical micelle concentrations of fatty acid soaps and the critical micelle concentration of soap mixtures. *The Journal of Physical Chemistry* **1954,** *58* (12), 1136-1141.
186. Tokiwa, F.; Ohki, K.; Kokubo, I., Gel Filtration of Mixtures of Surfactants on Sephadex. *Bulletin of the Chemical Society of Japan* **1968,** *41* (12), 2845-2848.
187. Barry, B. W.; Morrison, J. C.; Russell, G. F. J., Prediction of the critical micelle concentration of mixtures of alkyltrimethylammonium salts. *Journal of Colloid and Interface Science* **1970,** *33* (4), 554-561.
188. Schick, M. J.; Manning, D. J., Micelle formation in mixtures of nonionic and anionic detergents. *Journal of the American Oil Chemists Society* **1966,** *43* (3), 133-136.
189. Corkill, J. M.; Goodman, J. F.; Tate, J. R., Micellization in mixtures of anionic and non-ionic detergents. *Transactions of the Faraday Society* **1964,** *60*, 986-995.

190. Kuriyama, K., Temperature dependence of micellar weight of non-ionic surfactant in the presence of various additives. *Kolloid-Zeitschrift und Zeitschrift für Polymere* **1962,** *180* (1), 55-64.
191. Sugihara, G.; Mukerjee, P., High-pressure study of micelle formation in aqueous solutions of sodium perfluorooctanoate. *The Journal of Physical Chemistry* **1981,** *85* (11), 1612-1616.
192. Muller, N.; Simsohn, H., Investigation of micelle structure by fluorine magnetic resonance. V. Sodium perfluorooctanoate. *The Journal of Physical Chemistry* **1971,** *75* (7), 942-945.
193. Turro, N. J.; Lee, P. C. C., Perfluorinated" mini" micelles: energy transfer from benzophenone and determination of aggregation number. *The Journal of Physical Chemistry* **1982,** *86* (17), 3367-3371.
194. Attwood, D., Micelle formation by some antihistamines in aqueous solution. *Journal of Pharmacy and Pharmacology* **1972,** *24* (9), 751-752.
195. Mukerjee, P., Micellar properties of drugs: Micellar and nonmicellar patterns of self-association of hydrophobic solutes of different molecular structures — monomer fraction, availability, and misuses of micellar hypothesis. *Journal of Pharmaceutical Sciences* **1974,** *63* (6), 972-981.
196. Farhadieh, B.; Hall, N. A.; Hammarlund, E. R., Aggregation of Certain Medicinal Amines in Aqueous Solutions of Their Salts. *Journal of Pharmaceutical Sciences* **1967,** *56* (1), 18-23.
197. Attwood, D.; Udeala, O. K., Aggregation of antihistamines in aqueous solution. Self-association of some pyridine derivatives. *The Journal of Physical Chemistry* **1975,** *79* (9), 889-892.
198. Attwood, D., Aggregation of antiacetylcholme drugs in aqueous solution: micellar properties of some diphenylmethane derivatives. *Journal of Pharmacy and Pharmacology* **1976,** *28* (5), 407-409.
199. Attwood, D.; Florence, A. T.; Gillan, J. M. N., Micellar properties of drugs: Properties of micellar aggregates of phenothiazines and their aqueous solutions. *Journal of Pharmaceutical Sciences* **1974,** *63* (6), 988-993.
200. Attwood, D.; Gibson, J., Aggregation of antidepressant drugs in aqueous solution. *Journal of Pharmacy and Pharmacology* **1978,** *30* (1), 176-180.
201. Nambu, N.; Sakurai, S.; Nagai, T., Adsorption from Solution, Permeation through Cellulose Membrane, Partition Coefficient and Surface Tension of Several Antidepressants and Phenothiazines. *Chem. Pharm. Bull* **1975,** *23* (7), 1404-1410.
202. Levy, J. V., Surface tension effects of β-adrenergic blocking drugs. *Journal of Pharmacy and Pharmacology* **1968,** *20* (10), 813-815.
203. Hellenbrecht, D.; Lemmer, B.; Wiethold, G.; Grobecker, H., Measurement of hydrophobicity, surface activity, local anaesthesia, and myocardial conduction velocity as quantitative parameters of the non-specific membrane affinity of nine β-adrenergic blocking agents. *Naunyn-Schmiedeberg's Archives of Pharmacology* **1973,** *277* (2), 211-226.
204. Eckert, T.; Kilb, E.; Hoffmann, H., Über Molekülassoziationen des Cinchocain (Percain ®) und seiner höheren Homologen Beiträge zur Frage der Wirkung bei höheren Homologen oberflächenanästhetisch wirksamer Reihen; 1. Mitt. *Archiv der Pharmazie* **1964,** *297* (1), 31-39.
205. Johnson, E. M.; Ludlum, D. B., Aggregation of local anesthetics in solution. *Biochemical pharmacology* **1969,** *18* (11), 2675-2677.
206. Jaenicke, R., Bestimmung des Mizellgewichts von Assoziationskolloiden in der Ultrazentrifuge. *Kolloid-Zeitschrift und Zeitschrift für Polymere* **1966,** *212* (1), 36-45.

207. Hocking, C. S., Light-scattering Studies on Penicillin G Solutions. *Nature* **1951,** *168* (4271), 423-424.
208. Hauser, E. A.; Phillips, R. G.; Phillips, J. W., Penicillin and Streptomycin. *Science* **1947,** *106* (2764), 616-616.
209. Thakkar, A. L.; Wilham, W. L., Self-association of benzylpenicillin in aqueous solution: 1 H nuclear magnetic resonance study. *Journal of the Chemical Society D: Chemical Communications* **1971,** (7), 320-322.
210. Hauser, E. A.; Marlowe, G. J., The Colloidal Phenomena of Antibiotics. *The Journal of Physical Chemistry* **1950,** *54* (8), 1077-1087.
211. Kumler, W. D.; Alpen, E. L., Surface Tension and Conductivity of Penicillin Salts. *Science* **1948,** *107* (2787), 567-567.
212. Few, A. V.; Schulman, J. H., On the surface chemistry of sodium penicillin G. *Biochimica et Biophysica Acta* **1953,** *10*, 302-310.
213. Duff, D. G.; Giles, C. H., Dyestuffs. In *Water A Comprehensive Treatise: Aqueous Solutions of Amphiphiles and Macromolecules*, Franks, F., Ed. Springer US: Boston, MA, 1975; pp 169-207.
214. Attwood, D.; Tolley, J. A., Self-association of analgesics in aqueous solution: micellar properties of dextropropoxyphene hydrochloride and methadone hydrochloride. *Journal of Pharmacy and Pharmacology* **1980,** *32* (1), 533-536.
215. Perrin, J. H.; Wilham, W. L.; Thakkar, A. L., Aggregation of (+)-propoxyphene hydrochloride in aqueous solution: circular dichroism measurements. *Journal of Pharmacy and Pharmacology* **1972,** *24* (3), 257-259.
216. Conine, J. W., Drugs as Solubilizing Agents: Solubilization of Acids by Water-Soluble Amine Salts. *Journal of Pharmaceutical Sciences* **1965,** *54* (11), 1580-1585.
217. Scholtan, W., Kolloidchemische Eigenschaften von Salzen basisch substituierter Xanthon- und Thioxanthonderivate. *Kolloid-Zeitschrift* **1960,** *170*, 19-29.
218. Scholtan, W.; Gönnert, R., The relation between weight of micelles and the biological activity of xanthones and thioxanthones effective against bilharziasis. *Med. Chem. Abhandl. Med.-Chem. Forschungsstätten Farbenfabriken Bayer* **1956,** *5*, 314.
219. Bolton, S.; Guttman, D.; Higuchi, T., Complexes Formed in Solution by Homologs of Caffeine.**School of Pharmacy, University of Wisconsin, Madison: Interactions Between p-Hydroxybenzoic Acid and Ethyl, Propyl, and Butyl Derivatives of Theobromine, and Theophylline. *Journal of the American Pharmaceutical Association (Scientific ed.)* **1957,** *46* (1), 38-41.
220. Sinanoglu, O., Molecular Associations in Biology. *Academic Press, New York, NY* **1968**, 427-445.
221. Thakkar, A. L.; Tensmeyer, L. G.; Wilham, W. L., NMR evidence for self-association of theophylline in aqueous solution. *Journal of Pharmaceutical Sciences* **1971,** *60* (8), 1267-1269.
222. Soon, N. G., An Infrared Study of the Interaction of Caffeine and Theophylline with 9-Ethyladenine in Chloroform Solution. *Molecular Pharmacology* **1971,** *7* (2), 177.
223. Rauniyar, B. S.; Bhattarai, A., Study of conductivity, contact angle and surface free energy of anionic (SDS, AOT) and cationic (CTAB) surfactants in water and isopropanol mixture. *Journal of Molecular Liquids* **2021,** *323*, 114604.
224. Sheng, R.; Ding, Q. Y.; Ren, Z. H.; Li, D. N.; Fan, S. C.; Cai, L. L.; Quan, X. F.; Wang, Y.; Yi, M. T.; Zhang, Y. X.; Cao, Y. X.; Wang, H.; Wang, J. R.; Zhang, Q. H.; Qian, Z.

B., Interfacial and micellization behavior of binary mixture of amino sulfonate amphoteric surfactant and octadecyltrimethyl ammonium bromide: Effect of short chain alcohol and its chain length. *Journal of Molecular Liquids* **2021,** *334*, 116064.
225. Devi, Y. G.; Gurung, J.; Pulikkal, A. K., Micellar Solution Behavior of Cetylpyridinium Surfactants in 2-Propanol–Water Mixed Media at Different Temperatures. *Journal of Chemical & Engineering Data* **2021,** *66* (1), 368-378.
226. Üner, O.; Akkurt, N., Micellization and thermodynamics study of n-alkyl-4-methylpyridinium bromides in water and mixed water–ethanol media. *Journal of Molecular Liquids* **2022,** *352*, 118765.
227. Kumar, V.; Verma, R.; Satodia, D.; Ray, D.; Kuperkar, K.; Aswal, V. K.; Mitchell-Koch, K. R.; Bahadur, P., Contrasting effect of 1-butanol and 1,4-butanediol on the triggered micellar self-assemblies of C16-type cationic surfactants. *Physical Chemistry Chemical Physics* **2021,** *23* (35), 19680-19692.
228. Basnet, N.; Prasai, S.; Dominguez, H.; Ríos-López, M.; Adhikari, R.; Ghimire, M. P.; Bhattarai, A., Conductance Study of Aerosol-OT in Binary Mixed Solvents of Short-Chain Alcohol–Water Systems at Various Temperatures. *Journal of Chemical & Engineering Data* **2021,** *66* (1), 65-78.
229. Dutta, A.; Joy, M. T. R.; Ahsan, S. M. A.; Gatasheh, M. K.; Kumar, D.; Abdul Rub, M.; Anamul Hoque, M.; Majibur Rahman, M.; Hoda, N.; Islam, D. M. S., Physico-chemical parameters for the assembly of moxifloxacin hydrochloride and cetyltrimethylammonium chloride mixture in aqueous and alcoholic media. *Chinese Journal of Chemical Engineering* **2023,** *57*, 280-289.
230. Keshvarinezhad, M.; Ebrahimi, N.; Sadeghi, R., Liquid–Liquid Demixing Behavior of Aqueous 1-Butanol Solutions in the Presence of Various Organic and Inorganic Ammonium Salts: Effect of Temperature, Cation Alkyl Chain Length, and Anion Type of Salts on Salting Coefficients and Thermodynamic Functions. *Journal of Chemical & Engineering Data* **2023,** *68* (7), 1728-1738.
231. Lu, J.; González de Castilla, A.; Müller, S.; Xi, S.; Chapman, W. G., Dualistic Role of Alcohol in Micelle Formation and Structure from iSAFT Based Density Functional Theory and COSMOplex. *Industrial & Engineering Chemistry Research* **2023,** *62* (4), 1968-1983.
232. Ghosh, R.; Parida, C.; Chowdhuri, S., Hydrogen bonding behavior of ethanol-trifluoroethanol binary mixtures and its effects on the water structure and dynamics in ternary aqueous-ethanol-trifluoroethanol solutions. *Chemical Physics* **2023,** *572*, 111956.
233. Sharma, K.; Negi, S.; Kishore, K., Ultrasonic velocity and critical micellar concentration of glycerol monostearate in mixed organic solvent at 290 K. *Journal of surface science and technology* **2019**, 17-25.
234. Zana, R., Aqueous surfactant-alcohol systems: A review. *Advances in Colloid and Interface Science* **1995,** *57*, 1-64.
235. Gordon, J. E., *Organic chemistry of electrolyte solutions*. 1975.
236. Banik, R.; Mondal, B. B.; Sardar, R.; Ghosh, S., Comparative Study of the Aggregation Behavior of Some Ionic Surfactants with Nonionic Triton X-114 in Water and a Water/2,2,2-Trifluoroethanol Mixture. *Industrial & Engineering Chemistry Research* **2024,** *63* (7), 3057-3071.
237. Rodríguez, A.; del Mar Graciani, M.; Angulo, M.; Moyá, M. L., Effects of Organic Solvent Addition on the Aggregation and Micellar Growth of Cationic Dimeric Surfactant 12-3-12,2Br. *Langmuir* **2007,** *23* (23), 11496-11505.

238. Kumar, M.; Singh, V.; Choudhary, R.; kumar deb, D.; Singh, S.; Srivastava, A., Mixed Micellization of drug-excipients and its application to enhance the binding and encapsulation efficacy of ibuprofen in aqueous media. *Colloids and Surfaces A: Physicochemical and Engineering Aspects* **2021,** *628*, 127268.
239. Kumar, M.; Raj, S.; Thapa, U.; Singh, S.; Srivastava, A., Investigation the effect of sodium carboxymethylcellulose as polycounterion on cetirizine hydrochloride–sodium dodecyl sulphate mixed micelle. *Journal of Molecular Liquids* **2021,** *322*, 114973.
240. Kumar, M.; Khushi, K.; Bhardwaj, A.; Deb, D. K.; Singh, N.; Elahi, D.; Sharma, S.; Bajpai, G.; Srivastava, A., In-vitro study for Ibuprofen encapsulation, controlled release and cytotoxicity improvement using excipient-drugs mixed micelle. *Colloids and Surfaces A: Physicochemical and Engineering Aspects* **2022,** *654*, 130057.
241. Noriyuki, M.; Mariko, K.; Yasuko, N.; Shozo, M.; Hitoshi, S., Mechanism for the inducement of the intestinal absorption of poorly absorbed drugs by mixed micelles I. Effects of various lipid—bile salt mixed micelles on the intestinal absorption of streptomycin in rat. *International Journal of Pharmaceutics* **1980,** *4* (4), 271-279.
242. Attwood, D., *Surfactant systems: their chemistry, pharmacy and biology*. Springer Science & Business Media: 2012.
243. Attwood, D., The mode of association of amphiphilic drugs in aqueous solution. *Advances in Colloid and Interface Science* **1995,** *55*, 271-303.
244. Krishnadas, A.; Rubinstein, I.; Önyüksel, H., Sterically Stabilized Phospholipid Mixed Micelles: In Vitro Evaluation as a Novel Carrier for Water-Insoluble Drugs. *Pharmaceutical Research* **2003,** *20* (2), 297-302.
245. Lawrence, M. J.; Rees, G. D., Microemulsion-based media as novel drug delivery systems. *Advanced Drug Delivery Reviews* **2000,** *45* (1), 89-121.
246. Halliwell, W. H., Cationic Amphiphilic Drug-Induced Phospholipidosis. *Toxicologic Pathology* **1997,** *25* (1), 53-60.
247. Barbosa, L. R. S.; Itri, R.; Caetano, W.; de Sousa Neto, D.; Tabak, M., Self-Assembling of Phenothiazine Compounds Investigated by Small-Angle X-ray Scattering and Electron Paramagnetic Resonance Spectroscopy. *The Journal of Physical Chemistry B* **2008,** *112* (14), 4261-4269.
248. Glaser, E. M.; Newling, P. S. B., Side effects of chlorpromazine hydrochloride. *British Journal of Pharmacology and Chemotherapy* **1955,** *10* (4), 429.
249. Azum, N.; Rub, M. A.; Asiri, A. M., Energetics of Clouding Phenomenon in Amphiphilic Drug Imipramine Hydrochloride with Pharmaceutical Excipients. *Pharmaceutical Chemistry Journal* **2014,** *48* (3), 201-208.
250. Azum, N.; Rub, M. A.; Asiri, A. M.; Kashmery, H. A., Synergistic effect of an antipsychotic drug chlorpromazine hydrochloride with pluronic triblock copolymer: A physicochemical study. *Journal of Molecular Liquids* **2018,** *260*, 159-165.

Chapter-I

Comparative Studies on the aggregate formation of synthesized zwitterionic gemini and monomeric surfactants in the presence of amphiphilic antipsychotic drug chlorpromazine hydrochloride in aqueous solution: an experimental and theoretical approach

Comparative Studies on the aggregate formation of synthesized zwitterionic gemini and monomeric surfactants in the presence of amphiphilic antipsychotic drug chlorpromazine hydrochloride in aqueous solution: an experimental and theoretical approach ‡

Abstract

The formation of aggregates, which are widely used in the field of biochemistry and the medical industry, was formed and studied with different compositions of alkyl betaine gemini surfactants (C_{14}Ab) in conjugation with chlorpromazine hydrochloride (CPZ). The result was compared with a single-chain zwitterionic surfactant (C_{12}DmCB) of the same type with CPZ. Dynamic light scattering (DLS), confocal laser scanning microscopy (CLSM), and transmission electron microscopy (TEM) methods were used to distinguish the aggregates for CPZ/C_{14}Ab system in aqueous solutions above a certain mole fraction of the drug CPZ ($\alpha_{CPZ} = 0.2$). Time-resolved fluorescence decay measurements of acridine orange determine relative polarity near the headgroup regions of mixed micelle (CPZ/C_{14}Ab and CPZ/C_{12}DmCB) systems. The hydrophilic environment around the headgroup regions of the CPZ/C_{14}Ab system is different from the head group regions of the CPZ/C_{12}DmCB system. On the other hand, several theoretical studies have been employed (Clint, Rubingh, Motomura, and SPB) on mixed micellar systems to elucidate the different interaction parameters. Such systematic study of a zwitterionic gemini amphiphile and their interaction with other amphiphiles and an amphiphilic drug molecule is rare in the literature.

(‡ Published in *Soft Matter, 2023, 19 (41), 7995-8010*)

1. Introduction

Surfactants offer a fascinating range of applications in industry and daily life due to their amphiphilic properties.[1-4] The fundamental benefit of an amphiphilic molecule, which has dual solubility due to its structural properties (polar 'head' and nonpolar hydrocarbon chain), is preferential adsorption at the interface at low concentrations. Beyond a critical concentration, the hydrophobic 'tail' of the amphiphile separates from the solvent by self-aggregation, leading to the formation of nano-aggregates largely known as micelles.[5-7] This type of favorable interaction, known as the hydrophobic effect, minimizes the unfavorable contacts between hydrocarbons and water and releases the polar water molecules in bulk, leading to an increase in the entropy of the system by destroying the so-called 'iceberg structure' of water.[8, 9] The critical amphiphile concentration mandatory for the commencement of the formation of an aggregated assembly, referred generally to as a micelle, is called the critical micellar concentration (*cmc*).[10, 11] Mixed

micellar systems can consist of two or more types of amphiphiles available in the literature [5-7, 12-16] and belong to any combination of anionic, cationic, nonionic, and zwitterionic surfactants. Mixed surfactant systems almost always show an improvement in interfacial properties (e.g., lower *cmc*, greater surface activity, etc.) compared to their individual components.[13, 17] This behaviour of mixed surfactants allows their use at low concentrations in the cosmetics industry to avoid potential skin irritation.[12, 18, 19] The use of mixed surfactants in low concentration also significantly reduces the release to the environment compared to their individual components in mixed state, since a low concentration of mixed surfactants is necessary for the desired effect and therefore beneficial to the environment.[20] In the pharmaceutical field, mixed micelles have been shown to enhance the absorption of various water-insoluble drugs in the human body, as mixed micelle systems have been effectively used as effective drug carriers.[21-25] Most drugs commonly used as local anesthetics, antidepressants, sedatives, and antibiotics are amphiphilic, like conventional surfactants, and can form micellar aggregates in water with an aggregation number of 8 - 10.[26] The pharmacologic activity of these drugs requires a concentration well below their *cmc*s,[27] which are measured in vitro with a negligible number of drug monomers in the aggregated units. The use of amphiphilic drugs as self-carriers is not recommended because a higher drug concentration is required to form their micelle-like aggregates. Sometimes these amphiphilic drugs are not as lipophilic as required to form micelle-like aggregates.[28] Mixed micelles act as an appropriate drug carrier in aqueous medium for targeting the drug to specific sites within tissue due to their nanosized aggregate, reducing undesirable binding of drug to the other site during drug delivery and preventing numerous side effects.[29]

Gemini surfactants are the special class of surfactants studied extensively in recent times. These are composed by two amphiphilic segments connected by a spacer at or near the head group of individual amphiphiles.[30-32] Among the various studied gemini surfactants, cationic geminis have been extensively studied over anionic and non-ionic geminis as cationic gemini surfactants can be easily prepared in the laboratory and are also important from an industrial and pharmaceutical point of view.[33-37,41] Synthesis of zwitterionic gemini surfactants is found as a great difficulty in comparison with the other geminis. These types of surfactants have no counterions and also their structures contain the same number of positive and negative charges.[31] Due to their less skin-irritating, biocompatible, and other qualities, zwitterionic gemini surfactants are often used in drug delivery systems, clinical treatments, chemical compound analyses, and other applications[38-40]. Till

date, very few reports have been documented regarding the systematic study of zwitterionic gemini surfactants and their interaction with other surfactants in the literature.[31,38-40]

Chlorpromazine (CPZ, Figure 1), an amphiphilic phenothiazine class drug,[42] is sold in the market with the trade name 'Thorazine' or sometimes 'Largactil' among others. This drug is widely used to treat psychotic disorders, especially schizophrenia. It is also used to treat bipolar disorder, nausea, vomiting, and anxiety before surgery. This tricyclic amphiphilic compound containing a hydrophobic part as an amino group (Figure 1) has several side effects including cardiovascular, antihistamine and anticholinergic side effects[42-44] and brings phospholipidosis (a physiological condition of gathering excessive intracellular phospholipids)[45] due to the interaction of negative phosphate oxygen of the phospholipids found in the body with the protonated amine group of CPZ. To reduce these side effects, phenothiazine drugs are often used with a carrier (surfactants, polymers, block co-polymers etc.).[46]

The present study is mainly concerned with the aggregation behaviour of a gemini zwitterionic surfactant and a single chain zwitterionic surfactant having the same head group and more or less the same number of carbon atoms in the alkyl chain (Figure 1), in the presence of CPZ. Both surfactants were synthesized in the laboratory (see the Synthesis section). At an optimal concentration of CPZ, the formation of a non-spherical structure of zwitterionic gemini was observed. To understand the micellar aggregates at different stoichiometric mole fractions of zwitterionic surfactants and CPZ, various physicochemical techniques, such as tensiometry, steady-state and time-resolved fluorescence spectroscopy, steady-state anisotropy, confocal microscopy, dynamic light scattering (DLS), and transmission electron microscopy (TEM) were used in this study. Several theoretical models, including Clint, Rubingh, and SPB were also used. The understanding of the detailed parameters has been evaluated here on the characteristics of gemini-drug mixed micelles which may be applied to solubilization, drug delivery, and other areas of interest.

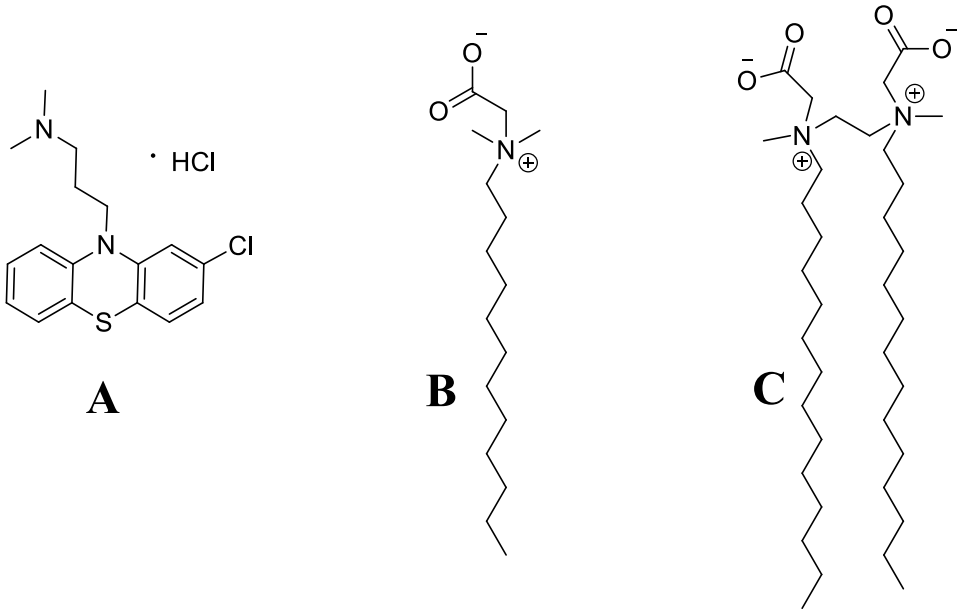

Figure. 1 Chemical structure of (A) Chlorpromazine hydrochloride (CPZ), (B) N-Dodecyl-N, N-dimethyl-2-ammonio-1-ethanecarbonate (C_{12}DmCB) and (C) 1, 2-bis[N-methyl-N-carboxymethyl tetradecylammonium] ethane (C_{14}Ab).

2. Experimental Procedures

2.1. Materials and instruments

N, N′-Dimethyldodecylamine (purity > 96%) was purchased from TCI Chemicals, and sodium chloroacetate (purity > 98%) from Sigma Aldrich and were used for the synthesis of zwitterionic surfactant (**1**). N, N′-Dimethylethylenediamine (purity > 99%), bromoacetic acid (purity > 98%), and 1-bromotetradecane (purity > 96%) were purchased from Spectrochem, India for the synthesis of zwitterionic gemini surfactant (**2**). Drug CPZ hydrochloride (≥ 98%) was purchased from Merck, India. Acridine orange hydrochloride (≥ 98%) was purchased from Merck, India. For the preparation and purification of synthesized surfactants, dry acetone, ethyl acetate, methanol, ethanol, and NaOH were used and purchased from Merck, India. The synthesized surfactants were characterized by FTIR and ^{1}H NMR. The IR spectra were recorded on a Perkin Elmer Spectrum-Two FT-IR spectrometer using KBr pallets. ^{1}H NMR spectra were recorded in $CDCl_3$ and CD_3OD

solutions at 500 MHz/ 400 MHz on a Bruker AC-500/ Brucker DPX-400 spectrometer using tetramethylsilane as an internal standard.

2.2. Synthesis and characterisation of zwitterionic surfactants

The detail steps of synthesis and characterisation of zwitterionic surfactants were represented in the supplementary information section.

2.3. Solution preparation for mixed-micelle

A stock solution of C_{12}DmCB, C_{14}Ab and CPZ was prepared using distilled water at 50.0, 5.0, 200.0 mmol L^{-1} respectively. Mixed micelle solutions for CPZ/ C_{12}DmCB and CPZ/ C_{14}Ab systems of various mole fractions at a particular total mixture concentration were prepared. Here, the mole fractions of CPZ, C_{12}DmCB and C_{14}Ab are denoted as α_{CPZ}, $\alpha_{C_{12}DmCB}$ and $\alpha_{C_{14}Ab}$ respectively. The mole fraction of the components and the total concentration of the mixtures are represented in Table 1.

2.4. Tensiometry

For surface tension measurements, Krüss (Germany) tensiometer was used applying ring detachment method. Concentrated stock solution (concentrations are mentioned in table 1) of surfactants in aqueous medium at a particular mole fraction of CPZ was added to water with a Hamilton micro syringe taking 5 min time for equilibration before each measurement. All measurements were done three times to examine reproducibility. The precision of the method was ± 0.1 $mN.m^{-1}$. To get the *cmc*, surface tension (γ) vs. log[surfactant] was plotted [cf. Figure 2]. From the breaks in the plot, *cmc* was obtained.

2.5. Turbidity measurement

Turbidity of the solutions was carried out by the measurement of transmittance of the solutions by SHIMADZU UV-1601 spectrophotometer (Made in Japan). A quartz cuvette of 1 cm path length was used. Surfactant solutions of different mole fractions of CPZ were prepared keeping the concentration of solution equal to the *cmc* corresponding to different mole fractions of drug. The percentage of transmittance (%*T*) of the different sets[47] was taken at 550 nm since no characteristic absorbance was found for both the surfactants and drug solutions at this particular wavelength.[48]

Turbidity (t) of different experimental sets was evaluated-using the equation, $t = 100 - \%T$. The whole experiment was carried out at room temperature (298.15 ± 0.01 K).

2.6. Dynamic Light Scattering (DLS) and Zeta potential measurement

DLS measurements were done in a Zetasizer nano ZS (Malvern, UK) at a scattering angle of 90° with a He–Ne laser (λ = 632.8 nm). All the solutions having concentrations just above the *cmc* at that particular mole fraction were filtered 3 times by membrane filters (porosity 0.25 μm) to eliminate larger particles. The zeta potential (ζ) measurement of solutions was repeated for three times in the same instrument and the average values of the results were reported.

2.7. Confocal Laser Scanning Microscopy (CLSM)

In this study, an inverted confocal fluorescence microscope with two-photon excitation (Zeiss-LSM 510 META Carl Zeiss, Jena, Germany) has been used. All the solutions having concentrations just above the *cmc* at that particular mole fraction was used. Acridine orange was used as a probe. 1 μM acridine orange was added during the sample preparation. The excitation wave length was maintained at 480 nm for acridine orange which was used as a probe. A drop of a solution with probe was placed on a glass slide and then it was covered with another thin slide. All experiments were repeated twice to check reproducibility.

2.8. Transmission Electron Microscopy (TEM)

10 μL sample solutions having concentrations just above the *cmc* of particular mole fraction were placed on carbon-coated copper grid with 300 mesh size to adsorb on it. Excess liquid on the copper grid was automatically removed from the filter paper on which it was placed. Freshly prepared 0.5 wt % aqueous uranyl acetate was used to stain it negatively. The samples were kept in a desiccator overnight. A JEOL-JEM 2100, Japan transmission electron microscope was used with an accelerating voltage of 100 kV.

2.9. Steady state fluorescence anisotropy study

Steady state fluorescence anisotropy measurements were performed using a Perkin Elmer LS55 (USA) fluorescence spectrophotometer attached to a fluorescence Peltier system PTP-1 including a glass cell of 1 cm path length. All the solutions having concentrations just above the *cmc* at that particular mole fraction was used in the experiment. Acridine orange was used for steady state

fluorescence anisotropy (r_{ss}) measurements with excitation wavelength 480 nm and emission wavelength 530 nm. r_{ss} is defined as:[5, 49, 50]

$$r_{ss} = \frac{I_v - GI_h}{I_v + 2GI_h} \quad (1)$$

Where I_h and I_v are the emission intensities which are horizontally and vertically polarized respectively, arising from vertically polarized excitation of the probe. Factor G is defined as:

$$G = \frac{I_v}{I_h} \quad (2)$$

All the anisotropy values were averaged over an integration time of 20 s.

2.10. Time-Resolved Fluorescence Study

Time-resolved fluorescence decay was carried out using a Horiba−Jobin−Yvon FluoroCube fluorescence lifetime system using a NanoLED at 500 nm (IBH, UK) as the excitation sources for acridine orange and TBX photon detection module was used as the detector. . All the solutions having concentrations just above the *cmc* at that particular mole fraction was used in the experiment. All the decay data were fitted by using IBH DAS-6 decay analysis software. The lamp profile was collected by using dilute micellar solution of sodium dodecyl sulfate as a scatterer in place of the sample. For the appropriate fittings, the χ^2 values were kept close to unity.

2.11. Electrical Conductivity Measurements

The electrical conductivity was measured with Eütech (Singapore) having a cell constant = 1 cm^{-1}. The temperature of the solution was kept constant at 298 K in a water bath with the accuracy of ± 0.1 K. 5 mL of solution of a particular mole fraction of CPZ (α_{CPZ}) having concentrations equal to the *cmc* of that particular mole fraction was placed in a container and the value of specific conductance (κ) was recorded. Each measurement was repeated for three times and the average value was recorded with an uncertainty within ± 2μS.

3. Results and discussions

3.1. Critical Micelle Concentration (*cmc*) and validity of Clint Model

Chlorpromazine hydrochloride (CPZ) is a water-soluble drug and aqueous solution was taken here for the experiments. During the addition of CPZ solution gradually into the aqueous medium, the

surface tension of the system decreases up to a certain minimum. Concentration corresponding to the minimum value of surface tension is defined as critical micelle concentration, *cmc*. In Figure 2, plots of surface tension versus log of total concentration of surfactant [S] are provided. The *cmc* values of synthesized surfactant, N-Dodecyl-N, N-dimethyl-2-ammonio-1-ethanecarbonate (C_{12}DmCB), 1,2-bis [N-methyl-N-carboxymethyl tetradecylammonium] ethane (C_{14}Ab) and drug CPZ are comparable with values reported earlier.[6, 33, 51-53] The *cmc* value of the drug CPZ appears at higher concentration because of its rigid hydrophobic part (Figure 2C). Hydrophobic interaction is the most important for the understanding of the micellization process.[54] During the addition of amphiphiles to aqueous media, the hydrophobic moiety of the molecule breaks the structure of the water molecules connected through hydrogen bonding and thus, water molecules are liberated from hydration shells[55] resulting in the increase in the entropy of the system. Geminis are composed of two amphiphilic segments connected by a spacer at or near the head group of individual amphiphiles. Due to its characteristic molecular structure (presence of double hydrophobic chains), it shows greater hydrophobicity than the single-chain amphiphiles having similar number of carbon atoms as each segment of gemini. Thus, micellization happens at lower concentrations in the case of gemini.[56] Therefore, from Table 2, it is evident that the *cmc* value of zwitterionic gemini surfactant C_{14}Ab is lower than that of C_{12}DmCB. From Table 2, it can be seen that with increasing the mole fraction of drug CPZ, the *cmc* value approaches the ideal values found using the Clint model. According to Clint theory,[57] the ideal value of *cmc*s for the mixture of surfactants can be predicted from the following equation (eq. 3) where it is considered that components of mixed-micelle are non-interacting:[58]

$$\frac{1}{cmc_{ideal}} = \sum_i^n \frac{\alpha_i}{cmc_i} \tag{3}$$

Here, α_i and cmc_i indicate the stoichiometric mole-fraction and *cmc* of the ith constituent of the mixed-micelle of ideal mixing of surfactants. Deviation of experimental *cmc* (cmc_{exp}) from the *cmc* proposed by Clint model suggests non-ideal mixing of monomer components. If $cmc_{ideal} < cmc_{exp}$ it is called positive deviation suggesting antagonistic interaction among the surfactant monomers. If $cmc_{ideal} > cmc_{exp}$, it is called negative deviation suggesting synergistic interaction. From Table 2, it is observed that in the present mixed system (CPZ/C_{12}DmCB), $cmc_{ideal} > cmc_{exp}$ indicating synergistic interaction between CPZ and C_{12}DmCB molecule, in other words attractive interaction takes place between the component molecules. On the other hand, repulsive interaction

takes place between CPZ and zwitterionic gemini surfactant C_{14}Ab. Reduced values of *cmc* than the ideal value in case of CPZ/C_{12}DmCB system for all stoichiometric mole fractions of CPZ (α_{CPZ}) clearly indicate that the drug molecules are attached to the stern layer of C_{12}DmCB micelle due to attractive electrostatic interaction. As a result of that, stable mixed micelle system form is formed. For CPZ/C_{14}Ab combination electrostatic repulsion occurs between the two head groups of gemini and head group of CPZ at the micellar surface during the formation of mixed micelle, it was overshadowed by large CPZ moiety with higher mole fraction of CPZ (α_{CPZ}). With an increase in the value of α_{CPZ}, the value of cmc_{exp} increases as compared to its ideal values in the case of CPZ/C_{14}Ab system at all mole fractions of CPZ (α_{CPZ}). This phenomenon regarding the deviation of cmc_{exp} values from cmc_{ideal} values (~ + 43% at $\alpha_{CPZ} = 0.6$) (cf. Table 2) infers that CPZ molecules are incorporated into the micelle formed by the C_{14}Ab as stated for similar systems in previous literature.[59]

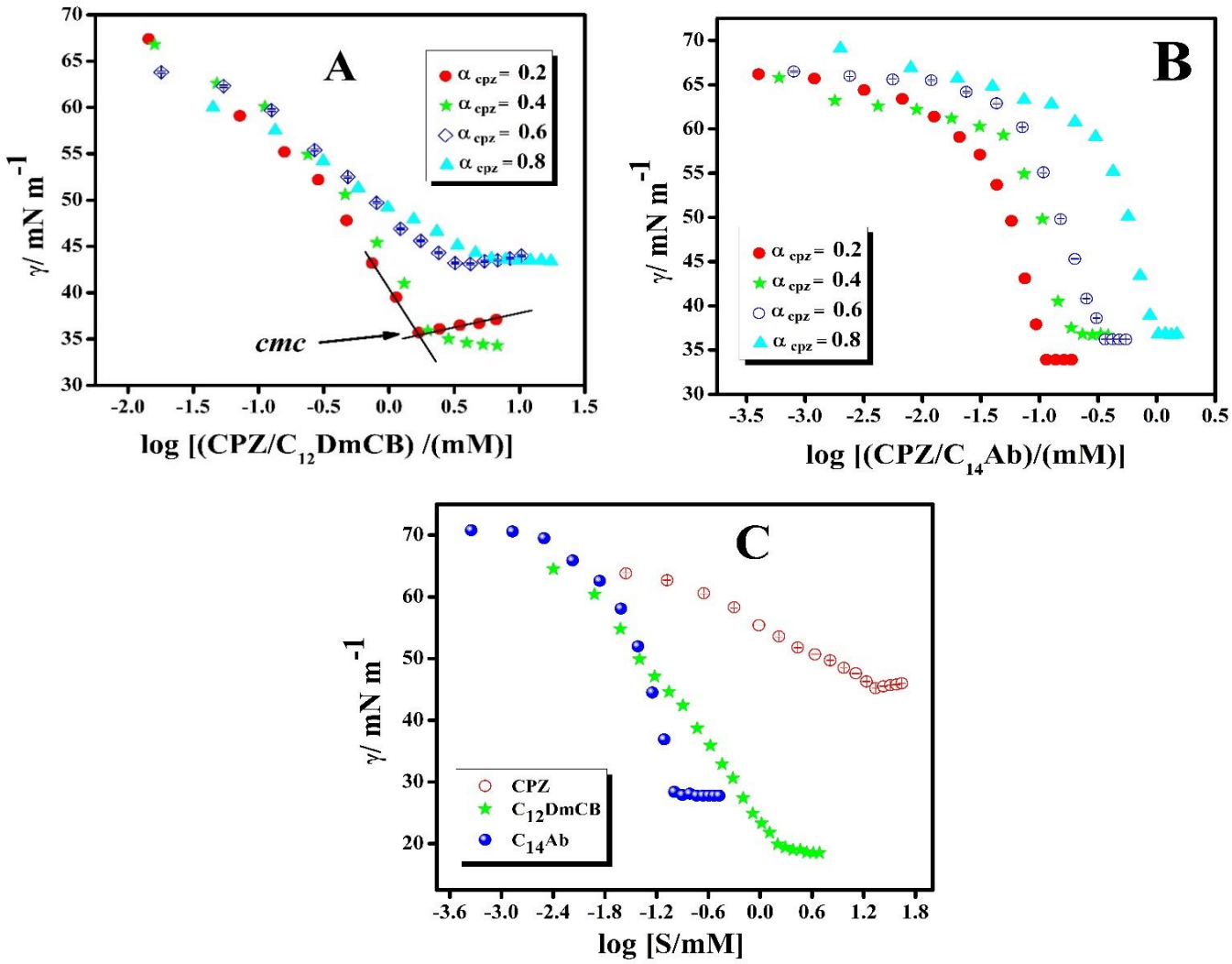

Figure. 2 Plots of surface tension (γ) vs. (A) log [CPZ/C_{12}DmCB (mM)], (B) log [CPZ/C_{14}Ab (mM)] at different mole fractions of CPZ and (C) log [pure components/mM] in water at 298.15 K.

3.2. Adsorption at air/water interface

Adsorption of amphiphiles at the air/water interface reduces the surface tension of the aqueous phase. Breaking of the hydrogen bonds at the surface of the aqueous phase with the addition of amphiphiles decreases the surface tension. The Gibbs surface excess (Γ_{max})[60-62] which signifies the amount of adsorbed surfactant molecules per unit area, can be obtained from the following equation:

$$\Gamma_{max} = -\frac{1}{2.303nRT}\lim_{C\to cmc}\left(\frac{d\gamma}{d\log C}\right)_{max} mol.m^{-2} \quad (4)$$

Here, $d\gamma/d\log C$ defines the slope of the surface tension vs log of concentration profile (Figure 2). R and T indicate the universal gas constant (8.314 J mol^{-1} K^{-1}) and temperature in Kelvin respectively and n indicates the number of ionic species adsorbed at the interface. For the system having only zwitterionic species in aqueous solution value of n is taken as 1[63] and for the drug species in aqueous solution value of n is taken as 2.[6] For the mixed system, the value of n can be determined theoretically considering complete ionisation of the ionic drug species by using the relation $n = n_1X_1 + n_2X_2$.[6] With increasing the amount of drug molecule, $\Gamma_{max}$is observed to decrease. This signifies that the drug molecule CPZ is less surface active than the zwitterionic molecule. The minimum area per molecule (A_{min}) can be calculated by the relation:

$$A_{min} = \frac{10^{18}}{N_A\Gamma_{max}}\ nm^2molecule^{-1} \quad (5)$$

Here, N_A is the Avogadro number. From Table 2, it is evident that with increasing the amount of CPZ, the A_{min} value increases. This signifies that monomers are packed less compactly in presence of drug molecules. The drug molecule having more rigid hydrophobic part occupies more area than both zwitterionic molecules. The calculated value of Γ_{max} for C_{12}DmCB is higher than the cationic surfactant CTAB and anionic surfactant SDS.[64, 65] This higher value of Γ_{max} comes as a result of larger hydrophilic head group compared to CTAB and SDS.[66] The calculated Γ_{max} value of C_{14}Ab is 7.33×10^{-6} mol m^{-2} which is close to the value of 6.34×10^{-6} mol m^{-2} reported earlier.[33] Higher Γ_{max} value of C_{14}Ab compared to C_{12}DmCB suggests that zwitterionic gemini is more surface active than the other. Another interesting fact is that though the zwitterionic gemini has more hydrophobic nature due to hydrophobic twin tails, it has lower A_{min} value than the C_{12}DmCB molecule. This reveals the fact that zwitterionic gemini is more closely packed at the interface. The reason behind this small area might be the overlapping of hydrophobic chains and formation of film.[33] Ideal value of minimum area per molecule (A_{min}^{ideal}) is calculated in Table 2 from the equation as follows:

$$A_{min}^{ideal} = X_1A_1 + X_2A_2 \quad (6)$$

Here, X_1 and A_1 are the micellar mole fraction and minimum area per molecule of component 1 and X_2 and A_2 are the micellar mole fraction and minimum area per molecule of component 2 respectively. It was observed that ideal values (A_{min}^{ideal}) are greater than the experimental values A_{min} i.e., the area occupied by the head group of amphiphiles in the mixed micelle (CPZ+

C_{12}DmCB / C_{14}Ab) is smaller than the ideal value. The smaller experimental values suggest some contraction in interfacial packing.[67] Efficiency of interfacial adsorption is denoted by the parameter pC_{20} which is the negative logarithm of C_{20} ($_pC_{20}$ = -logC_{20}). The concentration needed to decrease the surface tension of a solvent by 20 mM m^{-1} is defined as C_{20}. The system having better efficiency to adsorb at the air-water interface has the larger value of pC_{20}. From Table 2, it is seen that pC_{20} value of CPZ is lower than the other amphiphiles C_{12}DmCB and C_{14}Ab and mixture of CPZ + C_{12}DmCB / C_{14}Ab. The surface pressure (π_{cmc}) is defined as the difference between the surface tension of pure solvent (γ_0) and surface tension at *cmc* (γ_{cmc}), i. e.,

$$\pi_{cmc} = \gamma_0 - \gamma_{cmc} \tag{7}$$

π_{cmc} values of amphiphiles C_{12}DmCB and C_{14}Ab and mixture of CPZ+ C_{12}DmCB/C_{14}Ab are larger than the CPZ, indicating that amphiphiles have greater effectiveness in lowering the interfacial tension and CPZ has a lower tendency to adsorb at the air-liquid interface.

3.3. Thermodynamics of micellization

The standard free energy of micellization (ΔG_m^0) and interfacial adsorption (ΔG_{ad}^0) can be evaluated using regular solution theory considering negligible degrees of counterion dissociation [68, 69] as the following equations:

$$\Delta G_m^0 = RT\, ln\, X_{cmc} \tag{8}$$

$$\Delta G_{ad}^0 = \Delta G_m^0 - \frac{\pi_{cmc}}{\Gamma_{max}} \tag{9}$$

Here, X_{cmc} represents the *cmc* value in terms of mole fraction units. The calculated values are given in Table 2. The negative value of ΔG_m^0 indicates the spontaneity of the micellization process. The values for the mixed systems at all mole fractions are negative, which indicates that the process was spontaneous (Table 2). The negative values of the free energy of micellization are higher for mixed systems than for the drug, indicate that the formation of mixed micelles is energetically favorable than micellization of the drug CPZ. The negative ΔG_m^0 values for pure C_{12}DmCB and C_{14}Ab were found to be higher in magnitude than those for pure CPZ and CPZ-C_{12}DmCB/ C_{14}Ab mixed systems, indicating that the aggregation process is more spontaneous when involved with pure C_{12}DmCB/ C_{14}Ab, and this phenomenon is also supported by their *cmc* values. Also, more negative ΔG_m^0 values in case of CPZ/ C_{14}Ab system compared to the other signifies micellization

process is more favourable in the case of former than the latter. Higher negative value of ΔG_{ad}^{0} than ΔG_{m}^{0} signifies micellization which is a secondary process compared to the interfacial adsorption. Another thermodynamic parameter $G_{min}$is defined as change in free energy while transition occurs from bulk phase to air/solution interface of the amphiphiles in the system. The value of G_{min} can be calculated as follows:[70]

$$G_{min} = A_{min}\gamma_{min}N_A \quad (10)$$

Lower magnitude of G_{min} signifies the formation of more thermodynamically stable interface. From Table 2, it is apparent that magnitude of G_{min} is smaller than the ΔG_{ad}^{0} in most of the cases meaning the formation of more thermodynamically stable surface.

3.4. Packing parameter

Packing parameter for predicting the shape of the micelle can be obtained from the Israelachvili model[71] as follows:

$$P = \frac{v_c}{l_c A} \quad (11)$$

Here, *A* is the surface area of the hydrophilic head group which is equal to $A_{min}$of the components, v_c is the exclusive volume of the hydrophobic monomer and l_c is the maximum effective tail length per monomer in the micelle and was estimated from the Tanford formulas[72] following the relations:

$$l_c \leq l_{max} \approx (0.154 + 0.1265C_n)\ nm \quad (12)$$

$$v_c = (0.0274 + 0.0269C_n)\ nm^3 \quad (13)$$

Here, C_n is the number of carbon atoms in the monomeric hydrophobic saturated chain. For gemini surfactant, two l_c and two v_c were used in place of l_c and v_c respectively in equation 11.[73] The following equation was applied to determine v for mixed micelles:

$$v = \sum x_i v_{c,i} \quad (14)$$

Where i corresponds to the i^{th} species and x_i denotes the micellar mole fraction of the i^{th} species and $v_{c,i}$ corresponds to the exclusive volume of the i^{th} hydrophobic monomer obtained from equation 13.[74] In the case of drug CPZ, the amide group connected with two phenyl rings was treated as a saturated carbon bond to estimate l_c and v_c as the entire hydrophobic chain was also

participated in the formation of mixed micellisation. For determination of l_c in case of mixed micelles, the component with the longest hydrophobic tail length was taken into consideration.[74] In case of CPZ/C_{12}DmCB system l_c(C_{12}DmCB) > l_c(CPZ) and similarly for the system CPZ/C_{14}Ab l_c(C_{14}Ab) > l_c(CPZ). So, the hydrophobic tail length of C_{12}DmCB and C_{14}Ab was considered for CPZ/C_{12}DmCB and CPZ/C_{14}Ab systems respectively. From the P values (Table 2) it can be predicted the shape and the geometry of the aggregates. For spherical micelle the range of P value is 0 to 0.33; for cylindrical micelle, 0.33 to 0.5 and for bilayers and vesicles, 0.5 to 1.[7,75] High packing parameter value of the CPZ/C_{14}Ab system shows an indication of formation of non-spherical aggregates.[76]

3.5. Interaction between drug and zwitterionic surfactants: approach from the theoretical models

3.5.1. Rubingh Model

For understanding the ideal behaviour of the mixed micelles, Clint equation[77] is applicable which has been stated in equation (3). Deviation from experimentally calculated *cmc* from ideal *cmc* value would suggest that amphiphiles are interacting with each other and the system is non-ideal. Rubingh[78] proposed his theory for this non-ideal nature of mixed micelles formed in the bulk phase. The equation from which the composition of binary systems and interaction parameter (β) can be determined is as follows:

$$\frac{(X_1^R)^2\, ln[(\alpha_1 cmc/X_1^R cmc_1)]}{(1-X_1^R)^2\, ln[(1-\alpha_1)cmc/(1-X_1^R)cmc_2]} = 1 \qquad (15)$$

$$\beta^R = \frac{ln(\alpha_1 cmc/X_1 cmc_1)}{(1-X_1)^2} \qquad (16)$$

Here, X_1^R represents the micellar mole fraction of drug CPZ in the mixed system of drug-zwitterionic surfactants; cmc_1 is the *cmc* of drug CPZ and cmc_2 is the *cmc* of zwitterionic surfactants (C_{12}DmCB and C_{14}Ab). The equation 15 was solved by an iterative process to obtain X_1^R values. These X_1^R values were used to calculate interaction parameter (β^R). When the *cmc* of the mixture is less compared to the components of the mixture, it is called synergism and when the value is greater than the components, it is called antagonism. The conditions for synergism in a binary mixture of amphiphiles are (i) β^R is negative and (ii) $|\beta^R|$ > | ln (cmc_1/cmc_2) |. Positive

value of β^R signifies antagonism. The value of β is close to zero signifing ideal mixing. The magnitude of β^R is the highest for 0.2 mole fraction of drug CPZ of CPZ/C_{12}DmCB system ($\alpha_{CPZ} = 0.2$). The magnitude of interaction between amphiphile molecules depends on the synergism of the mixtures and the hydrophobic nature of amphiphiles in the solution. Increase in the mole fraction of the surfactant increases the hydrophobicity in the mixture and thus, we can observe the more negative value (Table 3) of the interaction parameter (β^R). In case of CPZ/C_{14}Ab combination, the value of β^R is -5.32 (Table 3) which indicates synergistic interaction at $\alpha_{CPZ} = 0.2$. However, for other mole fractions of CPZ, the values of interaction parameter (β^R) are undefined applying by iterative process; the reason of this may be unfavorable interaction between surfactant (C_{14}Ab) and drug CPZ. The surfactant C_{14}Ab has a more hydrophobic nature than C_{12}DmCB, it produces strong attractive interactions with drug as it is evident from the more negative β^R value (β^R = -5.32 for) of the C_{14}Ab/CPZ system. The micellar activity coefficients, $f_1$and $f_2$can be calculated from the equations as follows:

$$f_1 = exp[\,\beta^R(1 - X_1)^2] \tag{17}$$

$$f_2 = exp[\,\beta^R(X_1)^2] \tag{18}$$

The values of micellar activity coefficients f_1 and f_2 are less than unity for all the systems, that means, all the systems show non-ideal behavior and interaction of the mixed micellar system is attractive. If f_1 and f_2 terms are introduced in Clint's equation (eq. 3), then according to RST, eq. 3 can be transformed into the following equation:

$$\frac{1}{cmc_{cal}} = \frac{\alpha_1}{f_1 cmc_1} + \frac{\alpha_2}{f_2 cmc_2} \tag{19}$$

It is shown that, predicted *cmc* values (cmc_{cal}) found fair similarities with *cmc*s which were found by experimentally given in Table 3 after taking the values of activity coefficients measured by the equations 17 and 18. The ideal mole fraction of the component in the mixed micellar system can be calculated as follows using Motomura's approximation for ideal mixing:

$$X_{ideal} = \frac{\alpha_1 cmc_2}{\alpha_1 cmc_2 + \alpha_2 cmc_1} \tag{20}$$

The calculated values of X_1 and X_{ideal} are given in Table 3. From Table 3, it is seen the positive deviation of the values of X_1 from the values of X_{ideal}. The increased value of X_1 than X_{ideal}

indicates the greater contribution of CPZ in mixed micelle as expected, also declares that mixed system shows non-ideal behavior (synergism). Excess free energy of mixed micellization (G_{ex}), excess enthalpy (H_{ex}), and enthalpy of micellization (ΔH_m) can be evaluated from the following equation:[5, 79]

$$G_{ex} = H_{ex} = \Delta H_m = [X_1 \, ln \, f_1 + (1 - X_1) \, ln \, f_2]RT \quad (21)$$

The values of G_{ex} are presented in Table 4. The negative values of G_{ex} indicate that micellization process for mixed amphiphile systems is more favourable than the micellization of the pure components. The excess free energy of micellization signifies deviation from the ideal behavior (G_{ex}= ΔG_m−ΔG_m^{ideal}). The non-ideal free energy of micellization (ΔG_m) can be given by:

$$\Delta G_m = RT \, [X_1 \ln(X_1 f_1) + X_2 \ln(X_2 f_2)] \quad (22)$$

The free energy of micellization (ΔG_m) for an ideal mixing can be given by

$$\Delta G_m^{ideal} = RT[X_1 \ln(X_1) + X_2 \ln(X_2)] \quad (23)$$

ΔG_m and ΔG_m^{ideal} values were given in Table 4. From Table 4, it is evident that the free energy of micellization on a nonideal state (ΔG_m) has more negative values from the free energy of micellization on an ideal state (ΔG_m^{ideal}) for both the systems investigating here favoring the formation of mixed micelle. The entropy of micellization (ΔS_m) can be obtained by using the values of the enthalpy of micellization (ΔH_m) and free energy of micellization (ΔG_m) from eq. 24.

$$\Delta S_m = \frac{\Delta H_m - \Delta G_m}{T} \quad (24)$$

From Table 4, it is evident that ΔH_m values are more negative for CPZ/C_{12}DmCB system in comparison with CPZ/C_{14}Ab system demonstrating micellization process is more exothermic for CPZ/C_{12}DmCB system. The values of ΔS_m are positive for all the systems, especially for CPZ/C_{14}Ab system. Finally, it may be stated from $\left|\frac{T\Delta S_m}{\Delta G_m}\right|$ values (cf. Table 4), mixed micellization is entropy driven at higher mole fraction of CPZ.

3.5.2. SPB Model

Blankschtein et al. (SPB)[80-82] proposed a thermodynamic theory and also predicted quantitatively micellar composition (X_{SPB}), phase behavior and shape based on the hydrophobic, structural, and

electrical interactions between the binary components. This theoretical model was applied here to get the more appropriate values of the interaction parameter (β) particularly for those values which were undefined according to the Rubingh Model. Thus, Clint's equation is written in the following form in case of nonideal mixing of surfactants assuming activity coefficient (f) not equal to 1.

$$\frac{1}{cmc_{mix}} = \frac{\alpha_1}{f_1 cmc_1} + \frac{\alpha_2}{f_2 cmc_2} \tag{25}$$

Here, f denotes the activity coefficient of the surfactant in the mixed micelle and is obtained from the relations given below:

$$f_1 = exp\left[\frac{\beta(1-\alpha^*)^2}{kT}\right] \tag{26}$$

and

$$f_2 = exp\left[\frac{\beta(\alpha^*)^2}{kT}\right] \tag{27}$$

Here, β is the predicted interaction parameter between two surfactants 1 and 2 (1 stands for CPZ and 2 stands for each one of the zwitterionic surfactants), α^* represents the optimal micellar composition (denoted by X_{SPB} where the free energy of micellization reaches minimum). The following equation can be solved iteratively to find α* and β and by using these values, f can be obtained according to the equations (26) and (27) and α* is the trial mole fraction of CPZ and cmc_1 and cmc_2 values are taken from Table 2.

$$\frac{\beta(1-2\alpha^*)}{kT} + \ln\left[\frac{\alpha^*}{(1-\alpha^*)}\right] = \ln\left[\frac{\alpha_1 cmc_2}{(1-\alpha_1)cmc_1}\right] \tag{28}$$

It is observed from Table 4 that with increasing α_1 (α_{cpz}) for all the binaries the values of α^*(X_{SPB}, micellar mole fraction of CPZ) increase in case of CPZ/C_{12}DmCB system, while the opposite trend is observed for CPZ/C_{14}Ab in water system. Similar observation has been found in terms of X_1 (cf. Table 3) for CPZ/C_{12}DmCB system, where X_1increases with the increase of α_1. The β values are also found more negative with the increase in the mole fractions of surfactants and observed that more synergistic interaction in case of CPZ with zwitterionic gemini surfactants. The values of β^R and β have similarity in magnitude and the same trend has been observed for CPZ/C_{12}DmCB system (see Table 3 and Table 4) and also the undefined values of interaction parameter (β^R)

according to the Rubingh model for CPZ/C_{14}Ab system were obtained here (see β values in Table 4) by applying this thermodynamic model. The values of cmc_{cal} also show (Table 4) well similarity with the experimental values (Table 2) which have been calculated by using equation 25 with the help of equations 26 and 27.

3.6. Turbidity Measurements

In case of CPZ/ C_{12}DmCB system, for all the sample solutions of the corresponding mole fraction of drug CPZ (α_{CPZ}), no visual turbidity has been found.

To investigate the degree of turbidity of CPZ/C_{14}Ab system, a fixed wavelength of 550 nm was chosen as neither of the components (CPZ, C_{14}Ab) showed any absorbance at this particular wavelength. With increasing the mole fraction of drug CPZ in CPZ/C_{14}Ab system, turbidity of the system gradually increased up to $\alpha_{CPZ} = 0.6$ which is evident from the Figure 3A and B; after that, turbidity decreases. This characteristic sharp variation in the turbidity happens due to the transformation of smaller micelles into larger non−spherical aggregates. In Figure 3B, a point of inflection was also found.

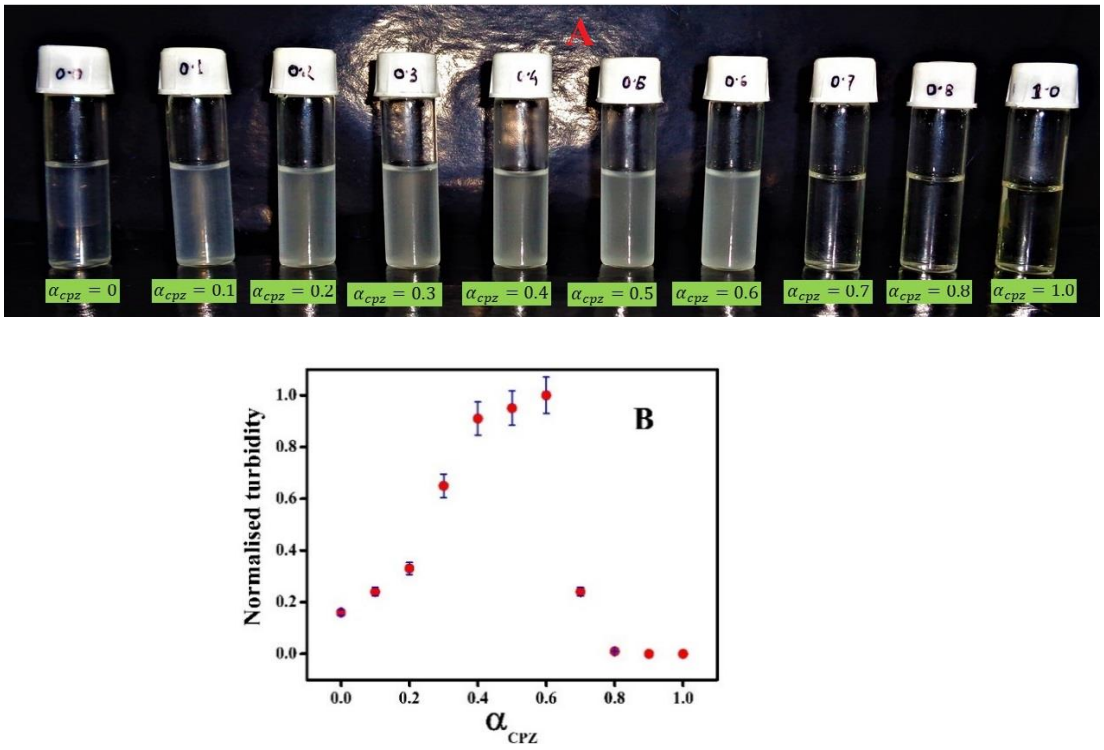

Figure. 3 Phase behaviors of (A) CPZ/C_{14}Ab system at different mole fractions of CPZ and (B) Normalized turbidity of CPZ/C_{14}Ab system at different mole fractions of CPZ.

3.7. Dynamic Light Scattering (DLS) Method and Confocal Laser Scanning Microscopy (CLSM)

The transformation of the structure of the aggregates can be identified from the hydrodynamic radius of the system. The DLS size distribution plots of CPZ/C_{12}DmCB and CPZ/C_{14}Ab aggregates are shown in supplementary information on pages S14 and S16 respectively. The C_{12}DmCB molecules form small aggregates in the micellar region in aqueous solution which is evident from DLS measurement. Also, no distinguished image from CLSM is found corresponding to the stable larger aggregates.

In the case of C_{14}Ab, the DLS method indicates that the hydrodynamic radii of CPZ/C_{14}Ab aggregates are comparatively larger at all mole fractions (α_{CPZ}). For pure C_{14}Ab solution at concentration ~ 0.1mM (*cmc* of C_{14}Ab), a clear bluish solution appears. DLS profile of this solution indicates that the hydrodynamic radius of aggregates is ~127-147 nm. DLS radius

distribution patterns for CPZ/C_{14}Ab mixtures are represented in supporting information on page S16. The range of hydrodynamic radius for these solutions ($\alpha_{CPZ} = 0.1{\sim}0.6$) is 147~553nm. Variation of hydrodynamic radius with the mole fraction of CPZ has been shown in Figure 4. At higher mole fraction ($\alpha_{CPZ} > 0.6$), the hydrodynamic radius of aggregates is comparatively small (~127 nm) due to the dissociation of larger aggregates which is also evident from the visual observation where clear solution appears. CLSM images are represented in Figure 5 for CPZ/C_{14}Ab mixture solution. Formation of larger aggregates can be confirmed from CLSM images. The nature of CLSM images is dependent on the distribution of the dye molecule (probe) used. Probe molecules are generally hydrophobic in nature and are able to stain the hydrophobic portion of the aggregates. In this case we used Acridine orange (AO) hydrochloride which is cationic in nature i.e., it contains both a hydrophilic and hydrophobic moiety. Therefore, it has the ability to stain the ionic micellar surface (contains a negatively charged $-COO^-$group) as well as the hydrophobic micellar core. Also, some portion of AO remains in bulk water solvent.[83] So, AO can stain the entire aggregated system and we get a larger micrograph having higher dimensions than DLS. However, some differential distribution of probe molecules must be present which gives differential contrast in staining of the entire system. From the CLSM images (Figure 5) it can be seen that the entire micrographs consist of smaller aggregates having different contrasts which confirms the aggregate formation of the system.

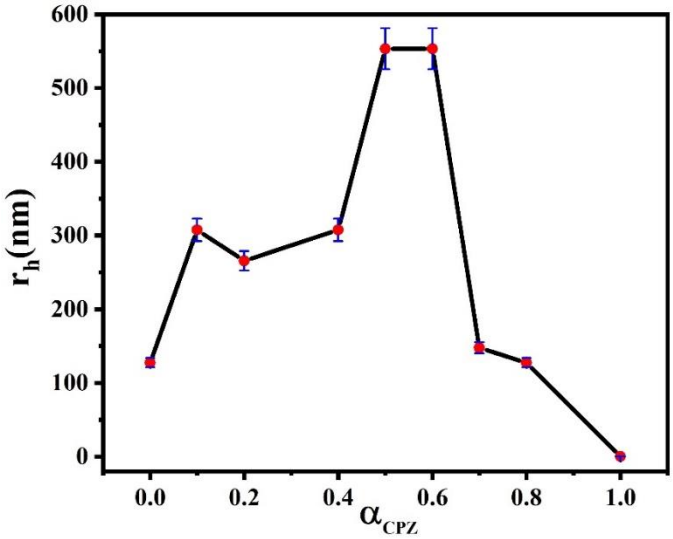

Figure. 4 Hydrodynamic radii of aggregates of the CPZ/ C_{14}Ab system at different mole fractions of CPZ at 298.15 K.

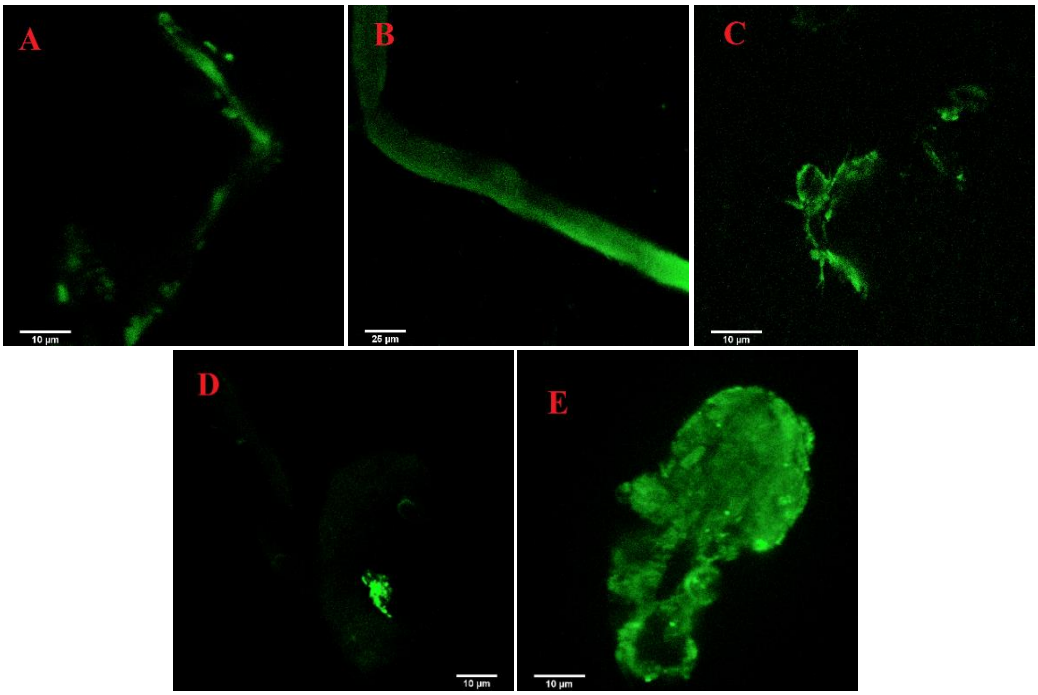

Figure. 5 Confocal laser scanning microscopic (CLSM) images of the CPZ/C_{14}Ab system at (A)-(C) α_{CPZ} =0.3; (D) α_{CPZ} =0.4; and (E) α_{CPZ} =0.6.

3.8. Transmission Electron Microscopy (TEM)

TEM experiments were done for lower mole fraction (α_{CPZ} = 0.1) and for higher mole fractions (α_{CPZ} = 0.4, 0.6) where the solution appears to be most turbid in case of CPZ/C_{14}Ab system to get authentic evidence of non-spherical aggregate formation. In case of CPZ/C_{12}DmCB system, as no turbid solution found for any mole fraction of drug and DLS experiments gave the indication of the presence of aggregates having hydrodynamic radius ≤ 10 nm, TEM experiment was not done here. The micrographs at α_{CPZ} = 0.1, 0.4 and 0.6 in case of CPZ/C_{14}Ab system have been represented in Figure 6A–F. The formation of large spherical aggregates (indicated with red arrows) at lower mole fraction CPZ (α_{CPZ} = 0.1) with diameter ~ 250 nm was confirmed from these images. The diameter of the spherical aggregates at α_{CPZ} = 0.4 was found to be ~ 200-340 nm. With increasing mole fraction of CPZ these spherical aggregates collapse and turn into non-spherical aggregates with larger size distributions which is clearly visible from the micrographs D, E and F at α_{CPZ} = 0.6. At this mole fraction the dimension of the aggregates was found to be (~200-470 nm). However, the micrographs obtained from the TEM experiment are comparatively smaller than the size distribution profiles obtained from the DLS. A couple of reasons can be proposed to interpret this observation:

1. DLS calculates the hydrodynamic size, or the size of the nanoparticle with any solvent molecules remaining bound to its surface. The direct observation is the intensity fluctuations produced by particle diffusion. The Stokes Einstein equation is then used to interpret the diffusion coefficient as a hydrodynamic size. The diffusion coefficient is compared to that of a hypothetical sphere traveling with the same diffusion coefficient. This measurement, which effectively yields a z-average distribution, weights the various size distributions differently, by size to the power of 6. i.e., larger particles are therefore given more weight, making the "average" size appear larger. Consequently, results.

2. An additional fact is that a thin electric dipole layer of solvent sticks to the surface of a dispersed particle when it moves through a liquid medium. This layer governs how the particle moves through the medium. Thus, as the particle moves under the influence of Brownian motion,

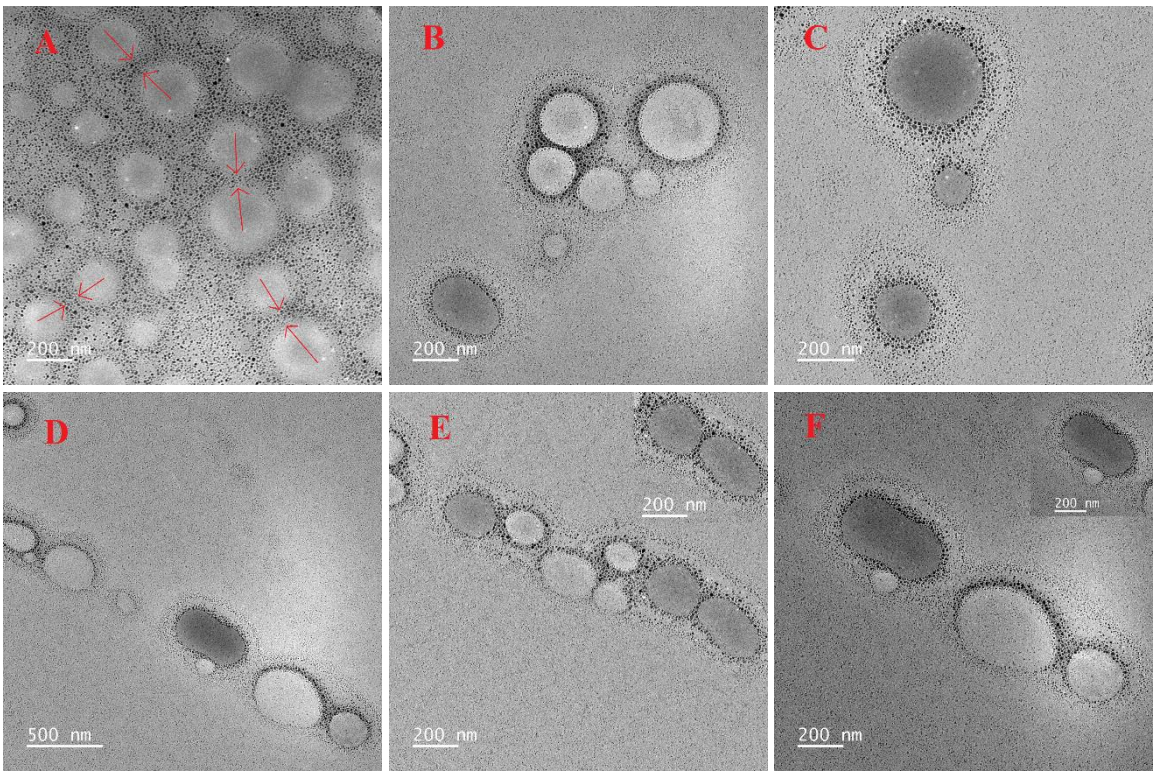

Figure. 6 TEM micrographs of the CPZ/C_{14}Ab system at (A) α_{CPZ} = 0.1; (B)-(C) α_{CPZ} = 0.4; and (D)-(F) α_{CPZ} = 0.6.

the hydrodynamic diameter provides us with information about the hydrophobic core and the solvent layer adhering to the particle. This hydration layer is absent while measuring size via TEM, therefore we only learn about the hydrophobic core. As a result, the hydrodynamic diameter is always larger than what TEM estimates.[84]

3.9. Fluorescence Polarization Anisotropy measurement

In the case of CPZ/C_{12}DmCB system with increasing mole fraction of CPZ, anisotropy gradually increases. Anisotropy value of acridine orange (AO) in water is found to be 0.013. In micellar system, this anisotropy value slightly increases. As the probe molecules enter the hydrophobic region of the micellar system, the restriction in rotational movement occurs and the anisotropy value increases (Figure 7A). Comparatively, a high anisotropy value is observed in the case of CPZ/C_{14}Ab system Figure 7B. This high anisotropy ($r > 0.14$) value indicates the formation of

larger aggregates which impose high restrictions on rotational movement of probe molecules. This anisotropy value shows a maximum at $\alpha_{CPZ} \sim 0.6$ and then decreases. This phenomenon indicates the transition of larger aggregates to smaller micellar aggregates which is also supported by the DLS profile and CLSM images.

3.10. Time-Resolved Fluorescence Decay Measurements

To get information about the local environment of a probe molecule, fluorescence lifetime measurement is an important tool. This method also gives information about the stability of the probe molecule in the excited state**.**

In the micellar system, the anisotropy decays of acridine orange are complex and data can be fitted using both double and single exponential decay.[85] For interfacial surfactant layer the average value of time scale is ~ 1 ns while for micellar system the value is ~ 1.7 ns.[86] For double exponential decay, the anisotropy value ($r(t)$) at time t with two relaxation components, τ_1 and τ_2:

$$r(t) = r_0 \left\{ a_1 e^{-t/\tau_1} + a_2 e^{-t/\tau_2} \right\} \quad (29)$$

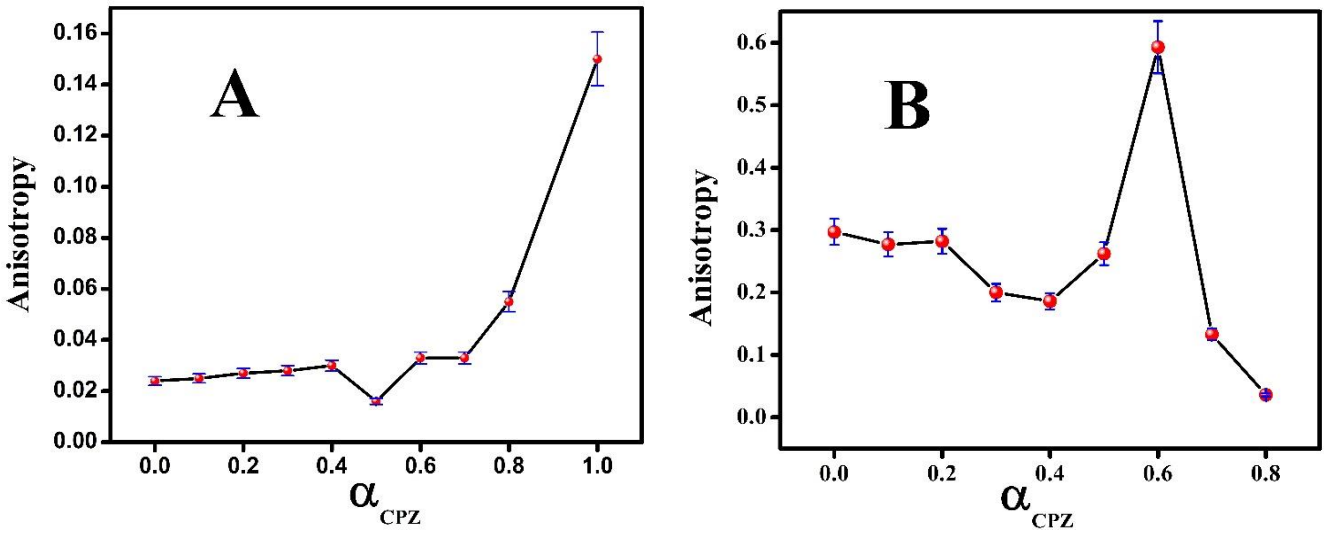

Figure. 7 Steady state fluorescence anisotropy (r) of (A) CPZ/C_{12}DmCB system and CPZ/ C_{14}Ab system at different mole fractions of CPZ at 298.15 K.

Here, r_0 indicates the anisotropy value at t = 0; a_1, a_2 are called the pre-exponential factors; in other words, a_1, a_2 are the contributing factors of each time scale component. Here, two

components originate from two different environments of the probe molecules located at the water-micelle interface and penetrated into the micelle.[80] Average value of the time scale τ_{av} is given by the equation as follows:

$$\tau_{av} = a_1\tau_1 + a_2\tau_2 \quad (30)$$

In case of C_{12}DmCB the hydrophilic portion of micelle is enclosed by single negatively charged carboxylate ion. When cationic drug CPZ is incorporated in the system, it comes adjacent to the polar headgroup regions of amphiphiles first and thus, the Na^+ ions from the head groups are replaced by the drug CPZ which increases the penetration of water molecules in the headgroup regions. As a result, the probe acridine orange (AO) molecule experiences a more hydrophilic environment which makes the rotation of AO less hindered and thus, the average value of life time (τ_{avg}) decreases with increasing molar ratio of CPZ (α_{CPZ}) up to $\alpha_{CPZ} = 0.4$ (refer to Table 5 and Figures 8 and 9). After that, as α_{CPZ} increases, single negatively charged carboxylate ion of C_{12}DmCB is not sufficient in holding cationic drug CPZ which restricts solubilization of CPZ at the outer portion of micelle system which is evident from the increasing τ_{avg} value after $\alpha_{CPZ} = 0.5$. In C_{14}Ab, two negatively charged carboxylate ions jointly attract cationic drug CPZ molecule and thus, water penetration around the headgroup regions increases rapidly which gives probe molecule more hydrophilic environment and less hindered movement that is evident from the decreasing average life time value (τ_{avg}). The values are provided in Table 5.

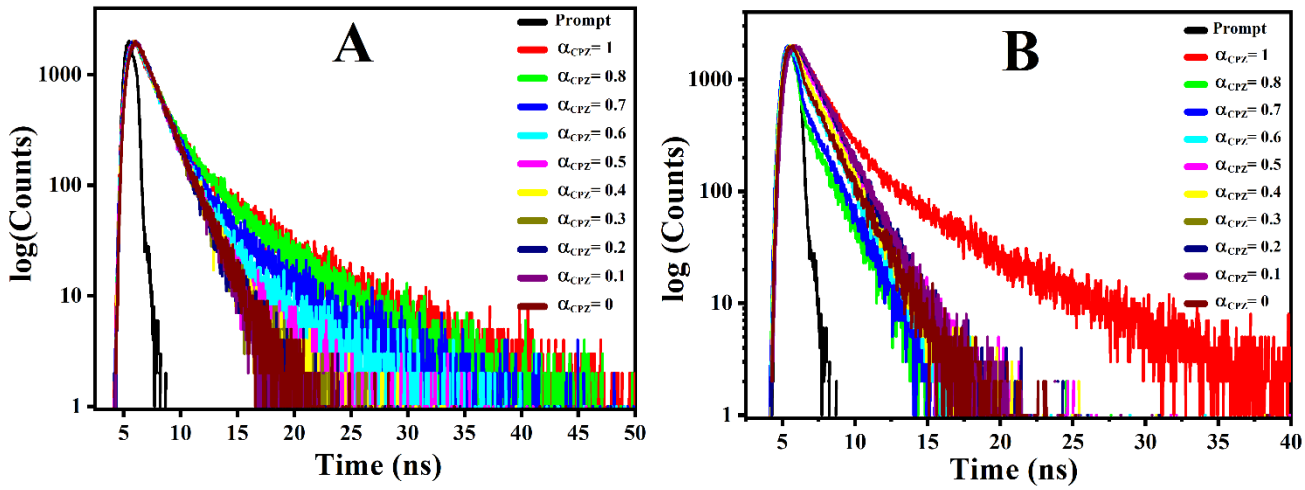

Figure. 8 Life time decay profile of solubilized acridine orange in water of (A) CPZ/ C_{12}DmCB and (B) CPZ/C_{14}Ab systems at different mole fractions of CPZ.

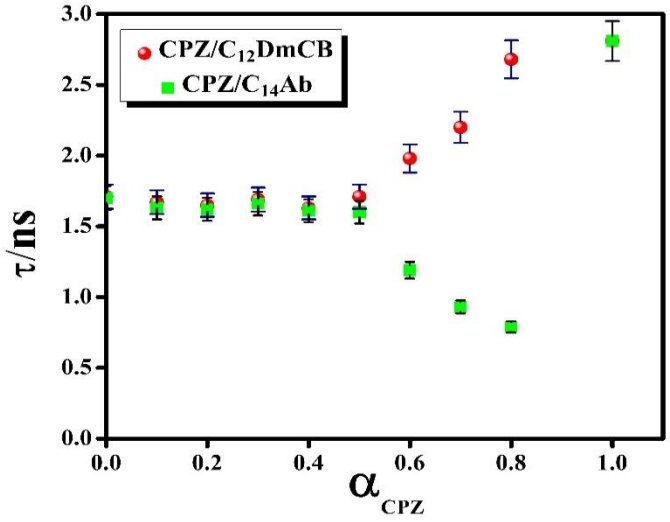

Figure. 9 Life time (τ) of solubilized acridine orange in water of CPZ/C_{12}DmCB and CPZ/ C_{14}Ab systems at different mole fractions of CPZ.

3.11. Zeta Potential (ζ) Measurement

The zeta potential (ζ) for both the systems CPZ/C_{12}DmCB and CPZ/C_{14}Ab was performed for different values of α_{CPZ}. The zeta potential (ζ) is defined as the potential difference between the diffusion medium and the stationary layer of solution close to the dispersed aggregates. This provides an idea of the stability of aggregates. The variation of zeta potential is represented in Figure 10. It was observed that the zeta potential varies from negative to positive value in both systems with increase of α_{CPZ}.

In case of CPZ/C_{12}DmCB system, the ζ value for 1.79 mM C_{12}DmCB micelle is −3.79 mV as it has negative surface charge of the micelle (Figure 10A). Addition of cationic drug CPZ, the negative charge of surface decreases with neutralization of surface charge density. Initially, a rapid increase in ζ value is observed up to $\alpha_{CPZ} = 0.2$, indicating strong interaction between cationic drug CPZ and anionic [C_{12}DmCB] micellar aggregates. A sudden decrease in ζ value is observed after $\alpha_{CPZ} = 0.2$ and a steady increment in ζ value is found up to $\alpha_{CPZ} = 0.6$ and then, it becomes constant. This rapid change in ζ value at $\alpha_{CPZ} = 0.2$ may happen due to the formation of elongated micelles which break down into small aggregates further increasing the mole fraction of CPZ.

Surface charge of C_{14}Ab micelle is negative (~ −4.12 mV) and the drug CPZ contains positive charge (~ +6.72 mV), so there is strong electrostatic attraction between these two to form a new aggregated structure (Figure 10B). With addition of CPZ drug, slight increase in the value of ζ is observed and it continues up to $\alpha_{CPZ} = 0.6$. After that, at higher mole fraction of drug, surface charge of the aggregates became saturated and there is no indication of increment of the size of aggregates obtained from DLS.

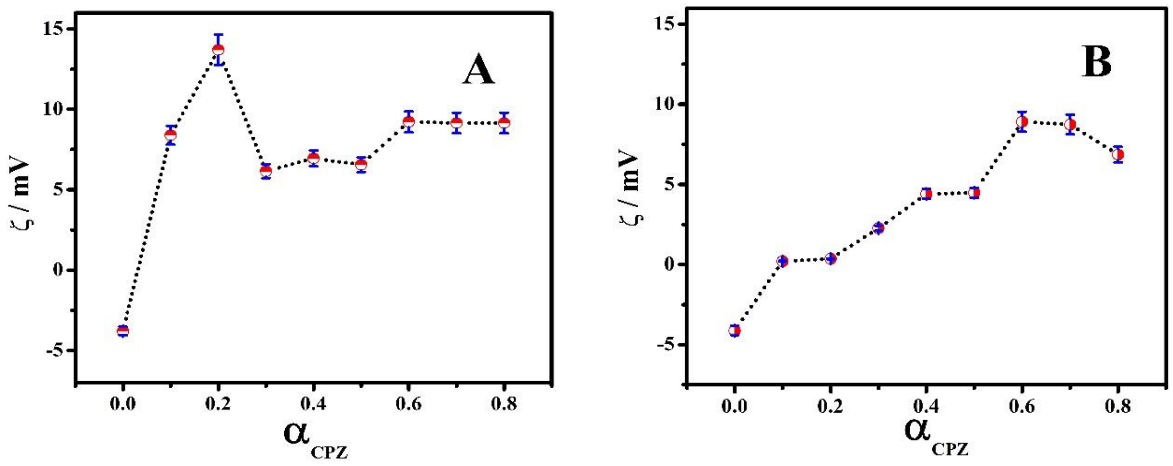

Figure. 10 Zeta potential (ζ) of (A) CPZ/C_{12}DmCB and (B) CPZ/C_{14}Ab systems at different mole fractions of CPZ.

3.12. Conductivity Measurements

To investigate the transition of the larger to smaller aggregates, electrical conductivity was measured. In case of CPZ/C_{12}DmCB system, with the addition of drug CPZ in aqueous C_{12}DmCB micelle, specific conductivity (κ) increases abruptly up to $\alpha_{CPZ} = 0.2$ and then, it remains within the range of 2.4-2.9 mS cm^{-1} (Figure 11A). In case of CPZ/C_{14}Ab system, specific conductivity value (κ) increases up to $\alpha_{CPZ} = 0.2$ and then suddenly starts falling and it remains almost saturated up to $\alpha_{CPZ} = 0.6$, indicating the formation of larger aggregates (Figure 11B). After $\alpha_{CPZ} = 0.6$, increased value of specific conductivity indicates the transformation of larger aggregates to smaller aggregates which is in agreement with the decreasing hydrodynamic radius in DLS profile.

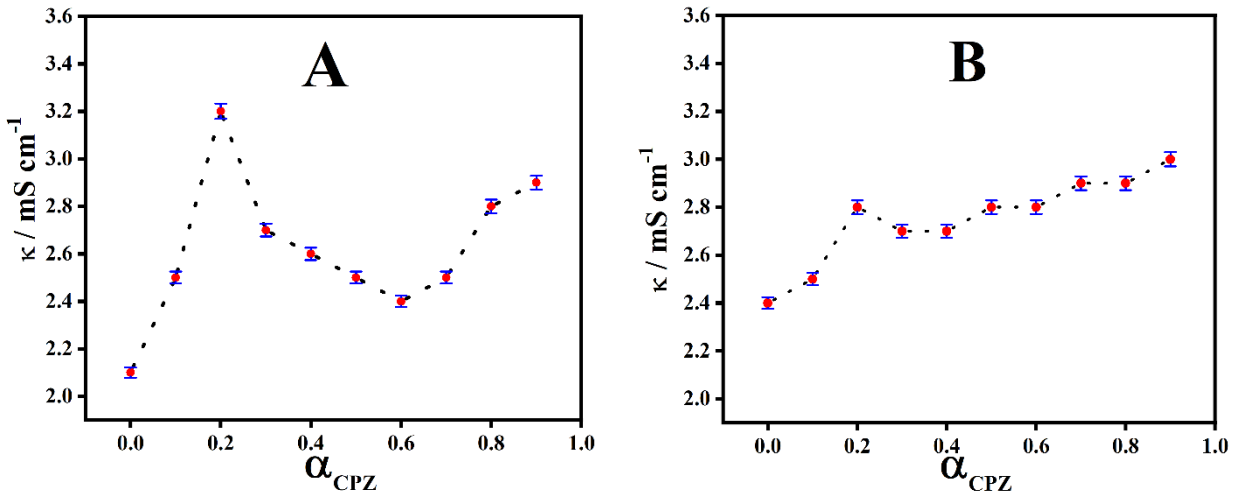

Figure. 11 Specific conductivity (κ) of (A) CPZ/C_{12}DmCB and (B) CPZ/C_{14}Ab systems at different mole fractions of CPZ.

4. Conclusion

In this work, the CPZ-assisted aggregate formation from a zwitterionic gemini surfactant was investigated. These aggregates were detected by DLS, confocal laser scanning microscopy, transmission electron microscopy (TEM) along with time-resolved anisotropy measurements. Time-resolved measurements of fluorescence decay were also performed, which provide information about the penetration of water molecules into the polar headgroup regions of the drug-surfactant system, which increases with the increasing mole fraction of drug in the system. The following conclusions can be drawn based on the obtained results:

1. With an increase in the value of α_{CPZ}, cmc_{exp} increases in comparison to its ideal values in the case of the CPZ/C_{14}Ab system indicating that CPZ molecules are absorbed into the micelle generated by C_{14}Ab.

2. The high packing parameter value of the CPZ/C_{14}Ab system gave an indication of the formation of large aggregates which was confirmed by confocal laser scanning microscopy (CLSM), transmission electron microscopy (TEM).

3. From $\left|\frac{T\Delta S_m}{\Delta G_m}\right|$ values (cf. Table 4) obtained from Rubingh model that, mixed micellization is entropy driven at higher mole fraction of CPZ for both the systems.

4. From the ΔG_m and ΔG_m^{ideal} values in Table 4, it can be stated that the free energy of micellization in a nonideal state (ΔG_m) has greater negative values than the free energy of micellization in an ideal state (ΔG_m^{ideal}) for both systems investigated here, favoring the formation of mixed micelles.

REFERENCES

1. J. F. Scamehorn, *Phenomena in mixed surfactant systems* 1986.
2. P. Holland, *ACS Symposium Series*, 1992, **501**, 31.
3. M. Malmsten, *Surfactants and polymers in drug delivery*, CRC Press, 2002.
4. T. F. Tadros, *Applied surfactants: principles and applications*, John Wiley & Sons, 2006.
5. S. Das, S. Ghosh and B. Das, *Journal of Chemical & Engineering Data*, 2018, **63**, 3784-3800.
6. N. Azum, M. A. Rub and A. M. Asiri, *Chinese Journal of Chemical Engineering*, 2018, **26**, 566-573.
7. T. Yadav, D. Tikariha, J. Lakra, A. K. Tiwari, S. K. Saha and K. K. Ghosh, *Journal of Surface Science and Technology*, 2014, **30**, 1-19.
8. D. Lombardo, M. A. Kiselev, S. Magazu and P. Calandra, *Advances in Condensed Matter Physics*, 2015, **2015**.
9. T. F. Tadros, *An introduction to surfactants*, de Gruyter, 2014.
10. A. Florence and D. Attwood, *Surfactant Systems: Their Chemistry, Pharmacy and Biology*, 1983.
11. Y. Lu, E. Zhang, J. Yang and Z. Cao, *Nano Research*, 2018, **11**, 4985-4998.
12. S. P. Moulik and S. Ghosh, *Journal of Molecular Liquids*, 1997, **72**, 145-161.
13. S. Ghosh, *Journal of Colloid and Interface Science*, 2001, **244**, 128-138.
14. G. S. Georgieva, S. E. Anachkov, I. Lieberwirth, K. Koynov and P. A. Kralchevsky, *Langmuir*, 2016, **32**, 12885-12893.
15. M. Barai, M. K. Mandal, H. Sultana, E. Manna, S. Das, K. Nag, S. Ghosh, A. Patra and A. K. Panda, *Journal of Surfactants and Detergents* 2020, **23**, 891-902.
16. T. Iwasaki, M. Ogawa, K. Esumi and K. Meguro, *Langmuir* 1991, **7**, 30-35.
17. M. Colic and N. Kallay, *Journal of Surface Science Technology* 1988, **4**, 53-66.
18. M. Garcia, I. Ribosa, J. S. Leal and F. Comelles, *Journal of the American Oil Chemists Society*, 1992, **69**, 25-29.
19. L. D. Rhein, A. Simion, R. L. Hill, R. H. Cagan, J. Mattai and H. I. Maibach, *Dermatology* 1990, **180**, 18-23.
20. T. C. Kibbey and K. F. Hayes, *Environmental science technology* 1997, **31**, 1171-1177.
21. B. J. Aungst and S. Phang, *International journal of pharmaceutics*, 1995, **117**, 95-100.
22. M. Noriyuki, K. Mariko, N. Yasuko, M. Shozo and S. Hitoshi, *International journal of pharmaceutics*, 1980, **4**, 271-279.
23. M. Kumar, K. Khushi, A. Bhardwaj, D. K. Deb, N. Singh, D. Elahi, S. Sharma, G. Bajpai and A. Srivastava, *Colloids and Surfaces A: Physicochemical and Engineering Aspects*, 2022, **654**, 130057.
24. M. Kumar, S. Raj, U. Thapa, S. Singh and A. Srivastava, *Journal of Molecular Liquids*, 2021, **322**, 114973.
25. M. Kumar, V. Singh, R. Choudhary, D. kumar deb, S. Singh and A. Srivastava, *Colloids and Surfaces A: Physicochemical and Engineering Aspects*, 2021, **628**, 127268.

26. D. Attwood, *Surfactant systems: their chemistry, pharmacy and biology*, Springer Science & Business Media, 2012.
27. D. Attwood, *Advances in colloid interface science* 1995, **55**, 271-303.
28. A. Krishnadas, I. Rubinstein and H. Önyüksel, *Pharmaceutical research*, 2003, **20**, 297-302.
29. M. J. Lawrence and G. D. Rees, *Advanced drug delivery reviews*, 2000, **45**, 89-121.
30. A. C. Williams and B. W. Barry, *Advanced drug delivery reviews* 2012, **64**, 128-137.
31. Y. Chevalier, *Current opinion in colloid interface science* 2002, **7**, 3-11.
32. A. V. Peresypkin and F. M. Menger, *Organic Letters*, 1999, **1**, 1347-1350.
33. Z. Xie and Y. Feng, *Journal of Surfactants and Detergents*, 2010, **13**, 51-57.
34. P. Renouf, D. Hebrault, J.-R. Desmurs, J.-M. Mercier, C. Mioskowski and L. Lebeau, *Chemistry and Physics of Lipids*, 1999, **99**, 21-32.
35. K. S. Sharma, C. Rodgers, R. M. Palepu and A. Rakshit, *Journal of colloid interface science* 2003, **268**, 482-488.
36. M. M. Khalaf, A. H. Tantawy, K. A. Soliman and H. M. Abd El-Lateef, *Journal of Molecular Structure*, 2020, **1203**, 127442.
37. N. Jahan, N. Paul, C. J. Petropolis, D. G. Marangoni and T. B. Grindley, *The Journal of Organic Chemistry*, 2009, **74**, 7762-7773.
38. A. Z. Naqvi, S. Noori and D. Kabir ud, *Colloids and Surfaces A: Physicochemical and Engineering Aspects*, 2015, **477**, 9-18.
39. S. Noori, A. Z. Naqvi, W. H. Ansari and D. Kabir ud, *Journal of Solution Chemistry*, 2015, **44**, 1292-1309.
40. A. Kumar, E. Alami, K. Holmberg, V. Seredyuk and F. Menger, *Colloids and Surfaces A: Physicochemical and Engineering Aspects* 2003, **228**, 197-207.
41. A. Srivastava, U. Thapa, M. Saha and M. Jalees, *Journal of Molecular Liquids*, 2019, **276**, 399-408.
42. E. Glaser and P. Newling, *British journal of pharmacology chemotherapy*, 1955, **10**, 429.
43. L. R. S. Barbosa, R. Itri, W. Caetano, D. de Sousa Neto and M. Tabak, *The Journal of Physical Chemistry B*, 2008, **112**, 4261-4269.
44. W. H. Halliwell, *Toxicologic pathology*, 1997, **25**, 53-60.
45. N. Azum, M. A. Rub and A. M. Asiri, *Pharmaceutical Chemistry Journal*, 2014, **48**, 201-208.
46. N. Azum, M. A. Rub, A. M. Asiri and H. A. Kashmery, *Journal of Molecular Liquids* 2018, **260**, 159-165.
47. X. Zhang, J. K. Jackson and H. M. Burt, *Journal of Biochemical and Biophysical Methods*, 1996, **31**, 145-150.
48. U. Subuddhi and A. K. Mishra, *Colloids and Surfaces B: Biointerfaces*, 2007, **57**, 102-107.
49. S. Ghosh and S. Mondal, *J. Surf. Sci. Technol*, 2012, **28**, 179-195.
50. N. Azum, A. Z. Naqvi, M. A. Rub and A. M. Asiri, *Journal of Molecular Liquids*, 2017, **240**, 189-195.
51. A. Kumar and A. Mandal, *Journal of Molecular Liquids*, 2017, **243**, 61-71.
52. D. Attwood and P. Fletcher, *Journal of Pharmacy and Pharmacology*, 1986, **38**, 494-498.
53. D. Attwood, E. Boitard, J. P. Dubes and H. Tachoire, *The Journal of Physical Chemistry*, 1992, **96**, 11018-11021.
54. J. J. H. Nusselder and J. B. Engberts, *Journal of colloid interface science* 1992, **148**, 353-361.
55. J. Israelachvili and H. Wennerström, *Nature*, 1996, **379**, 219-225.

56. M. Panda, N. Fatma and M. Kamil, *Zeitschrift für Physikalische Chemie* 2019, **233**, 707-720.
57. S. Ghosh, G. B. Ray and S. Mondal, *Fluid Phase Equilibria*, 2015, **405**, 46-54.
58. J. H. Clint, *Surfactant Aggregation*, Springer Netherlands, 2012.
59. A. Dey, V. Sandre, D. G. Marangoni and S. Ghosh, *The Journal of Physical Chemistry B*, 2018, **122**, 3974-3987.
60. T. Chakraborty and S. Ghosh, *Journal of Surfactants and Detergents*, 2008, **11**, 323-334.
61. A. Ridell, H. Evertsson, S. Nilsson and L.-O. Sundelöf, *Journal of Pharmaceutical Sciences*, 1999, **88**, 1175-1181.
62. D. Tikariha, B. Kumar, S. Ghosh, A. K. Tiwari, S. K. Saha, N. Barbero, P. Quagliotto and K. K. Ghosh, *Journal of Nanofluids*, 2013, **2**, 316-324.
63. S. Gao, Z. Song, D. Zhu, F. Lan and Q. Jiang, *RSC Advances*, 2018, **8**, 33256-33268.
64. B. Gao, Y. Yu and L. Jiang, *Colloids and Surfaces A: Physicochemical and Engineering Aspects*, 2007, **293**, 210-216.
65. M. J. Puchana-Rosero, M. A. Adebayo, E. C. Lima, F. M. Machado, P. S. Thue, J. C. P. Vaghetti, C. S. Umpierres and M. Gutterres, *Colloids and Surfaces A: Physicochemical and Engineering Aspects*, 2016, **504**, 105-115.
66. Z. H. Asadov, S. M. Nasibova, R. A. Rahimov, G. A. Ahmadova and S. M. Huseynova, *Journal of Molecular Liquids*, 2017, **225**, 451-455.
67. S. Ghosh and T. Chakraborty, *The Journal of Physical Chemistry B*, 2007, **111**, 8080-8088.
68. K. Tsubone, Y. Arakawa and M. J. Rosen, *Journal of Colloid and Interface Science*, 2003, **262**, 516-524.
69. R. Miller, V. Dutschk and V. B. Fainerman, *The Journal of Adhesion*, 2004, **80**, 549-561.
70. G. Sugihara, A. Miyazono, S. Nagadome, T. Oida, Y. Hayashi and J.-S. Ko, *Journal of Oleo Science*, 2003, **52**, 449-461.
71. J. N. Israelachvili, *Intermolecular and Surface Forces*, Elsevier Science, 2015.
72. S. Krimm, *Journal of Polymer Science: Polymer Letters Edition*, 1980, **18**, 687-687.
73. Z. Liang, C. Wang and J. Huang, *Colloids and Surfaces A: Physicochemical and Engineering Aspects*, 2003, **224**, 213-220
74. U. Farooq, A. Ali, R. Patel and N. A. Malik, *Journal of Molecular Liquids*, 2017, **234**, 452-462.
75. N. Azum, M. A. Rub, A. M. Asiri and W. A. Bawazeer, *Colloids and Surfaces A: Physicochemical and Engineering Aspects*, 2017, **522**, 183-192.
76. R. K. Mahajan, S. Mahajan, A. Bhadani and S. Singh, *Physical Chemistry Chemical Physics*, 2012, **14**, 887-898.
77. J. H. Clint, *Journal of the Chemical Society, Faraday Transactions 1: Physical Chemistry in Condensed Phases*, 1975, **71**, 1327-1334.
78. D. N. Rubingh, *Solution Chemistry of Surfactants*, 1979, **Vol. 1**.
79. M. A. Rub, N. Azum, A. M. Asiri, S. Y. M. Alfaifi and S. S. Alharthi, *Journal of Molecular Liquids*, 2017, **227**, 1-14.
80. C. Sarmoria, S. Puvvada and D. Blankschtein, *Langmuir* 1992, **8**, 2690-2697.
81. S. Puvvada and D. Blankschtein, *Molecular—Thermodynamic Theory of Mixed Micellar Solutions*, American Chemical Society, 1992.
82. A. Shiloach and D. Blankschtein, *Langmuir* 1998, **14**, 4105-4114.
83. A. K. Shaw and S. K. Pal, *The Journal of Physical Chemistry B*, 2007, **111**, 4189-4199.
84. A. P. Ramos, *Nanocharacterization Techniques*, William Andrew Publishing, 2017, 99-110.

85. S. Aygün, B. M. Beşer, M. Acar and K. Meral, *Journal of Fluorescence*, 2020, **30**, 849-857.
86. D. A. Piasecki and M. J. Wirth, *The Journal of Physical Chemistry*, 1993, **97**, 7700-7705.

Table 1. The mole fraction-based formulation for the preparation of mixed micelles in aqueous medium.

CPZ/C_{12}DmCB in water				
α_{CPZ}	$\alpha_{C_{12}DmCB}$	CPZ (mmol L^{-1})	C_{12}DmCB (mmol L^{-1})	Total concentration (mmol L^{-1})
0.0	1.0	0.0	50.0	50.0
0.1	0.9	5.0	45.0	50.0
0.2	0.8	10.0	40.0	50.0
0.3	0.7	15.0	35.0	50.0
0.4	0.6	20.0	30.0	50.0
0.5	0.5	25.0	25.0	50.0
0.6	0.4	30.0	20.0	50.0
0.7	0.3	35.0	15.0	50.0
0.8	0.2	40.0	10.0	50.0
0.9	0.1	45.0	5.0	50.0
1.0	0.0	200.0	0.0	200.0
CPZ/C_{14}Ab in water				
α_{CPZ}	$\alpha_{C_{14}Ab}$	CPZ (mmol L^{-1})	C_{14}Ab (mmol L^{-1})	Total concentration (mmol L^{-1})
0.0	1.0	0.0	5.0	5.0
0.1	0.9	0.5	4.5	5.0
0.2	0.8	1.0	4.0	5.0
0.3	0.7	1.5	3.5	5.0
0.4	0.6	2.0	3.0	5.0
0.5	0.5	2.5	2.5	5.0
0.6	0.4	3.0	2.0	5.0
0.7	0.3	3.5	1.5	5.0
0.8	0.2	4.0	1.0	5.0
0.9	0.1	4.5	0.5	5.0
1.0	0.0	200.0	0.0	200.0

Standard uncertainties in terms of concentration (mmol L^{-1}) = $\pm$ 2%

Table 2. Experimental Critical Micellar Concentrations (*cmc*), Calculated ideal Critical Micellar Concentrations according to Clint equation, The surface pressure (π_{cmc}), Minimum area per molecule (A_{min}), Ideal minimum area per molecule (A_{min}^{ideal}), Efficiency of interfacial adsorption (pC_{20}), Standard free energy of micellization (ΔG_m^0), Standard free energy of interfacial adsorption (ΔG_{ad}^0), Surface tension at *cmc* (γ_{cmc}), Minimum free energy of the surface with maximum adsorption (G_{min}), packing parameter (P) at 298.15 K.

α_{CPZ}	cmc (exp)	cmc $(ideal)$	π_{cmc} $(mN.m^{-1})$	$10^6\Gamma_{max}$ $(mol\,m^{-2})$	A_{min}^{ideal} $(nm^2$ $/molecule)$	A_{min} $(nm^2$ $/molecule)$	pC_{20}	ΔG_m^0 $(kJ.mol^{-1})$	ΔG_{ads}^0 $(kJ.mol^{-1})$	γ_{cmc} $(\pm 0.2\,mN.m^{-1})$	G_{min} $(kJ.mol^{-1})$	P
CPZ/C_{12}DmCB in water												
0	1.79		50.9	3.98	0.42	0.42	3.28	-25.63	-38.39	19.6	4.91	0.50
0.2	1.68	2.19	35.1	3.33	0.76	0.49	2.83	-25.78	-36.31	35.5	16.2	0.45
0.4	1.99	2.82	34.6	3.15	1.10	0.53	2.79	-25.36	-36.34	35.7	23.7	0.46
0.6	3.53	3.98	28.0	1.61	1.45	1.03	2.57	-23.94	-41.34	42.8	37.3	0.25
0.8	6.01	6.73	27.1	0.79	1.79	2.09	1.92	-22.62	-56.80	43.5	47.0	0.13
1.0	21.8		25.6	0.77	2.14	2.14	1.63	-19.43	-52.51	45.0	58.0	0.21
CPZ/C_{14}Ab in water												
0	0.10		38.2	7.33	0.23	0.23	4.27	-32.73	-37.94	32.7	4.45	0.92
0.2	0.11	0.13	37.3	5.02	0.61	0.33	4.18	-32.49	-39.93	33.9	12.4	0.66
0.4	0.19	0.17	34.6	3.50	0.99	0.47	3.92	-31.19	-41.07	36.6	21.8	0.48
0.6	0.36	0.25	35.2	3.64	1.37	0.46	3.73	-29.58	-39.25	36.1	29.9	0.51
0.8	1.04	0.50	34.1	2.86	1.75	0.58	3.19	-26.97	-38.90	36.8	38.9	0.42
1.0	21.8		25.6	0.77	2.14	2.14	1.63	-19.44	-52.51	45.0	58.0	0.21

Standard uncertainties in terms of cmc, Γ_{max}, A_{min}, π_{cmc}, ΔG_m^0, and pC_{20} are ± 0.01%, ± 0.04%, ± 0.04%, ± 0.03%, ± 0.02% and ± 0.03% respectively.

Table 3. Mole fractions of CPZ (α_{Cpz}), Micellar activity coefficients (f_1, f_2), Micellar mole fraction (X_1, X_2), Interaction parameter (β^R), Calculated critical micellar concentrations (cmc_{cal}) according to regular solution theory (RST), Ideal micellar mole fraction (X_{ideal}).

α_{CPZ}	f_1	f_2	X_1	X_2	β^R	$\beta^R_{ave.}$	cmc_{cal} (RST) mM	X_{ideal} (Motomura)
CPZ/C_{12}DmCB in water								
0.8	0.74	0.95	0.29	0.71	-0.58	-2.01	5.99	0.25
0.6	0.52	0.97	0.18	0.82	-0.97		3.53	0.11
0.4	0.16	0.86	0.22	0.84	-3.01		1.99	0.05
0.2	0.09	0.90	0.17	0.83	-3.48		1.68	0.02
CPZ/C_{14}Ab in water								
0.8	-	-	-		-			0.020
0.6	-	-	-		-			0.006
0.4	-	-	-		-			0.003
0.2	0.012	0.960	0.087	0.913	-5.32		0.112	0.001

The uncertainty limit of cmc_{cal}**(RST)**, X_1**(RST)**, β^R**(RST)**, f_1**(RST)** and f_2**(RST)** are ± 3, ± 3, ± 4, ± 5 and ± 5% respectively.

Table 4. Activity coefficients (f_1, f_2), Trial mole fraction (α^*), critical micellar concentrations according to Regular Solution Theory (cmc_{cal}), Interaction parameter (β), Nonideal Free Energy of Micellization (ΔG_m), Nonideal Entropy of Micellization (ΔS_m), Free Energy of Micellization for Ideal Mixing (ΔG_m^{ideal}), and $|T\Delta S_m/\Delta G_m|$ at Various Stoichiometric Mole Fractions of CPZ/C_{12}DmCB and CPZ/C_{14}Ab in water systems at different mole fraction of CPZ (α_{CPZ}) at 298.15 K.

α_{CPZ}/α_1	f_1	f_2	α^* (X_{SPB})	cmc_{cal} (RST) mM	β	G_{ex}/ H_{ex}/ ΔH_m kJ.mol^{-1}	ΔG_m kJ.mol^{-1}	ΔS_m J.K^{-1}mol^{-1}	ΔG_m^{ideal} kJ.mol^{-1}	$\left\|\frac{T\Delta S_m}{\Delta G_m}\right\|$
CPZ/C_{12}DmCB in water										
0.8	0.75	0.95	0.29	6.01	-0.58	-0.29	-1.79	0.005	-1.50	0.84
0.6	0.53	0.98	0.19	3.53	-0.97	-0.36	-1.55	0.004	-1.19	0.77
0.4	0.16	0.86	0.22	1.99	-3.01	-1.29	-2.62	0.004	-1.32	0.51
0.2	0.09	0.90	0.17	1.68	-3.48	-1.22	-2.35	0.004	-1.13	0.48
CPZ/C_{14}Ab in water										
0.8	2.32	1.000	0.008	0.51	0.86	0.02	-0.09	0.0004	-0.12	1.00
0.6	0.77	0.999	0.009	0.25	-0.26	-0.01	-0.14	0.0004	-0.13	0.93
0.4	0.07	0.996	0.040	0.16	-2.82	-0.27	-0.68	0.0014	-0.42	0.60
0.2	0.01	0.968	0.080	0.11	-5.13	-0.94	-1.63	0.0023	-0.69	0.42

The uncertainty limits of cmc_{cal} (RST), β, f, ΔH_m, ΔG_m, ΔS_m **and** ΔG_m^{ideal} are ± 3, ± 4, ± 2, ± 5, ± 5, ± 5 and ± 4% respectively.

Table 5. Time-Resolved Decay Parameter of CPZ/C_{12}DmCB and CPZ/C_{14}Ab systems at different mole fractions of CPZ.

α_{CPZ}	$\tau_1(ns)$	a_1	$\tau_2(ns)$	a_2	$\tau_{avg}(ns)$	χ^2
			CPZ/C_{12}DmCB			
0.0	1.71	1.00	-	-	1.71	1.03
0.1	1.67	1.00	-	-	1.67	0.97
0.2	1.65	1.00	-	-	1.65	1.14
0.3	1.69	1.00	-	-	1.69	1.05
0.4	1.63	1.00	-	-	1.63	1.11
0.5	1.59	0.84	2.39	0.16	1.71	1.07
0.6	1.63	0.90	5.29	0.09	1.98	1.18
0.7	1.59	0.82	4.94	0.18	2.20	0.99
0.8	1.59	0.71	5.41	0.29	2.68	1.13
1.0	1.59	0.72	6.08	0.27	2.81	1.00
			CPZ/C_{14}Ab			
0.0	1.70	1.00	-	-	1.70	1.06
0.1	1.63	1.00	-	-	1.63	0.99
0.2	1.62	1.00	-	-	1.62	0.99
0.3	1.66	1.00	-	-	1.66	0.92
0.4	1.61	1.00	-	-	1.61	1.09
0.5	1.60	1.00	-	-	1.60	1.24
0.6	0.13	0.29	1.64	0.70	1.19	1.09
0.7	0.18	0.48	1.63	0.52	0.93	1.25
0.8	0.58	0.15	1.68	0.42	0.79	1.16
1.0	1.59	0.72	6.08	0.27	2.81	1.00

The standard uncertainty of τ_{avg} is ± 5%.

Supporting Information

Synthesis and characterization of zwitterionic surfactant: N-Dodecyl-N,N′-dimethyl-2-ammonio-1-ethanecarbonate (1)

8.52 g (0.04 mole, 1 equiv.) of N, N′-Dimethyldodecylamine (**3**) was mixed with 5.1 g (0.044 mole, 1.1 equiv.) of sodium chloroacetate (**4**) in 50 mL methanol/water mixture (1:3, v/v) and was refluxed for overnight at 78-80°C. The solvent was removed in vacuo and the residue was dissolved in dry acetone and filtered to remove unreacted **4** and salt so formed. The filtrate was collected and the acetone was removed in *vacuo* to get the desired product **1** as a highly viscous and colourless liquid (Scheme 1).

Yield: (10.04 g, 93%). IR: 3417 (broad peak), 2919, 2851, 1620 cm^{-1}. ^{1}H NMR ($CDCl_3$, 400 MHz) δ (ppm): 0.90 [t, 3H, *J* 8Hz, **$\underline{CH_3}$**$(CH_2)_{11}$-], 1.27– 1.33 [m, 18H, CH_3**$\underline{(CH_2)_9}$**-CH_2-CH_2-], 1.70 [br s, 2H, $CH_3(CH_2)_9$-**$\underline{CH_2}$**-CH_2-N-], 3.29 (s, 6H, (**$\underline{CH_3}$**$)_2$N-), 3.56-3.58 (m, 2H, $CH_3(CH_2)_{10}$-**$\underline{CH_2}$**-N-), 4.36 [s, 2H, -N-**$\underline{CH_2}$**-COO-]. ^{13}C NMR (100 MHz) δ (ppm): 14.12, 22.72, 22.88, 26.51, 29.45, 29.74, 29.74, 29.75, 29.81, 31.97, 42.76, 51.32, 57.98, 64.06, 64.36, 167.72.

Scheme 1

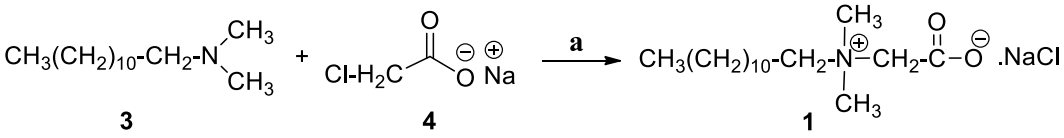

Scheme 1. Reaction condition, a: refluxed for overnight at 78-80°C in methanol/water mixture (1:3, v/v).

Synthesis and characterization of zwitterionic gemini surfactant 1,2-Bis[N-methyl-N-carboxymethyltetradecylammonium] ethane (2):

Zwitterionic gemini surfactant 2 was prepared via 2 steps (a & b) as follows:

a. Synthesis of N, N′-dimethyl-N, N′-bis-(tetradecyl)-ethylenediamine (**5**)

To a stirred solution of N, N′-Dimethylethylenediamine (**6**, 0.025 mol, 2.2 g, 1 eq.v.) in 20 mL dry ethanol, 1-bromotetradecane (**7**, 0.055 mol, 16 g, 1.1 equivalent) and 3 g NaOH were added and the resulting mixture was refluxed for overnight at 78℃. The resulting solution was filtered to remove the inorganic salt so formed. The filtrate was quenched with 10 mL conc. hydrochloric acid, yielding hydrochloride salt of N, N′-Dimethyl-N, N′-bis-(tetradecyl)-ethylenediamine (**5**) as a white solid. After washing the solid with chloroform, it was dissolved in 30 mL 10% aqueous NaOH solution at room temperature. The upper organic layer was collected and washed three times with brine. It was then dried in vacuum to get the desired product **5** as a white solid (Scheme 2).

Yield: (11.65 g, 78%). IR: 2955, 2932, 2852, 1470 cm^{-1}. ^1H NMR ($CDCl_3$, 500 MHz) δ (ppm): 0.90 [t, 6H, *J* 8 Hz, 2C**H**$_3$$(CH_2)_{11}$-], 1.27- 1.33 [m, 44H, 2CH_3**(CH$_2$)$_{11}$**CH_2-], 1.44- 1.48 [m, 4H, 2$CH_3(CH_2)_{11}$**CH$_2$**CH_2N-], 2.25 [s, 6H, 2CH_2N**CH$_3$**], 2.31- 2.34 [t, 4H, *J* 4.5 Hz, 2$CH_3(CH_2)_{11}CH_2$**CH$_2$**N] and 2.46 [s, 4H, N**CH$_2$CH$_2$**N].

Scheme 2

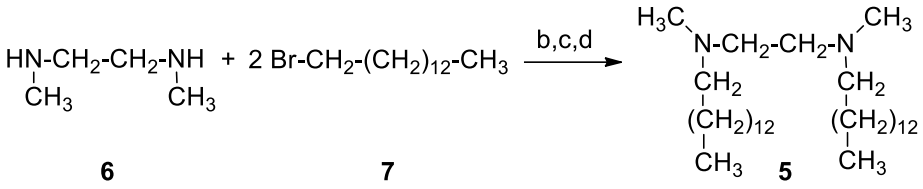

Scheme 2. Reaction condition b: NaOH/ refluxed for overnight in dry EtOH at 78°C; c: concentrated HCl; d: 10% NaOH at room temperature.

b. Synthesis of 1,2-bis[N-methyl-N-carboxymethyltetradecylammonium] ethane (2)

To a stirred solution of 2-bromoacetic acid (0.05 mol, 7 g) in 50 mL methanol, NaOH (0.05 mol, 2 g) was added in batches under an ice bath. The temperature of the reaction bath was then slowly raised to 50°C and then cooled to room temperature after 30 min. Afterwards, N, N$^/$-dimethyl-N, N$^/$-bis-(tetradecyl)-ethylenediamine (**5**) (0.025 mol, 2 g) and 0.4 g KI were added dropwise to the reaction mixture. The mixture was refluxed for 4 days, then cooled to room temperature and filtered to remove insoluble materials. The filtrate was evaporated under reduced pressure. The residue was then dissolved in 20 mL of 2-propanol and was filtered. The filtrate after crystallization gave the desired product 1,2-bis[N-methyl-N-carboxymethyltetradecyl-ammonium] ethane (**2**) as a colourless solid (Scheme 3).

Yield: (7.55 g, 53%). IR: 3435 (broad peak), 2920, 2851, 1627 cm^{-1}. ^1H NMR (CD_3OD, 400 MHz): δ 0.80 [t, 6H, *J* 8 Hz, 2(**CH$_3$**$(CH_2)_{13}$-)], 1.19–1.31 [m, 44H, 2(CH_3**(CH$_2$)$_{11}$**-CH_2-CH_2-)], 1.70 [m,

4H, 2($CH_3(CH_2)_{11}$-**CH_2**-CH_2-N-)], 3.22 [s, 6H, 2(**CH_3**N-)], 3.53 [m, 4H, 2($CH_3(CH_2)_{12}$-**CH_2**-N-)], 3.80 [s, 4H, -N**CH_2CH_2**N-], 4.19 [s, 4H, 2(-N-**CH_2**-COO-)]. ^{13}C NMR (100 MHz) δ (ppm): 13.08, 20.87, 22.09, 22.34, 26.01, 28.87, 29.08, 29.21, 29.27, 29.36, 29.40, 31.67, 48.83, 53.09, 61.33, 61.49, 63.76, 167.03.

Scheme 3

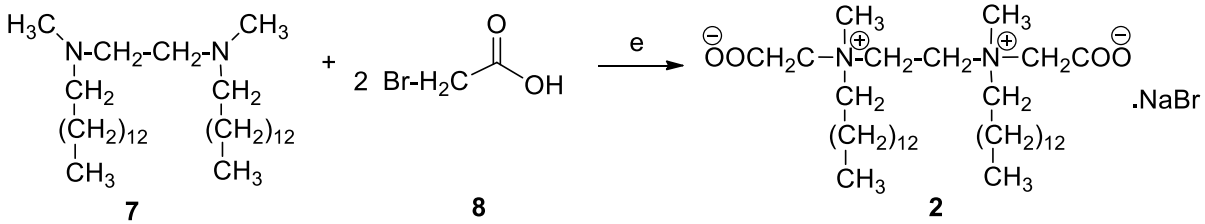

Scheme 3. Reaction condition, e: NaOH & KI/ refluxed for 60 h in MeOH.

FT-IR spectrum of zwitterionic surfactant: N-Dodecyl-N,N-dimethyl-2-ammonio-1-ethanecarbonate (1)

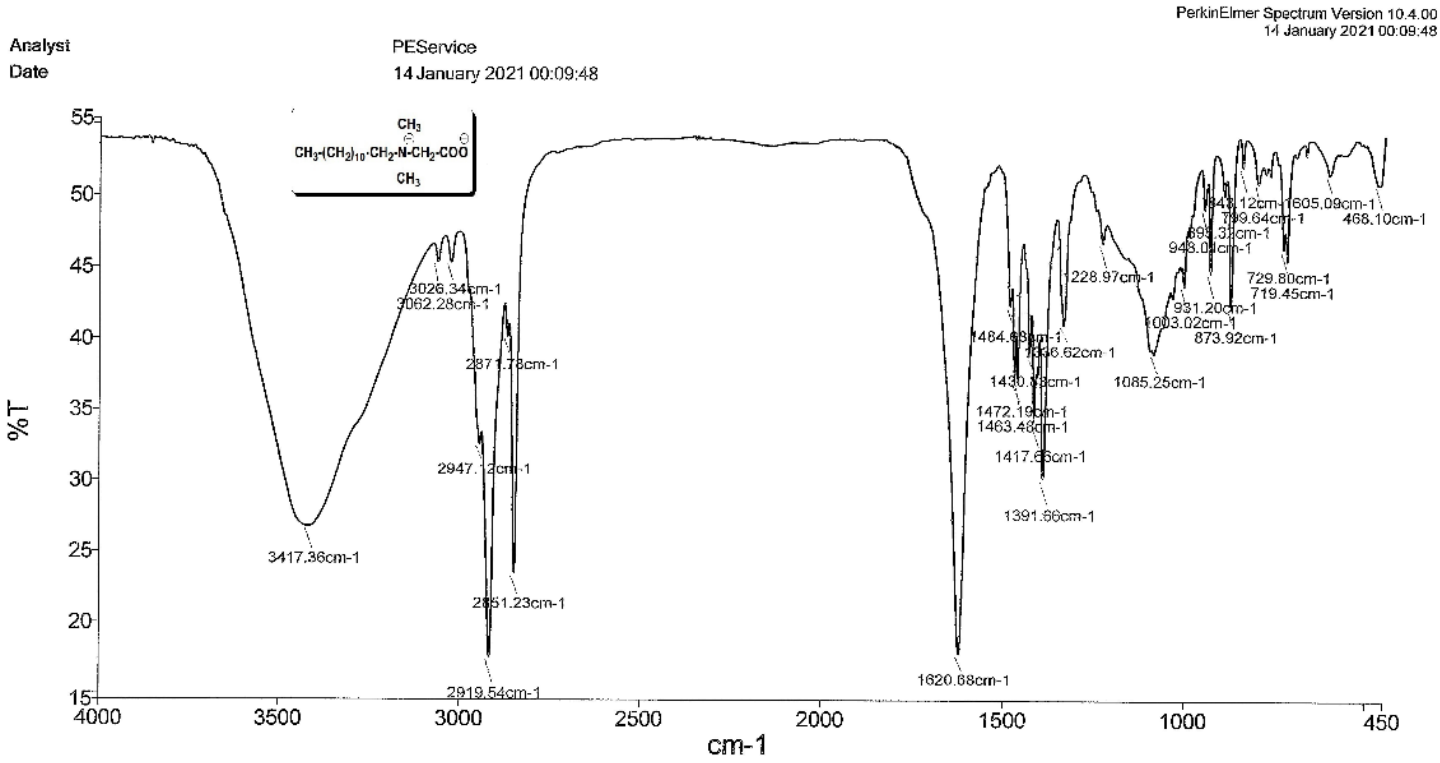

FT-IR Spectrum of N-Dodecyl-N,N-dimethyl-2-ammonio-1-ethanecarbonate

^{1}H-NMR spectrum of zwitterionic surfactant: N-Dodecyl-N,N-dimethyl-2-ammonio-1-ethanecarbonate (1)

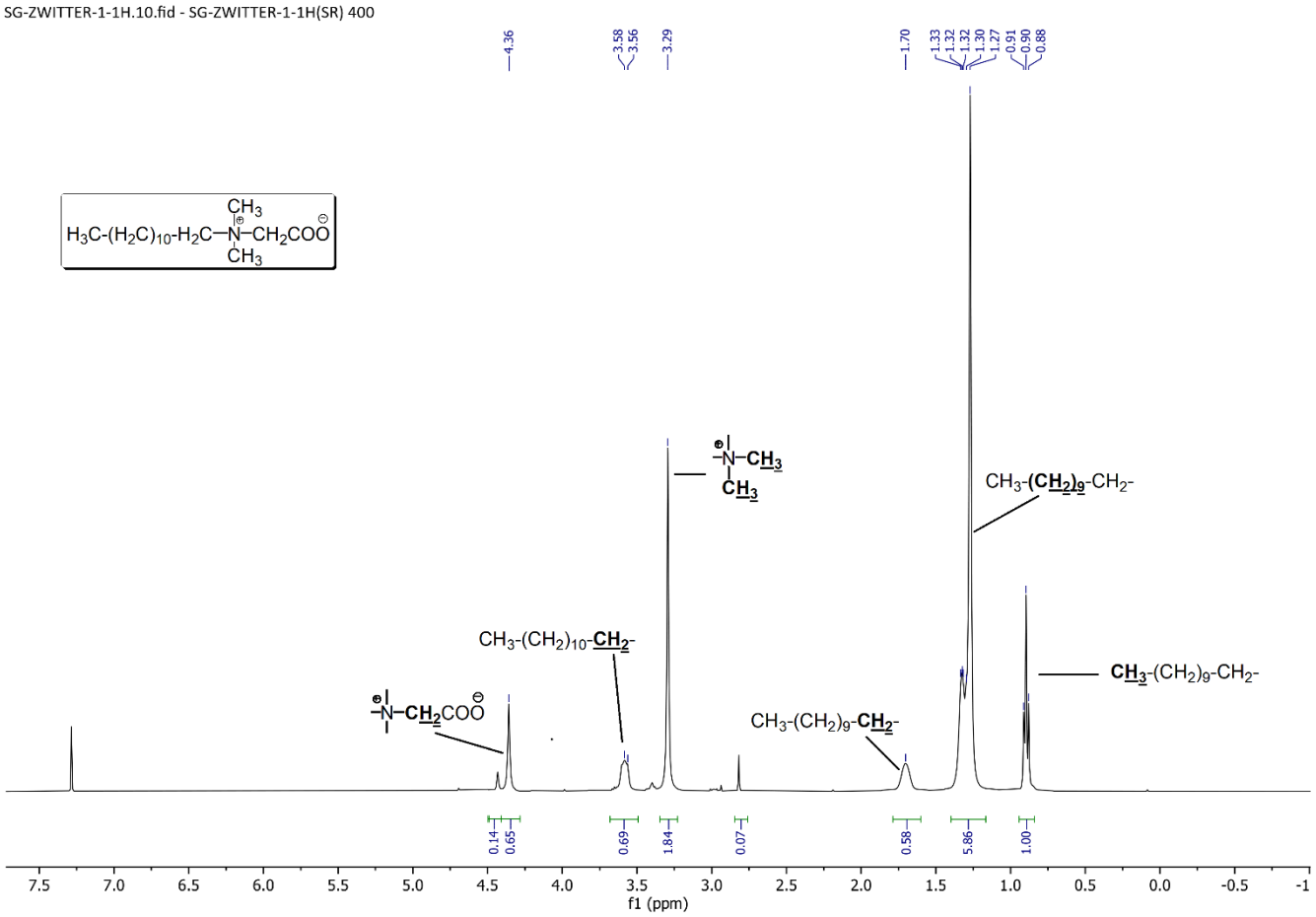

^{13}C-NMR spectrum of zwitterionic surfactant: N-Dodecyl-N,N-dimethyl-2-ammonio-1-ethanecarbonate (1)

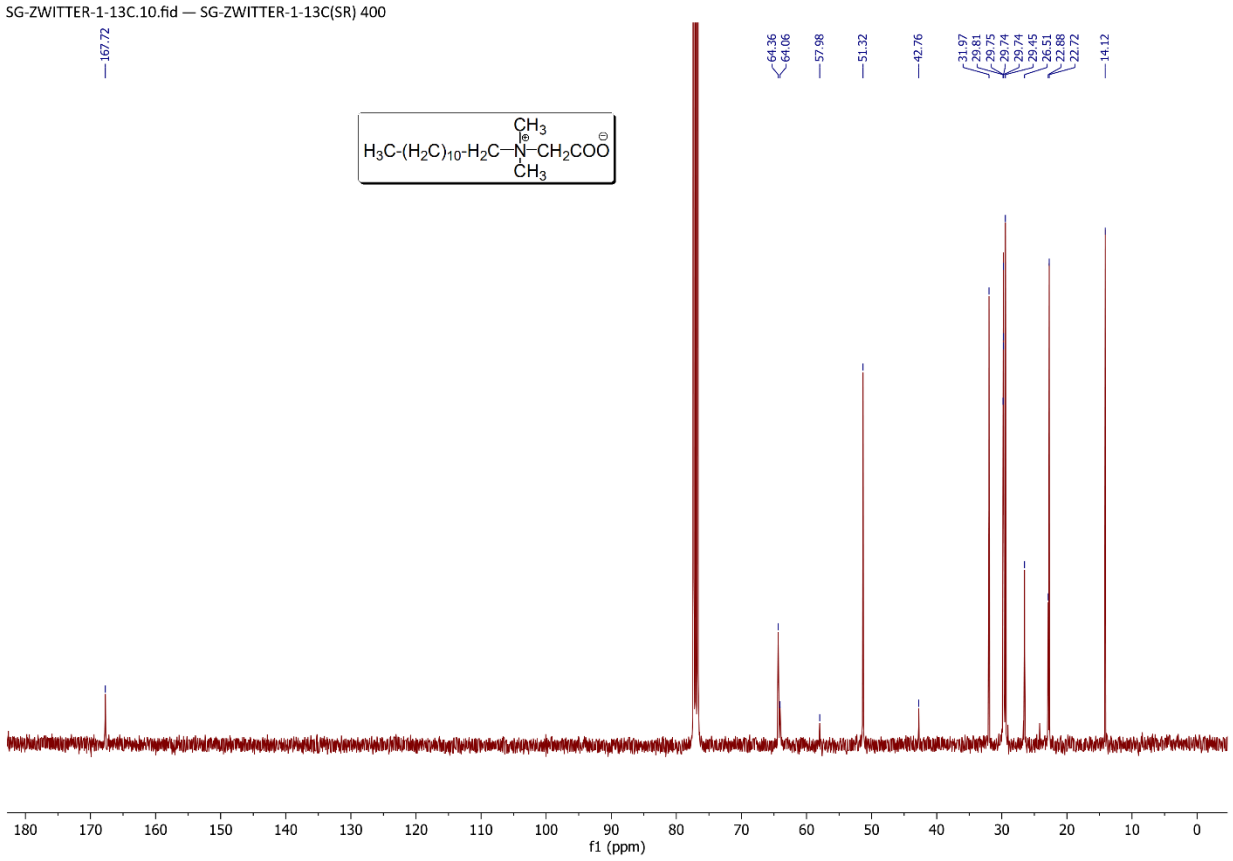

Synthesis and characterization of zwitterionic gemini surfactant 1,2-Bis[N-methyl-N-carboxymethyltetradecylammonium] ethane (2):

FT-IR spectrum of N, N/-dimethyl-N, N/-bis-(tetradecyl)-ethylenediamine (5)

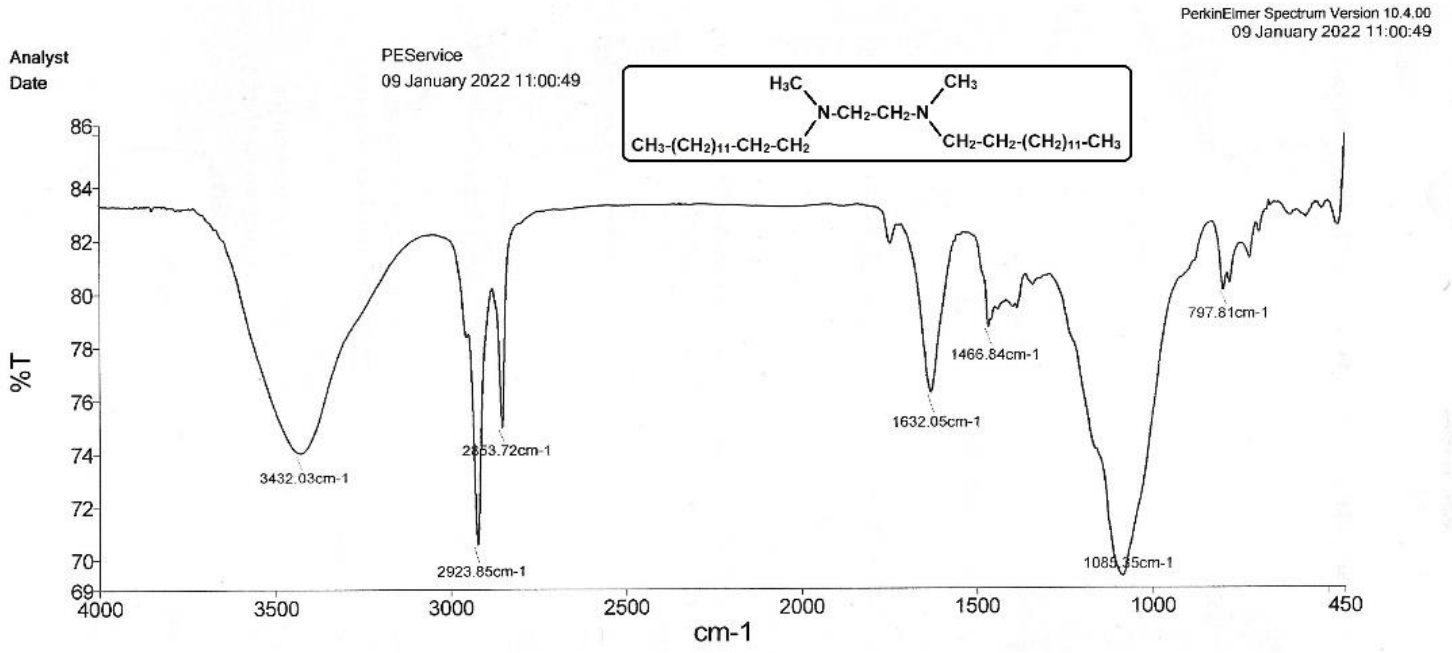

^{1}H-NMR spectrum of N, N$^{/}$-dimethyl-N, N$^{/}$-bis-(tetradecyl)-ethylenediamine (**5**)

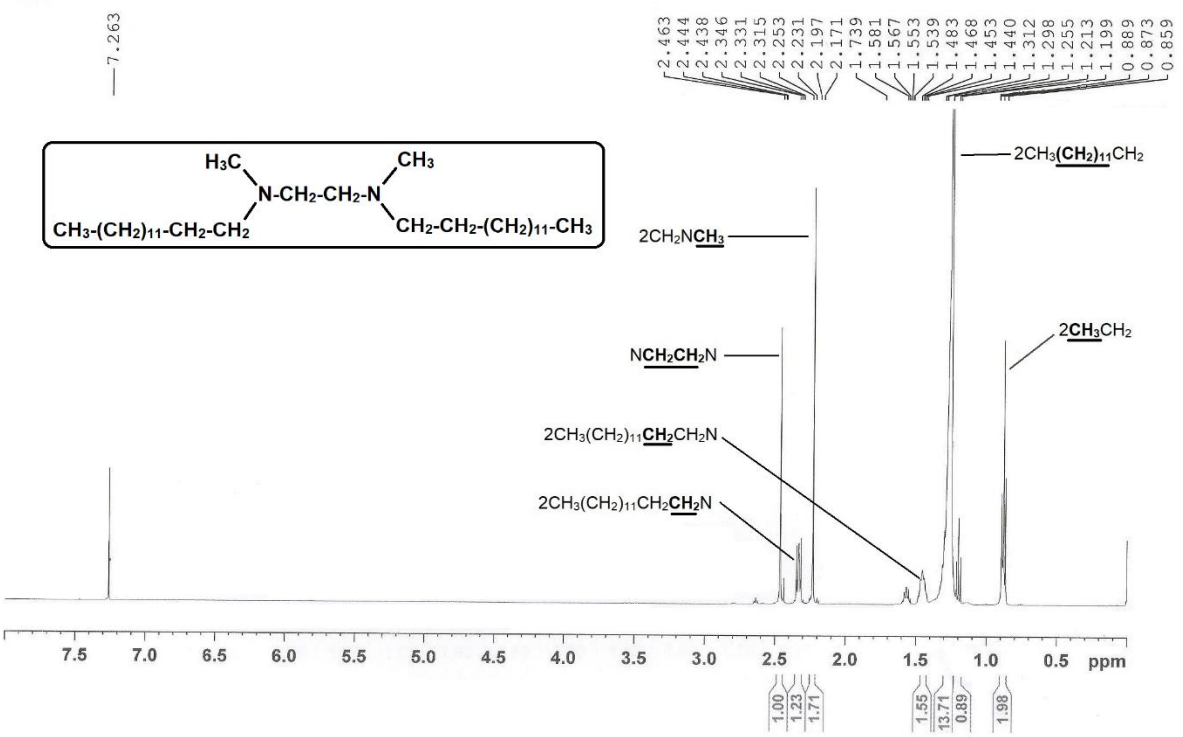

b. Synthesis of 1,2-bis[N-methyl-N-carboxymethyltetradecylammonium] ethane (2)

FT-IR spectrum of 1,2-bis[N-methyl-N-carboxymethyltetradecylammonium] ethane (2)

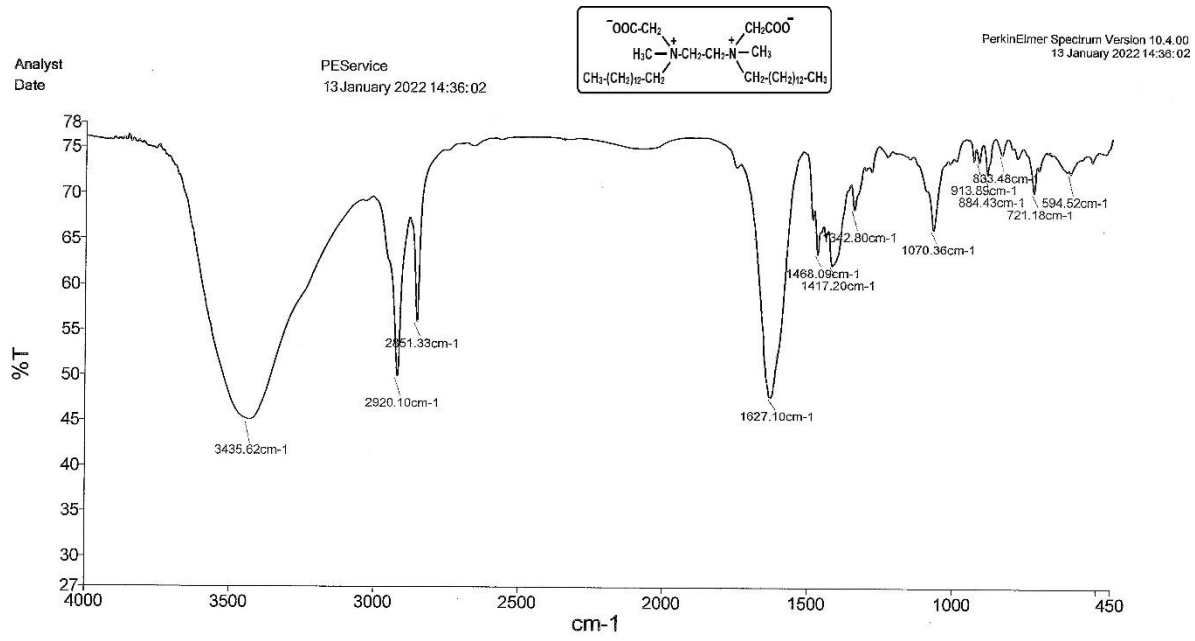

FT-IR of N,N/-Dimethyl-N,N/-bis-(tetradecyl)-ethylenediamine

^{1}H-NMR spectrum of 1,2-bis[N-methyl-N-carboxymethyltetradecylammonium] ethane (2)

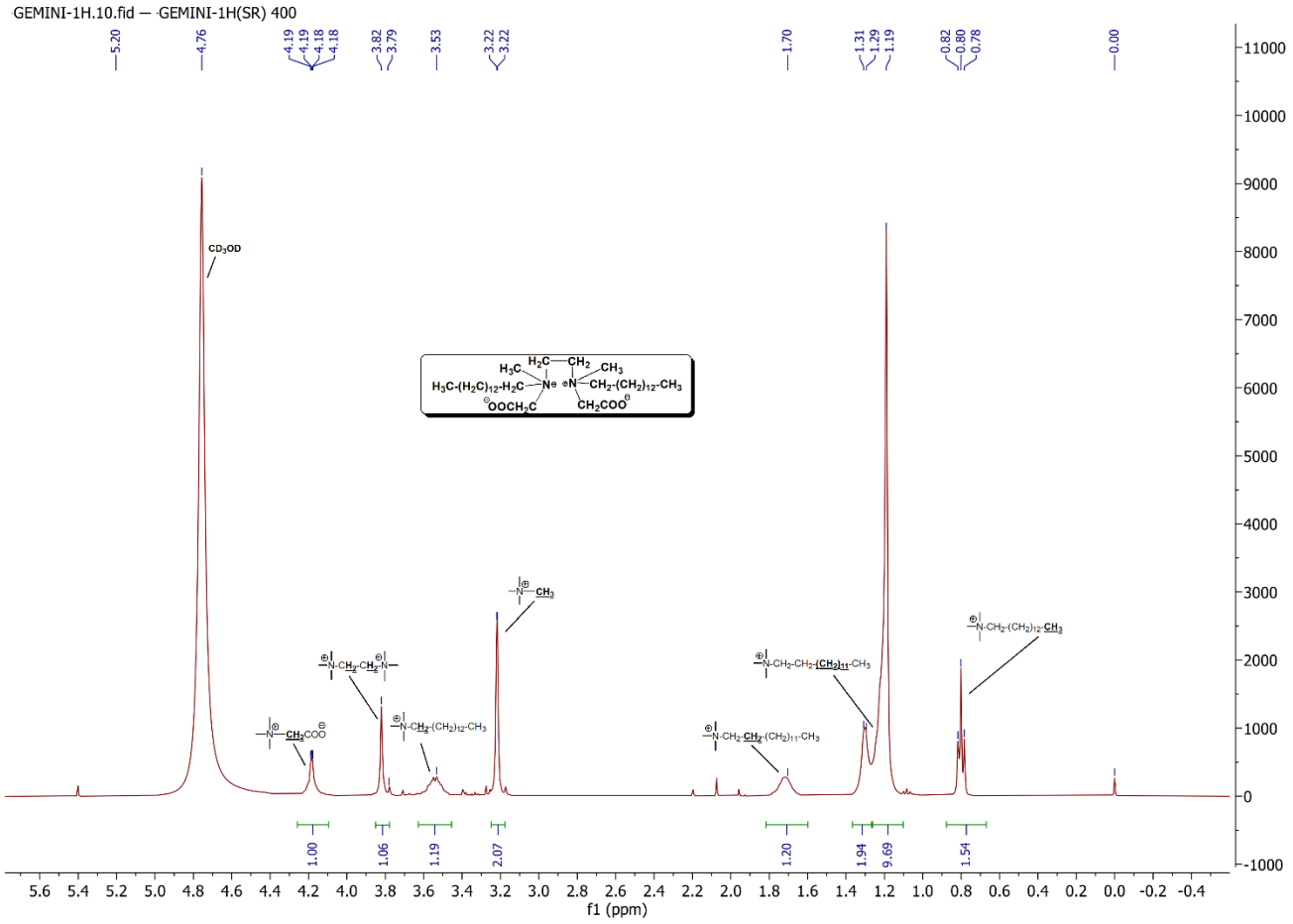

^{13}C-NMR spectrum of 1,2-bis[N-methyl-N-carboxymethyltetradecylammonium] ethane (2)

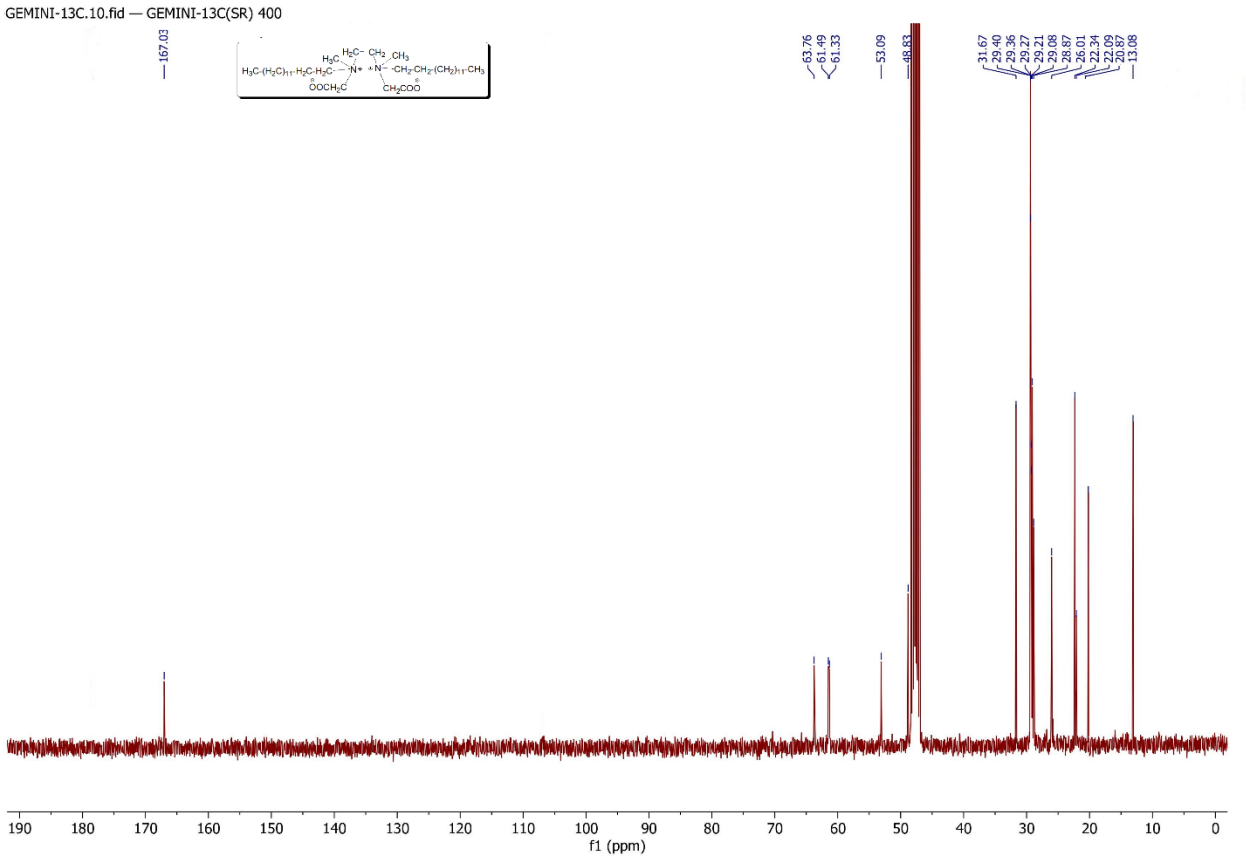

Dynamic light scattering (DLS) size distribution plots of CPZ/C_{12}DmCB system

$\alpha_{CPZ} = 0$

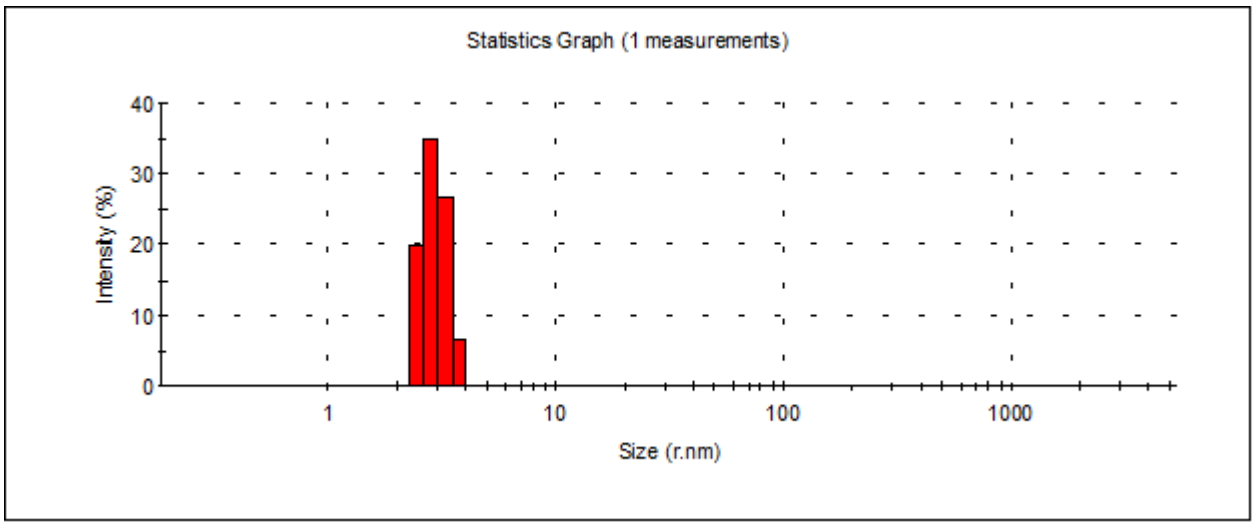

$\alpha_{CPZ} = 0.2$

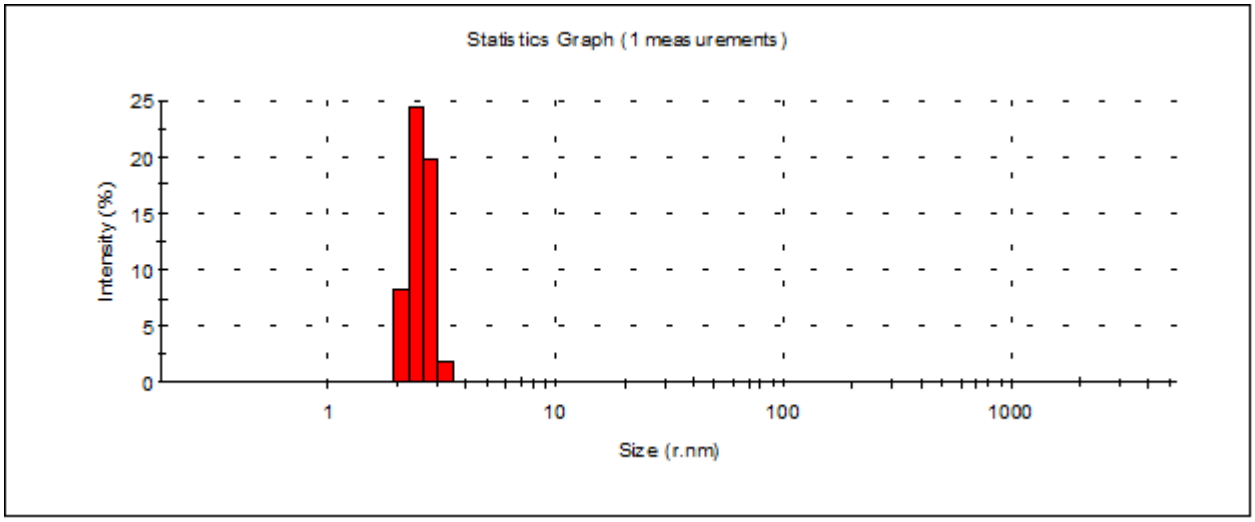

$\alpha_{CPZ} = 0.6$

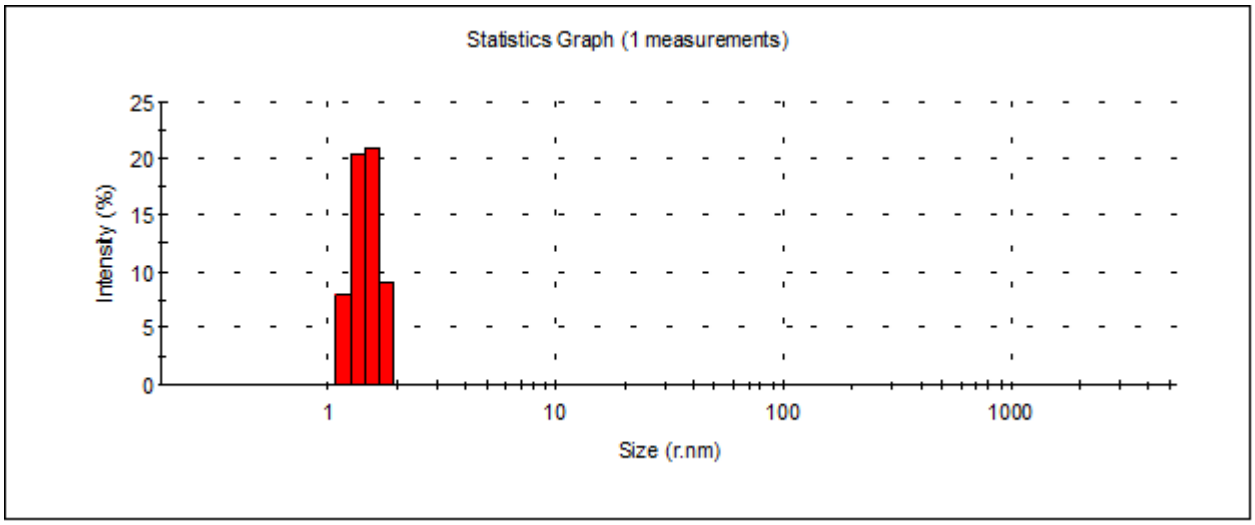

$\alpha_{CPZ} = 0.8$

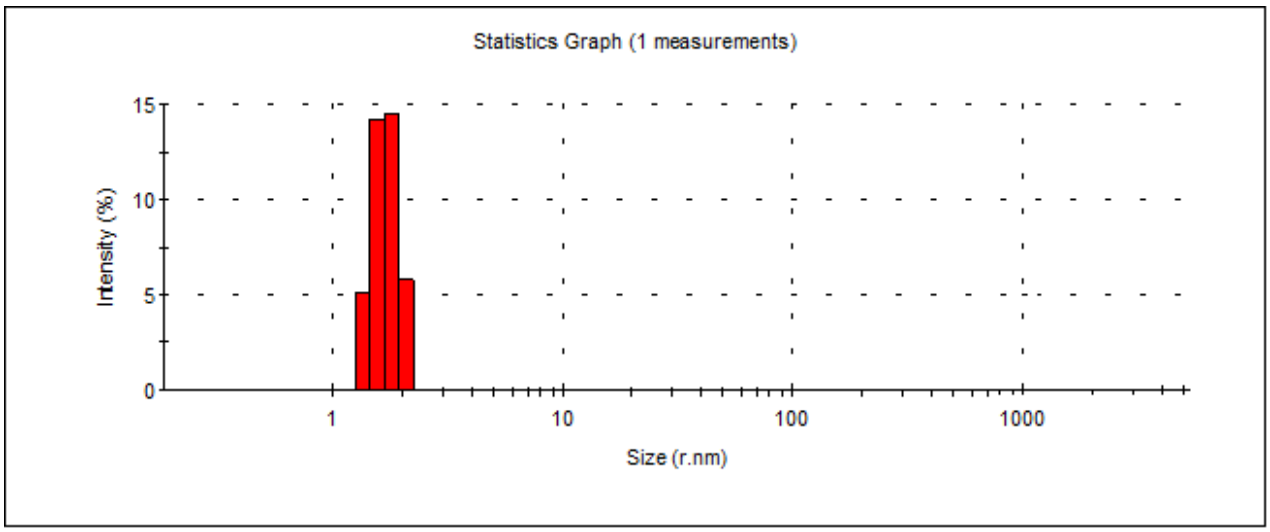

Dynamic light scattering (DLS) size distribution plots of CPZ/C_{14}Ab system

$\alpha_{CPZ} = 0$

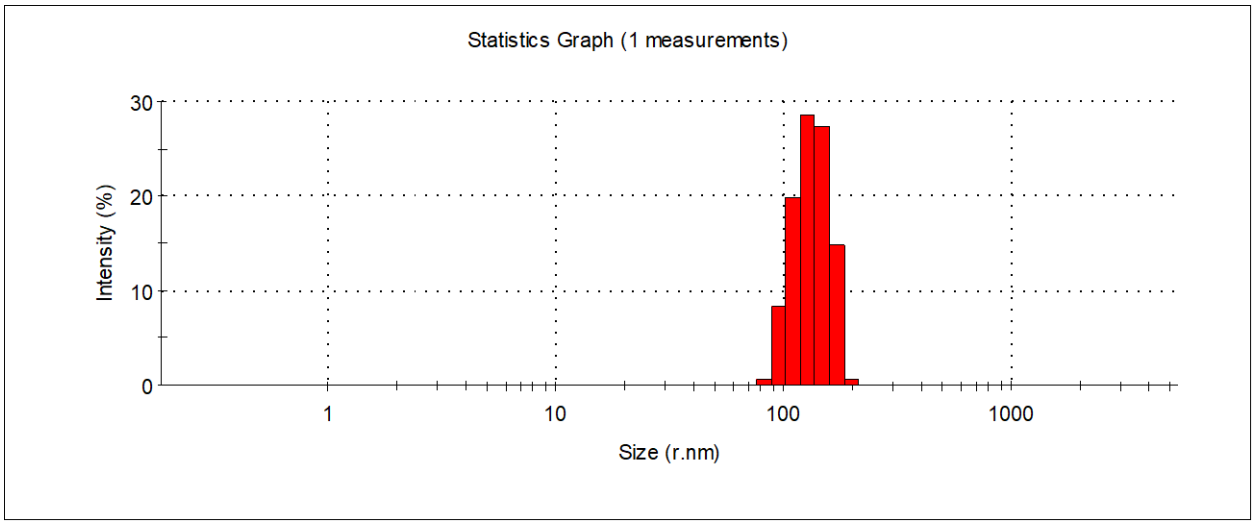

$\alpha_{CPZ} = 0.1$

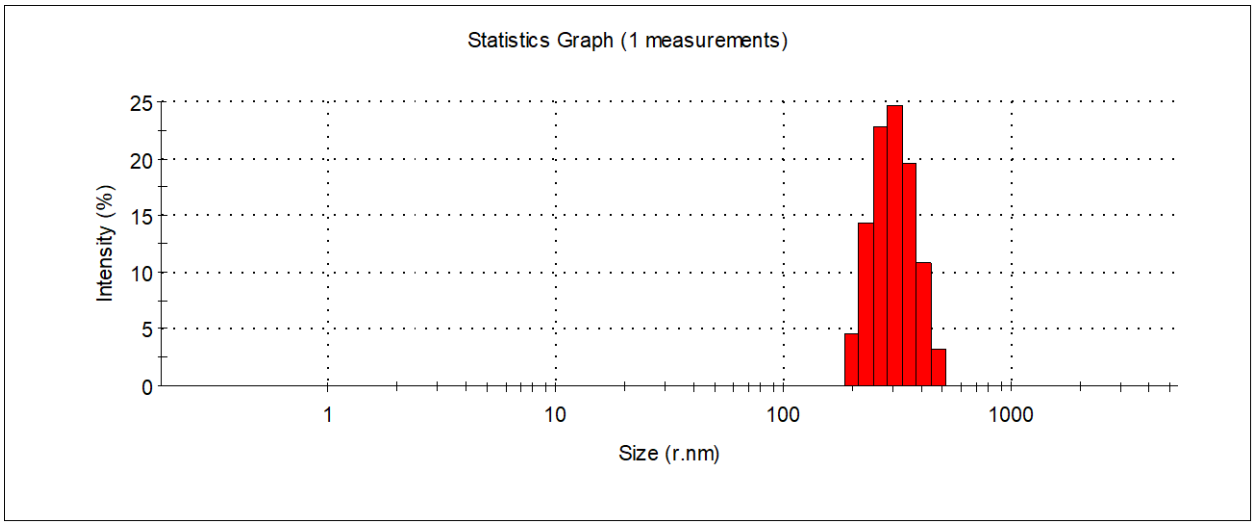

$\alpha_{CPZ} = 0.2$

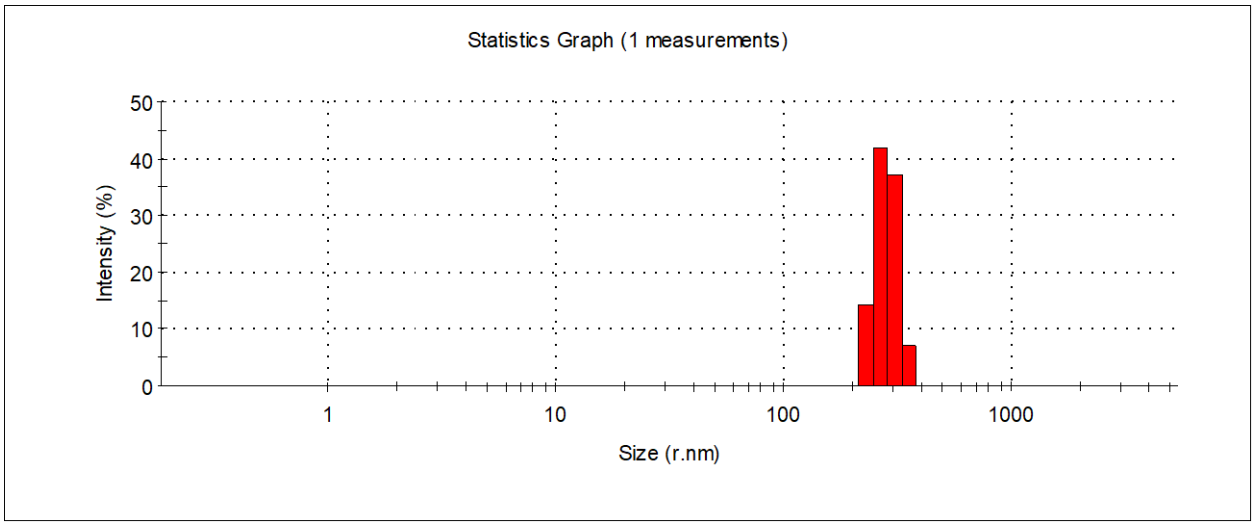

$\alpha_{CPZ} = 0.4$

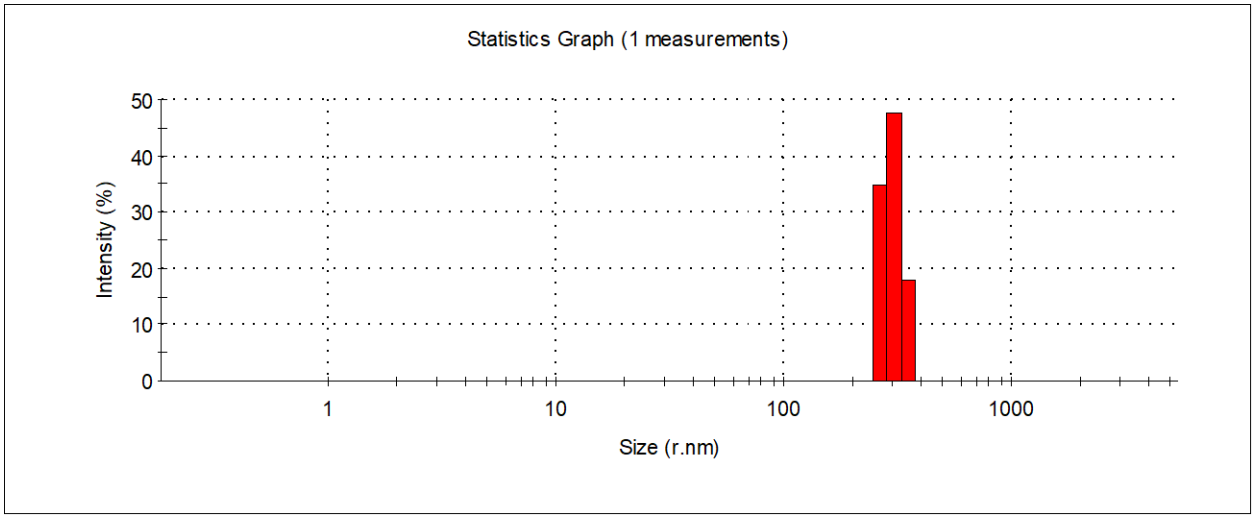

$\alpha_{CPZ} = 0.5$

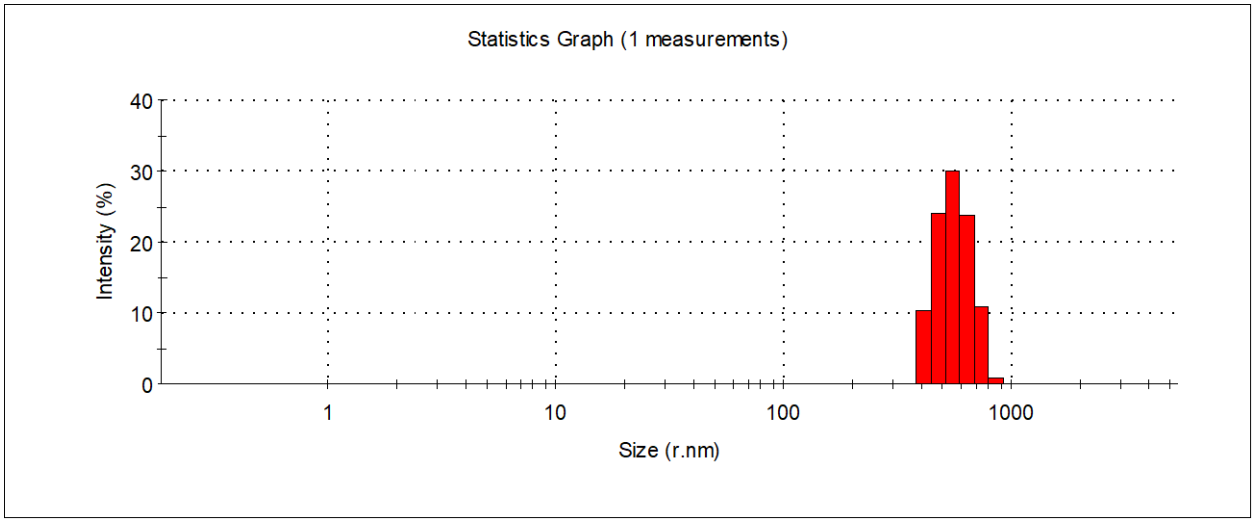

$\alpha_{CPZ} = 0.6$

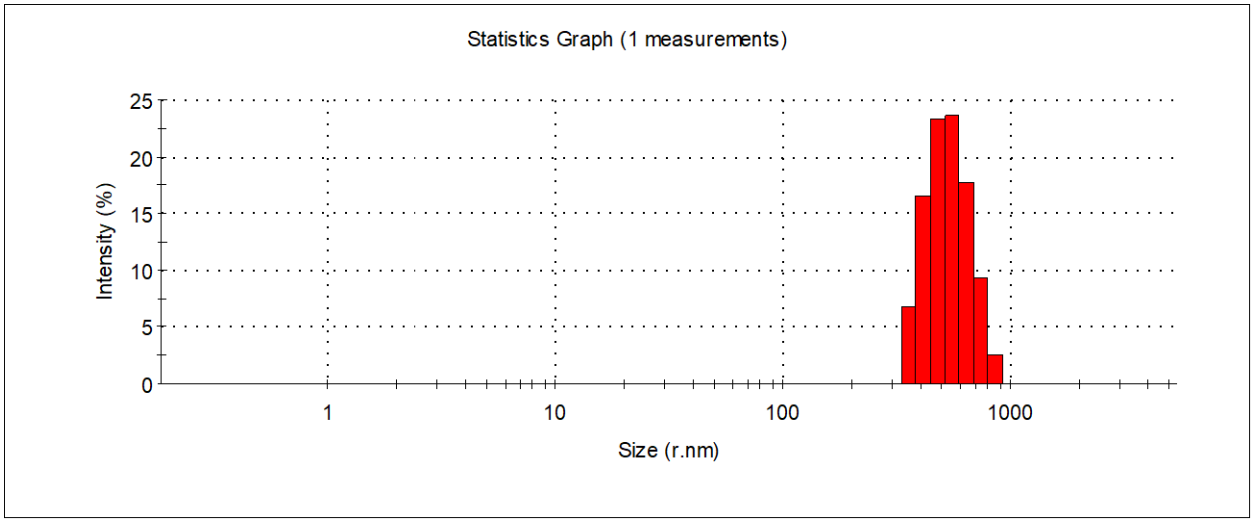

$\alpha_{CPZ} = 0.8$

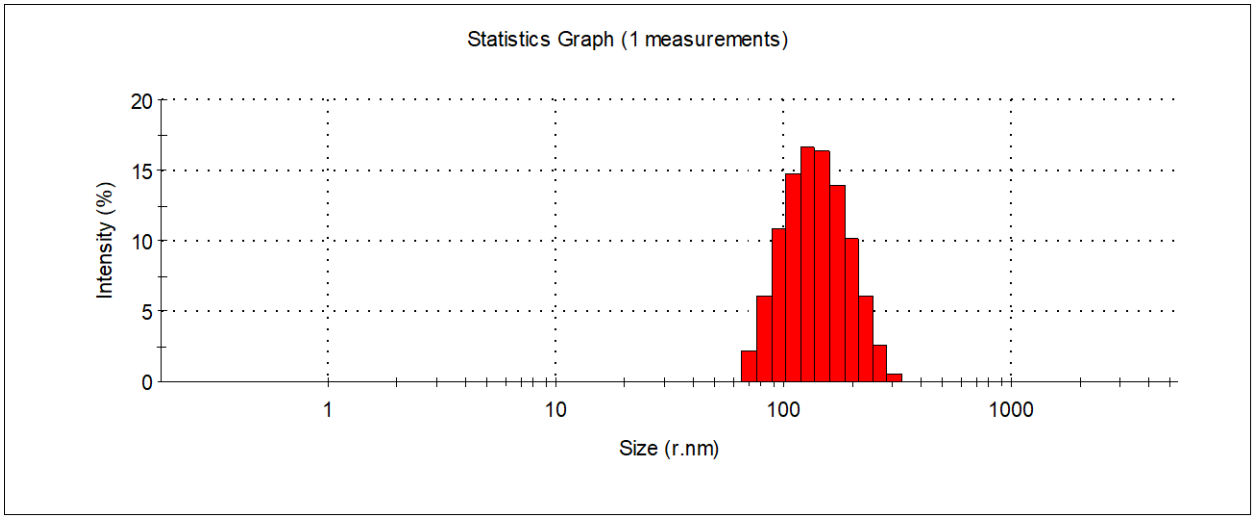

$\alpha_{CPZ} = 1.0$

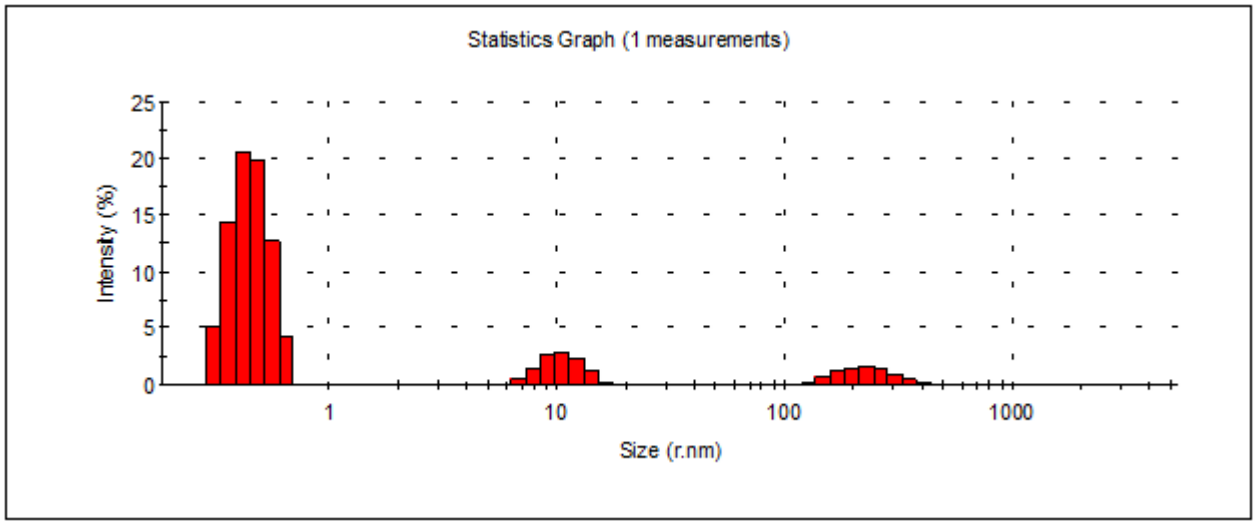

Chapter-II

Comparative Study of the Aggregation behaviour of some ionic surfactants with non-ionic Triton X-114 in water and water-TFE mixture

Comparative Study of the Aggregation behaviour of some ionic surfactants with non-ionic Triton X-114 in water and water-TFE mixture ‡

Abstract

The influence of 2,2,2-trifluoroethanol (TFE) on the micellar properties of ionic surfactants hexadecyltrimethylammonium bromide (CTAB), hexadecyltrimethylammonium p-toluenesulfonate (CTAT), sodium dodecyl sulfate (SDS), N-lauroylsarcosine sodium salt (SDDS) and non-ionic surfactant Triton X-100 (TX-100) in aqueous solutions was studied using tensiometry, electrical conductivity, fluorimetry, time-resolved fluorescence study and microcalorimetry. With increasing concentrations of TFE, the micellar charge densities of the ionic head groups decrease causing a decrease in CMC of ionic-surfactant solutions (SDS, SDDS, CTAB, and CTAT) in micellar solutions. However, for non-ionic surfactant TX-114, the polar head group undergoes some conformational changes causing an increase in the value of CMC. Time-resolved fluorescence decay measurement was done to get evidence of penetration of TFE molecules into the stern layer of the micelle. The micellar aggregation number declines with increasing concentration of solvent indicating higher concentration of mixed solvent reduces the number of monomers needed for micellization for ionic surfactants whereas for non-ionic TX-114 it indicates some structural changes of the molecule forming the micelle in the presence of TFE.

(‡ Published in *Industrial & Engineering Chemistry Research 2024 63 (7), 3057-3071*)

1. Introduction

In recent years, a broad community of surface chemists has shown a great deal of scientific interest in the physicochemical modifications of surface-active agents in an attempt to improve the functionality of surfactant formulations. In this context, various additives, including salts[1], solvents [2], polymers,[3] drugs,[4] etc., have been introduced to the micellization environment of amphiphilic systems to achieve the desired features with various industrial importance in cosmetics,[5] food products,[6] enhanced oil recovery,[7] and pharmaceuticals.[8] Among all the additives, non-aqueous alcohol solvents have been examined the most in amphiphile-water-solvent ternary systems using both theoretical and experimental approaches.[9-17] The exceptional solubilizing and hydrogen bonding potential of alcohols distinguish them as solvents of choice.[18] Moreover, alcohols possess a dual character of serving as either cosurfactants or cosolvents as a motif to modify the critical

micelle concentration (CMC) in the self-assembly of amphiphilic systems.[19] The present study has opted to use 2,2,2 trifluoroethanol (TFE), a fluorinated alcohol,[20,21] due to its great demand as a cosolvent in molecular biology, particularly during the denaturation process of proteins.[22,23] More importantly, TFE has been extensively reported in the literature in elucidation of the secondary structures of biological macromolecules, including polypeptides and proteins.[24,25] The presence of electron-withdrawing trifluoromethyl (CF_3) group in TFE imparts unique qualities as a solvent compared to other conventional alcohols.[26-28] TFE has the advantage of being highly soluble in water, irrespective of having a hydrophobic -CF_3 terminal. Fatima et al.[29] has performed a comparative analysis to investigate the effects of TFE and ethanol solvents on the thermal stability of an ionic liquid [EMIM][DCA]) in TFE/ethanol binary mixture. TFE has been reported as a solvent medium in many organic synthesis reactions.[30,31] Nevertheless, there has not been substantial attention on surfactant aggregation in TFE solvent.[32,33]

Surfactants[34,35] also known as surface-active agents, are widely recognized for their ability to self-assemble into various shaped micellar-like aggregates (usually spherical) in liquid medium at and above a certain concentration, which is referred to as the critical micelle concentration (CMC). The most important feature of amphiphilic systems, which accounts for their distinct properties in solution, is the coexistence of hydrophilic head and hydrophobic tail moieties in a single molecule. According to the charge of the hydrophilic moiety, surfactants have been categorized as cationic,[36] anionic,[37] non-ionic[38] and zwitterionic.[4]

Cationic surfactants contain positive charged head groups (alkyl quaternary ammonium salts, amine salts, amine oxides, phosphonium salts, etc.) along with negatively charged counterions (mostly Cl^- and Br^-).

Anionic surfactants hold negatively charged head groups and positively charged counterions. Head groups may be alkyl-sulfates, sulfosuccinates, carboxylates, N-acyl amino acids, sulfonates, etc. Counterions may be positively charged alkali metal ions (Na^+/K^+) or quaternary ammonium cations.

Nonionic surfactants possess no electrical charges. These are miscible in water due to the presence of polar functionality present in their structures. Polyoxyethylenes, alkylpolyglucosides, polyglycidols, N-based glucamine surfactants belong to this class.

Zwitterionic surfactants contain both positive and negative charged centers. The origin of positive charge is contributed generally by ammonium ions and negative charge by sulfates, sulfonates, carboxylate ions. Depending upon the variation of pH they can be used either as cationic or anionic surfactants. Imidazole derivatives, betaines and phosphatides belong to this class.

Ionic surfactants can form an ordered self-assembled structure accomplished by small and strongly hydrophilic head groups at the interface whereas, non-ionic surfactants having long and weakly hydrophilic head groups form a disordered layer.

Lately, a novel class of non-conventional gemini surfactants, also referred to as dimeric or bis-surfactants, have come into the light of colloid science, which are comprised of two hydrophobic and two hydrophilic moieties.[39,40] Combinations of specific alcohols and surfactants are capable of working in collaboration to improve individual performance.[41] In order to solubilize membrane proteins for structural analysis, surfactants are utilized. Selecting the proper surfactant or combination of surfactants that replicates the native lipid bilayer and stabilizes protein folding is an important step in determining the structure of membrane proteins.[42-44] Keeping in mind the utility of TFE in protein chemistry, the change in the physicochemical properties of surfactant solutions mediated by TFE is interesting to study from an overall perspective.

In this article, a comparative study of the micellization behaviour of non-ionic Triton X-114 with conventional cationic hexadecyltrimethylammonium bromide (CTAB), hexadecyltrimethylammonium p-toluenesulfonate (CTAT) and anionic sodium dodecyl sulfate (SDS), N-lauroylsarcosine sodium salt (SDDS) surfactants has been performed using different techniques, such as tensiometry, conductometry, steady state and time resolved fluorimetry and microcalorimetry. In the literature, such comparative discussions taking special emphasis on uncharged surfactants in the light of charged surfactants are rare. The polar protic solvent TFE has been found to modify the solution properties of the surfactants in an attractive and beneficial way. Kumar et al.[45] has observed that 1-octanol can promote higher-order transitions in CTAB micelles (ellipsoidal → rodlike → wormlike). In a similar study, Patel et al.[46] has reported rodlike CTAT micelle to vesicle transition in 1-hexanol solvent. Mahbub et al.[47] has examined the effect of aqueous alcohol (methanol and ethanol) solvent on CTAB-SDS mixed micelles. Recently, our research group investigated the solvency effect of TFE on HEC-SDDS system to enhance the hydrophobicity of the medium.[48] For non-ionic surfactants, cloud point (CP) is the most important

physical parameter. An extensive literature survey finds that alcohols can have an impact on clouding development.[49,50] The non-ionic Triton X-114 (TX-114) is widely used commercially. [51-53] The micellar properties of the Triton X family mainly depend on the oxyethylene unit (EO). The length of the polar $(EO)_n$ head group (where n denotes the number of oxyethylene units) influences strongly the micellar properties.[54] Here, several thermodynamic parameters of micellization have been presented to simplify the comparative study. The deliberate construction of these conjugates aligns with our motif in this work. Each of the observations that are highlighted is a novel undertaking.

Although there are complexities of interpretation in the systems studied, the conclusive results may be beneficial in understanding similar biological systems including proteins and polypeptides. Throughout extensive research, the mechanisms underlying the interaction between TFE and proteins still remain somewhat unclear. Moreover, there are a lot of unsolved questions regarding the protein-surfactant binding processes. The aggregation of surfactants in TFE medium can be a useful model for protein-TFE as well as protein-surfactant interaction behaviors.

2. Experimental procedures

2.1. Materials and methods

Sodium dodecyl sulfate (SDS) (purity ≥ 98.5%), N-lauroylsarcosine sodium salt (SDDS) (purity ≥ 97%), hexadecyltrimethylammonium bromide (CTAB) (purity ≥ 98%) hexadecyltrimethylammonium p-toluenesulfonate (CTAT) (purity ≥ 98.5%) and Triton X-114 (TX-114) were purchased from Merck, India. 2,2,2-Trifluoroethanol (purity 99%) was bought from SRL, India. Cetylpyridinium chloride monohydrate (CPC) (purity 98%), Coumarin 153 **(**purity ~ 99%**)** and pyrene (purity ≥ 98%) were also purchased from Merck, India. Pyrene was recrystallized before use.

2.1.1. Tensiometry

Surface tension measurements were done using Krüss (Germany) tensiometer applying ring detachment process. Concentrated stock solution (~15 times of the CMC) of surfactants in aqueous and TFE/water medium at a particular volume was added to the respective medium with a Hamilton micro syringe keeping 5 min time for equilibration before each of the measurements. Measurements were done thrice to check reproducibility. The accuracy of the method was found to be ± 0.1 $mN.m^{-}$

[1]. To obtain the CMC, Surface tension (γ) vs. log [surfactant] was plotted and from the break points in the plot desired CMC values were obtained.

2.1.2. Electrical Conductivity Measurements

The electrical conductivity measurements were done with Eütech (Singapore) with cell constant = 1 cm^{-1}. The temperature of the solution was kept constant at 298 K with a water bath with the accuracy of ± 0.1 K. 6 mL of solvent was placed in a container and surfactant solution prepared in the particular solvent (∼15 times of the CMC) was added gradually using a Hamilton micro syringe. The value of specific conductance (κ) was recorded after each addition followed by uniform mixing. Each measurement was repeated thrice and the average value was recorded with an uncertainty within ± 2 μS. The CMC values were obtained from the break points in the specific conductance (κ) vs concentration of surfactant plots.

2.1.3. Preparation of pyrene solution

Pyrene (purity ≥ 98%) purchased from Merck, India was used here after recrystallization. 1 mM of a stock solution of pyrene was prepared in absolute ethanol and sonicated properly to dissolve. The stock solution was used in the experiment where the final concentration of pyrene in the surfactant solution is $\sim 10^{-6}$ (M).

2.1.4. Fluorimetry

Fluorescence measurements were performed using a Perkin Elmer LS55 fluorescence spectrophotometer. The temperature was kept constant at 298 K using a water-flow thermostat which is connected to the internal cell compartment. The concentration of surfactant solutions was used above the CMC. The excitation of pyrene was done at 332 nm and emission spectra were recorded at 373 and 384 nm which correspond to its first and third vibrational peaks, respectively. The slits used in excitation and emission were 9 and 4 nm, respectively. A scan speed of 250 nm per minute was used. The values of aggregation number (N_{agg}) were determined by a fluorescence quenching method of pyrene using (CPC) as a quencher. The pyrene solution was added to the individual solutions of surfactants and its concentration was kept low enough (~ 10^{-6} (M)) to avoid its excimer formation. The quencher was added gradually and the intensity was recorded for further analysis.

2.1.5. Microcalorimetry

Isothermal titration calorimetric (ITC) measurements were done using an GE Microcal ITC 200 (Northampton, USA) microcalorimeter in the temperature range 298–323 K. Surfactant concentration of the solutions was taken ~10 times its CMC and it was added gradually (3 µL at each step) maintaining equal time intervals (210 s) into 1.352 mL solvent taken in a cell under constant stirring (300 rpm). The heat released or absorbed at each step of dilution of the surfactant solutions in water and TFE/water medium was recorded and the enthalpy change per mole of surfactant was calculated with the help of the ITC software. Each measurement was repeated twice to check reproducibility. The enthalpy of micellization (ΔH_m^0) was calculated from the experiment. The experimental data was fitted using the Sigmoidal Boltzmann equation and thus CMC and enthalpy of micellization were obtained from the enthalpogram.

2.1.6. Time-Resolved Fluorescence Study

Time-resolved fluorescence decay was carried out using a Horiba−Jobin−Yvon FluoroCube fluorescence lifetime system using NanoLED at 450 nm (IBH, UK) as the excitation source and emission was set at 544 nm for coumarin 153 with TBX photon detection module as the detector. All the decay data were fitted by using IBH DAS-6 decay analysis software. The lamp profile was collected by using a dilute micellar solution of sodium dodecyl sulfate as a scatterer in place of the sample. For the appropriate fittings, the $\chi 2$ values were kept close to unity.

3. Results and discussions

3.1. Critical micelle concentration (CMC)

Critical micelle concentration can be determined from tensiometry, where the surface tension (γ) value of the solution was plotted against the logarithm of the concentration of the surfactant. From the break point of the tensiometric plot, the CMC value can be determined (Figure 1). An initial increase in surface tension followed by its decrease was observed for a number of systems in Figure 1. This can be explained as follows:

TFE molecules can form cooperative hydrogen bonds with water molecules due to its H-donation ability accomplished by the presence of a of highly electronegative -CF_3 moiety. Thus, it can break the H-bonding network among water molecules at the air/water interface as well as in the bulk.

Also, due to the presence of a hydrophobic -CF_3 terminal, the population of TFE molecules at the air/water interface is significant which is evident from the low surface tension values of the water/TFE mixture.

During the addition of surfactants to aqueous media, the hydrophobic moiety of the surfactant breakdowns the structure of the water molecules connected through hydrogen bonding and thus reduces the interfacial tension. In the case of mixed solvents (water/TFE mixture) the structure of the water molecules was significantly altered by cooperative hydrogen bonding between TFE and water molecules. At higher concentrations of TFE (i.e., $\geq$ 15% (v/v)), the air/solvent interface is significantly populated by TFE molecules which break down the H-bonding network of water molecules. In such cases, if amphiphilic molecules are added, they will replace some of the hydrophobic TFE molecules present at the interface due to the higher hydrophobicity of amphiphiles than TFE. Therefore, the population of TFE decreases initially at the interface and again the hydrogen bonding network among water molecules is reestablished to some extent which increases the surface tension up to a certain amount and an initial increase on the curves was observed. However, with the gradual addition of amphiphiles, the hydrogen bonding network of water molecules is disrupted again by the hydrophobic moiety of amphiphiles and thus the surface tension value decreases and maxima on curves (surface tension (γ) vs. log [Surfactant (mM)] plot) was observed.

The inflection point obtained from the plot of specific conductance (κ) against surfactant concentration indicates CMC (Figure 2). CMC can also be determined using an enthalpogram by analyzing it through the sigmoidal Boltzmann equation (discussed in the ITC section). The experimental CMC values in aqueous media are quite similar to the data available in the literature. For anionic surfactants SDS and SDDS obtained CMC values are 8.9 mM and 16.9 mM, whereas the reported CMC values are 8.0 mM and 14.3 mM respectively.[55] For cationic surfactants CTAB and CTAT obtained CMC values are 0.77 mM and 0.22 mM which is also similar to the available literature data of 0.82 mM [55] and 0.24 mM [56] respectively. The obtained CMC value of non-ionic TX-114 in aqueous media is 0.23 mM which is also in good agreement with the literature data of 0.24 mM.[57]

From the experimental results, it can be seen that for the ionic surfactants (cationic: CTAB, CTAT and anionic: SDS, SDDS), CMC decreases with increasing concentration of TFE in the surfactant

solution whereas CMC value increases slightly in case of non-ionic surfactant TX-114 (Table 1). The reason behind this behaviour of TFE is that it can act as a cosolvent and also as a cosurfactant.

(a) In the case of ionic surfactants, TFE molecule enter the surface layer of the micelle which increases the average distance between the ionic head groups. As a result, micellar charge density decreases and thus, CMC decreases.[58] With increasing amount of TFE added, CMC value declines (see Table. 1) owing to the increased solubilization of TFE in the surface layer of the micelle.

(b) In the case of non-ionic surfactant TX-114, CMC remains almost unchanged for the lowest concentrations of TFE (up to 5% v/v) and slightly increases for higher concentrations of TFE. This is because of the hydrogen bonding ability of TFE molecules with the oxygen of the oxyethylene groups of the TX-114 in the palisade layer.[59,60] Moreover, the dielectric constant (ε) of TFE is smaller than the water (ε value is 80.1 for water and 8.55 for TFE) and repulsion between two polar head groups in the surfactants is increased by the decrease in the dielectric constant of the medium which disfavors the micellization process and thus, increases the CMC.[33]

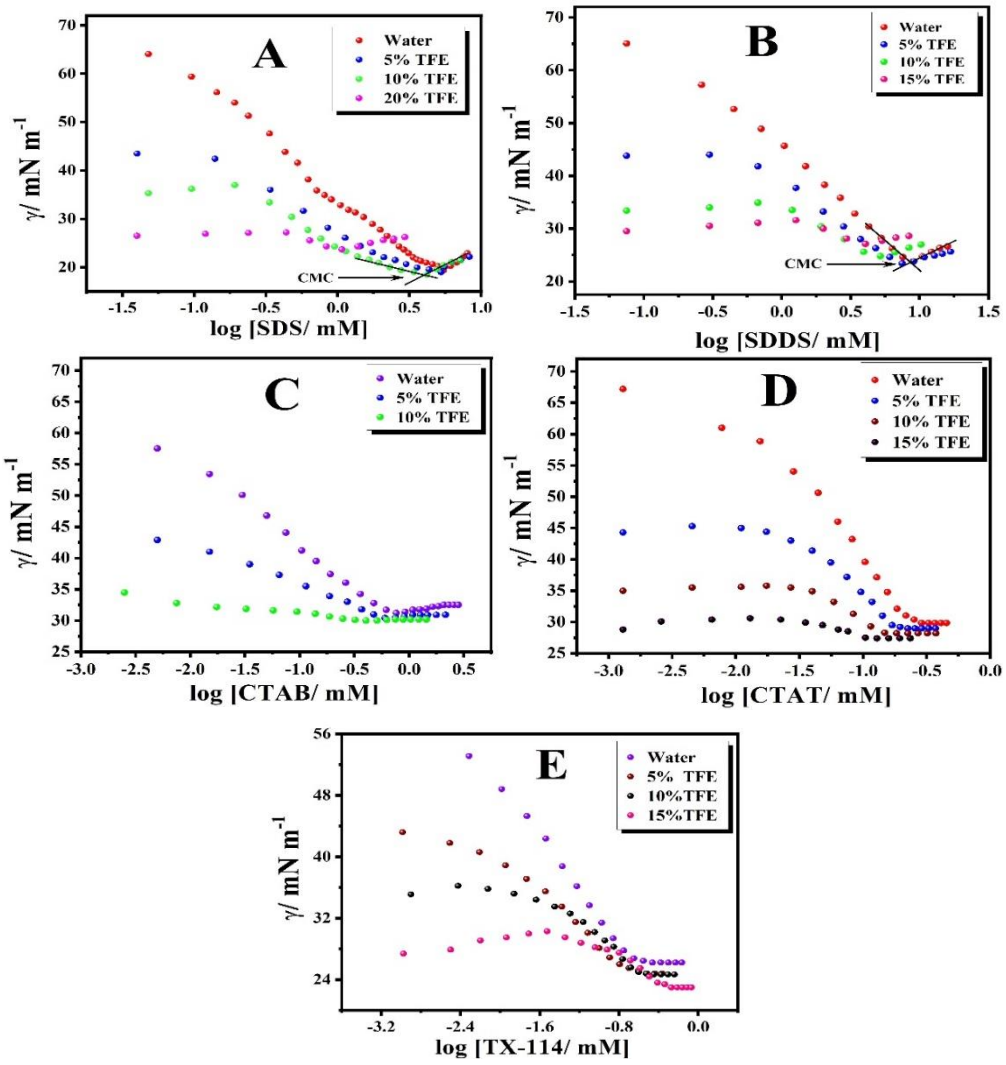

Figure 1. Plots of surface tension (γ) vs. (A) log [SDS (mM)], (B) log [SDDS (mM)], (C) log [CTAB (mM)], (D) log [CTAT (mM)] and (E) log [TX-114 (Mm)] in water and water/TFE mixed solvent at 298.15 K.

3.2. Counterion binding (β)

The ability of ionic micelles to bind with counterions can be determined from the specific conductance vs concentration (Figure 2) plot using the following equation (1)

$$\beta = 1 - \frac{S_2}{S_1} \quad (1)$$

where S_1 and S_2 are the pre- and post-micellar slopes respectively obtained from specific conductance vs concentration plots. The values are represented in Table 1. The detailed procedure was described earlier.[61, 62]

These values provide information regarding the electrostatic interactions between the charged micellar surface and counterion which are located very close to each other. With an increase in the volume percentage of TFE, micellar surface charge density decreases and thus, counterion binding (β) also decreases.[63]

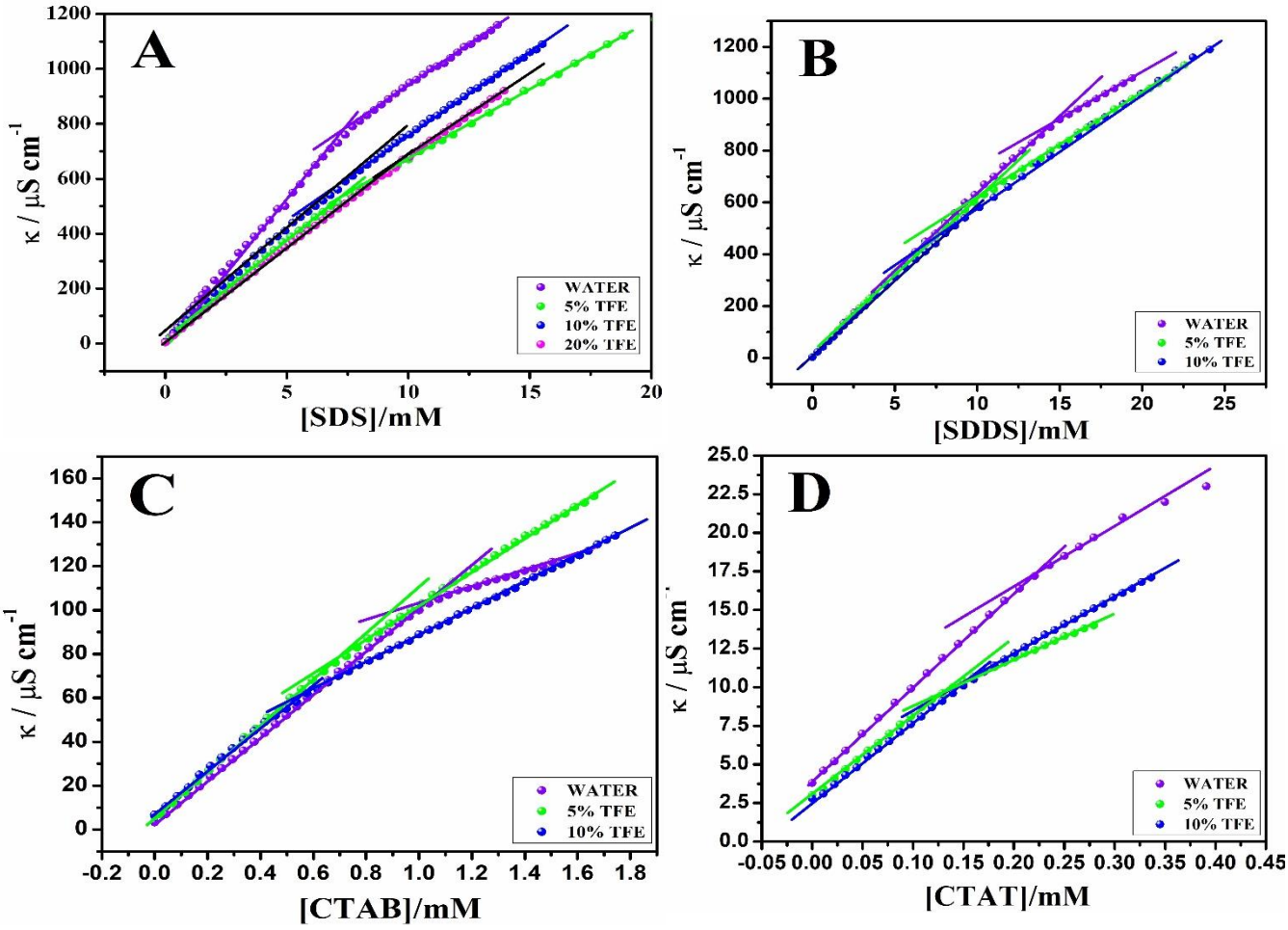

Figure 2. Conductivity (κ) vs (A) [SDS], (B) [SDDS], (C) [CTAB] and (D) [CTAT] systems in water and water/TFE mixed solvent at 298.15 K.

3.3. Adsorption at the Air/Solvent Interface

With the addition of amphiphile molecules to the water and water/TFE medium, surface tension (γ) decreases as they populate themselves at the air/water interface. This decrease in γ value continues until the adsorption of amphiphile at the air/water interface reaches maximum. At a particular concentration, the γ value remains almost unchanged. This concentration of amphiphile is called CMC and the corresponding surface tension value is denoted as γ_{cmc} which signifies the efficiency of the surfactant to occupy at the air/water interface. The surface excess concentration can be determined using the Gibbs adsorption equation (2),

$$\Gamma_{max} = -\frac{1}{2.303nRT}\lim_{C\to cmc}\left(\frac{d\gamma}{d\log C}\right)_{max} mol.m^{-2} \quad (2)$$

where R and T represent the universal gas constant (8.31 J mol^{-1} K^{-1}) and absolute temperature respectively, C is the concentration in molarity of the surfactants and n indicates the number of species in the solution which is taken as 2 for the ionic amphiphiles (SDS, SDDS, CTAB and CTAT) and 1 in case of nonionic surfactant (TX-114). Though the above equation is valid for ideal solution, it can be applied for binary solvents also.[64, 65] Minimum area per adsorbed amphiphile molecule at solvent/air interface (A_{min}) was calculated from the following equation (3) (considering complete monolayer formation at CMC):

$$A_{min} = \frac{10^{18}}{N_A \times \Gamma_{max}} \quad (3)$$

Here N_A indicates the Avogadro's number.

Another important parameter which is called surface pressure (π_{cmc}) can be calculated from the following equation, (4)

$$\pi_{cmc} = \gamma_{solvent} - \gamma_{cmc} \quad (4)$$

where $\gamma_{solvent}$ and γ_{cmc} represent the values of surface tension of the TFE/water mixture without any amphiphile and surface tension of TFE/water mixture with surfactant at the CMC, respectively. The decrease in Γ_{max} value was observed with an increase in the vol% of TFE in water (see Table 1). This signifies that surfactant monomers have more tendency to occupy the air/solvent interface at lower solvent concentrations. From Table 1, it can be seen that A_{min} tends to increase with a decrease in the value of Γ_{max} which indicates surfactant monomers are more closely packed at lower concentrations of solvent. π_{cmc} also decreased with increasing concentration of organic solvent in the mixture which implies lower effectiveness in lowering the interfacial tension with increasing concentration of TFE.[66]

The increasing value of A_{min} per surface molecule with increasing (v/v) % of TFE is the consequence of lower population of surfactants at the air-liquid interface at higher percentage of TFE (Table 1). The decreasing trend of Γ_{max} with increasing concentration of the solvent can be described with the following factors

(a) changing of the water structure with the addition of TFE

(b) the interaction between TFE and surfactants

(c) the presence of TFE at the interface.[67]

The standard Gibbs free energy of micellization ΔG_m^0 was obtained for ionic amphiphiles by using the following equations (5) and (6)

$$\Delta G_m^0 = (1+\beta) RT\ InX_{cmc} \quad (5)$$

and for nonionic amphiphiles by

$$\Delta G_m^0 = RT\ InX_{cmc} \quad (6)$$

where β signifies the counterion binding obtained conductometrically.

The standard free energy of interfacial adsorption at the air/solvent interface can be obtained from the equation (7) [64, 68-70]

$$\Delta G_{ads}^0 = \Delta G_m^0 - \frac{\Pi_{cmc}}{\Gamma_{max}} \quad (7)$$

The higher negative ΔG_{ads}^0 value signifies the higher tendency of the surfactant to be adsorbed at the interface. From the Table 1, it is observed that the value of ΔG_{ads}^0 increases with increasing (v/v) % of TFE.

3.4. Gordon Parameter (G)

The capability of a solvent to promote amphiphile self-assembly is controlled by the solvophobic effect and may be associated with solvent cohesiveness which can be characterized via its Gordon parameter (G).[71] For binary mixtures, it can be determined from experimental values of the surface tension of various homogeneous mixtures. Gordon parameters were determined from the equation:

$$G = \frac{\gamma_{sol}}{V_m^{\frac{1}{3}}} \quad (8)$$

where γ_{sol} represents the surface tension of the mixed solvent and V_m represents the molar volume of the mixed solvent. Table 2 shows the values of Gordon parameters for the various mixtures used as bulk phases in the micellar solution under study. These parameters indicate the decrease of cohesiveness with an increase in concentration of TFE solvent and as a result, solvation of the hydrophobic tail in the bulk phase increases as the solvophobic effect decreases. Moyá et al.[72]

showed that G was linearly dependent on ΔG_m^0 which was similar with the present experimental observation.

3.5. Aggregation Number (Nagg) and Micropolarity

The effects of solvent on the micellar aggregation number of the amphiphiles can be observed by quenching of a fluorescence probe (pyrene) with a known concentration of a quencher (CPC was used here). The following equation (9) which is used to determine the aggregation number of the surfactants in the water and water/TFE system can be determined by using the following:

$$ln\frac{F_0}{F} = \frac{N_{agg}[Q]}{[S]-CMC} \quad (9)$$

where F_0 and F represent the respective fluorescence intensities of the probe with surfactants in the absence and presence of quencher $[S]$ and $[Q]$ denotes the molar concentrations of surfactant and quencher, respectively. The aggregation number (N_{agg}) was evaluated from $ln\frac{F_0}{F}$ vs $[Q]$ plot and the fitting at various concentrations of a quencher (Figure 3). The experimental values in aqueous media obtained in this work are quite similar to the available reports e.g., N_{agg} of SDS in aqueous media was found to be 105 whereas literature reports on N_{agg} of SDS found in the range 40-100 [73]; for TX-114 the obtained N_{agg} value in aqueous medium from our experiment was found to be 48 which is very close to the available reported value 44.[74] However, the aggregation number of SDDS and CTAB was found to be 76 and 52 whereas available literature suggests the values 88 [75] and 80 [76] respectively. The deviation between these values was observed as N_{agg} values depend on the concentration and here the concentrations of the surfactant solutions taken was ~5 times of their CMC which is different from the available literature.[73] It was found that N_{agg} value decreases with increasing solvent concentration implying the increase in hydrophobicity of the solvent with increasing concentration of TFE.

The micropolarity of the pyrene in the micellar environment was evaluated from the ratio of the fluorescence intensities of the first and third vibronic peaks (I_1/I_3) in fluorescence spectra of pyrene. From Table 2, it was observed that micropolarities of micelles as a function of solvent concentration gradually decrease. This can be demonstrated by the solubilization of TFE at the air/solvent interface. Pyrene is located in the palisade layer of the micelle which is close to the surface of the micelle. Increasing the concentration of TFE makes the medium non-polar and as a result, pyrene

molecules sense a more non-polar environment which is evident from the decrease in (I_1/I_3) value. Also, from Table 1, it was found that increasing the concentration of TFE results in an increase in the A_{min} value of the amphiphiles which forces the pyrene molecule to locate closer to the micellar surface, i.e., a more non-polar environment and as a consequence, the (I_1/I_3) value decreases.[66]

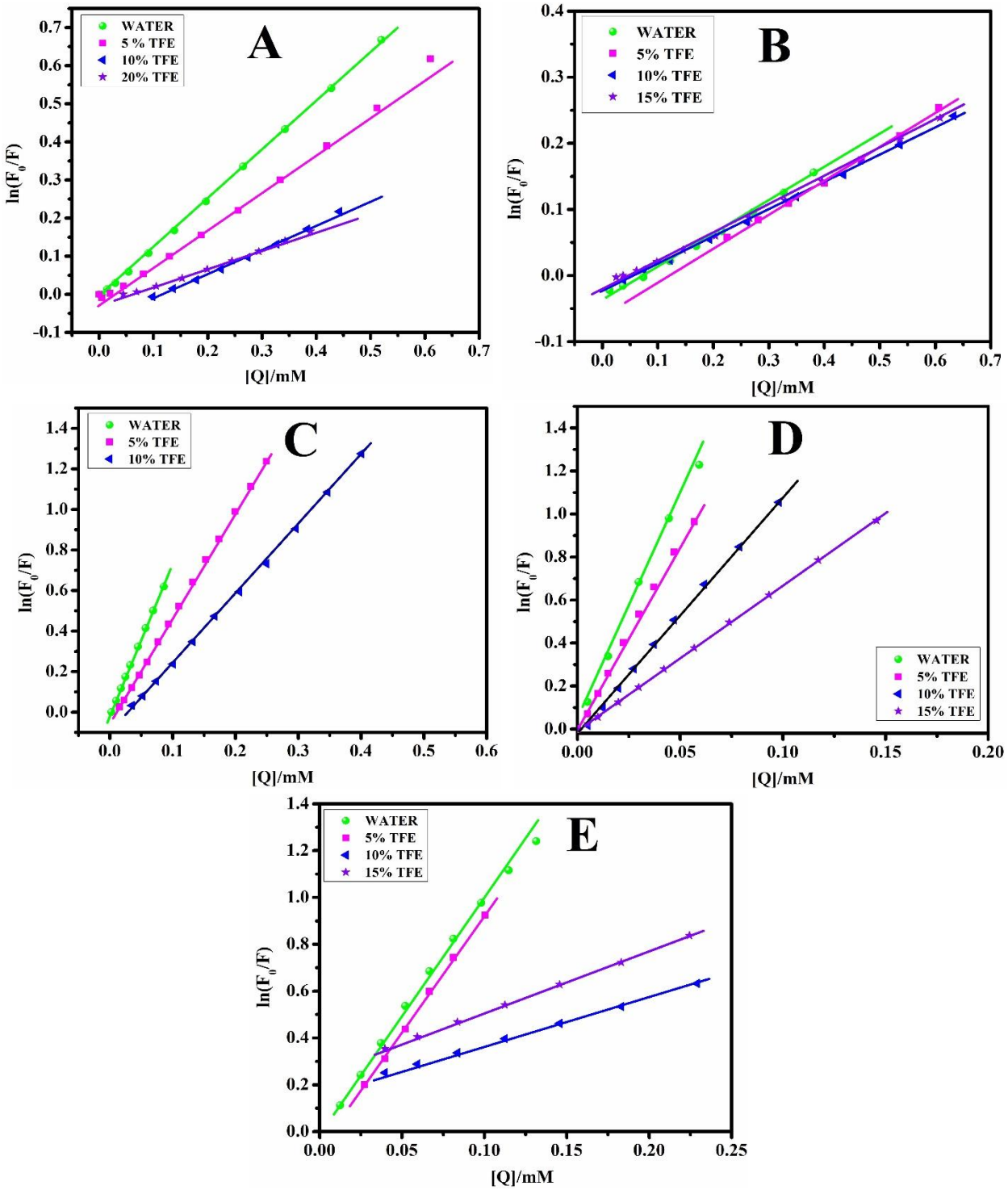

Figure 3. Plot of ln [F_0/F] vs [CPC (mM)] in case of (A) [SDS], (B) [SDDS], (C) [CTAB], (D) [CTAT] and (E) [TX-114] in water and water/TFE mixed solvent at 298.15 K.

3.6. Packing Parameter (P)

The micelle structure can be determined from the packing parameter (P). The packing properties of amphiphiles depend on three parameters.

(i) The volume (v) of hydrophobic chains of incompressible liquid is determined using the Tanford equation (10)

$$v = (0.0274 + 0.0269C_n) \quad (10)$$

(ii) The maximum effective length, called the critical chain length l_c. For saturated hydrophobic chains with n_c carbon atoms, the equation (11)

$$l_c \leq l_{max} \approx (0.154 + 0.1265C_n) \quad (11)$$

According to Israelachvili,[77] the geometry of the micellar aggregates can be predicted from the packing parameter (P) represented as equation (12),

$$P = \frac{v}{A_{min} \times l} \quad (12)$$

For P < 1/3, micelle will be spherical; it is non-spherical when 1/3 < P < 1/2; in case of 1/2 < P < 1, it is vesicle or bilayer and inverted structures when P > 1. From Table 2, it was found that the shape of the aggregates for water and also in mixed solvent is spherical in nature.

3.7. Isothermal titration calorimetry (ITC)

The change in enthalpy values obtained from ITC at 298.15 K for micellization are represented in Table 1. The calorimetric titration curves with the heat-flow with time for selective TFE concentrations of the surfactants are represented in Figure 4. There are three distinct regions in the calorimetric profile: [78]

(a) The premicellar region where dilution of concentrated surfactant solution (concentration ≈10 times the CMC) happens.

(b) The middle portion where a sharp decrease or increase is generally observed as a consequence of the dilution of a fraction of micelles into free monomers.

(c) The post-micellar region where dilution of the micelles occurs.

The enthalpograms are generally "sigmoidal" in nature and the curves are fitted using the sigmoidal Boltzmann equation; [79] and CMC can be obtained from the inflection point in the intermediate section of the enthalpogram.[78, 80-85] To determine CMC more precisely, a plot of the first derivative of the enthalpy change was employed with the corresponding enthalpogram as a function of the concentration of the amphiphile.[84] For the micellization of SDDS in water and in 15% of (v/v) TFE, endo- and exothermic processes were observed respectively. In all other cases, the change in enthalpy is exothermic ($\Delta H_m^0 < 0$) in nature (Figure 4). The CMC values evaluated from enthalpograms are in conformity with the CMCs obtained from other methods, i.e., tensiometry and conductometry (Table 1). The initial enthalpy of dilution [$\Delta H_{dil}^0(initial)$] can be obtained from the intersection of the vertical line passing through the CMC and the pre-micellar line (Figure 4). Similarly, the initial enthalpy of dilution [$\Delta H_{dil}^0(final)$] was obtained from the intersection of the vertical line passing through the CMC and the post-micellar line. For some enthalpograms, however, the initial enthalpy of dilution was considered as the heat of the first injection assuming complete demicellisation occurs in the system.[86, 87] The change of enthalpy due to the micellization process (ΔH_m^0) is evaluated from the difference between $\Delta H_{dil}^0(initial)$ and $\Delta H_{dil}^0(initial)$ values. Similar enthalpograms have also been observed earlier for other systems also.[82, 83, 88-92] Moreover, the value of enthalpy at high surfactant concentrations tends to approach zero, while in some cases for the post-micellar region, a plateau is found below zero value. These phenomena were observed earlier.[80, 81]

Micellization of SDS and CTAB in water and water/TFE solution is found to be exothermic (Table 1) and CMC of SDS has been determined to be 9.04 mM in water and 7.99 mM in 20 % (v/v) of TFE at 298.15 K. CMC of CTAB in water has been found to be 0.55 mM. However, micellization of SDDS in water has been found to be endothermic (2.02 kJ.mol^{-1}) whereas, it is exothermic (-6.96 kJ.mol^{-1}) in 15 % (v/v) of TFE. CMC of SDDS in water and 15 % (v/v) of TFE was found to be 13.7 mM and 16.22 mM respectively.

The discrepancy in the magnitudes of CMCs obtained by ITC and other various methods is due to the fact that there are some systematic differences between these methods [93] and CMC is a method-dependent quantity.[94, 95] Also, CMC does not represent a particular concentration, rather it corresponds to a small range of concentrations and different methods generate slightly different values.

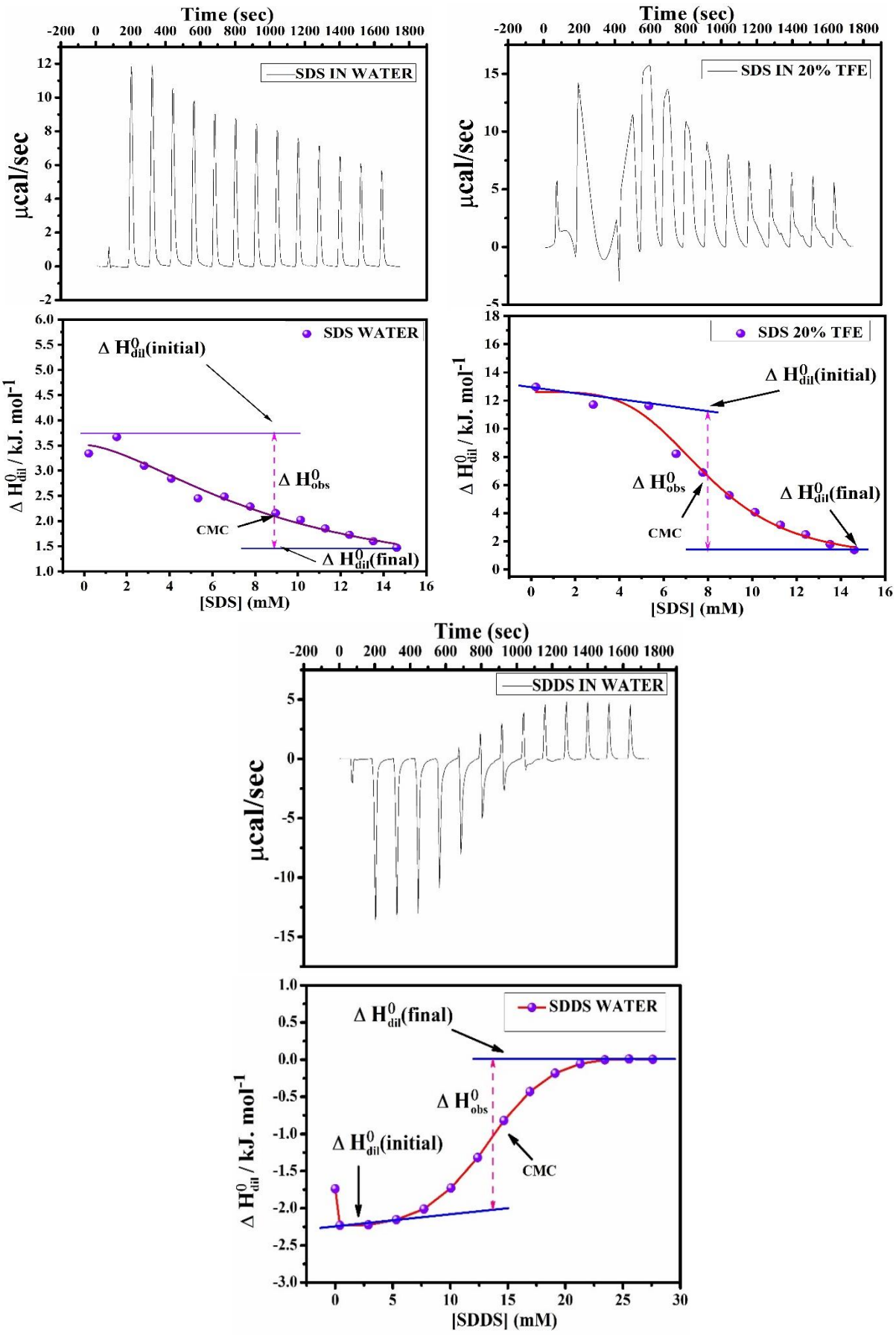
Time (sec)
SDS IN WATER
µcal/sec
SDS WATER
Δ H0dil(initial)
Δ H0obs
CMC
Δ H0dil(final)
Δ H0dil / kJ. mol-1
[SDS] (mM)
SDS IN 20% TFE
SDS 20% TFE
SDDS IN WATER
SDDS WATER
[SDDS] (mM)

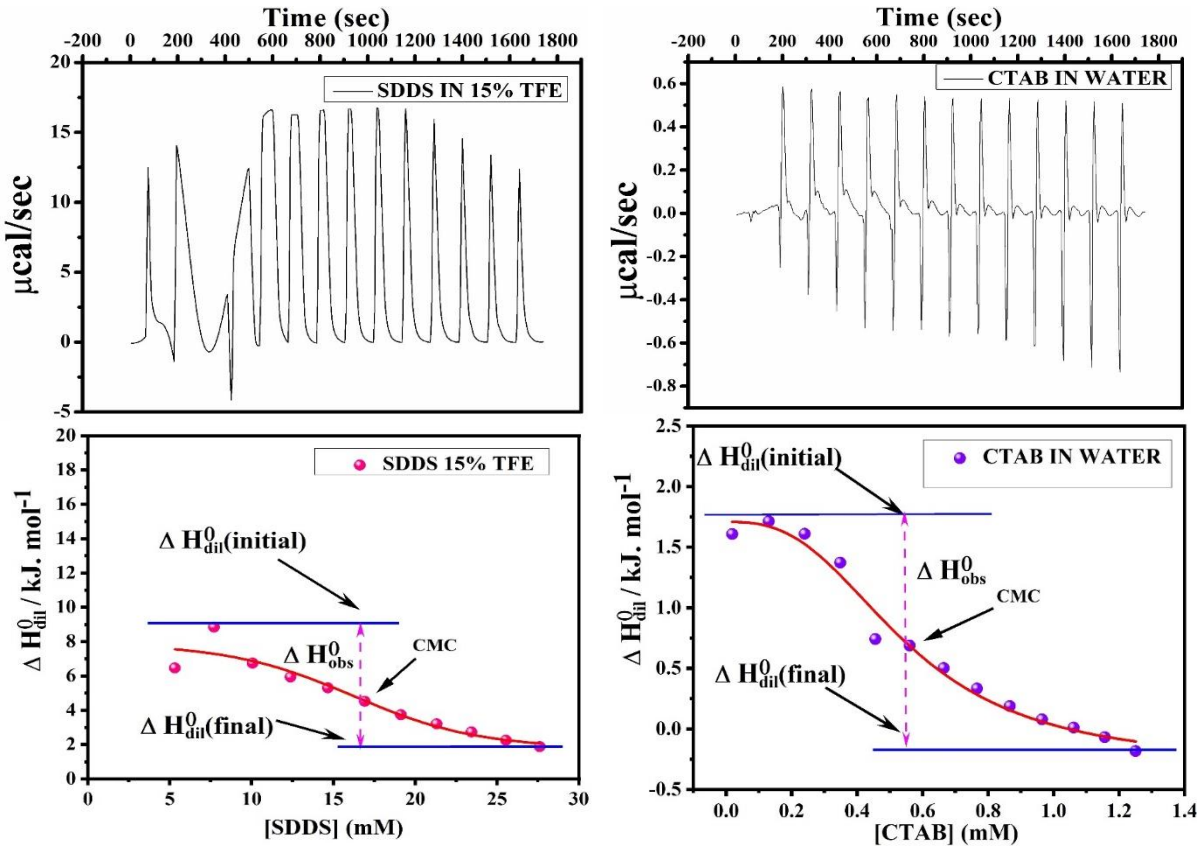

Figure 4. Calorimetric titration curves of various systems (For each plot: top row: raw calorimetric traces (heat flow vs. time), bottom row: integration of peaks with thermodynamic parameters) in water and water/TFE mixed solvent at 298.15 K.

3.8. Time-Resolved Fluorescence Decay Measurements

Fluorescence lifetime measurement gives us information regarding the local environment of a probe molecule. This method also gives indication of the stability of the probe molecule in the excited state**.**

The anisotropy decay value of coumarin 153 (C153) in aqueous solution is bi exponential with a time constant of ~1.70 ns.[96] The anisotropy decays in the micellar system are complicated and data can be analyzed using double exponential decay. The anisotropic decay value ($r(t)$) at time t with two relaxation components τ_1,τ_2 can be represented as equation (13)

$$r(t) = r_0 \left[a_1 e^{-t/\tau_1} + a_2 e^{-t/\tau_2} \right] \quad (13)$$

where r_0 represents the anisotropy value at t = 0 and a_1, a_2 are termed as the pre-exponential factor i.e., the contributing factor of each time scale component. The two components appear from two different environments of the probe molecules located at the water-micelle/solvent-micelle interface and penetrate into the hydrophobic core of the micelle. The average relaxation time value (τ_{av}) can be expressed by the following equation (14):

$$\tau_{av} = a_1\tau_1 + a_2\tau_2 \quad (14)$$

The decay profile was represented in Figure 5. The τ_{av} values have been represented in Table 3. Two interesting aspects have been found in this experimental observation.

(I) In case of ionic amphiphiles (SDS, SDDS, CTAB and CTAT), fluorescence lifetime of C153 slightly increases or remains more or less constant as the TFE concentration is increased. The reason behind this phenomenon can be attributed to the fact that an increased amount of TFE makes the micellization process more favourable, as has been discussed earlier. As the micellization process becomes more favourable, the environment around the probe molecule C153 turns more hydrophobic and thus, its movement turns out to be more restricted. In other words, C153 molecules become less accessible to the quencher TFE as the micellization process turns more favourable. This results in an increased lifetime value for C-153. Moreover, it has been discussed earlier that increased concentration of TFE locates it in the surface layer of the micelle near the polar head group which means that TFE molecules are not accessible to the hydrophobic core where the probe molecule generally locates itself which in turn makes it inaccessible to the TFE molecules for quenching.

(II) For non-ionic surfactant TX-114, fluorescence lifetime of the probe molecule decreases as the concentration of TFE is increased (Table 3) i.e., a dynamic quenching has been observed here. TFE molecules here act as both cosolvent (at low concentration) and cosurfactant (at high concentration). At low concentration, TFE extensively forms cooperative hydrogen bonds with water molecules as it can operate as H-donor due to the presence of highly electronegative -CF_3 moiety. In that case, TFE molecules are located in the outer region of the micelle. With increasing concentration, TFE molecules start penetrating the palisade layer of the micelle as it can form hydrogen bond with the oxygen of the oxyethylene groups of the TX-114 in the palisade layer.[59, 60] To interpret this quenching phenomenon, the Stern–Volmer equation can be employed as follows:

$$\frac{\tau_0}{\tau} = 1 + K_{SV}[Q] \quad (15)$$

Here, τ and τ_0 represent the fluorescence lifetime of probe C153 in the presence and absence of TFE, respectively. K_{SV} represents the Stern–Volmer constant and $[Q]$ denotes the free quencher concentration. In the case of a large excess of quencher, $[Q]$ is assumed to be the total quencher concentration.[97] From this plot of $\frac{\tau_0}{\tau}$ versus [Q], bimolecular quenching constant k_q can be evaluated from Stern–Volmer type equation (16),

$$\frac{\tau_0}{\tau} = 1 + k_q\tau_0[Q] = 1 + K_D[Q] \quad (16)$$

Figure 6 depicts the τ_0/τ vs $[Q]$ plot. From the slope of the mentioned plot, K_D value can be obtained as 0.1653 M^{-1} and k_q as 4.108×10^7 M^{-1} s^{-1}.

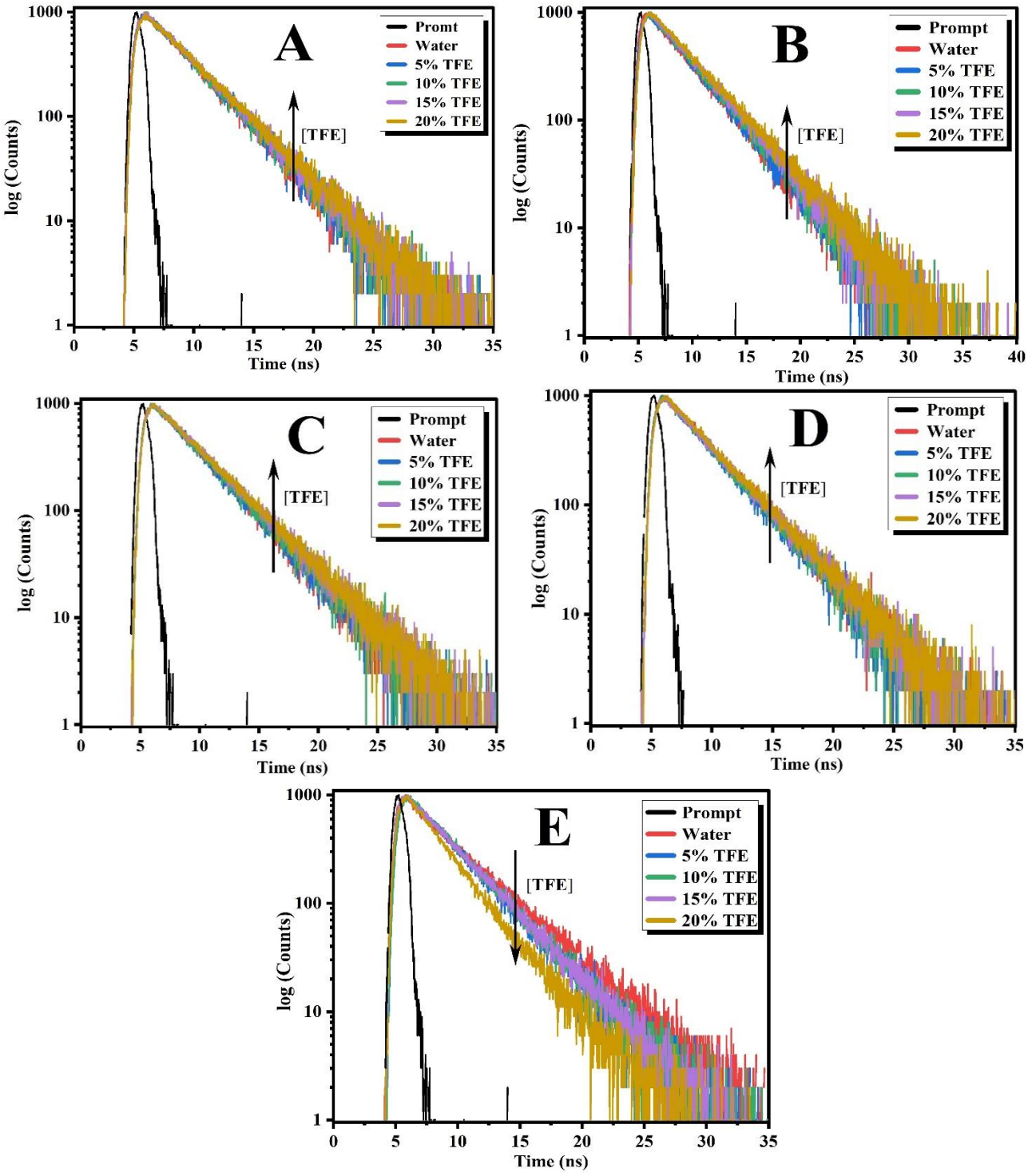

Figure 5. Life time decay profile of coumarin 153 in case of (A) [SDS], (B) [SDDS], (C) [CTAB], (D) [CTAT] and (E) TX-114 in water and water/TFE mixed solvent at 298.15 K.

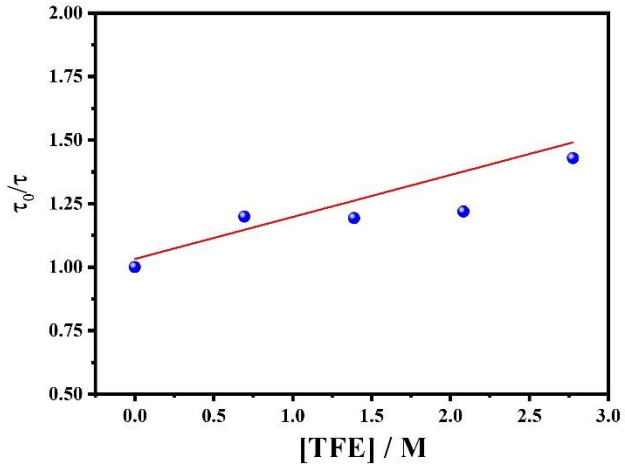

Figure 6. Stern–Volmer plot for the quenching of the fluorescence life time of coumarin 153 by TFE in aqueous solution of TX-114 at 298.15 K.

From these results, it can be concluded that a fraction of C153 and TFE molecules are located at the palisade layer and also in the outer region of the micellar core.

4. Conclusions

The decrease of CMC of micellar solutions of ionic-surfactants (SDS, SDDS, CTAB, CTAT) with increasing concentration of TFE can be justified by the decrease of micellar charge density of the ionic head groups as TFE molecules are prone to enter the surface layer of the micelle. This is also consistent with the time-resolved fluorescence anisotropy decay measurement of coumarin 153 used as a probe. The anisotropy decay values of C153 were more or less constant with increasing concentration of TFE for the ionic surfactants which confirm that quencher TFE molecules are not located at a palisade layer of the micelle.

However, a completely different observation has been found in the case of non-ionic TX-114. At lower concentrations of TFE, CMC values are more or less constant, but these increase at higher concentrations of TFE. This happens due to the fact that for non-ionic TX-114, the charge density of the polar head groups is not worth considering and thus the destabilizing effect due to the decrease of the dielectric constant with small increasing TFE concentration can be ignored at lower concentrations of TFE. However, at higher concentrations of TFE, some conformational changes occur in the polar head group of TX-114 which increases the steric repulsion of the head groups. Similar observation has also been found by Civera et al.[56] in the case of TX-165 molecules.

The nature of the interaction of TFE with the micelle formed by non-ionic TX-114 as well as ionic amphiphiles is rarely found in literature and with the assistance of time-resolved fluorescence decay study it was found that quenching of the fluorescence lifetime of the probe was occurred in case of TX-114/TFE system due to the penetration of TFE into the palisade layer of the micelle by the assistance of hydrogen bonding between these two molecules; the systematic study of this kind is fairly new in literature which may pave the way for understanding the nature of interaction in similar biological systems as combination of appropriate detergents replicates the property of native lipid bilayer and stabilizes membrane proteins which is an important step for determining the structure of those proteins and also in pharmaceutical industry.

REFERENCES

1. Abdul Rub, M.; Koya Pulikkal, A.; Azum, N.; Asiri, A. M., The assembly of amitriptyline hydrochloride + triton X-45 (non-ionic surfactant) mixtures: Effects of simple salt and urea. *Journal of Molecular Liquids* **2022,** *356*, 118997.
2. Hirpara, D.; Patel, B.; Chavda, V.; Kumar, S., Micellization of conventional and gemini surfactants in aquoline: A case of exclusively water based deep eutectic solvent. *Journal of Molecular Liquids* **2022,** *362*, 119672.
3. Mondal, B. B.; Banik, R.; Ghosh, S., Detailed physicochemical study and thermodynamic aspects of the interaction between nonionic cellulose derivative hydroxyethyl cellulose and anionic surfactant sodium N-dodecanoyl sarcosinate in aqueous media. *Journal of the Taiwan Institute of Chemical Engineers* **2023,** *149*, 104982.
4. Banik, R.; Das, S.; Ghosh, A.; Ghosh, S., Comparative studies on the aggregate formation of synthesized zwitterionic gemini and monomeric surfactants in the presence of the amphiphilic antipsychotic drug chlorpromazine hydrochloride in aqueous solution: an experimental and theoretical approach. *Soft Matter* **2023,** *19* (41), 7995-8010.
5. Serna, J.; Narváez Rincón, P. C.; Falk, V.; Boly, V.; Camargo, M., Methodology for Emulsion Design Based on Emulsion Science and Expert Knowledge. Part 2: An Application in the Cosmetics Sector. *Industrial & Engineering Chemistry Research* **2021,** *60* (14), 5220-5235.
6. Fenton, T.; Gholamipour-Shirazi, A.; Daffner, K.; Mills, T.; Pelan, E., Formulation and additive manufacturing of polysaccharide-surfactant hybrid gels as gelatin analogues in food applications. *Food Hydrocolloids* **2021,** *120*, 106881.
7. Chowdhury, S.; Shrivastava, S.; Kakati, A.; Sangwai, J. S., Comprehensive Review on the Role of Surfactants in the Chemical Enhanced Oil Recovery Process. *Industrial & Engineering Chemistry Research* **2022,** *61* (1), 21-64.
8. Lu, Z.; Zongjie, G.; Qianyu, Z.; Xueyan, L.; Kexin, W.; Baoyan, C.; Ran, T.; Fang, R.; Hui, H.; Huali, C., Preparation and characterization of a gemini surfactant-based biomimetic complex for gene delivery. *European Journal of Pharmaceutics and Biopharmaceutics* **2023,** *182*, 92-102.

9. Lu, J.; González de Castilla, A.; Müller, S.; Xi, S.; Chapman, W. G., Dualistic Role of Alcohol in Micelle Formation and Structure from iSAFT Based Density Functional Theory and COSMOplex. *Industrial & Engineering Chemistry Research* **2023,** *62* (4), 1968-1983.
10. Keshvarinezhad, M.; Ebrahimi, N.; Sadeghi, R., Liquid–Liquid Demixing Behavior of Aqueous 1-Butanol Solutions in the Presence of Various Organic and Inorganic Ammonium Salts: Effect of Temperature, Cation Alkyl Chain Length, and Anion Type of Salts on Salting Coefficients and Thermodynamic Functions. *Journal of Chemical & Engineering Data* **2023,** *68* (7), 1728-1738.
11. Dutta, A.; Joy, M. T. R.; Ahsan, S. M. A.; Gatasheh, M. K.; Kumar, D.; Abdul Rub, M.; Anamul Hoque, M.; Majibur Rahman, M.; Hoda, N.; Islam, D. M. S., Physico-chemical parameters for the assembly of moxifloxacin hydrochloride and cetyltrimethylammonium chloride mixture in aqueous and alcoholic media. *Chinese Journal of Chemical Engineering* **2023,** *57*, 280-289.
12. Basnet, N.; Prasai, S.; Dominguez, H.; Ríos-López, M.; Adhikari, R.; Ghimire, M. P.; Bhattarai, A., Conductance Study of Aerosol-OT in Binary Mixed Solvents of Short-Chain Alcohol–Water Systems at Various Temperatures. *Journal of Chemical & Engineering Data* **2021,** *66* (1), 65-78.
13. Kumar, V.; Verma, R.; Satodia, D.; Ray, D.; Kuperkar, K.; Aswal, V. K.; Mitchell-Koch, K. R.; Bahadur, P., Contrasting effect of 1-butanol and 1, 4-butanediol on the triggered micellar self-assemblies of C 16-type cationic surfactants. *Physical Chemistry Chemical Physics* **2021,** *23* (35), 19680-19692.
14. Üner, O.; Akkurt, N., Micellization and thermodynamics study of n-alkyl-4-methylpyridinium bromides in water and mixed water–ethanol media. *Journal of Molecular Liquids* **2022,** *352*, 118765.
15. Devi, Y. G.; Gurung, J.; Pulikkal, A. K., Micellar Solution Behavior of Cetylpyridinium Surfactants in 2-Propanol–Water Mixed Media at Different Temperatures. *Journal of Chemical & Engineering Data* **2021,** *66* (1), 368-378.
16. Sheng, R.; Ding, Q. Y.; Ren, Z. H.; Li, D. N.; Fan, S. C.; Cai, L. L.; Quan, X. F.; Wang, Y.; Yi, M. T.; Zhang, Y. X.; Cao, Y. X.; Wang, H.; Wang, J. R.; Zhang, Q. H.; Qian, Z. B., Interfacial and micellization behavior of binary mixture of amino sulfonate amphoteric surfactant and octadecyltrimethyl ammonium bromide: Effect of short chain alcohol and its chain length. *Journal of Molecular Liquids* **2021,** *334*, 116064.
17. Rauniyar, B. S.; Bhattarai, A., Study of conductivity, contact angle and surface free energy of anionic (SDS, AOT) and cationic (CTAB) surfactants in water and isopropanol mixture. *Journal of Molecular Liquids* **2021,** *323*, 114604.
18. Ghosh, R.; Parida, C.; Chowdhuri, S., Hydrogen bonding behavior of ethanol-trifluoroethanol binary mixtures and its effects on the water structure and dynamics in ternary aqueous-ethanol-trifluoroethanol solutions. *Chemical Physics* **2023,** *572*, 111956.
19. Shah, S. K.; Chatterjee, S. K.; Bhattarai, A., Micellization of cationic surfactants in alcohol — water mixed solvent media. *Journal of Molecular Liquids* **2016,** *222*, 906-914.
20. Shida, N.; Takenaka, H.; Gotou, A.; Isogai, T.; Yamauchi, A.; Kishikawa, Y.; Nagata, Y.; Tomita, I.; Fuchigami, T.; Inagi, S., Alkali Metal Fluorides in Fluorinated Alcohols: Fundamental Properties and Applications to Electrochemical Fluorination. *The Journal of Organic Chemistry* **2021,** *86* (22), 16128-16133.

21. Moreno, A.; Liu, T.; Ding, L.; Buzzacchera, I.; Galià, M.; Möller, M.; Wilson, C. J.; Lligadas, G.; Percec, V., SET-LRP in biphasic mixtures of fluorinated alcohols with water. *Polymer Chemistry* **2018,** *9* (17), 2313-2327.
22. Mohanta, D.; Jana, M., Can 2, 2, 2-trifluoroethanol be an efficient protein denaturant than methanol and ethanol under thermal stress? *Physical Chemistry Chemical Physics* **2018,** *20* (15), 9886-9896.
23. Hossain, M.; Huda, N.; Bhuyan, A. K., A surprisingly simple three-state generic process for reversible protein denaturation by trifluoroethanol. *Biophysical Chemistry* **2022,** *291*, 106895.
24. Ohgi, H.; Imamura, H.; Sumi, T.; Nishikawa, K.; Koga, Y.; Westh, P.; Morita, T., Two different regimes in alcohol-induced coil–helix transition: effects of 2, 2, 2-trifluoroethanol on proteins being either independent of or enhanced by solvent structural fluctuations. *Physical Chemistry Chemical Physics* **2021,** *23* (10), 5760-5772.
25. Pereira, A. F.; Piccoli, V.; Martínez, L., Trifluoroethanol direct interactions with protein backbones destabilize α-helices. *Journal of Molecular Liquids* **2022,** *365*, 120209.
26. Burakowski, A.; Gliński, J.; Czarnik-Matusewicz, B.; Kwoka, P.; Baranowski, A.; Jerie, K.; Pfeiffer, H.; Chatziathanasiou, N., Peculiarity of Aqueous Solutions of 2,2,2-Trifluoroethanol. *The Journal of Physical Chemistry B* **2012,** *116* (1), 705-710.
27. Gerig, J. T., Toward a Molecular Dynamics Force Field for Simulations of 40% Trifluoroethanol–Water. *The Journal of Physical Chemistry B* **2014,** *118* (6), 1471-1480.
28. Vymětal, J.; Vondrášek, J., Parametrization of 2,2,2-Trifluoroethanol Based on the Generalized Amber Force Field Provides Realistic Agreement between Experimental and Calculated Properties of Pure Liquid as Well as Water-Mixed Solutions. *The Journal of Physical Chemistry B* **2014,** *118* (35), 10390-10404.
29. Fatima, U.; Riyazuddeen; Dhakal, P.; Shah, J. K., Comparative Study of Influence of Ethanol and 2,2,2-Trifluoroethanol on Thermophysical Properties of 1-Ethyl-3-methylimidazolium Dicyanamide in Binary Mixtures: Experimental and MD Simulations. *Journal of Chemical & Engineering Data* **2021,** *66* (1), 101-115.
30. Yuan, H.; Wu, Y.-Z.; Fang, Y.-H.; Chen, C.-H.; Liang, C.; Mo, D.-L., Synthesis of Spirooxindole-1,2-oxazinan-5-ones through 2,2,2-Trifluoroethanol Promoted [3 + 3] Cycloaddition of N-Vinyl Oxindole Nitrones and Oxyallyl Cations. *The Journal of Organic Chemistry* **2023,** *88* (23), 16155-16166.
31. Zhu, G.; Chen, J.; Duan, J.; Liao, H.; Zhu, X.; Li, Z.; McCulloch, I.; Yue, W., Fluorinated Alcohol-Processed N-Type Organic Electrochemical Transistor with High Performance and Enhanced Stability. *ACS Applied Materials & Interfaces* **2022,** *14* (38), 43586-43596.
32. Civera, C.; Arias, C.; Elorza, M. A.; Elorza, B.; García-Blanco, F.; Galera-Gómez, P. A., Hydrophobicity enhancement in micelles of Triton X-165 by the presence of the cosolvent 2,2,2 trifluoroethanol (TFE). *Journal of Molecular Liquids* **2014,** *199*, 29-34.
33. García-Blanco, F.; Elorza, M. A.; Arias, C.; Elorza, B.; Gómez-Escalonilla, I.; Civera, C.; Galera-Gómez, P. A., Interactions of 2,2,2-trifluoroethanol with aqueous micelles of Triton X-100. *Journal of Colloid and Interface Science* **2009,** *330* (1), 163-169.
34. Chen, W.; Geng, X.; Liu, W.; Ding, B.; Xiong, C.; Sun, J.; Wang, C.; Jiang, K., A Comprehensive Review on Screening, Application, and Perspectives of Surfactant-Based Chemical-Enhanced Oil Recovery Methods in Unconventional Oil Reservoirs. *Energy & Fuels* **2023,** *37* (7), 4729-4750.
35. Raffa, P.; Wever, D. A. Z.; Picchioni, F.; Broekhuis, A. A., Polymeric Surfactants: Synthesis, Properties, and Links to Applications. *Chemical Reviews* **2015,** *115* (16), 8504-8563.

36. Gonçalves, R. A.; Holmberg, K.; Lindman, B., Cationic surfactants: A review. *Journal of Molecular Liquids* **2023,** *375*, 121335.
37. Shi, D.; Liu, Z.; Shao, F.; Li, X.; Sun, X.; Hou, X.; Xiao, Y.; Hei, Y.; Xie, E.; Leng, W., Self-assembly of anionic surfactant and its effect on oil–water interface: Implications for enhanced oil recovery. *Applied Surface Science* **2023,** *611*, 155666.
38. Saw, R. K.; Sinojiya, D.; Pillai, P.; Prakash, S.; Mandal, A., Experimental Investigation of the Synergistic Effect of Two Nonionic Surfactants on Interfacial Properties and Their Application in Enhanced Oil Recovery. *ACS Omega* **2023,** *8* (13), 12445-12455.
39. Wang, Y.; Zheng, C.; Shi, L.; Hou, J.; Jiang, C.; Zhang, L., Properties and Aggregation Behavior of Gemini Surfactants for Heavy Oil Recovery in High Temperature and Salinity Conditions. *Energy & Fuels* **2023,** *37* (20), 15687-15698.
40. Gyani Devi, Y.; Koya Pulikkal, A.; Gurung, J., Research Progress on the Synthesis of Different Types of Gemini Surfactants with a Functionalized Hydrophobic Moiety and Spacer. *ChemistrySelect* **2022,** *7* (45), e202203485.
41. Zdziennicka, A.; Jańczuk, B., Modification of adsorption, aggregation and wetting properties of surfactants by short chain alcohols. *Advances in Colloid and Interface Science* **2020,** *284*, 102249.
42. Jiang, R.; Wu, X.; Xiao, Y.; Kong, D.; Li, Y.; Wang, H., Tween 20 regulate the function and structure of transmembrane proteins of Bacillus cereus: Promoting transmembrane transport of fluoranthene. *Journal of Hazardous Materials* **2021,** *403*, 123707.
43. Varlas, S.; Blackman, L. D.; Findlay, H. E.; Reading, E.; Booth, P. J.; Gibson, M. I.; O'Reilly, R. K., Photoinitiated Polymerization-Induced Self-Assembly in the Presence of Surfactants Enables Membrane Protein Incorporation into Vesicles. *Macromolecules* **2018,** *51* (16), 6190-6201.
44. Chipot, C.; Dehez, F.; Schnell, J. R.; Zitzmann, N.; Pebay-Peyroula, E.; Catoire, L. J.; Miroux, B.; Kunji, E. R. S.; Veglia, G.; Cross, T. A.; Schanda, P., Perturbations of Native Membrane Protein Structure in Alkyl Phosphocholine Detergents: A Critical Assessment of NMR and Biophysical Studies. *Chemical Reviews* **2018,** *118* (7), 3559-3607.
45. Kumar, V.; Mitchell-Koch, K. R.; Marapureddy, S. G.; Verma, R.; Thareja, P.; Kuperkar, K.; Bahadur, P., Self-Assembly and Micellar Transition in CTAB Solutions Triggered by 1-Octanol. *The Journal of Physical Chemistry B* **2022,** *126* (40), 8102-8111.
46. Patel, V.; Ray, D.; Singh, K.; Abezgauz, L.; Marangoni, G.; Aswal, V. K.; Bahadur, P., 1-Hexanol triggered structural characterization of the worm-like micelle to vesicle transitions in cetyltrimethylammonium tosylate solutions. *RSC Advances* **2015,** *5* (107), 87758-87768.
47. Mahbub, S.; Rana, S.; Abdul Rub, M.; Hoque, M. A.; Kabir, S. E.; Asiri, A. M., Influence of Alcohol/Temperature on the Interaction of Sodium Dodecyl Sulfate with Cetyltrimethylammonium Bromide: Experimental and Theoretical Study. *Journal of Chemical & Engineering Data* **2019,** *64* (10), 4376-4389.
48. Mondal, B. B.; Banik, R.; Ghosh, S., Impact of 2,2,2-trifluoroethanol (TFE) on hydrophobicity enhancement in the aggregation of sodium N-dodecanoyl sarcosinate (SDDS) with nonionic hydroxyethyl cellulose. *Colloids and Surfaces A: Physicochemical and Engineering Aspects* **2024,** *681*, 132781.
49. Rony, M. R. I.; Khan, J. M.; Jahan, I.; Joy, M. T. R.; Hasan, T.; Kumar, D.; Ahmad, A.; Rana, S.; Hoque, M. A., Influences of alcohols, urea and polyethylene glycol on the cloudy formation nature and physico-chemical parameters of the mixture of triton X-100 and

ceftriaxone sodium salt. *Colloids and Surfaces A: Physicochemical and Engineering Aspects* **2023,** *677*, 132410.
50. Rasel Ahmed, M.; Abdul Rub, M.; Idrish Ali, M.; Rana, S.; Rahman, M.; Kumar, D.; Asiri, A. M.; Anamul Hoque, M., The phase separation, interaction forces and thermodynamics of sodium alginate and TX-100 mixture in the manifestation of alcohols: UV–visible and cloud point measurement studies. *Journal of Molecular Liquids* **2022,** *361*, 119479.
51. Ishkhanyan, H.; Ziolek, R. M.; Barlow, D. J.; Lawrence, M. J.; Poghosyan, A. H.; Lorenz, C. D., NSAID solubilisation promotes morphological transitions in Triton X-114 surfactant micelles. *Journal of Molecular Liquids* **2022,** *356*, 119050.
52. Mukherjee, A.; Ghosh, S.; Pal, M.; Singh, B., Deciphering the effective sequestration of DNA bounded bioactive small molecule Safranin-O by non-ionic surfactant TX-114 and diminution its cytotoxicity. *Journal of Molecular Liquids* **2019,** *289*, 111116.
53. Kangkamano, T.; Witsapan, W.; Numnuam, A.; Subba, J. R.; Jayeoye, T. J., Colorimetric hydrogen peroxide and glucose sensors based on the destruction of micelle-protected iron (ii) complex probes. *New Journal of Chemistry* **2023,** *47* (23), 11261-11274.
54. Peng, J.; Song, X.; Li, X.; Jiang, Y.; Liu, G.; Wei, Y.; Xia, Q., Molecular Dynamics Study on the Aggregation Behavior of Triton X Micelles with Different PEO Chain Lengths in Aqueous Solution. *Molecules* **2023,** *28* (8), 3557.
55. Ghosh, S.; Mondal, S.; Das, S.; Biswas, R., Spectroscopic investigation of interaction between crystal violet and various surfactants (cationic, anionic, nonionic and gemini) in aqueous solution. *Fluid Phase Equilibria* **2012,** *332*, 1-6.
56. Patel, V.; Chavda, S.; Aswal, V. K.; Bahadur, P., Effect of a hydrophilic PEO–PPO–PEO copolymer on cetyltrimethyl ammonium tosylate solutions in water. *Journal of Surfactants and Detergents* **2012,** *15*, 377-385.
57. Sun, T.; Gao, S.; Chen, Q.; Shen, X., Investigation on the interactions between hydrophobic anions of ionic liquids and Triton X-114 micelles in aqueous solutions. *Colloids and Surfaces A: Physicochemical and Engineering Aspects* **2014,** *456*, 18-25.
58. Rao, I. V.; Ruckenstein, E., Micellization behavior in the presence of alcohols. *Journal of Colloid and Interface Science* **1986,** *113* (2), 375-387.
59. Wolszczak, M.; Miller, J., Characterization of non-ionic surfactant aggregates by fluorometric techniques. *Journal of Photochemistry and Photobiology A: Chemistry* **2002,** *147* (1), 45-54.
60. Behera, K.; Pandey, M. D.; Porel, M.; Pandey, S., Unique role of hydrophilic ionic liquid in modifying properties of aqueous Triton X-100. *J. Chem. Phys* **2007,** *127* (18), 184501.
61. Ghosh, S., Surface Chemical and Micellar Properties of Binary and Ternary Surfactant Mixtures (Cetyl Pyridinium Chloride, Tween-40, and Brij-56) in an Aqueous Medium. *Journal of Colloid and Interface Science* **2001,** *244* (1), 128-138.
62. Das, C.; Chakraborty, T.; Ghosh, S.; Das, B., Mixed micellization of anionic–nonionic surfactants in aqueous media: a physicochemical study with theoretical consideration. *Colloid and Polymer Science* **2008,** *286* (10), 1143.
63. Das, S.; Naskar, B.; Ghosh, S., Influence of temperature and organic solvents (isopropanol and 1,4-dioxane) on the micellization of cationic gemini surfactant (14-4-14). *Soft Matter* **2014,** *10* (16), 2863-2875.
64. Das, C.; Das, B., Thermodynamic and Interfacial Adsorption Studies on the Micellar Solutions of Alkyltrimethylammonium Bromides in Ethylene Glycol (1) + Water (2) Mixed Solvent Media. *Journal of Chemical & Engineering Data* **2009,** *54* (2), 559-565.

65. Rodrı´guez, A.; Mar Graciani, M. a. d.; Fernández, G.; Moyá, M. a. L., Effects of glycols on the thermodynamic and micellar properties of TTAB in water. *Journal of Colloid and Interface Science* **2009,** *338* (1), 207-215.
66. Das, S.; Mondal, S.; Ghosh, S., Physicochemical Studies on the Micellization of Cationic, Anionic, and Nonionic Surfactants in Water–Polar Organic Solvent Mixtures. *Journal of Chemical & Engineering Data* **2013,** *58* (9), 2586-2595.
67. Sulthana, S. B.; Bhat, S. G. T.; Rakshit, A. K., Studies of the Effect of Additives on the Surface and Thermodynamic Properties of Poly(oxyethylene(10)) Lauryl Ether in Aqueous Solution. *Langmuir* **1997,** *13* (17), 4562-4568.
68. Tikariha, D.; Ghosh, K. K.; Barbero, N.; Quagliotto, P.; Ghosh, S., Micellization properties of mixed cationic gemini and cationic monomeric surfactants in aqueous-ethylene glycol mixture. *Colloids and Surfaces A: Physicochemical and Engineering Aspects* **2011,** *381* (1), 61-69.
69. Chauhan, M. S.; Sharma, K.; Kumar, G.; Chauhan, S., A conductometric study of dimethylsulfoxide effect on micellization of sodium dodecyl sulfate in dilute aqueous electrolyte solutions. *Colloids and Surfaces A: Physicochemical and Engineering Aspects* **2003,** *221* (1), 135-140.
70. Sjoeberg, M.; Henriksson, U.; Waernheim, T., Deuteron nuclear magnetic relaxation of [1,1-2H] hexadecyltrimethylammonium bromide in micellar solutions of nonaqueous polar solvents and their mixtures with water. *Langmuir* **1990,** *6* (7), 1205-1211.
71. Gordon, J. E., *Organic chemistry of electrolyte solutions*. Wiley: 1975.
72. Rodríguez, A.; del Mar Graciani, M.; Angulo, M.; Moyá, M. L., Effects of Organic Solvent Addition on the Aggregation and Micellar Growth of Cationic Dimeric Surfactant 12-3-12,2Br. *Langmuir* **2007,** *23* (23), 11496-11505.
73. Basu Ray, G.; Chakraborty, I.; Ghosh, S.; Moulik, S. P., A critical and comprehensive assessment of interfacial and bulk properties of aqueous binary mixtures of anionic surfactants, sodium dodecylsulfate, and sodium dodecylbenzenesulfonate. *Colloid and Polymer Science* **2007,** *285* (4), 457-469.
74. Rub, M. A., Effect of additives (TX-114) on micellization and microstructural phenomena of amphiphilic ibuprofen drug (sodium salt): Multi-technique approach. *Journal of Luminescence* **2018,** *197*, 252-265.
75. Ghosh, S.; Ray, G. B.; Mondal, S., Physicochemical investigation on the bulk and surface properties of the binary mixtures of N-methyl-N-dodecanoyl sodium glycinate (SDDS) and N-methyl-N-decanoyl glucamine (MEGA 10) in aqueous medium. *Fluid Phase Equilibria* **2015,** *405*, 46-54.
76. Mondal, S.; Ghosh, S.; Moulik, S. P., Colloidal Dispersions of Lipids and Curcumin, and the Solubility and Degradation Kinetics of the Latter in Micellar Solution. *Soft Materials* **2015,** *13* (2), 118-125.
77. Israelachvili, J. N., Intermolecular and surface force, 2nd ed.; Academic Press: London. **1991,** *Chapter 17, p 370.*
78. Galgano, P. D.; El Seoud, O. A., Micellar properties of surface active ionic liquids: A comparison of 1-hexadecyl-3-methylimidazolium chloride with structurally related cationic surfactants. *Journal of Colloid and Interface Science* **2010,** *345* (1), 1-11.
79. Páhi, A. B.; Király, Z.; Mastalir, Á.; Dudás, J.; Puskás, S.; Vágó, Á., Thermodynamics of Micelle Formation of the Counterion Coupled Gemini Surfactant Bis(4-(2-

dodecyl)benzenesulfonate)-Jeffamine Salt and Its Dynamic Adsorption on Sandstone. *The Journal of Physical Chemistry B* **2008,** *112* (48), 15320-15326.
80. Geng, F.; Liu, J.; Zheng, L.; Yu, L.; Li, Z.; Li, G.; Tung, C., Micelle Formation of Long-Chain Imidazolium Ionic Liquids in Aqueous Solution Measured by Isothermal Titration Microcalorimetry. *Journal of Chemical & Engineering Data* **2010,** *55* (1), 147-151.
81. Łuczak, J.; Markiewicz, M.; Thöming, J.; Hupka, J.; Jungnickel, C., Influence of the Hofmeister anions on self-organization of 1-decyl-3-methylimidazolium chloride in aqueous solutions. *Journal of Colloid and Interface Science* **2011,** *362* (2), 415-422.
82. Beyer, K.; Leine, D.; Blume, A., The demicellization of alkyltrimethylammonium bromides in 0.1M sodium chloride solution studied by isothermal titration calorimetry. *Colloids and Surfaces B: Biointerfaces* **2006,** *49* (1), 31-39.
83. Loh, W.; Brinatti, C.; Tam, K. C., Use of isothermal titration calorimetry to study surfactant aggregation in colloidal systems. *Biochimica et Biophysica Acta (BBA) - General Subjects* **2016,** *1860* (5), 999-1016.
84. Kessler, A.; Zeeb, B.; Kranz, B.; Menéndez-Aguirre, O.; Fischer, L.; Hinrichs, J.; Weiss, J., Isothermal titration calorimetry as a tool to determine the thermodynamics of demicellization processes. **2012,** *83* (10), 105104.
85. Majhi, P. R.; Moulik, S. P., Energetics of Micellization: Reassessment by a High-Sensitivity Titration Microcalorimeter. *Langmuir* **1998,** *14* (15), 3986-3990.
86. Anderson, S. L.; Rovnyak, D.; Strein, T. G., Direct Measurement of the Thermodynamics of Chiral Recognition in Bile Salt Micelles. **2016,** *28* (4), 290-298.
87. Chadha, C.; Singh, G.; Singh, G.; Kumar, H.; Kang, T. S., Modulating the mixed micellization of CTAB and an ionic liquid 1-hexadecyl-3-methylimidazollium bromide via varying physical states of ionic liquid. *RSC Advances* **2016,** *6* (44), 38238-38251.
88. Bijma, K.; B. F. N. Engberts, J.; J. Blandamer, M.; M. Cullis, P.; M. Last, P.; D. Irlam, K.; Giorgio Soldi, L., Classification of calorimetric titration plots for alkyltrimethylammonium and alkylpyridinium cationic surfactants in aqueous solutions. *Journal of the Chemical Society, Faraday Transactions* **1997,** *93* (8), 1579-1584.
89. Mehrian, T.; de Keizer, A.; Korteweg, A. J.; Lyklema, J., Thermodynamics of micellization of n-alkylpyridinium chlorides. *Colloids and Surfaces A: Physicochemical and Engineering Aspects* **1993,** *71* (3), 255-267.
90. Pires, P. A. R.; El Seoud, O. A. In *Benzyl (3-Acylaminopropyl) Dimethylammonium Chloride Surfactants: Structure and Some Properties of the Micellar Aggregates*, Smart Colloidal Materials, 2006; Springer Berlin Heidelberg: 2006; pp 131-141.
91. Shimizu, S.; Pires, P. A. R.; El Seoud, O. A., Thermodynamics of Micellization of Benzyl(2-acylaminoethyl)dimethylammonium Chloride Surfactants in Aqueous Solutions: A Conductivity and Titration Calorimetry Study. *Langmuir* **2004,** *20* (22), 9551-9559.
92. Shimizu, S.; Pires, P. A. R.; Loh, W.; El Seoud, O. A., Thermodynamics of micellization of cationic surfactants in aqueous solutions: consequences of the presence of the 2-acylaminoethyl moiety in the surfactant head group. *Colloid and Polymer Science* **2004,** *282* (9), 1026-1032.
93. Rudra, S.; Dasmandal, S.; Mahapatra, A., Binding interaction of sodium-N-dodecanoyl sarcosinate with hemoglobin and myoglobin: Physicochemical and spectroscopic studies with molecular docking analysis. *Journal of Colloid and Interface Science* **2017,** *496*, 267-277.
94. Prasad, M.; Chakraborty, I.; Rakshit, A. K.; Moulik, S. P., Critical Evaluation of Micellization Behavior of Nonionic Surfactant MEGA 10 in Comparison with Ionic

Surfactant Tetradecyltriphenylphosphonium Bromide Studied by Microcalorimetric Method in Aqueous Medium. *The Journal of Physical Chemistry B* **2006,** *110* (20), 9815-9821.
95. Smith, O. E. P.; Waters, L. J.; Small, W.; Mellor, S., CMC determination using isothermal titration calorimetry for five industrially significant non-ionic surfactants. *Colloids and Surfaces B: Biointerfaces* **2022,** *211*, 112320.
96. Seth, D.; Sarkar, S.; Sarkar, N., Dynamics of Solvent and Rotational Relaxation of Coumarin 153 in a Room Temperature Ionic Liquid, 1-Butyl-3-methylimidazolium Octyl Sulfate, Forming Micellar Structure. *Langmuir* **2008,** *24* (14), 7085-7091.
97. Lakowicz, J. R., *Principles of fluorescence spectroscopy*. Springer: 2006.

Table 1. Experimental CMC, surface pressure (π_{CMC}), minimum area per molecule (A_{min}), standard free energy of micellization (ΔG_m^0), standard free energy of interfacial adsorption (ΔG_{ad}^0), surface tension at CMC (γ_{CMC}), minimum free energy of the surface with maximum adsorption (G_{min}), and counterion binding (β) at 298.15 K.

% $\left(\frac{v}{v}\right)$ TFE	CMC (mM)			π_{CMC} ($mN.m^{-1}$)	$10^6\Gamma_{max}$ ($mol.m^{-2}$)	A_{min} $\left(\frac{nm^2}{molecule}\right)$	ΔH_m^0 ($kJ.mol^{-1}$)	ΔG_m^0 ($kJ.mol^{-1}$)	ΔG_{ads}^0 ($kJ.mol^{-1}$)	γ_{CMC} ($mN.m^{-1}$)	G_{min} ($kJ.mol^{-1}$)	β
	ST	COND	ITC									
SDS												
0	8.99	7.89	9.04	50.8	1.73	0.95	-2.198	-27.68	-51.18	20.6	11.78	0.42
5	8.51	7.74		24.1	0.46	3.58	-	-27.44	-66.53	19.2	41.39	0.30
10	8.14	6.93		15	0.45	3.68	-	-26.52	-43.15	19.0	42.11	0.25
20	4.84	6.47	7.99	2.3	0.43	3.88	-9.587	-23.33	-16.07	23.3	54.45	0.05
SDDS												
0	16.9	13.49	13.7	47.4	2.22	0.74	2.02	-27.56	-43.91	23.8	10.60	0.41
5	15.48	8.99		19.4	2.19	0.75		-26.59	-32.57	23.2	10.48	0.35
10	13.18	8.71		7.36	1.48	1.12		-25.10	-27.06	24.8	16.72	0.25
15	9.54		16.2	1.56	0.719	2.31	-6.966	-22.73	-20.36	27.0	37.56	0.10
CTAB												
0	0.77	1.03	0.55	38.6	1.23	1.86	-1.892	-43.81	-83.18	31.3	35.06	0.62
5	0.61	0.70		11.5	0.322	2.29	-	-38.13	-54.18	30.2	41.65	0.38
10	0.40	0.52		4.3	0.059	7.28	-	-36.48	-54.90	29.7	130.22	0.28
CTAT												
0	0.22	0.21		40.6	2.67	0.62	-	-43.90	-57.73	30.1	11.24	0.45
5	0.17	0.14		14.1	1.95	0.84	-	-44.86	-52.01	29.1	14.72	0.46
10	0.14	0.13		6.1	1.02	1.61	-	-39.15	-44.98	28.2	27.34	0.26
15	0.10			1	0.50	3.30	-	-	-	27.5	54.65	-
TX-114												
0	0.23			43.8	3.04	0.54	-	-29.98	-55.92	26.5	8.61	-
5	0.19			19.4	2.64	0.63	-	-30.35	-38.20	24.8	9.41	-
10	0.23			9.6	2.22	0.75	-	-29.79	-39.16	24.8	11.20	-
15	0.47			3.5	1.55	1.06	-	-27.96	-32.50	23.1	14.74	-

Standard uncertainties in terms of **CMC**, Γ_{cmc}, A_{min}, π_{cmc}, ΔG^0_m, and are ± 0.01%, ± 0.04%, ± 0.04%, ± 0.03%, ± 0.02% respectively.

Table 2. Aggregation Number (Nagg), Micropolarity, Packing Parameter (P), and Gordon Parameter (G) of SDS, SDDS, CTAB, CTAT and TX-114.

% $\left(\frac{v}{v}\right)$	G	N_{agg}	$\frac{I_1}{I_3}$	P
SDS				
0	-	105	0.89	0.22
5	16.19	83	0.86	0.058
10	12.63	53	0.82	0.056
20	9.89	46	0.87	0.053
SDDS				
0	-	76	0.97	0.28
5	16.19	72	0.89	0.27
10	12.63	70	0.88	0.18
15	9.89	67	0.86	0.09
CTAB				
0	-	52	1.09	0.11
5	16.19	38	1.08	0.09
10	12.63	25	1.07	0.03
CTAT				
0	-	37	1.03	0.33
5	16.19	32	0.98	0.25
10	12.63	20	0.98	0.13
15	9.89	13	1.04	0.06
TX-114				
0	-	48	1.13	0.38
5	16.19	48	1.09	0.33
10	12.63	9	1.05	0.28
15	9.89	12	1.08	0.19

Table 3. Time-Resolved Decay Parameter of SDS, SDDS, CTAB, CTAT, TX-114) in water and water/TFE mixed solvent at 298.15 K

% $\left(\frac{v}{v}\right)$ **TFE**	$\tau_1(ns)$	a_1	$\tau_2(ns)$	a_2	$\tau_{avg}(ns)$	χ^2
			SDS			
0	3.86	0.64	2.89	0.36	3.51	1.0954
5	3.85	0.98	0.31	0.02	3.77	1.0651
10	3.95	0.96	0.31	0.04	3.82	1.0813
15	4.02	0.96	0.24	0.04	3.86	1.0620
20	4.01	0.92	1.94	0.08	3.86	1.1339
			SDDS			
0	3.55	0.78	2.56	0.22	3.33	1.0005
5	3.90	0.91	1.14	0.09	3.66	0.9991
10	4.13	0.95	0.18	0.05	3.94	1.0083
15	4.11	0.88	1.97	0.12	3.86	1.0359
20	4.12	0.91	2.03	0.09	3.94	1.0601
			CTAB			
0	4.13	0.94	0.23	0.06	3.88	1.0712
5	3.97	0.93	0.45	0.07	3.71	1.0649
10	4.25	0.94	0.32	0.06	4.02	1.0661
15	4.27	0.99	0.35	0.01	4.21	1.0995
20	4.12	0.98	0.21	0.02	4.06	1.1800
			CTAT			
0	3.85	0.85	2.21	0.15	3.60	1.0637
5	3.66	0.92	0.18	0.08	3.37	0.9832
10	3.80	0.85	1.82	0.15	3.51	1.1050
15	3.96	0.84	1.92	0.16	3.63	1.0404
20	4.01	0.92	0.30	0.08	3.71	1.1295
			TX-114			
0	4.12	0.97	0.95	0.03	4.02	1.1402
5	3.77	0.89	0.10	0.11	3.36	1.1817
10	4.06	0.83	0.09	0.17	3.38	1.1173
15	3.65	0.72	2.40	0.28	3.30	1.0522
20	2.91	0.94	1.42	0.06	2.82	1.1055

The standard uncertainty of τ_{avg} is ± 5%.

Chapter-III

A physicochemical investigation of the complex formation by β-Cyclodextrin with Triton X-100 and Triton X-114 and their aggregation behaviour in aqueous solution: An experimental approach

A physicochemical investigation of the complex formation by β-Cyclodextrin with Triton X-100 and Triton X-114 and their aggregation behaviour in aqueous solution: An experimental approach

Abstract

The nature of complexation and binding affinity of Triton-X (TX-100 and TX-114) within β-cyclodextrin (β-CD) were investigated in an aqueous solution using various experimental approaches. The results obtained from analyzing experimental parameters (e.g., critical micelle concentration (*cmc*), aggregation number (N_{agg}), Stern-Volmer constant, and particle size distribution) have been used to determine the nature of complexation.

The DLS data provide strong evidence for the complexation process as well as the hydrophobic interaction between β-CD and Triton-X monomers. Utilizing the Benesi-Hildebrand method, the stoichiometry and binding constants for β-CD and Triton-X complexes have been determined. Such systematic and comparative study of Triton-X and β-CD is rare in the literature which can have potential applications in understanding various physicochemical aspects of drug delivery, solubilization, and other areas of interest.

1. Introduction

Cyclodextrins (CDs) are macrocyclic oligosaccharides which are linked by α-1,4-glucosidic bonds.[1] It was found by French chemist Antoine Villiers in 1891 as the fermented by-product of potato-starch. This truncated conelike oligosaccharides can be classified in terms of the number of d-glucose units as α-, β-, and γ-CDs. They are made up of six, seven, and eight α-(1-4) D-glucopyranose units, respectively. Seven units of glucose make up the oligosaccharide β-cyclodextrin (β-CD), which has a toroidal shape and a hydrophilic outer side.[2] With the help of these intriguing properties, they can bind selectively with some organic molecules into their cavities to create stable host-guest inclusion complexes, exhibiting remarkable molecular selectivity and enantioselectivity. The size of the interior cavity of these oligosaccharides, which are typically cone-shaped, varies from 4 to 8 Å depending on how many sugar units make up the macrocycle. The two rims are defined differently in the literature, with the smaller one typically being referred to as the primary rim or head and the bigger one frequently being referred to as the secondary rim or tail. In the cone structure, the O-H groups on the outward side of the cone provide the hydrophilic qualities while the C-H bonds-oriented inward provides a comparatively hydrophobic cavity. In addition, non-bonding electron pairs of oxygen atoms in the glycoside bonds point inward, toward

the cavity, resulting in high electronic density which makes the nature of the cavity of CD as Lewis basic.[3] The typical structure of cyclodextrin gives them their remarkable physico-chemical characteristics, particularly their capacity to form host-guest complexes. The presence of hydrophilic and hydrophobic regions, excess electron density, and highly structured water molecules all contribute to the development of host-guest complexes with a range of substances, including medicines,[4-6] surfactants, polymers[3, 7, 8] and essential oils.[9] The characteristics of the guest molecules are significantly impacted by the development of inclusion complexes. In particular, the inclusion complex lowers the guest molecule's chemical potential, which improves solubilization and controls the characteristics of volatilization.[10-12] In the last 120 years of development, especially in its rapid progress since the 1980s, many scientists have contributed in the progress of these fascinating molecules and promoted their practical application in almost every sector of industry.[13, 14] CD-based molecular recognition and assembly has been the focus of supramolecular chemistry over the past decades, mainly due to its excellent molecular binding ability to a variety of organic and bioactive substrates, both in aqueous solutions and solids.[15-18] Additionally, the self-assembly of CDs can lead to the formation of numerous molecular-level nanostructures with distinctive topological characteristics, including catenanes, (pseudo) rotaxanes, supramolecular polymers, crosslinked hydrogels and networks, functionalized nanoparticles, etc.[19-28]

Additionally, the superior biocompatibility and low toxicity of CDs make inclusion complexes suitable for a wide range of applications, including those in the food industries,[29] pharmaceutical,[11] medical,[30] and cosmetic,[31, 32] as well as electronic technology[33, 34] and other fields. Research on the creation of inclusion complexes between CDs and surfactants is highly dynamic. Not only due to their great relevance for the pharmaceutical, food, and cosmetic industries, but also due to the fact that these mixtures have a propensity for creating intricate supramolecular aggregates as a result of the careful balancing of numerous forces. Additionally, the nearly limitless selection of surfactants on hand and their responsiveness to various stimuli make this a very rich field for colloidal scientists seeking the spontaneous synthesis of complex materials from basic building blocks. A third component, specifically a different kind of surfactant or polymer, can be added to the mixture as a further important parameter to influence the supramolecular assembly of CD/surfactants inclusion complexes.[35] The system becomes especially complex as specific host-guest interactions, long-range electrostatic and dispersion forces, and directional, short-range hydrogen bridge between adjacent CD molecules interact. Either emphasizing the structure and stimulus-responsiveness of

the inclusion complexes or the thermodynamics of binding here, we present an updated and thorough analysis of the thermodynamic factors defining the development of the inclusion complex between simple surfactant and cyclodextrins. A significant amount of CD has been used as modifiers in the creation of electrochemical sensors because of its exceptional host-guest supramolecular recognition capacity.[36-38] Much work has gone into creating CD polymers that allow for increased CD loading in order to boost the recognition capacity of β-CD.[39, 40] These polymers, however, have a small surface area. Porous CD-metal organic frameworks (CD-MOFs), which were created by CD and alkali metal ions, have recently been reported by a number of research groups. These CD-MOFs exhibit extremely selective gas adsorption for gases like CO_2 and HCHO due to their well-defined porous architectures with high surface area and high porosity.[41-43]

Surfactants are amphiphilic compounds that have the ability to reduce the surface tension of water, as well as other solvents.[44] Since many years ago, surfactants have been used extensively in the pharmaceutical industry, cosmetic products, household cleaners, and various industrial formulations and processing, such as solubilizers, wetting agents, emulsifiers, and separation of metal ions, organic molecules, enzymes, etc..[45-47] A simplified model of bio-membranes has been created using surfactant micelles.[48] Surfactants are anticipated to accommodate the poorly soluble important chemical components in water in medicinal formulations by forming a surfactant micelle.[49-51] Nonionic surfactants typically form micelles in very diluted solutions and are biodegradable, less toxic, more stable, and mild in nature. Nonionic surfactants typically become less soluble as temperature rises; as a result, at a specific higher temperature, precipitation or phase separation occurs, causing the solution to become turbid or hazy. Additionally, nonionic surfactants are chemically more efficient molecular species when compared to other types of surfactants, making them ideal for use as excipients in pharmaceutical formulations and drug delivery.[52, 53] They are also used to help with solubilization[54] and to increase the stability of drug carrier emulsions.[55] One of the detergents that is frequently used in laboratories, businesses, and for research reasons is Triton X. It can also be used to lyse cells and remove their proteins and organelles.[56] It is one of the often-used ingredients in influenza vaccines. Triton X is frequently employed in biochemical applications, such as solubilizing proteins and recovering membrane components under mild nondenaturing circumstances.[56]

In this study, a host-guest complexation between β-CD and two surfactants belongs to the Triton X family (Triton X-114, Triton X-100) series was explored. Tensiometry, fluorescence, dynamic light scattering (DLS), time-resolved fluorescence study, UV–visible spectroscopy were used to investigate the progress of inclusion complexes. The impact of β-CD in Triton X on the aggregation number, polarity, critical micelle concentration (*cmc*) has been investigated. Using the Benesi-Hildebrand approach, the binding constants and binding mode for cyclodextrin/ Triton-X complexes have been found and particle size for a 1:1 complex was also determined using DLS. The information obtained from comparative investigation can be useful in wide range of applications of amphiphile-cyclodextrins inclusion compound.

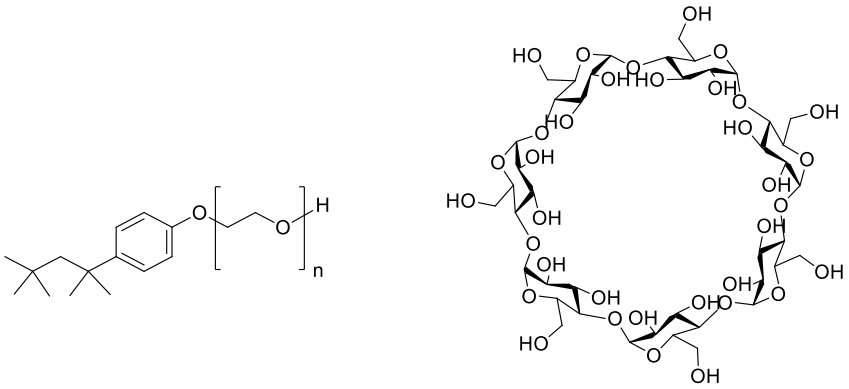

Figure 1. Chemical structure of (A) Triton X (n= 9-10 for Triton X-100; n= 7 for Triton X-114) (B) β-Cyclodextrin (β-CD).

2. Experimental Procedures

2.1. Materials and methods

Triton X-114, Triton X-100, β-cyclodextrin (≥ 97%), cetylpyridinium chloride monohydrate (CPC) (purity 98%), coumarin 153 **(**purity ~ 99%**)** and pyrene (purity ≥ 98%) were purchased Merck, India. Pyrene was recrystallized before use.

2.2. Tensiometry

Krüss (Germany) tensiometer was employed with the ring detachment method for surface tension measurements. Concentrated stock solution [~ 15 times of critical micelle concentration (cmc)] of Triton X prepared at various mole fractions of β-CD in aqueous medium was added to that parent solution of β-CD of that particular mole fraction with a Hamilton micro syringe, giving it five minutes to equilibrate before each measurement. To test the reproducibility of all measurements, they were performed three times. The approach had an accuracy of ± 0.1 $mN.m^{-1}$. Surface tension (γ) vs. log [surfactant] was plotted to obtain the *cmc* of triton X [cf. Figure 2]. The value of *cmc* was obtained from the breaks in the plot.

2.3. Fluorimetry

Utilizing a Perkin Elmer LS55 fluorescence spectrophotometer, measurements of fluorescence were performed. A water-flow thermostat attached to the inside cell compartment was used to maintain the temperature at 298 K. Surfactant solutions with a concentration exceeding the *cmc* were used. Pyrene was excited at 332 nm, and emission spectra were acquired at 373 and 384 nm, which correspond to its first and third vibrational peaks, respectively. Excitation and emission were conducted using slits that were 9 and 4 nm, respectively. 250 nm per minute was chosen as the scan speed. Using cetylpyridinium chloride (CPC) as a quencher, the values of aggregation number (N_{agg}) were ascertained using the pyrene fluorescence quenching method. The concentration of the pyrene solution was kept low enough (~10^{-6} (M)) when it was introduced to the various surfactant solutions to prevent the creation of its eximer. The quencher was gradually added, and the intensity was noted for future studies.

2.4. Steady-state spectral measurements

A Shimadzu 1601 UV-vis spectrophotometer from Japan and a Perkin-Elmer LS 55 fluorescence spectrophotometer from the United States were used, respectively, to record the absorption and fluorescence emission spectra, respectively. With an excitation wavelength of 270 nm and emission slit widths of 10 nm and 5 nm, emission spectra of Triton X were captured in the range of 290–350 nm. Freshly prepared solutions were used for all spectroscopic measurements.

2.5. Dynamic light scattering (DLS) measurement

DLS measurements were performed in a Zetasizer Nano ZS (Malvern, UK) at a scattering angle of 90° using a He-Ne laser (λ= 632.8 nm). All solutions having concentrations just over the *cmc* at that mole fraction were filtered three times with membrane filters (porosity: 0.25 μm) to remove larger particles. The particle sizes of the solutions were measured three times in the same instrument to check the reproducibility.

2.6. Time-resolved fluorescence study

Time-resolved fluorescence decay was performed utilising a Horiba-Jobin-Yvon FluoroCube fluorescence lifetime system with 450 nm NanoLEDs (IBH, UK) as excitation sources for the probe, coumarin 153 and a TBX photon detection module as the detector. Using the IBH DAS-6 decay analysis software, all of the decay data were fitted. The sodium dodecyl sulphate micellar solution was used as a scatterer in place of the sample to obtain the lamp profile. The χ^2 values were kept somewhat near to 1 for the proper fits.

3. Results and discussion

3.1. Effects of β-CD on Critical Micelle Concentration

When surfactant solution was gradually added into the aqueous medium, the surface tension of the system decreases up to a certain minimum. Concentration corresponding to the minimum value of surface tension is defined as critical micelle concentration, *cmc*. In the Figure 2, plots of surface tension versus log of total concentration of surfactant [Triton X] are provided. Hydrophobic interaction is the most important for the understanding of micellization process.[57] When amphiphiles are added to aqueous media, the hydrophobic moiety of the molecule breaks the structure of the water molecules connected through hydrogen bonding and thus, water molecules are liberated from hydration shells [58] which results the increase in the entropy of the system. With increasing hydrophobicity of the system, micellization appears in lower concentration of the surfactants. Therefore, from Table 1, it is evident that *cmc* value of TX-114 at different molefractions of β-CD is lower (10-25 %) than that of TX-100 excepting very high molefraction of β-CD ($\alpha_{\beta-CD}$= 0.8 and 0.1). From the Table 1, it can also be seen that with increasing the mole fraction of β-CD, the *cmc* value also increases.

The hydrocarbon tail of the non-ionic surfactant plays an important role here. The alkyl chain of the amphiphile is more likely to be incorporated into the hydrophobic cavity of β-CD and its polar oxyethylene headgroup remains outside of the cavity. Addition of β-CD breaks the original structure of micelle and releases the monomers which are then encapsulated into the β-CD cavity. Due to inclusion of monomer into the β-CD cavity more surfactant is required to form micelles which leads to the increase in *cmc* values for the both systems.

The amphiphilic molecules preferentially adsorb at the air/solution interface than the bulk phase. Gibbs adsorption equation [59, 60] is employed to calculate the amount of adsorbed amphiphile per unit area of the surface as follows:

$$\Gamma_{\max} = -\frac{1}{2.303nRT}\lim_{C\to cmc}\left(\frac{d\gamma}{d\log C}\right)_{max} \text{mol.m}^{-2} \quad (1)$$

Here, $d\gamma/d\log C$ denotes the slope of the surface tension (γ) vs log of concentration profile (Figure 2). R and T indicate universal gas constant (8.31 J mol^{-1} K^{-1}) and temperature in Kelvin scale respectively and n denotes number of ionic species adsorbed at the interface. For non-ionic systems in aqueous solution, the value of n is taken as unity. With increasing the mole fraction of β-CD molecule, there is no significant trend in the value of $\Gamma_{\max}$ observed in both the systems. The minimum area per molecule (A_{min}) can be calculated by the relation:

$$A_{min} = \frac{10^{18}}{N_A\Gamma_{max}}\, nm^2 molecule^{-1} \quad (2)$$

where N_A signifies the Avogadro number. From Table 1, it is apparent that with increasing mole fraction of β-CD, the A_{min} values are somewhat greater in case of β-CD/TX-100 system than β-CD/TX-114 system. This signifies the less compact packing of monomers with increasing concentration of β-CD in case of β-CD/TX-100 system.

An important term which is a measure of the efficiency of adsorption of the amphiphiles is pC_{20}

which is defined as follows:

$$pC_{20} = -logC_{20} \quad (3)$$

where C_{20} is the concentration of surfactant required to reduce the surface tension of the solvent by 20 mN m^{-1}.[61] Higher value of pC_{20} signifies the requirement of lower concentration to reduce the

surface tension by 20 mN m^{-1} i.e., the amphiphile is more surface active. The value of pC_{20} decreases with increase in mole fraction of β-CD for both the systems. The reduction in the value of pC_{20} is more in the case of β-CD/ TX-100 system than β-CD/ TX-114 which reveals the fact that β-CD/TX-114 system has better efficiency of adsorption (Table 1). In the presence of β-CD, mixtures show a lower value of pC_{20} which means that β-CD reduces the surface activity of the systems (Table 1). In another word, in presence of β-CD, more amphiphile is needed to reduce the surface tension by same magnitude, i.e., β-CD delays the aggregation of the surfactants and so *cmc* value increases.

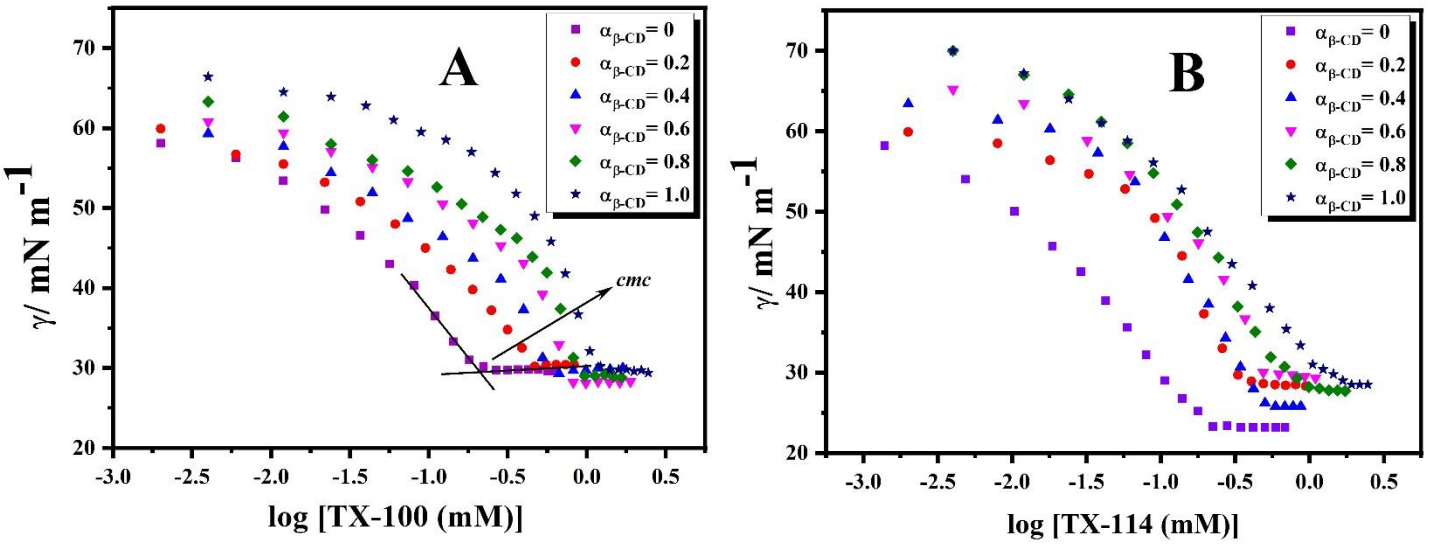

Figure 2. Plots of surface tension (γ) vs. (A) log [TX-100 (mM)], (B) log [TX-114 (mM)] at different mole fractions of β-CD in water at 298.15 K.

3.2. Thermodynamics

The standard value of Gibbs free energy of micellization (ΔG_m^0) is evaluated from the equation as given below [62] :

$$\Delta G_m^0 = RT \ln X_{cmc} \quad (4)$$

where, X_{cmc} represents the *cmc* in terms of mass fraction units and R and T indicate universal gas constant (8.31 J mol^{-1} K^{-1}) and temperature in Kelvin scale respectively. ΔG_m^0 values are negative for both the systems and for all mole fractions of β-CD; but the magnitude decreases with the increase in the mole fraction of β-CD which indicates that though the micellization is a

thermodynamically favourable, it becomes less spontaneous in presence of β-CD (Table 1). The variations of the enthalpic and entropic contributions make consequence of either an increase or decrease in ΔG_m^0 values. The release of water molecules by breaking the clusters surrounding the amphiphiles is responsible for the increase of entropy and spontaneity of the system during formation of micelles. β-CD traps the hydrophobic tails of the amphiphile and thus, breaks the cluster of water molecule surrounding the surfactant monomers before micellization. Therefore, magnitude of entropy gained during micellization process reduces and thus, accordingly, ΔG_m^0 values become less negative in presence of β-CD. The standard free energy of interfacial adsorption (ΔG_{ad}^0) is evaluated by using [63]

$$\Delta G_{ad}^0 = \Delta G_m^0 - \frac{\pi_{cmc}}{\Gamma_{max}} \quad (5)$$

In the above relation, π_{cmc} is the surface pressure at the *cmc* which is defined as:

$$\pi_{cmc} = \gamma_0 - \gamma_{cmc} \quad (6)$$

Here, γ_0 and γ_{cmc} are termed as the surface tension values of pure solvent and the solution at *cmc*. The calculated ΔG_{ad}^0 values are negative indicating the spontaneous adsorption processes. The more negative ΔG_{ad}^0 values than the corresponding ΔG_m^0 values indicate that adsorption is the primary process whereas, micellization is secondary one. An important thermodynamic parameter, G_{min} is defined as free energy change of the amphiphiles during transition from bulk phase to the air/solution interface in the system. G_{min} can be obtained from the relation as follows [64] :

$$G_{min} = A_{min}\gamma_{cmc}N_A \quad (7)$$

The parameter, G_{min} includes the contributions of γ_{cmc} and A_{min} which are important in the process of monolayer formation. The significance of G_{min} is that the amount of work is needed to form a surface area per mole or the change of Gibbs free energy change per mole in transition of amphiphile molecules from the bulk phase to the surface phase of solution. Lower value of Gibbs free energy signifies the formation of more thermodynamically stable surface. The calculated values are provided in the Table 1. The lower values (20- 40%) of G_{min} in case of β-CD/ TX-114 system compared to β-CD/TX-100 system inferred the formation of thermodynamically stable surfaces in that system.

The phenyl ring of Triton X is 3.0 Å wide and 5.0 Å long [65] which is small to fit inside the cavity of β-CD of which inner diameter is 7.8 Å wide and 7.8 Å long.[66] From the previously reported NMR results, it is evident that the hydrocarbon part, phenyl group and a part of the EO chain next to the phenyl group has proximity with the protons (H-3 and H-5) of the β-CD [65] that supports the incorporation of the hydrophobic portion of the surfactant molecule into the β-CD cavity with the polar oxyethylene headgroup remaining exposed to the solvent outside of the cavity. To interpret the association of surfactant molecule with β-CD, three types of interactions is to be considered: (a) van der Waals interactions, (b) hydrogen bonding interactions and (c) hydrophobic interactions.[67, 68] However, the resultant of these factors is measured in this study by the use of thermodynamic parameters.

Nonionic surfactants like TX-100 and TX-114 have tendency to form strong hydrogen bonding with water.[69] As TX-100 contains greater number of oxyethylene (EO) units (10), the hydrogen bonding with water is stronger in this case than the TX-114 and also it is supposed to form more random coil conformation before complexation with β-CD; while for TX-114 with smaller EO units (8) it is expected to form more linear conformation with trans geometry.[70] Therefore, the largest decrease of enthalpy and entropy is detected for the β-CD/TX-100 system after complex formation owing to its loss of random coil conformation of the EO units. In case of β-CD/TX-114, this decrease of enthalpy and entropy is less due to its smaller number of EO units. This is the reason behind the less spontaneous micellization process of β-CD/TX-100 system evident from the less negative ΔG_m^0 values (Table 1) of that system compared to the other at particular mole fraction of β-CD.

3.3. Aggregation numbers (N_{agg}) of β-CD/TX-100 and β-CD/TX-114 systems

The fluorescence quenching method by using pyrene as a probe is used for the determination of micellar aggregation numbers (N_{agg}).[71] Cetylpyridinium chloride (CPC) is used here as a quencher. The fluorescent probe (pyrene) distributes itself among micelles with a quencher CPC and with micelles without CPC. To evaluate N_{agg}, the following equation is used [72] :

$$ln\frac{F_0}{F} = \frac{N_{agg}[Q]}{[S]-cmc} \quad (8)$$

where, F_0 and F represent the fluorescence intensities corresponding to the first vibronic peak of pyrene at 373 nm in the presence and absence of CPC respectively, $[S]$ is the total concentration of surfactant mixture and $[Q]$ represents the concentration of the CPC.

A linear plot is obtained between $ln\frac{F_0}{F}$ vs $[Q]$ graph (Figure 3) having slope equals to $N_{agg}/([S] - cmc)$, giving values of N_{agg}. The values of N_{agg} for β-CD/TX-100 and β-CD/TX-114 mixtures were determined from using plots in Figure 3. Data were presented in Table 2 as well. Increasing mole fraction of β-CD tends to increase the N_{agg} values probably due to formation of larger closely packed aggregates. The N_{agg} value of β-CD/ TX-114 having lower mole-fraction of β-CD ($\alpha_{\beta-CD}$= 0.2) is higher than that of β-CD/ TX-100. This is understandable from the fact that TX-114 molecule contains smaller number of oxyethylene monomers and thus makes it more hydrophobic in nature compared to TX-100. As a consequence, TX-114 tends to form aggregate having greater number of monomer than TX-100. However, with increasing mole-fraction of β-CD (for $\alpha_{\beta-CD}$= 0.4, 0.6, 0.8), complexation process with TX-100 is probably more favourable which tends to form β-CD/ TX-100 micelles with higher number of monomers which is reflected from the higher N_{agg} values of β-CD/ TX-100 system than the β-CD/ TX-114 combination.

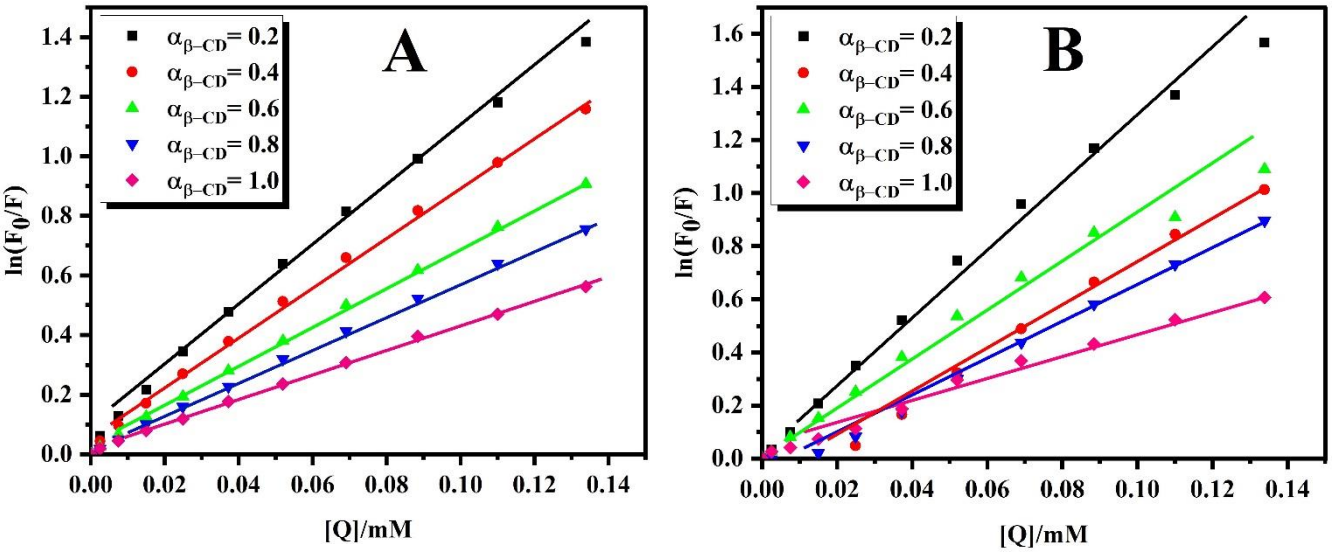

Figure 3. Plot of ln [F₀/F] vs [CPC (mM)] in case of (A) TX-100 (B) TX-114 in various mole fractions of β-CD at 298.15 K

3.4. Microenvironment

Micropolarity and dielectric constant are two important parameters determined here by steady state quenching of fluorescence of pyrene with a suitable quencher CPC. Micropolarity was measured using micellar solution of each component of both the systems above *cmc*. Figure 3 represents the fluorescence spectra of pyrene having concentration of 10^{-6} M in aqueous micellar solutions at varying quencher (CPC) concentrations. The value of the ratio $\frac{I_1}{I_3}$ < 1 signifies the non-polar environment around the probe, pyrene and $\frac{I_1}{I_3}$ > 1 signifies the polar surroundings.[73] From the Table 2, it is evident that the $\frac{I_1}{I_3}$ ratio equals to 1.10–1.14 which depicts that the probe is solubilized near the polar region of the aggregates. Also, the calculated $\frac{I_1}{I_3}$ ratio is somewhat higher in case of β-CD/TX-114 system than the other. This observation can be illustrated by considering water penetration in the systems. The more compact arrangement of headgroup, the more difficult it is to penetrate by the water molecules. On the other hand, less compact headgroup arrangement makes the micellar system more vulnerable to penetrate by water molecules. TX-100 contains greater number of PEO chain, therefore, it undergoes more water penetration and thus, magnitude of micropolarity decreases compared to the other system including TX-114.[74, 75]

The apparent dielectric constant (D_{exp}) of the medium (environment around the pyrene in the micelle) can be calculated [76, 77] from the following relation

$$\frac{I_1}{I_3} = 1.00461 + 0.01253D_{exp} \quad (9)$$

The D_{exp} values follow the similar trend as the ratio $\frac{I_1}{I_3}$ (Table 2). The nature of the hydrophobic environment can be further interpreted in terms of quenching by evaluating first-order quenching rate constant using Stern–Volmer equation as follows:

$$\frac{F_0}{F} = 1 + K_{SV}[Q] \quad (10)$$

where, K_{SV} is Stern–Volmer binding constant and $[Q]$ represents the concentration of the CPC. The value of K_{SV} depends on the solubility of the quencher and probe in the micellar system. Greater solubility implies higher K_{SV} value. The value of K_{SV} declines with increasing mole fraction of β-

CD which implies increasing hydrophobicity of the medium. Also, K_{SV} values are higher in case of β-CD/TX-114 system than the other which indicates the more hydrophobic nature of the system.

3.5. UV absorption of TX-100 and TX-114

Aqueous solution of Triton X shows absorption maxima at 275 nm with a shoulder peak at 285 nm (Figure 4). With increasing concentration of Triton X from below *cmc* to above the *cmc* absorbance also increases with a slight red shift. Similar observation has also been observed by Gratzer and Beaven [78] and Ray and Némethy [79] with differential observation of molar absorptivity and vibrational structures of Triton X.

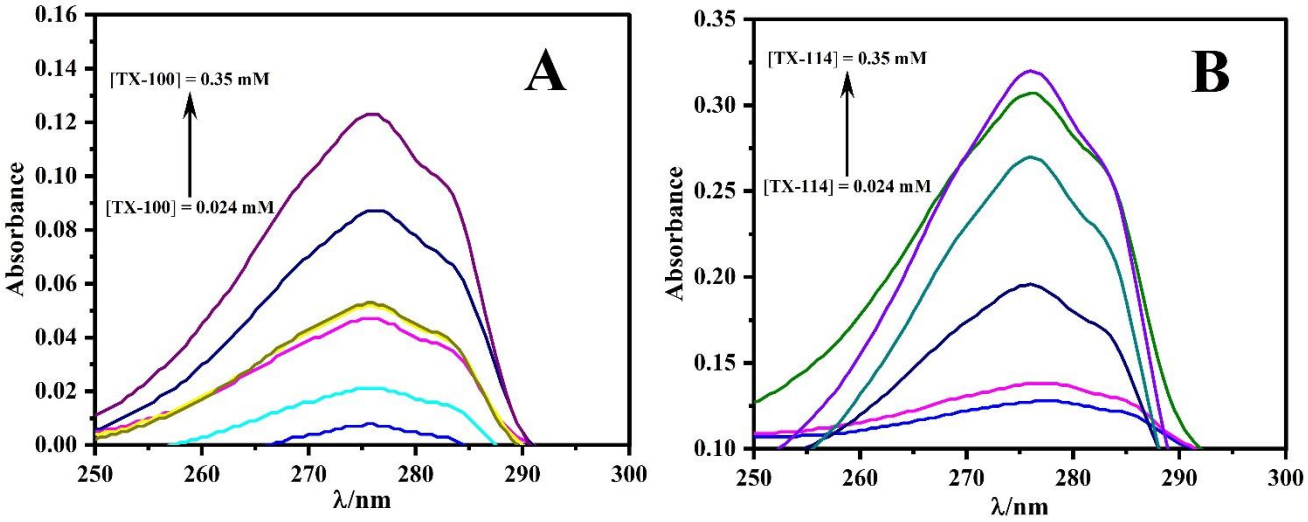

Figure 4. Absorption spectrum of (A) TX-100 (B) TX-114 with variation of its concentration in water at 298.15 K.

3.6. UV absorption of β-CD/TX-100 and β-CD/TX-114 systems

The UV absorbance spectra of β-CD/Triton X system has been shown in Figure 5. With increasing concentration of β-CD from 1.0×10^{-3} M to 8.0×10^{-3} M, absorbance increases or remains constant or slightly decreases. Another important fact is that with increasing β-CD concentration, the spectral band of Triton X becomes more distinct than the previous one and poorly defined shoulder peak becomes more apparent as well. Also, a slight red shift of absorbance has been observed with

increasing the concentration of β-CD to 8.0 × 10^{-3} M. Crooks [80] have explained the similar kind of observation by an electron donating species that is non absorbing called as auxochrome. Auxochrome modifies the absorption of parent molecule containing chromophore. In this study, combination of phenyl ring of Triton X and the electron donating hydroxyl and glycosidic oxygens of β-CD are likely to act as auxochrome which is responsible for the red shift in the UV absorption spectra.

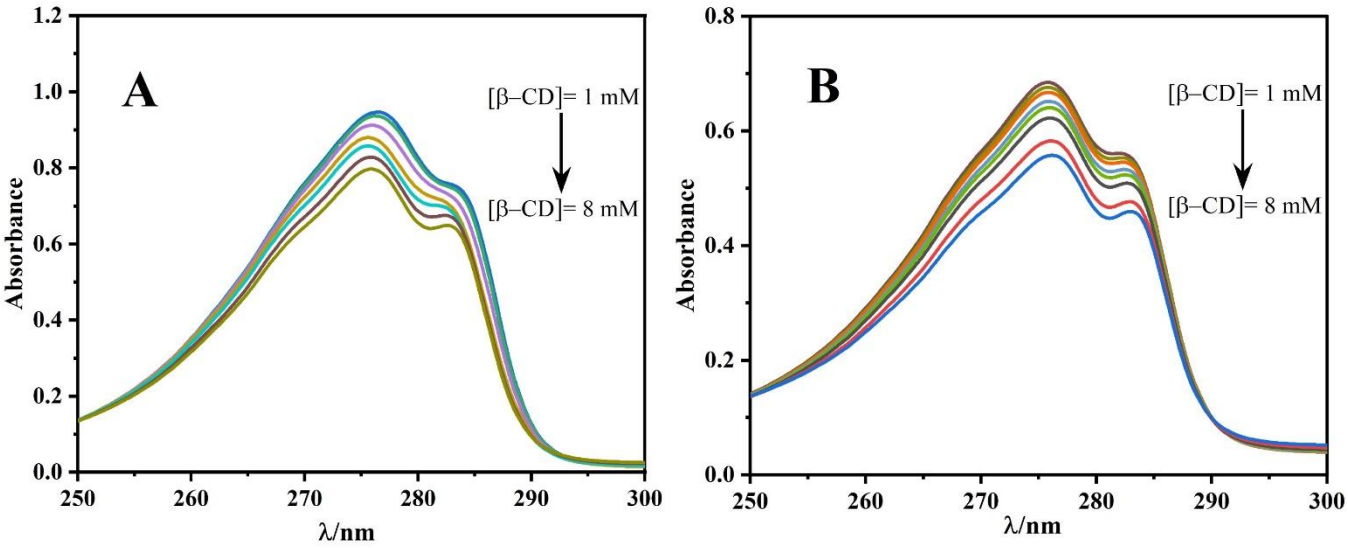

Figure 5. Absorption spectrum of (A) TX-100 (B) TX-114 with variation of concentration of β-CD in water at 298.15 K

3.7. Measurement of steady state emission Spectra

Figure 6 represents the increase in fluorescence emission spectra of TX-100. The fluorescence spectrum shows a peak positioned around 305 nm. The intensity was recorded at the peak maxima at 305 nm. The fluorescence intensity increases with increasing concentrations of β-CD (Fig. 6A). This gives the indication of incorporation of monomeric units within the β-CD cavity. The modified Benesi−Hildebrand equation [81, 82] can be applied to get an idea about the binding between β-CD/surfactant interactions. Here, the systematic titration data have been used to determine the binding pattern of β-CD/surfactant systems following the equation 11:

$$\frac{1}{\Delta F} = \frac{1}{\Delta F_{max}} + \frac{1}{K\Delta F_{max}} \frac{1}{[\beta CD]^n} \qquad (11)$$

where $\Delta F = F_x - F_0$ and $\Delta F_{max} = F_\infty - F_0$; F_0, F_x, and F_∞ are the fluorescence intensities of surfactant in absence of β-CD, at an intermediate β-CD concentration, and final β-CD concentration, respectively. K and n represents the binding constant and stoichiometric coefficient, respectively. The graphical plots of $^1/_{\Delta F}$ vs $^1/_{[\beta CD]}$ gives a straight line which

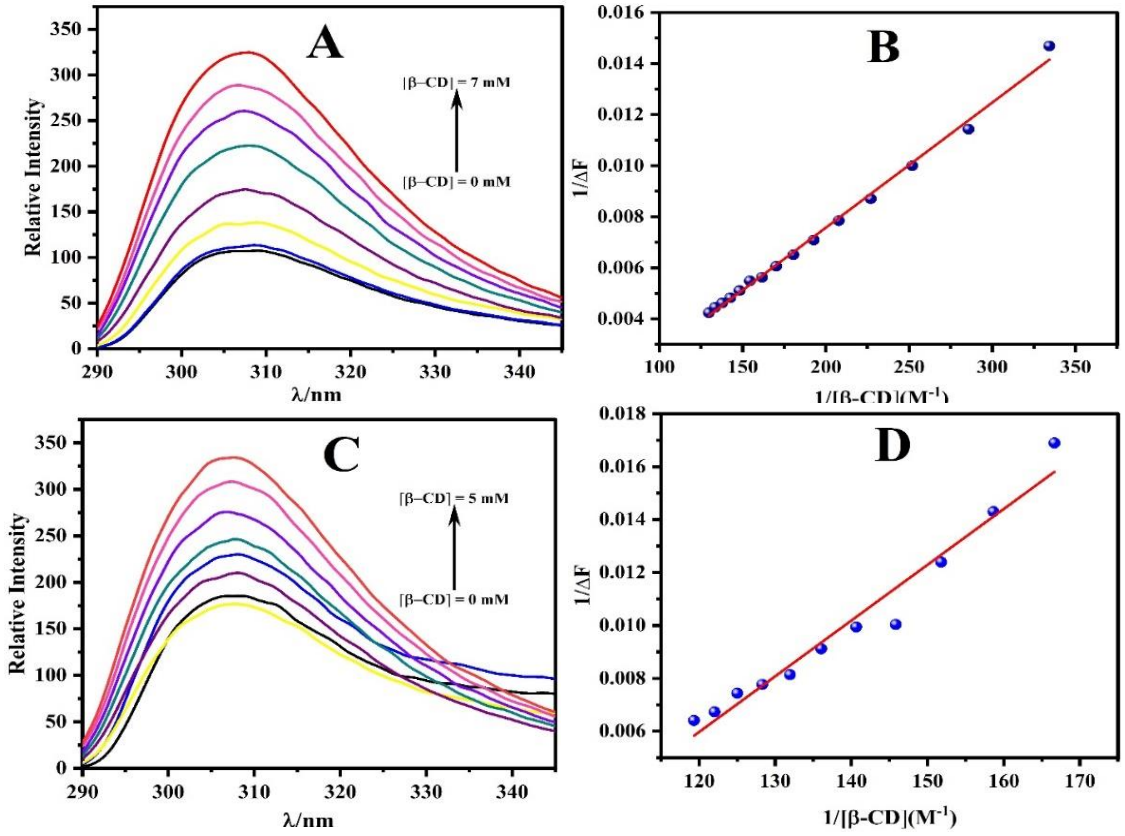

Figure 6. Fluorescence spectrum of (A) TX-100, (C) TX-114 and corresponding $\frac{1}{\Delta F}$ vs $\frac{1}{[\beta CD]}$ plot of (B) TX-100, (D) TX-114 with variation of concentration of β-CD in water at 298.15 K.

confirms 1:1 binding mode between β-CD and surfactant, and the binding constant value is 5.102 M^{-1} for β-CD/TX-100 (Fig. 6B). In case of β-CD/TX-114 system, similar nature of fluorescence spectra is observed (Fig. 6C) and considering the plot of $^1/_{\Delta F}$ vs $^1/_{[\beta CD]}$ (Fig. 6D), the value of K is 0.79 M^{-1}. The comparatively low value in case of β-CD/TX-114 system than β-CD/TX-100

system is observed due to more hydrophobic nature of TX-114 which tends to form more stable aggregate than TX-100 discussed earlier. The more stable aggregates of TX-114 are reluctant to form complex with β-CD and thus, forms less stable complex.

3.8. Dynamic light scattering (DLS) measurement

The dynamic light scattering (DLS) technique is frequently employed to investigate the particle size distribution of self-assembled nanostructures produced in aqueous surfactant solutions [57]. Figure 7 displays the aggregate size distribution for aqueous solutions of triton-X and their mixtures with varying concentrations of β-CD. Hydrodynamic diameter in the absence of β-CD found for the TX-100 and TX-114 micelles are ~ 458.7 nm and above 1100 nm respectively. An interesting observation was found in the presence of β-CD for both the systems.

In case of β-CD/ TX-100 system micelles having hydrodynamic diameter ~7 nm is found to be present with varying mole-fraction of β-CD. The aggregates with hydrodynamic diameter ranging from 100 to 1000 nm are found to be absent in the presence of β-CD which reveals the fact that TX-100 monomers having random coil conformation due to oxyethylene (EO) units before complexation with β-CD undertake complexation with β-CD breaking the random coil structure.

A completely different observation was found in the case of β-CD/ TX-114 system. Aggregates having hydrodynamic diameter greater than 1000 nm which is similar to the uncomplexed TX-114 are found to be predominant in solution in the presence of β-CD. Although the size of the aggregates in the presence of 1.0 mM β-CD are found to be ~ (300-500) nm. The probable reason behind this differential observation of the two different systems is that TX-114 molecule is more hydrophobic in nature as it contains a smaller number of oxyethylene groups compared to TX-100. Thus, TX-114 tends to form stable aggregates which are reluctant to form complex with β-CD. However, at higher mole fraction of β-CD (1.0 mM), the complexation process with TX-114 is comparatively more favourable which is reflected in the disappearance of the aggregates having higher diameter (~1000 nm).

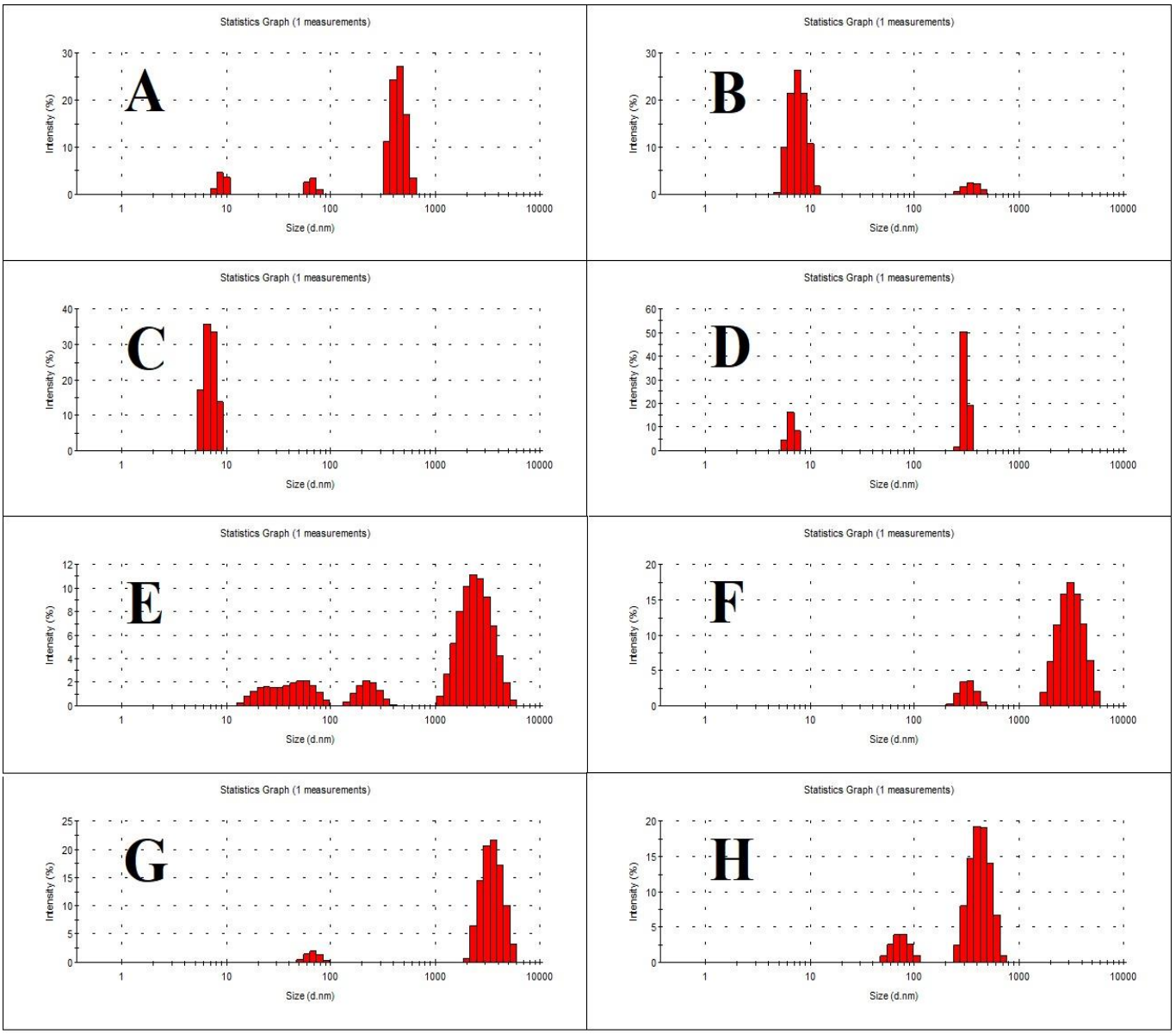

Figure 7. DLS profile of (A)-(D) β-CD/ TX-100 and (E)-(H) β-CD/ TX-114 systems with variation of mole-fraction of β-CD; (A) $\alpha_{\beta-CD}$= 0.0, (B) $\alpha_{\beta-CD}$= 0.6, (C) $\alpha_{\beta-CD}$= 0.8, (D) $\alpha_{\beta-CD}$= 1.0 and (E) $\alpha_{\beta-CD}$= 0.0, (F) $\alpha_{\beta-CD}$= 0.6, (G) $\alpha_{\beta-CD}$= 0.8, (H) $\alpha_{\beta-CD}$= 1.0.

3.9. Time-resolved fluorescence decay Measurements

Time-resolved fluorescence decay measurement provides the information regarding environment around a probe molecule and stability in its excited state. The anisotropic decay value ($r(t)$) can be expressed at time t with two relaxation components τ_1, and τ_2 as:

$$r(t) = r_0 \left[a_1 e^{-t/\tau_1} + a_2 e^{-t/\tau_2} \right] \quad (12)$$

where r_0 represents the anisotropy value at t = 0 and a_1, and a_2 are termed as the pre-exponential factor i.e., the contributing factor of each time scale component. Two components appear from two different environments of the probe molecules (here coumarin 153) located in the amphiphile/water interface and hydrophobic core of micelle. The average time value (τ_{av}) can be expressed as follows:

$$\tau_{av} = a_1\tau_1 + a_2\tau_2 \quad (13)$$

The life time decay profiles have been represented in Figure 8. In absence of amphiphile, the probe molecule is mainly distributed between the air/water interface and hydrophobic core of the β-CD. When concentrated solution of surfactant was added gradually, the probe molecules are distributed to the hydrophobic portion of the monomers. In this circumstance, τ_{av} value remains more or less constant. After attaining the critical micellar concentration, majority of the probe molecules gets distributed to the hydrophobic core of the micelle. In this case, τ_{av} value of the probe starts increasing. From τ_{av} vs conc of the surfactant plot (Fig. 9), we can also get the *cmc* value from intersection point of the two lines representing the change of τ_{av} with concentration of the amphiphile. The average life time values of the probe have been given in the Table 3.

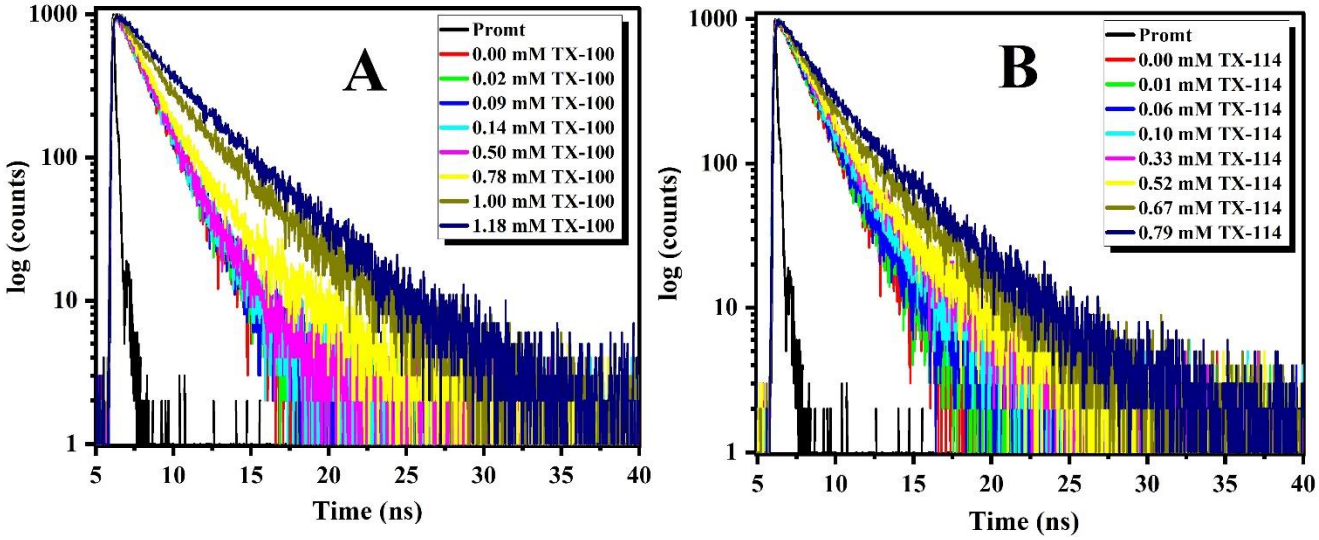

Figure 8. Life time decay profile of solubilized coumarin 153 of (A) TX-100 and (B) TX-114 systems with variation of its concentration at 0.6 mM β-CD.

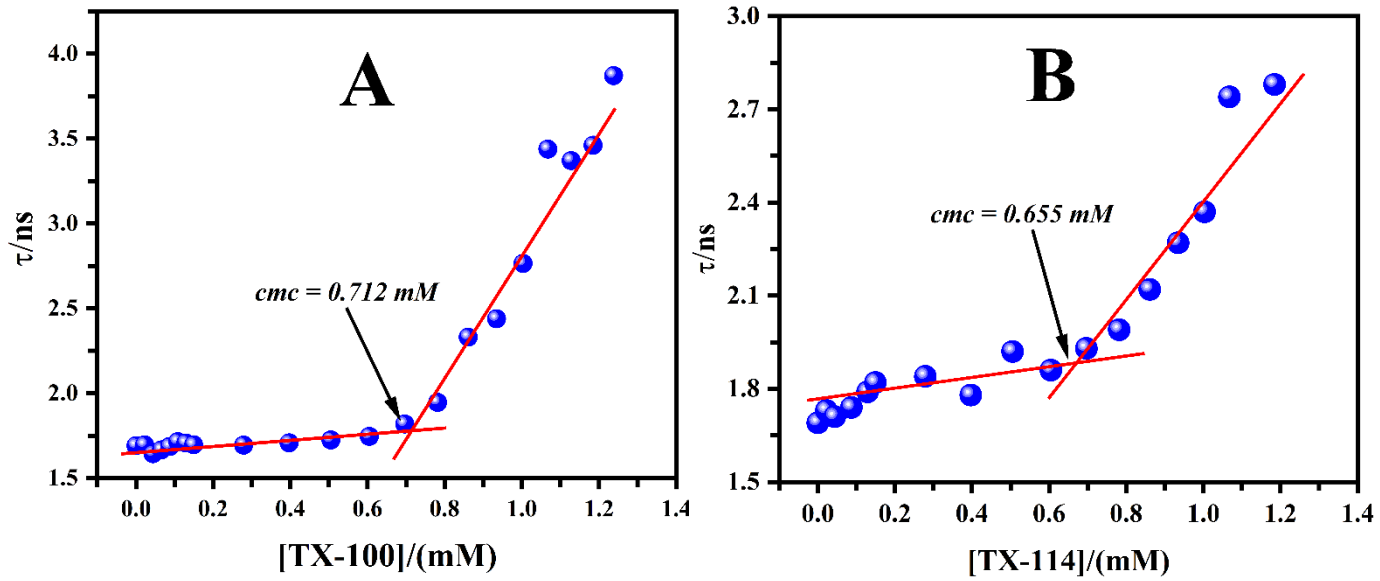

Figure 9. Life time (τ) of solubilized Coumarin 153 vs concentration of (A) TX-100 and (B) TX-114 systems at 0.6 mM β-CD.

4. Conclusions

In this study, molecular interactions have been discussed between TX-114/ TX-100 and β-cyclodextrin via tensiometry, fluorimetry, UV–VIS spectrophotometry, time-correlated single photon counting and dynamic light scattering. The *cmc* of both the systems increases with increasing concentration of β-cyclodextrin. Benesi-Hildebrand plots have been used to get confirmation of the 1:1 stoichiometry of the inclusion complexes. Addition of β-cyclodextrin delayed micellization for both the systems. It was observed that inclusion complex with TX-100 is somehow more stable than the other due to its less hydrophobic nature.

Incorporation of Triton X molecule into β-cyclodextrin causes a marked increase in fluorescence intensity occurring from phenyl moiety of the surfactant. This increment suggests a change in the microenvironment around the phenyl groups of amphiphile. Also, change in the microenvironment indicates a change in the hydrophobicity that results from inclusion of TX-molecules within the hydrophobic cavity of β-CD.

The greater value of A_{min} in case of β-CD/ TX-100 system than β-CD/ TX-114 signifies more compact packing of monomers with increasing concentration of β-CD. Negative values of ΔG_m^0 and ΔG_{ad}^0 for both the systems in all mole fractions of β-CD signify thermodynamically stable micellization and adsorption processes respectively. However, the magnitude decreases with the increase in the mole fraction of β-CD which indicates that stable micellization and adsorption processes become less spontaneous in presence of β-CD. The more negative ΔG_{ad}^0 values than the corresponding ΔG_m^0 values signify adsorption process as primary process and micellization is secondary. Therefore, the study provided important information regarding the interaction between β-CD and nonionic Triton X surfactant. The above information can be useful in wide range of applications of β-cyclodextrin and non-ionic surfactant and it demands further research.

REFERENCES

1. S. V. Kurkov and T. Loftsson, *International journal of pharmaceutics*, 2013, **453**, 167-180.
2. S. S. Wu, M. Wei, W. Wei, Y. Liu and S. Liu, *Biosensors and Bioelectronics*, 2019, **129**, 58-63.

3. A. J. M. Valente and O. Söderman, *Advances in Colloid and Interface Science*, 2014, **205**, 156-176.
4. W.-C. Geng, J. L. Sessler and D.-S. Guo, *Chemical Society Reviews*, 2020, **49**, 2303-2315.
5. S. Jacob and A. B. Nair, *Drug Development Research*, 2018, **79**, 201-217.
6. M. E. Davis and M. E. Brewster, *Nature Reviews Drug Discovery*, 2004, **3**, 1023-1035.
7. G. Lazzara and S. Milioto, *The Journal of Physical Chemistry B*, 2008, **112**, 11887-11895.
8. A. E. Tonelli, *Polymer*, 2008, **49**, 1725-1736.
9. V. Budhwar, *Asian Journal of Pharmaceutics (AJP)*, 2018, **12**.
10. G. Murtaza, *Acta Pol Pharm*, 2012, **69**, 581-590.
11. A. Singh, Z. A. Worku and G. Van den Mooter, *Expert Opinion on Drug Delivery*, 2011, **8**, 1361-1378.
12. T. Loftsson and M. E. Brewster, *Journal of Pharmaceutical Sciences*, 2012, **101**, 3019-3032.
13. G. Crini, *Chemical Reviews*, 2014, **114**, 10940-10975.
14. N. Sharma and A. Baldi, *Drug Delivery*, 2016, **23**, 729-747.
15. S. Engel, N. Möller and B. J. Ravoo, *Chemistry – A European Journal*, 2018, **24**, 4741-4748.
16. D. Prochowicz, A. Kornowicz and J. Lewiński, *Chemical Reviews*, 2017, **117**, 13461-13501.
17. S. S. Jambhekar and P. Breen, *Drug Discovery Today*, 2016, **21**, 356-362.
18. K. Ariga, M. Naito, Q. Ji and D. Payra, *CrystEngComm*, 2016, **18**, 4890-4899.
19. G. Liu, Q. Yuan, G. Hollett, W. Zhao, Y. Kang and J. Wu, *Polymer Chemistry*, 2018, **9**, 3436-3449.
20. G. Cutrone, J. M. Casas-Solvas and A. Vargas-Berenguel, *International Journal of Pharmaceutics*, 2017, **531**, 621-639.
21. F. Caldera, M. Tannous, R. Cavalli, M. Zanetti and F. Trotta, *International Journal of Pharmaceutics*, 2017, **531**, 470-479.
22. W.-F. Lai, A. L. Rogach and W.-T. Wong, *Chemical Society Reviews*, 2017, **46**, 6379-6419.
23. R. Mejia-Ariza, L. Graña-Suárez, W. Verboom and J. Huskens, *Journal of Materials Chemistry B*, 2017, **5**, 36-52.
24. H. Masai and J. Terao, *Polymer Journal*, 2017, **49**, 805-814.
25. A. Costoya, A. Concheiro and C. Alvarez-Lorenzo, *Molecules*, 2017, **22**, 230.
26. S. M. N. Simões, A. Rey-Rico, A. Concheiro and C. Alvarez-Lorenzo, *Chemical Communications*, 2015, **51**, 6275-6289.
27. Y. Chen and Y. Liu, *Advanced Materials*, 2015, **27**, 5403-5409.
28. A. Harada, Y. Takashima and M. Nakahata, *Accounts of Chemical Research*, 2014, **47**, 2128-2140.
29. G. Astray, J. C. Mejuto, J. Morales, R. Rial-Otero and J. Simal-Gándara, *Food Research International*, 2010, **43**, 1212-1218.
30. J. Wang, L. Liu, J. Chen, M. Deng, X. Feng and L. Chen, *European Polymer Journal*, 2019, **118**, 222-230.
31. H.-J. Buschmann and E. Schollmeyer, *Journal of cosmetic science*, 2002, **53**, 185-192.
32. A. C. Santos, F. Morais, A. Simões, I. Pereira, J. A. D. Sequeira, M. Pereira-Silva, F. Veiga and A. Ribeiro, *Expert Opinion on Drug Delivery*, 2019, **16**, 313-330.
33. J. Chen, Y. Huo, S. Li, Y. Huang and S. Lv, *Composites Communications*, 2019, **16**, 117-123.
34. Y. Wang, G. Ning, Y. Wu, S. Wu, B. Zeng, G. Liu, X. He and K. Wang, *Biosensors and Bioelectronics*, 2019, **124-125**, 82-88.

35. C. Galant, C. Amiel and L. Auvray, *Macromolecular Bioscience*, 2005, **5**, 1057-1065.
36. S. S. Upadhyay, P. K. Kalambate and A. K. Srivastava, *Electrochimica Acta*, 2017, **248**, 258-269.
37. S. Palanisamy, K. Thangavelu, S.-M. Chen, V. Velusamy, M.-H. Chang, T.-W. Chen, F. M. A. Al-Hemaid, M. A. Ali and S. K. Ramaraj, *Sensors and Actuators B: Chemical*, 2017, **243**, 888-894.
38. M. Zhang, H. T. Zhao, X. Yang, A. J. Dong, H. Zhang, J. Wang, G. Y. Liu and X. C. Zhai, *Sensors and Actuators B: Chemical*, 2016, **229**, 190-199.
39. N. Morin-Crini and G. Crini, *Progress in Polymer Science*, 2013, **38**, 344-368.
40. X. Zhang, L. Wu, J. Zhou, X. Zhang and J. Chen, *Journal of Electroanalytical Chemistry*, 2015, **742**, 97-103.
41. R. A. Smaldone, R. S. Forgan, H. Furukawa, J. J. Gassensmith, A. M. Z. Slawin, O. M. Yaghi and J. F. Stoddart, *Angewandte Chemie International Edition*, 2010, **49**, 8630-8634.
42. L. Wang, X.-Y. Liang, Z.-Y. Chang, L.-S. Ding, S. Zhang and B.-J. Li, *ACS Applied Materials & Interfaces*, 2018, **10**, 42-46.
43. H. Li, N. Lv, X. Li, B. Liu, J. Feng, X. Ren, T. Guo, D. Chen, J. Fraser Stoddart, R. Gref and J. Zhang, *Nanoscale*, 2017, **9**, 7454-7463.
44. M. J. Rosen and J. T. Kunjappu, *Surfactants and interfacial phenomena*, John Wiley & Sons2012.
45. M. A. Rub, N. Azum, F. Khan and A. M. Asiri, *The Journal of Chemical Thermodynamics*, 2018, **121**, 199-210.
46. D. Kumar and M. A. Rub, *Tenside Surfactants Detergents*, 2018, **55**, 78-84.
47. D. Kumar and M. A. Rub, *Journal of Molecular Liquids*, 2018, **269**, 1-7.
48. L. E. Buckingham, M. Balasubramanian, R. M. Emanuele, K. E. Clodfelter and J. S. Coon, *International Journal of Cancer*, 1995, **62**, 436-442.
49. D. Attwood, A. Florence, D. Attwood and A. Florence, *Surfactant Systems: Their chemistry, pharmacy biology*, 1983, 698-777.
50. M. Abdul Rub, N. Azum and A. M. Asiri, *Journal of Chemical & Engineering Data*, 2017, **62**, 3216-3228.
51. M. A. Rub, M. S. Sheikh, F. Khan, S. B. Khan and A. M. Asiri, *Zeitschrift für Physikalische Chemie*, 2014, **228**, 747-767.
52. S. Chauhan, K. Sharma, K. Kumar and G. Kumar, *Journal of Surfactants and Detergents*, 2014, **17**, 161-168.
53. R. Abbas, C. Ihmels, S. Enders and J. Gmehling, *Fluid Phase Equilibria*, 2011, **306**, 181-189.
54. S. Schreier, S. V. P. Malheiros and E. de Paula, *Biochimica et Biophysica Acta (BBA) - Biomembranes*, 2000, **1508**, 210-234.
55. D. Attwood and A. T. Florence, Wiley Online Library, Chapman & Hall, London, United Kingdom1983.
56. M. A. R. Khan, M. R. Amin, S. Mahbub, M. M. Alam, M. A. Rub, M. A. Hoque, M. A. Khan and A. M. Asiri, *Journal of Surfactants and Detergents*, 2019, **22**, 613-623.
57. J. J. H. Nusselder and J. B. F. N. Engberts, *Journal of Colloid and Interface Science*, 1992, **148**, 353-361.
58. J. Israelachvili and H. Wennerström, *Nature*, 1996, **379**, 219-225.
59. M. J. Rosen and F. Zhao, *Journal of Colloid and Interface Science*, 1983, **95**, 443-452.
60. Q. Zhou and M. J. Rosen, *Langmuir*, 2003, **19**, 4555-4562.

61. J. Rosen, New Jersey: John Wiley & Sons, Inc2004.
62. R. Zana, *Langmuir*, 1996, **12**, 1208-1211.
63. M. J. Rosen and S. Aronson, *Colloids and Surfaces*, 1981, **3**, 201-208.
64. G. Sugihara, A. Miyazono, S. Nagadome, T. Oida, Y. Hayashi and J.-S. Ko, *Journal of Oleo Science*, 2003, **52**, 449-461.
65. V. K. Smith, T. T. Ndou and I. M. Warner, *Applied Spectroscopy*, 1992, **46**, 659-668.
66. F. Cramer, W. Saenger and H.-C. Spatz, *Journal of the American Chemical Society*, 1967, **89**, 14-20.
67. M. Bastos, L. E. Briggner, I. Shehatta and I. Wadsö, *The Journal of Chemical Thermodynamics*, 1990, **22**, 1181-1190.
68. Y. Inoue, T. Hakushi, Y. Liu, L. Tong, B. Shen and D. Jin, *Journal of the American Chemical Society*, 1993, **115**, 475-481.
69. H. Schott, *Journal of Colloid and Interface Science*, 1973, **43**, 150-155.
70. M. J. Schick, *Nonionic surfactants: physical chemistry*, CRC Press1987.
71. C. C. Ruiz and J. Aguiar, *Molecular Physics*, 1999, **97**, 1095-1103.
72. N. J. Turro and A. Yekta, *Journal of the American Chemical Society*, 1978, **100**, 5951-5952.
73. K. Rohatgi-Mukherjee, *Fundamentals of photochemistry*, New Age International1978.
74. N. Muller, *Reaction kinetics in micelles, ed. E. A. Cordes*, Plennum, New York1973.
75. S. Berr, R. R. Jones and J. S. Johnson Jr, *The Journal of physical chemistry*, 1992, **96**, 5611-5614.
76. N. Turro, P. Kuo, P. Somasundaran and K. Wong, *The Journal of Physical Chemistry*, 1986, **90**, 288-291.
77. K. S. Sharma, P. A. Hassan and A. K. Rakshit, *Colloids and Surfaces A: Physicochemical and Engineering Aspects*, 2006, **289**, 17-24.
78. W. B. Gratzer and G. H. Beaven, *The Journal of Physical Chemistry*, 1969, **73**, 2270-2273.
79. G. Nemethy and A. Ray, *Journal of Physical Chemistry*, 1971, **75**, 804-808.
80. J. Crooks, Academic Press, London, New York, San Francisco1978.
81. H. A. Benesi and J. Hildebrand, *Journal of the American Chemical Society*, 1949, **71**, 2703-2707.
82. R. Sanan, T. S. Kang and R. K. Mahajan, *Physical Chemistry Chemical Physics*, 2014, **16**, 5667-5677.

Table 1. Critical Micellar Concentrations (*cmc*), surface pressure (π_{cmc}), minimum area per molecule (A_{min}), efficiency of interfacial adsorption (pC_{20}), standard free energy of micellization (ΔG_m^0), standard free energy of interfacial adsorption (ΔG_{ad}^0), surface tension at *cmc* (γ_{cmc}), minimum free energy of the surface with maximum adsorption (G_{min}) at 298.15 K.

$\alpha_{\beta-CD}$	*cmc*	π_{cmc} ($mN.m^{-1}$)	$10^6\Gamma_{max}$ ($mol^{-1}m^{-1}$)	A_{min} ($nm^2/molecule$)	pC_{20}	ΔG_m^0 ($kJ.mol^{-1}$)	ΔG_{ads}^0 ($kJ.mol^{-1}$)	γ_{cmc} ($\pm$ 0.2 $mN.m^{-1}$)	G_{min} ($kJ.mol^{-1}$)
TX-100 in β-CD									
0	0.266	40.7	4.55	0.36	1.71	-30.35	-39.29	29.7	6.52
0.2	0.420	41.2	4.00	0.42	1.51	-29.22	-39.52	30.2	7.56
0.4	0.583	42.0	4.36	0.38	1.32	-28.40	-38.04	29.3	6.72
0.6	0.714	43.2	4.85	0.34	0.98	-27.90	-36.81	28.2	5.82
0.8	0.893	41.4	4.77	0.35	0.80	-27.35	-36.03	29.0	6.08
1.0	1.148	41.9	6.05	0.27	0.45	-26.73	-33.66	29.7	4.91
TX-114 in β-CD									
0	0.239	48.2	4.70	0.35	2.11	-30.61	-40.86	23.2	4.93
0.2	0.321	41.6	5.80	0.29	1.11	-29.88	-37.05	28.9	4.98
0.4	0.493	45.3	6.66	0.25	1.11	-28.82	-35.62	26.2	3.93
0.6	0.529	41.3	5.89	0.28	1.05	-28.65	-35.66	30.0	5.09
0.8	0.952	43.4	5.91	0.28	0.92	-27.19	-34.54	28.2	4.77
1.0	1.580	42.9	4.51	0.37	0.82	-25.93	-35.44	28.5	6.32

Standard uncertainties in terms of ***cmc***, Γ_{max}, A_{min}, π_{cmc}, ΔG^0_m, and pC_{20} are ± 0.01%, ± 0.04%, ± 0.04%, ± 0.03%, ± 0.02% and ± 0.03% respectively.

Table 2. Aggregation Number (N_{agg}), Micropolarity, Packing Parameter (P), Apparent dielectric constant (D_{exp}) and Stern–Volmer binding constant (K_{SV}) of TX-100 and TX-114 in different mole fractions of β-CD.

$\alpha_{\beta-CD}$	N_{agg}	I_1/I_3	D_{exp}	K_{SV}
TX-100 in β-CD				
0.2	37	1.113	8.64	19.88
0.4	42	1.111	8.51	14.70
0.6	45	1.105	8.00	10.08
0.8	46	1.134	10.31	7.97
1.0	44	1.137	10.60	5.38
TX-114 in β-CD				
0.2	43	1.123	9.46	30.11
0.4	38	1.126	9.66	14.74
0.6	43	1.115	8.78	14.32
0.8	41	1.118	9.01	13.50
1.0	54	1.139	10.73	6.66

Table 3. Time-Resolved Decay Parameter of Coumarin 153 of TX-100 and TX-114 at 0.6 mM β-CD.

[Triton X]$/mM$	$\tau_1(ns)$	a_1	$\tau_2(ns)$	a_2	$\tau_{avg}(ns)$	χ^2
TX-100 in 0.6 mM β-CD						
0.0	0.95	0.05	1.77	0.95	1.69	1.15
0.02	0.95	0.07	1.79	0.93	1.69	1.08
0.09	1.22	0.20	1.86	0.80	1.68	1.04
0.14	1.10	0.16	1.87	0.84	1.69	1.17
0.50	1.43	0.54	2.26	0.46	1.72	1.00
0.78	1.45	0.46	2.71	0.54	1.94	1.10
1.00	1.58	0.27	3.80	0.73	2.76	1.11
1.18	1.99	0.22	4.39	0.73	3.46	1.06
TX-114 in 0.6 mM β-CD						
0.0	0.95	0.05	1.77	0.95	1.69	1.15
0.01	0.89	0.02	1.76	0.98	1.73	1.03
0.05	1.04	0.06	1.82	0.94	1.74	1.04
0.10	1.35	0.41	2.42	0.59	1.82	1.02
0.33	1.38	0.42	2.67	0.58	1.92	0.99
0.52	1.31	0.33	2.68	0.67	1.99	1.06
0.67	1.54	0.42	3.92	0.58	2.37	0.98
0.79	1.59	0.29	4.02	0.71	2.78	1.03

Standard uncertainty of τ_{avg} is ± 5%

Chapter-IV

An interface, micellar, and thermodynamic investigation of bile salts and Brij-30 binary mixtures

An interface, micellar, and thermodynamic investigation of bile salts and Brij-30 binary mixtures

Abstract

The nature of the binding of bile salts with nonionic Brij-30 were systematically investigated in aqueous solution using a range of experimental techniques. Parameters such as critical micelle concentration (CMC), particle size distribution, time-correlated single photon counting (TCSPC) were meticulously analyzed to elucidate the nature of the complexation. Dynamic light scattering (DLS) data provided the evidence for the complexation process and the hydrophobic interactions between bile salts with Brij-30. This comprehensive and systematic study, which is rarely addressed in existing literature, offers significant insights into the physicochemical properties relevant to drug delivery, solubilization, and other applications.

1. Introduction

Bile acid salts can be classified as steroid biosurfactants. The hydrophobic surface of the molecule is represented by the convex plane of the steroid skeleton (β-side), whereas the hydrophilic surface (α-side) of the molecule is portrayed by the concave plane of the steroid skeleton. These steroids, with a rigid and planar structure called the cyclopentanephenanthrene nucleus, function as hydrophobic molecules and have the ability to self-organize into micelles when in contact with water, similar to traditional surfactants. Bile salts are referred to as biplanar amphiphiles due to their unique hydrophobicity characterized by two distinct planes in their steroid skeleton, unlike typical surfactants with a polar head and hydrophobic tail. This distinctive feature enables them to form relatively small micelles having an aggregation number of 2 to 15 etc. The structural features of the anions of bile acids in their micelles consisting of a single component allow them to effectively bind to substances such as cholesterol,[1, 2] various drugs,[3-6] and morphine hydrochlorides[7] (resulting in a depot effect). Nevertheless, micelles exhibit limited ability to accommodate molecules because of their small dimensions. It is crucial to increase the hydrophobic phase of their micelles because of their pharmaceutical application. To achieve this, it may be necessary to use conventional non-ionic surfactants.[8-16]

Bile salts have a significant function in the process of fat solubilization during digestion.[17, 18] However, there is an important distinction.[10] The hydrophilic portion (concave side) of bile salts consists of carboxylate ions (–COO) and hydroxyl (–OH) groups, in addition to the steroid ring system. The separation between their hydrophilic and hydrophobic areas is not distinct, and their

micelles are created through a process starting with hydrophobic interaction and followed by hydrogen bonding.[18] When compared to sodium deoxycholate (NaDC), sodium cholate (NaC) has an extra -OH group, which increases its solubility in water and critical micellar concentration (CMC). The CMCs of bile salts have been evaluated using a variety of analytical techniques, including fluorescence,[19, 20] surface tension,[21] NMR[19] and calorimetry,[22] and the acceptable CMCs of NaC and NaDC at room temperature are 16 mM and 6 mM, respectively.[20] In addition to aiding in fat digestion, bile salts also have a role to play in the digestion of animal fat and various other biological processes. These substances, which are both compatible with living tissues and capable of breaking down naturally, are extensively utilized to transport drugs that repel water, as well as cosmetics and vitamins.[20, 23-28] The solubilization of fat-soluble vitamin E is attributed to the formation of mixed micelles involving bile salt, cholesterol, fatty acids, and monoglycerides.[29] Additionally, bile acids have been utilized in the field of supramolecular synthesis[30] and have played a role in the advancement of photorheological fluids.[31]

Extensive research has been conducted on Polyoxyethylene ether (POE) surfactants such as Brij-30 in pharmaceutical systems[30, 31] because of their low levels of toxicity. Bile salts, which are molecules that occur naturally in the body, are important for normal bodily functions, are compatible with living organisms, and can break down naturally when they come into contact with water. Due to their favorable compatibility with pharmaceutical products, they have been utilized to enhance the solubility of several drugs that are not easily soluble in water, such as griseofulvin,[32] glutethimide,[32] digoxin,[33] leucotriene-D4 antagonists,[34] and gemfibrozil.[35] The solubilization of dilute bile salt solutions is caused by the small micelles formed that have a low aggregation number, which is attributed to the hindrance caused by the large steroidal skeleton.

Nevertheless, when bile salts such as deoxycholates[33, 36, 37] are present in higher concentrations, they undergo a transformation in their structure. This transformation is facilitated by the intermolecular hydrogen bonding that occurs between the hydroxyl and carboxyl groups, as well as the partial way in which hydrophobic interactions occur. As a result, the micelles' hydrophobic domain expands, forming a helical structure or a polymer-like aggregation. Consequently, this increases its ability to dissolve hydrophobic substances.[36] Additionally, similar outcomes could be obtained by utilizing a combination of bile salts and surface-active agents in the form of mixed micelles. These mixed micelles are known to create elongated cylindrical structures resembling worms, resulting in

enhanced solubilization ability.[38-40] During our review of the literature, we discovered that the majority of studies examining the creation of mixed micelles and their subsequent uses in the field of pharmaceuticals focus on phospholipids and bile salts. These investigations typically require the utilization of organic solvents, such as, chloroform and methanol for the manufacturing process. So, in this study, we aim to provide an analysis of the flow characteristics and viscoelastic properties of a combination of sodium cholate (NaC) and the typical non-ionic surfactant Brij-30, which is referred to as mixed micelles. The preparation of these mixed micelles is simple and does not require the use of organic solvents. Additionally, they are highly suitable for use in pharmaceutical research. While going through the literature, we found most of the investigations having the objective of studying the formation of mixed micelles and their consequent pharmaceutical applications involve phospholipids and bile salts which need the use of organic solvents like chloroform and methanol for fabrication. Therefore, in this endeavour, we present the rheological characterization, i.e., flow behaviour and viscoelastic properties of mixed micelles of sodium cholate (NaC) and conventional non-ionic surfactant Brij-30. Such mixed micelles are easy to prepare without the aid of organic solvents.

There have been very few reported studies investigating the impact of bile salts on the structural transformation of non-ionic micelles. Furthermore, no attempts have been made so far to explore how various stimuli impact the alteration of microstructure in Brij-30 micelles when bile salts are present. Taking into account all these factors, our current study aimed to investigate how bile salts affect the dimensions and structure of Brij-30 micelles under different solution conditions. Interesting results could be obtained by conducting a comprehensive investigation into the micellization and transition of Brij-30 micelles when exposed to two bile salts (NaC and NaDC) and external triggers. Our study seeks to conduct thorough examinations of the behavior of mixed micelles composed of aqueous Brij-30 and bile salt. By doing so, we aim to enhance our comprehension of the molecular interactions that significantly influence the process of fat digestion and other biologically significant processes.

2. Experimental Procedures

2.1. Materials and methods:

Brij-30 (Purity ~ 95%), Sodium cholate (Purity ≥ 99%), Sodium deoxycholate (Purity ≥ 97%) [cf. Figure 1] Coumarin 153 **(**purity ~ 99%**)** were purchased Merck, India.

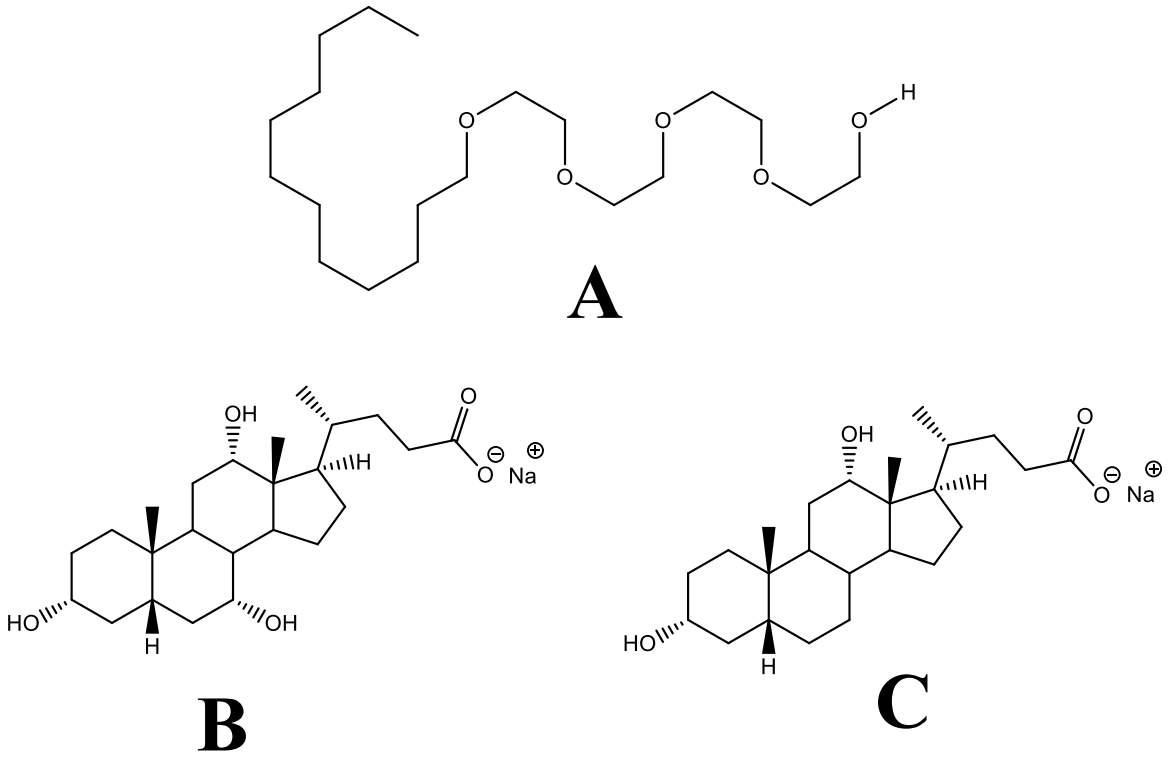

Figure 1. Chemical structure of (A) Brij-30, (B) Sodium cholate, and (C) Sodium deoxycholate.

2.2. Tensiometry

Surface tension measurements were performed using a Krüss (Germany) tensiometer and the ring detachment technique. The concentrated stock solution of specific mole fraction was added to aqueous medium with a Hamilton micro syringe giving it five minutes to equilibrate before each

measurement. All measurements were carried out three times in order to assess their reproducibility. The method was accurate within ± 0.1 $mN.m^{-1}$. To calculate the CMC, surface tension (γ) vs. log [surfactant] was plotted [cf. Figure 2]. The break point in the plot were used to derive the CMC.

2.3. Dynamic Light Scattering (DLS) and Zeta potential measurement

DLS measurements were carried out using a He-Ne laser (λ = 632.8 nm) in a Zetasizer nano ZS (Malvern, UK) at a scattering angle of 90°. To remove bigger particles, all of the solutions were filtered three times via membrane filters (porosity 0.25 µm). The average values of the data were then reported.

2.4. Time-Resolved Fluorescence Study.

Utilizing a Horiba-Jobin-Yvon FluoroCube fluorescence lifetime system with 450 nm NanoLEDs (IBH, UK) as the excitation sources for the probe coumarin 153 and a TBX photon detection module as the detector, time-resolved fluorescence decay was carried out. The emission was recorded at 544 nm. All of the decay data were fitted using IBH DAS-6 decay analysis software. To obtain the lamp profile, sodium dodecyl sulphate micellar solution was utilized as a scatterer instead of the sample. For the correct fit, the $\chi 2$ values were kept slightly close to 1.

3. Results and discussion

3.1. CMC of mixed system

The tensiometric plots are represented in the Figure 2. Additional data regarding the interfacial parameters has been given in the Table 1. CMC_{mix} decreased with increasing mole fraction of Brij-30 in the mixture. The CMC_{mix} values obtained from the tensiometric experiment were in between that of Brij-30 and NaC/ NaDC (Table 1).

.

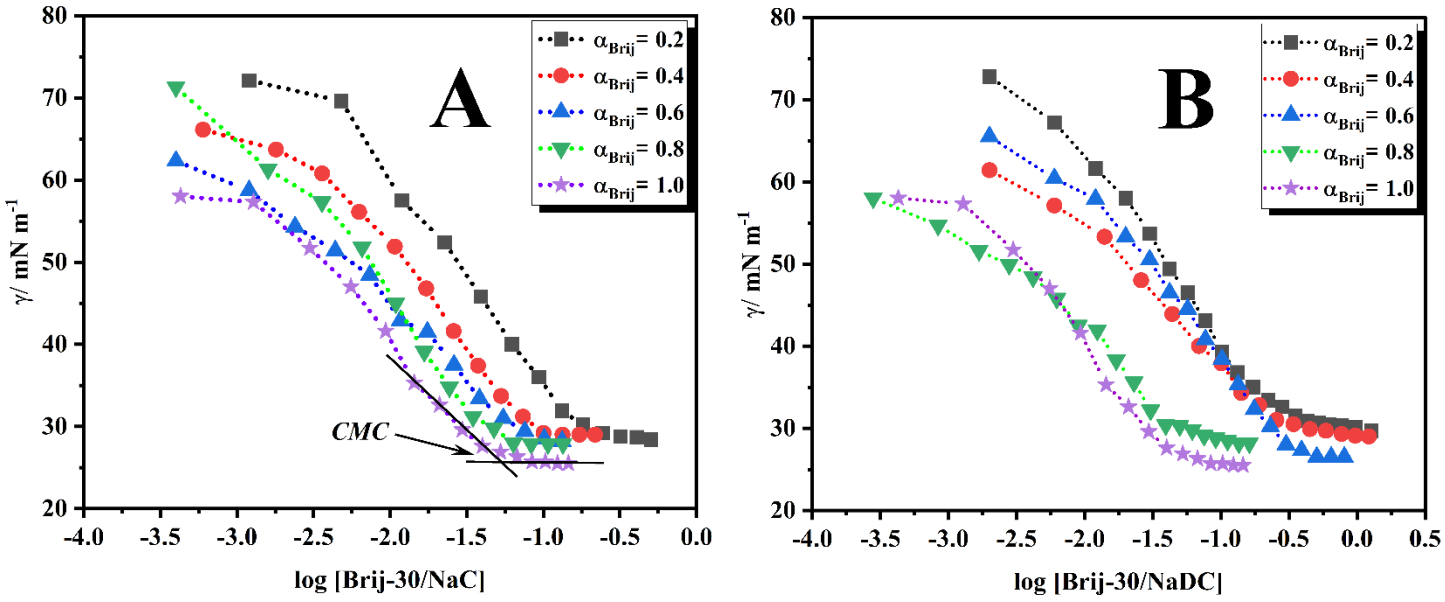

Figure 2. Plots of surface tension (γ) vs. (A) log [Brij-30/ NaC], (B) log [Brij-30/ NaDC] at different mole fractions of Brij-30 at 298.15 K.

3.2. Interfacial properties

The Gibbs adsorption equation was used to estimate the surface excess (Γ_{max}) and minimum area per head group of the amphiphile (A_{min}) at maximum adsorption of the investigated surfactants and their mixtures at the air/ solution interface as following:[41, 42]

$$\Gamma_{max} = -\frac{1}{2.303nRT}\lim_{C\to cmc}\left(\frac{d\gamma}{d\log C}\right)_{max} mol.m^{-2} \quad (1)$$

The slope of the surface tension (γ) vs. log of concentration profile is shown in Figure 2. The symbols R and T stand for the universal gas constant (8.31 J mol^{-1} K^{-1}), the temperature in Kelvin, and n is the number of ionic species adsorbed at the interface, respectively.

The relation $n = n_1X_1 + n_2X_2$ can be used to find the value of n for the mixed system.

The highest slope value of $\frac{d\gamma}{d\log C}$ at CMC was determined by fitting γ value with log C in a two-dimensional polynomial equation of the type.[43]

$$\gamma = a + b\,logC + c\,(logC)^2 \quad (2)$$

where the polynomial equation's coefficients are represented by a, b, and c. The $\frac{\mathrm{d}\gamma}{\mathrm{d}\log \mathrm{C}}$ was evaluated from the relation,

$$\frac{d\gamma}{dlogC} = b + 2c \quad (3)$$

Γ_{max} is seen to increase as mole fraction of Brij-30 is increased. As a result, the Brij-30 molecule is shown to have higher surface activity than the bile salts (NaC/ NaDC). The minimum area per head group (A_{min}) of the amphiphile at CMC can be evaluated by the following equation:

$$A_{min} = \frac{10^{18}}{N_A \Gamma_{max}} \quad (4)$$

where N_A denotes the Avogadro number. The A_{min} value decreases as the amount of Brij-30 increases, as shown in Table 1. This means that in the presence of a Brij-30 molecule, monomers are packed more densely. The bile salt molecules with the more rigid hydrophobic part takes up more space than the Brij-30 molecule.

According to the equation below, the standard value of the Gibbs free energy of micellization (ΔG_m^0) is calculated:[44]

$$\Delta G_m^0 = RT\, ln\, X_{CMC} \quad (5)$$

where R and T stand for the universal gas constant (8.31 J mol^{-1} K^{-1}) and temperature in Kelvin, respectively, and X_{CMC} is the CMC expressed in terms of mass fraction units. Despite being thermodynamically advantageous, micellization becomes less spontaneous with increasing mole fraction of bile salts, as shown by the fact that ΔG_m^0 values are negative for both systems and for all mole fractions of Brij-30, but the magnitude decreases with increasing mole fraction of NaC/ NaDC (Table 1). More -ve value of $\Delta G\,{}_m^0$ for Brij-30/ NaC system than Brij-30/ NaDC indicates that micellization of Brij-30/ NaC system is more spontaneous than the other one. Variations in the enthalpic and entropic contributions are a result of either rising or falling of ΔG_m^0 levels. Entropy and spontaneity of the system rise during micelle formation due to the release of water molecules caused by fracturing the clusters enclosing the amphiphiles. In order to break down the water molecule cluster enclosing the surfactant monomers prior to micellization, bile salts have smaller hydrophobic tails than Brij-30 amphiphile. As a result, the amount of entropy gained during the

micellization process in presence of bile salts was reduced, and as a result, the negative values of ΔG_m^0 were reduced in the presence of NaC/ NaDC.

ΔG_{ad}^0 is the standard free energy of interfacial adsorption calculated using the following equation[45]

$$\Delta G^{\,0}_{ads} = \Delta G^{\,0}_{m} - \frac{\pi_{CMC}}{\Gamma_{max}} \quad (6)$$

The standard state defined here as the hypothetical state of ideal solution having unit mole fraction.

Surface pressure (π_{CMC}) of the amphiphiles at the air/ solution interface was calculated as:

$$\pi_{CMC} = \gamma_{water} - \gamma_{CMC} \quad (7)$$

The π_{CMC} values of the bile salts are the lowest than the mixtures of bile salts and Brij-30 as well as the pure Brij-30, indicating that bile salts are less effective at lowering interfacial tension and have a lower tendency to adsorb at the air-liquid interface.

The experimental results are presented in Table 1. Micellization of Brij-30 was more spontaneous than NaC/ NaDC ($\Delta G^{\,0}_{m}$ for Brij-30 is more -ve than that for NaC/ NaDC). As a result, $\Gamma_{max}(\text{Brij}-30) > \Gamma_{max}(\text{NaC/ NaDC})$ and the values of their mixture were intermediate; the trend of A_{min} values was opposite to the value of Γ_{max}. Higher $A_{min}(\text{NaC/ NaDC})$ values than Brij-30 signify the flat orientation of the bile salt at the interface. For both pure NaC/ NaDC and its binary mixes with Brij-30 at all compositions, it was determined that the ratio of $\Delta G^{\,0}_{ad}/\,\Delta G^{\,0}_{m}$ was greater than 1.3 indicating that the transfer of surfactant monomers to the interface was two times more thermodynamically spontaneous than the transfer of surfactant monomers into the micelles from the bulk. The ratio for NaC/ NaDC was greater than 2.4, showing greater spontaneity in the transfer process mentioned above. ΔG^S_{min} is an important thermodynamic parameter which is defined as the free energy change of the amphiphiles in the system during the transition from bulk phase to air/ solution interface. ΔG^S_{min} can be calculated using the following relationship:

$$\Delta G^S_{min} = A_{min}\gamma_{CMC}N_A \quad (8)$$

The developed surface is more thermodynamically stable or exhibits higher surface activity when the ΔG^S_{min} is lower. The estimated values are reported in Table 1. ΔG^S_{min} is less for all the mixture

components of Brij-30/ NaC system than Brij-30/ NaDC (Table 1). The negative deviation of ΔG_{min}^{S} from the ideal line suggests synergistic interaction at the interface. Pure Brij-30 has the lowest ΔG_{min}^{S} value, while NaC/ NaDC has the highest value. A surface that has a lower Gibbs free energy value has a surface that is more thermodynamically stable. Table 1 presents the calculated values. The creation of thermodynamically stable surfaces in the Brij-30/ NaDC system was implied by the lower values of ΔG_{min}^{S} in that system compared to the Brij-30/ NaC system. The term pC_{20} is an important term that measures the efficiency of amphiphile adsorption and is defined as follows:

$$pC_{20} = -logC_{20} \quad (9)$$

where C_{20} is the concentration of surfactant required to reduce the surface tension of the solvent by 20 mM m^{-1}.[46] A higher pC_{20} value indicates that a lower concentration is needed to reduce surface tension by 20 mM m^{-1}, indicating that the Brij-30 is more surface active. pC_{20} declines with increasing mole fraction of bile salts in both systems (Table 1). In the presence of NaC/ NaDC, mixtures have a lower pC_{20} value, indicating that NaC/ NaDC decreases the surface activity of the systems (Table 1). In other words, the presence of bile salts requires more amphiphile to reduce surface tension by the same magnitude, implying that bile salts delayed surfactant aggregation.

3.3. Interaction parameters of mixed micelle

The components can interact in a mixed micelle in a positive or negative way. Synergism results from favourable interactions, whereas it is antagonistic for adverse interactions.[47] The Clint equation can be used to understand the nature of interaction between the components of a pair of surfactants in relation to their ideal mixtures (i.e., without synergism or antagonism) as follows:

$$\frac{1}{CMC_{mix}} = \frac{\alpha_{NaC/\,NaDC}}{CMC_{NaC/\,NaDC}} + \frac{1-\alpha_{NaC/\,NaDC}}{CMC_{Brij}} \quad (10)$$

where $\alpha_{NaC/\,NaDC}$ is the mole fraction of NaC/ NaDC in solution, and $CMC_{NaC/\,NaDC}$, CMC_{Brij} and CMC_{mix} are the CMCs of NaC/ NaDC, Brij-30 and their mixture, respectively. A non-ideal mixture (components interacting) would deviate from the relation, and Clint's prediction for synergistic or antagonistic interactions would be either lower or higher than the CMC_{mix}. In Table 1, the measured CMC_{mix} of NaC/ NaDC and Brij-30 is shown along with the correlation of CMC calculated from the Clint equation. Since there is both synergism and antagonism between the binary combinations, it can be seen that the experimental CMC_{mix} is lower than the CMC by Clint

in case of Brij-30/ NaC system and experimental CMC_{mix} is higher than the CMC calculated by Clint for Brij-30/ NaDC system indicating nonideality.

Table 1 shows that the components of the Brij-30/ NaC binary system exhibited synergism whereas Brij-30/ NaDC shows antagonism. The objective was to look at how structural changes between sodium cholate and sodium deoxycholate affect interactions with nonionic cosurfactants. Previous research with conventional surfactants[48-54] predicted that a more hydrophobic bile salt (NaDC) would cause stronger synergism with nonionic cosurfactants due to increased hydrophobic interactions. However, when the characteristics of the interaction of Brij-30/ NaC and Brij-30/ NaDC binary systems (Table 1) are examined, it is clear that a more hydrophilic bile salt (NaC) forms stronger contacts with the Brij-30. The fact is that sodium cholate has two α-axial hydroxyl groups at the C7 and C12 sites, whereas sodium deoxycholate has only one α-axial hydroxyl group at C12; this explains why it has a stronger synergistic impact. The number of α-axial hydroxyl groups is obviously significant for micelle stability. It is assumed that the side of the steroid skeleton of the bile salts in the investigated aggregates is oriented toward the hydrophobic core of the micelles, whereas the polar heads of Brij-30 are situated at the aggregates' surface. Median plain of Brij-30 is perpendicular to both the hydrophobic surface of the micelles and the axial α-hydroxyl groups of the bile salts. This most likely orientation allows hydrogen bond formation between the proton acceptor oxyethylene moiety of the polar head group of the Brij-30 and the α-axial hydroxyl groups of bile salts. Both the hydrophobic interaction and the generation of hydrogen bonds make micellar structures more stable. In case of Brij-30/ NaC, the extend of hydrogen bond formation is higher due to two α-axial hydroxyl groups at the C7 and C12 sites than Brij-30/ NaDC which contains only one α-axial hydroxyl group at C12. As a result, the CMC values of Brij-30/ NaC micelles are lower than those predicted by Clint's theory of ideal mixtures.

3.4. Dynamic Light Scattering (DLS) Method

The hydrodynamic diameter of the system can be used to determine how the aggregates' structure has changed. The DLS size distribution plots of the Brij-30/ NaC and Brij-30/ NaDC aggregates are displayed in Figure 3. The hydrodynamic diameters of the components of Brij-30/ NaC system are comparatively smaller at all mole fractions (α_{Brij}) than the Brij-30/ NaDC system (cf. Figure 4). The most probable hydrodynamic diameter of the aggregates in case of Brij-30/ NaC system having composition α_{Brij}= 0.2 is ~ 396.1 nm while for Brij-30/ NaDC system, the value is ~ 1484

nm having composition α_{Brij}= 0.2 (Figure 4). Similar observation was found for other compositions (α_{Brij}= 0.4, 0.6, 0.8) also in both the systems (Brij-30/ NaC and Brij-30/ NaDC). In the mixed micellar system, the dominant factor determining the size of the aggregates is the charge distribution around the head group. The smaller hydrodynamic diameter values in case of Brij-30/ NaC system implies lower charge density of the head group formed by the oxyethylene group of Brij-30 and axial hydroxyl groups at the C7 and C12 sites of NaC. In case of Brij-30/ NaDC system, charge density of the head group formed by the oxyethylene group of Brij-30 is higher than the other system as only one α-axial hydroxyl group at C12 of NaDC is available for hydrogen bonding. Because of increased charge repulsion of the head group, larger aggregates were formed for Brij-30/ NaDC system depicted in the Figure 3.

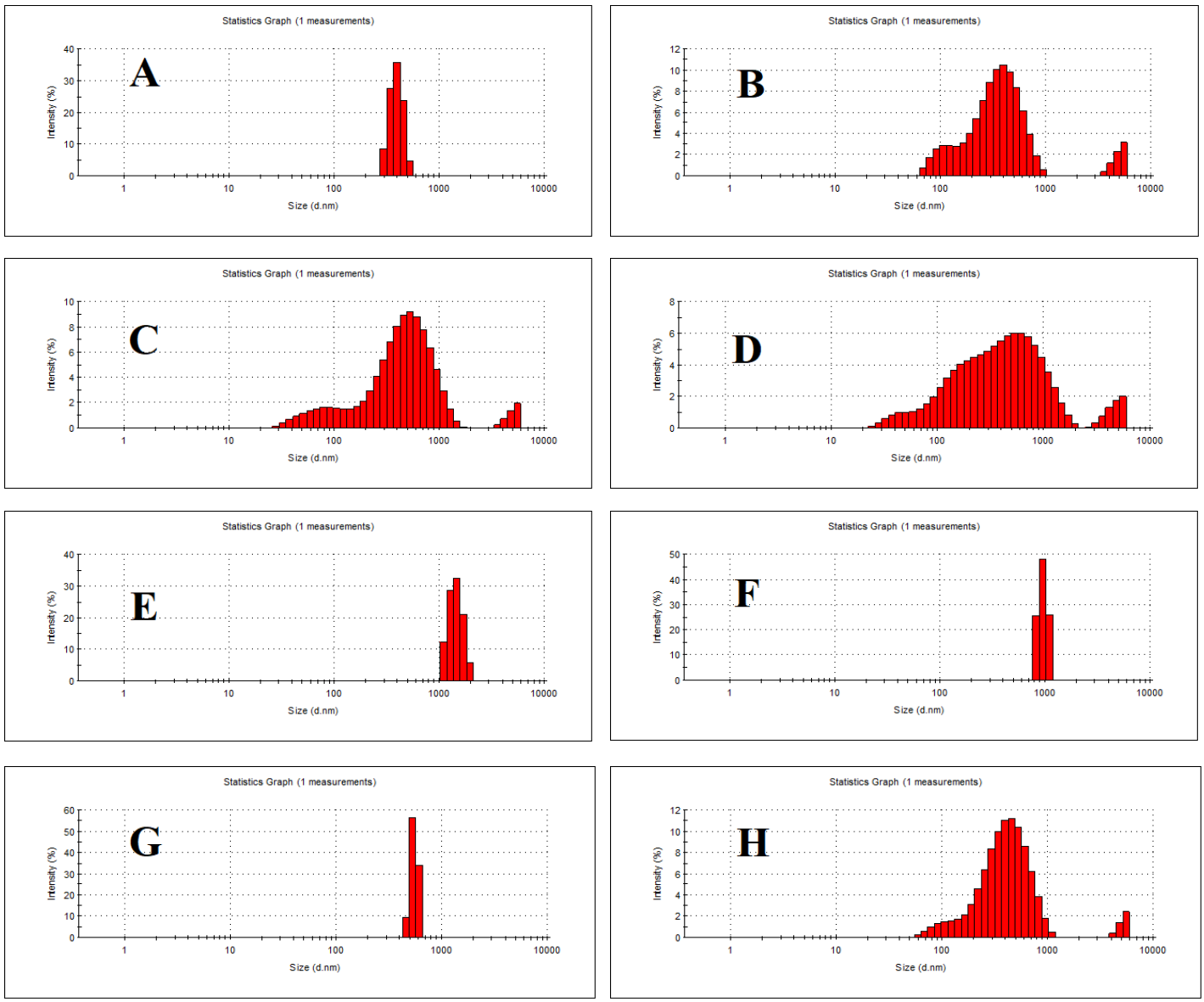

Figure 3. DLS profile of (A)-(D) Brij-30/ NaC and (E)-(H) Brij-30/ NaDC systems with variation of mole-fraction of Brij-30; (A) α_{Brij}=0.2, (B) α_{Brij}=0.4, (C) α_{Brij}=0.6, (D) α_{Brij}=0.8 and (E) α_{Brij}=0.2, (F) α_{Brij}=0.4, (G) α_{Brij}=0.6, (H) α_{Brij}=0.8.

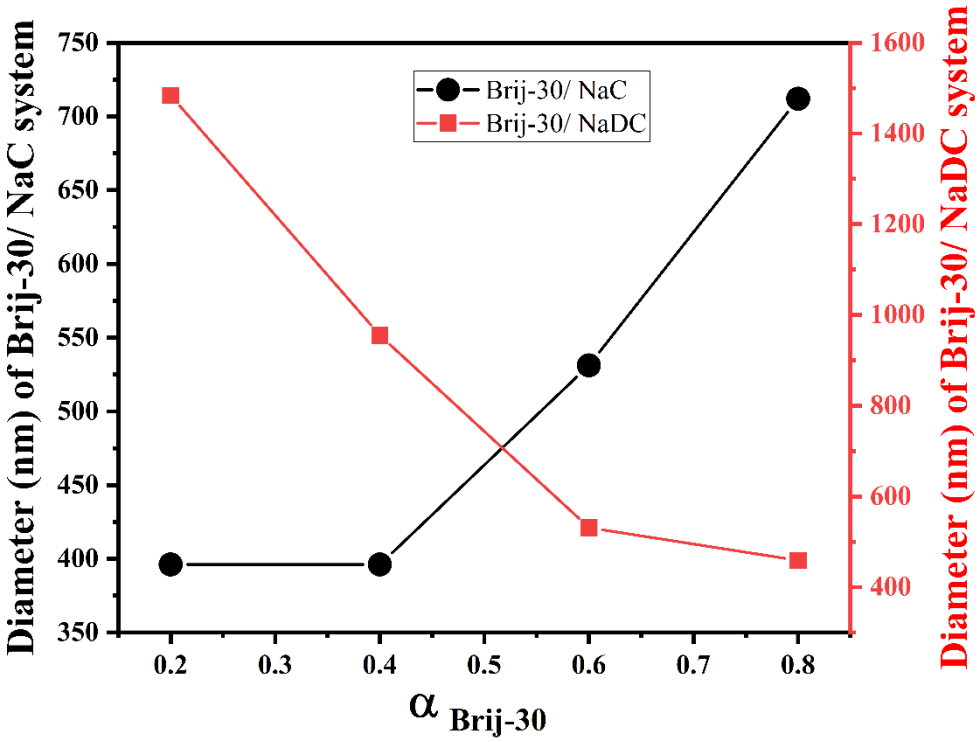

Figure 4. Hydrodynamic diameter (nm) vs mole fraction of Brij-30 plot for Brij-30/ NaC and Brij-30/ NaDC systems.

3.5. Time-Resolved Fluorescence Decay Measurements:

Time-Resolved Fluorescence Measurements of decay give information about the surroundings of a probe molecule and its stability in its excited state. Two relaxation components, τ_1,τ_2, can be used to express the anisotropic decay value ($r(t)$) at time t as follows:

$$r(t) = r_0 \left[a_1 e^{-t/\tau_1} + a_2 e^{-t/\tau_2}\right] \quad (11)$$

where a_1, a_2 are referred to as the pre-exponential factor, i.e., the contributing factor of each time scale component, and r_0 represents the anisotropy value at t = 0. The two components are a result of the probe molecules' two distinct environments, which are the micelle's hydrophobic core and the amphiphile/ water interface. The expression for the average time value (τ_{av}) is as follows:

$$\tau_{av} = a_1\tau_1 + a_2\tau_2 \quad (12)$$

Life time decay profile of solubilized probe (coumarin 153) in presence of Brij-30/ NaC and Brij-30/ NaDC systems has been represented in Figure 5. The probe molecule primarily distributed itself to the air/ water interface. The probe molecules were distributed to the hydrophobic region of the mixed micelle as a concentrated surfactant solution was gradually added. In this situation, the probe's τ_{av} value starts to rise. The increase in τ_{av} value implies the more hydrophobic environment near the hydrophobic core of the mixed micelle where the probe molecules are distributed at the maximum extend. In case of Brij-30/ NaC system, charge density of the head group is lower due to greater extend of H-bonding formed by the oxyethylene group of Brij-30 and axial hydroxyl groups at the C7 and C12 sites of NaC which makes the micellar structure more compact. In that case, it is difficult to penetrate into the hydrophobic core of the micelle for the probe molecule which is evident from the lower τ_{av} values for Brij-30/ NaC system compared to the Brij-30/ NaDC system. Again, in case of Brij-30/ NaDC system charge density of the head group formed by the oxyethylene group of Brij-30 is comparatively higher than the other system as only one α-axial hydroxyl group at C12 of NaDC is involved here for hydrogen bonding. Because of increased charge repulsion micellar aggregates were less compact which facilitates the penetration of probe molecules into the hydrophobic core of micelle and thus, higher τ_{av} values were observed.

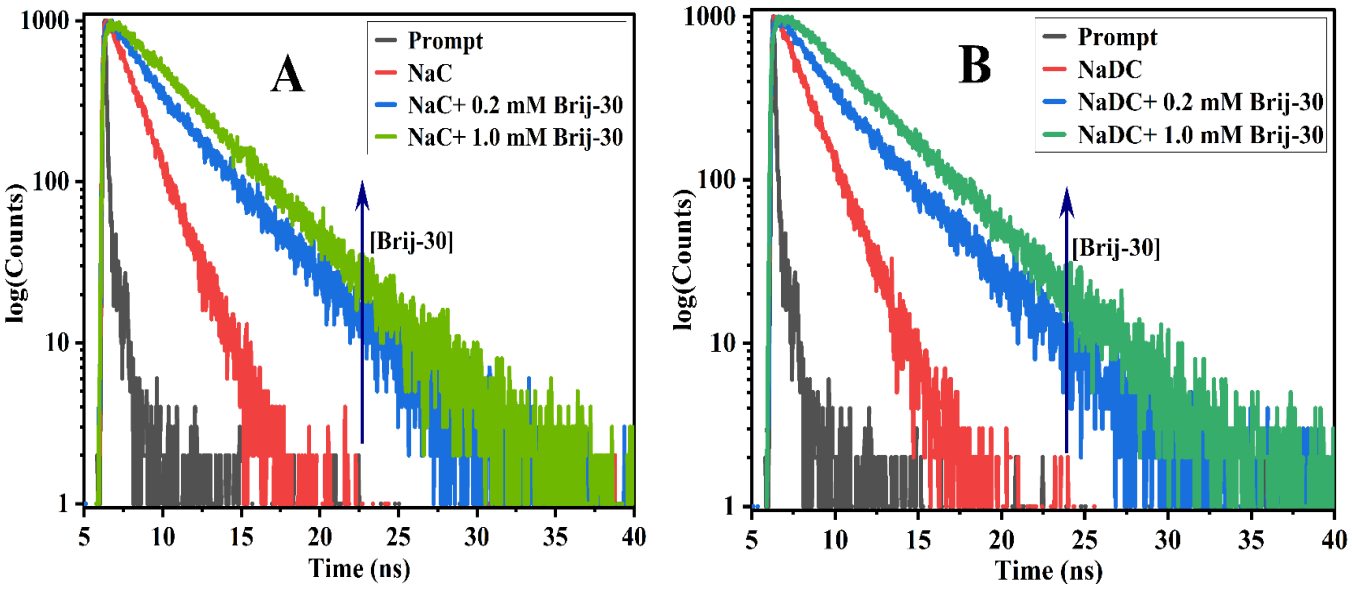

Figure 5. Life time decay profile of solubilized Coumarin 153 in presence of (A) Brij-30/ NaC and (B) Brij-30/ NaDC systems with variation of concentration of Brij-30.

4. Conclusions

In this study, time-correlated single photon counting (TCSPC), tensiometry, and dynamic light scattering (DLS) have all been used to discuss the molecular interactions between bile salts (NaC/ NaDC) and Brij-30. As the mole fraction of bile salts increases, the CMC of both systems does as well. Micellization was delayed in both systems in presence of bile salts.

It was found that NaC which is less hydrophobic in nature due to presence of additional axial hydroxyl group at the C7, creates stronger synergistic interactions with oxyethylenes of Brij-30. Again, antagonistic interaction was found in case of Brij-30/ NaDC system due to lack of one axial hydroxyl group at C7. Brij-30 molecules have higher surface activity than the bile salts (NaC/ NaDC). Decrease of A_{min} value with increase in the amount of Brij-30 implies that monomers are packed more densely in the presence of Brij-30 molecule. Bile salt molecules with the more rigid hydrophobic part takes up more space than the Brij-30 molecule. More -ve value of $\Delta G\ ^{0}_{m}$ for Brij-30/ NaC system than Brij-30/ NaDC implies that micellization of Brij-30/ NaC system is more spontaneous. Lower experimental $\mathrm{CMC_{mix}}$ than the CMC calculated by Clint in case of Brij-30/ NaC system and higher experimental $\mathrm{CMC_{mix}}$ than the CMC calculated by Clint for Brij-30/ NaDC system indicates nonideality. Also, higher τ_{av} values of probe for Brij-30/ NaDC system than Brij-30/ NaC system implies less compact micellar structure of the former facilitating more penetration of probe molecules into the hydrophobic micellar core.

REFERENCES

1. Massa, M.; Compari, C.; Fisicaro, E., On the mechanism of the cholesterol lowering ability of soluble dietary fibers: Interaction of some bile salts with pectin, alginate, and chitosan studied by isothermal titration calorimetry. *Frontiers in Nutrition* **2022,** *9*, 968847.
2. Lu, M.; Sun, J.; Zhao, Y.; Zhang, H.; Li, X.; Zhou, J.; Dang, H.; Zhang, J.; Huang, W.; Qi, C., Prevention of high-fat diet-induced hypercholesterolemia by Lactobacillus reuteri Fn041 through promoting cholesterol and bile salt excretion and intestinal mucosal barrier functions. *Frontiers in Nutrition* **2022,** *9*, 851541.
3. Kumar, D.; Azum, N.; Rub, M. A.; Asiri, A. M., Interfacial and spectroscopic behavior of phenothiazine drug/bile salt mixture in urea solution. *Chemical Papers* **2021,** *75* (8), 3949-3956.
4. Lupo, N.; Steinbring, C.; Friedl, J. D.; Le-Vinh, B.; Bernkop-Schnürch, A., Impact of bile salts and a medium chain fatty acid on the physical properties of self-emulsifying drug delivery systems. *Drug Development and Industrial Pharmacy* **2021,** *47* (1), 22-35.

5. Khafagy, E.-S.; Almutairy, B. K.; Abu Lila, A. S., Tailoring of Novel Bile Salt Stabilized Vesicles for Enhanced Transdermal Delivery of Simvastatin: A New Therapeutic Approach against Inflammation. *Polymers* **2023,** *15* (3).
6. Sohail, M. I.; Dönmez-Cakil, Y.; Szöllősi, D.; Stockner, T.; Chiba, P., The Bile Salt Export Pump: Molecular Structure, Study Models and Small-Molecule Drugs for the Treatment of Inherited BSEP Deficiencies. *International Journal of Molecular Sciences* **2021,** *22* (2).
7. Poša, M.; Tepavčević, V.; Grbović, L.; Mikulić, M.; Pavlović, K., Hydrophobicity and self-association (micellization) of bile salts with a lactone or lactam group in a steroid skeleton. *Journal of Physical Organic Chemistry* **2021,** *34* (2), e4133.
8. Jójárt, B.; Poša, M.; Fiser, B.; Szőri, M.; Farkaš, Z.; Viskolcz, B., Mixed Micelles of Sodium Cholate and Sodium Dodecylsulphate 1:1 Binary Mixture at Different Temperatures – Experimental and Theoretical Investigations. *PLOS ONE* **2014,** *9* (7), e102114.
9. Jójárt, B.; Viskolcz, B.; Poša, M.; Fejer, S. N., Global optimization of cholic acid aggregates. *The Journal of Chemical Physics* **2014,** *140* (14).
10. Madenci, D.; Egelhaaf, S. U., Self-assembly in aqueous bile salt solutions. *Current Opinion in Colloid & Interface Science* **2010,** *15* (1), 109-115.
11. Mikov, M.; Fawcett, J. P., Bile acids: chemistry, biosynthesis, analysis, chemical & metabolic transformations and pharmacology. *Eur. J. Drug Metab. Pharmacokinet* **2006,** *31*, 133-134.
12. Pártay, L. B.; Jedlovszky, P.; Sega, M., Molecular Aggregates in Aqueous Solutions of Bile Acid Salts. Molecular Dynamics Simulation Study. *The Journal of Physical Chemistry B* **2007,** *111* (33), 9886-9896.
13. Poša, M.; Popović, K.; Ćirin, D.; Farkaš, Z., Binary mixed micelles of polysorbates (Tween 20 and Tween 60) and bile salts (Na-hyodeoxycholate and Na-cholate): Regular solution theory and change of pKa values of micellar bile acid – a novel approach to estimate of the stability of the mixed micelles. *Fluid Phase Equilibria* **2015,** *396*, 1-8.
14. Poša, M.; Sebenji, A., Determination of number-average aggregation numbers of bile salts micelles with a special emphasis on their oxo derivatives—The effect of the steroid skeleton. *Biochimica et Biophysica Acta (BBA) - General Subjects* **2014,** *1840* (3), 1072-1082.
15. Yang, L.; Fawcett, J. P.; Østergaard, J.; Zhang, H.; Tucker, I. G., Mechanistic Studies of the Effect of Bile Salts on Rhodamine 123 Uptake into RBE4 Cells. *Molecular Pharmaceutics* **2012,** *9* (1), 29-36.
16. Yang, L.; Fawcett, J. P.; Zhang, H.; Tucker, I. G., Effect of 12-oxochenodeoxycholate on the pharmacokinetics and pharmacodynamics of morphine 6-glucuronide in Wistar rats. *Journal of Pharmacy and Pharmacology* **2013,** *65* (4), 561-566.
17. Maldonado-Valderrama, J.; Wilde, P.; Macierzanka, A.; Mackie, A., The role of bile salts in digestion. *Advances in Colloid and Interface Science* **2011,** *165* (1), 36-46.
18. Mukhopadhyay, S.; Maitra, U., Chemistry and biology of bile acids. *Current Science* **2004,** *87* (12), 1666-1683.
19. Gouin, S.; Zhu, X. X., Fluorescence and NMR Studies of the Effect of a Bile Acid Dimer on the Micellization of Bile Salts. *Langmuir* **1998,** *14* (15), 4025-4029.
20. Subuddhi, U.; Mishra, A. K., Micellization of bile salts in aqueous medium: A fluorescence study. *Colloids and Surfaces B: Biointerfaces* **2007,** *57* (1), 102-107.
21. Jana, P. K.; Moulik, S. P., Interaction of bile salts with hexadecyltrimethylammonium bromide and sodium dodecyl sulfate. *The Journal of Physical Chemistry* **1991,** *95* (23), 9525-9532.

22. Simonović, B. R.; Momirović, M., Determination of critical micelle concentration of bile acid salts by micro-calorimetric titration. *Microchimica Acta* **1997,** *127* (1), 101-104.
23. Glomme, A.; März, J.; Dressman, J. B., Predicting the Intestinal Solubility of Poorly Soluble Drugs. In *Pharmacokinetic Profiling in Drug Research*, **2006**; pp 259-280.
24. Okazaki, A.; Mano, T.; Sugano, K., Theoretical Dissolution Model of Poly-Disperse Drug Particles in Biorelevant Media. *Journal of Pharmaceutical Sciences* **2008,** *97* (5), 1843-1852.
25. Dongowski, G.; Fritzsch, B.; Giessler, J.; Härtl, A.; Kuhlmann, O.; Neubert, R. H. H., The influence of bile salts and mixed micelles on the pharmacokinetics of quinine in rabbits. *European Journal of Pharmaceutics and Biopharmaceutics* **2005,** *60* (1), 147-151.
26. Parks, D. J.; Blanchard, S. G.; Bledsoe, R. K.; Chandra, G.; Consler, T. G.; Kliewer, S. A.; Stimmel, J. B.; Willson, T. M.; Zavacki, A. M.; Moore, D. D.; Lehmann, J. M., Bile Acids: Natural Ligands for an Orphan Nuclear Receptor. *Science* **1999,** *284* (5418), 1365-1368.
27. Small, D. M., The Physical Chemistry of Cholanic Acids. In *The Bile Acids Chemistry, Physiology, and Metabolism: Volume 1: Chemistry*, Nair, P. P.; Kritchevsky, D., Eds. Springer US: Boston, MA, **1971**; pp 249-356.
28. Hoffman, K., Waterfront redevelopment as an urban revitalization tool: Boston's waterfront redevelopment plan. *Harv. Envtl. L. Rev.* **1999,** *23*, 471.
29. Gallo-Torres, H. E., Obligatory role of bile for the intestinal absorption of vitamin E. *Lipids* **1970,** *5* (4), 379-384.
30. Tamminen, J.; Kolehmainen, E., Bile Acids as Building Blocks of Supramolecular Hosts. *Molecules* **2001,** *6* (1), 21-46.
31. Lee, H.-Y.; Diehn, K. K.; Sun, K.; Chen, T.; Raghavan, S. R., Reversible Photorheological Fluids Based on Spiropyran-Doped Reverse Micelles. *Journal of the American Chemical Society* **2011,** *133* (22), 8461-8463.
32. Rosen, M. J.; Kunjappu, J. T., *Surfactants and interfacial phenomena*. John Wiley & Sons: **2012**.
33. Robson, R. J.; Dennis, E. A., The size, shape, and hydration of nonionic surfactant micelles. Triton X-100. *The Journal of Physical Chemistry* **1977,** *81* (11), 1075-1078.
34. Kresheck, G. C.; Hwang, J., Phase separation properties of several aqueous alkyldimethylphosphine oxide/phospholipid mixtures and their potential use for protein purification. *Chemistry and Physics of Lipids* **1995,** *76* (2), 193-199.
35. Altschuler, M.; Heddens, D. K.; Diveley, R. R., Jr.; Kresheck, G. C., Plasmid DNA isolation utilizing a novel nonionic detergent. *Biotechniques* **1994,** *17* (3), 434, 436.
36. Paradies, H. H., Shape and size of a nonionic surfactant micelle. Triton X-100 in aqueous solution. *The Journal of Physical Chemistry* **1980,** *84* (6), 599-607.
37. Biaselle, C. J.; Millar, D. B., Studies on Triton X-100 detergent micelles. *Biophysical Chemistry* **1975,** *3* (4), 355-361.
38. Streletzky, K.; Phillies, G. D. J., Temperature dependence of Triton X-100 micelle size and hydration. *Langmuir* **1995,** *11* (1), 42-47.
39. Kumbhakar, M.; Goel, T.; Mukherjee, T.; Pal, H., Role of Micellar Size and Hydration on Solvation Dynamics: A Temperature Dependent Study in Triton-X-100 and Brij-35 Micelles. *The Journal of Physical Chemistry B* **2004,** *108* (50), 19246-19254.

40. Brown, W.; Rymden, R.; Van Stam, J.; Almgren, M.; Svensk, G., Static and dynamic properties of nonionic amphiphile micelles: Triton X-100 in aqueous solution. *The Journal of Physical Chemistry* **1989,** *93* (6), 2512-2519.
41. Rosen, M. J.; Zhao, F., Binary mixtures of surfactants. The effect of structural and microenvironmental factors on molecular interaction at the aqueous solution/air interface. *Journal of Colloid and Interface Science* **1983,** *95* (2), 443-452.
42. Zhou, Q.; Rosen, M. J., Molecular Interactions of Surfactants in Mixed Monolayers at the Air/Aqueous Solution Interface and in Mixed Micelles in Aqueous Media: The Regular Solution Approach. *Langmuir* **2003,** *19* (11), 4555-4562.
43. Mukherjee, I.; Mukherjee, S.; Naskar, B.; Ghosh, S.; Moulik, S. P., Amphiphilic behavior of two phosphonium based ionic liquids. *Journal of Colloid and Interface Science* **2013,** *395*, 135-144.
44. Zana, R., Critical Micellization Concentration of Surfactants in Aqueous Solution and Free Energy of Micellization. *Langmuir* **1996,** *12* (5), 1208-1211.
45. Rosen, M. J.; Aronson, S., Standard free energies of adsorption of surfactants at the aqueous solution/air interface from surface tension data in the vicinity of the critical micelle concentration. *Colloids and Surfaces* **1981,** *3* (3), 201-208.
46. Rosen, M. J., *Surfactants and Interfacial Phenomena, 3rd Edn. NewYork: JohnWiley and Sons*. Inc: **2004**.
47. Ray, G. B.; Chakraborty, I.; Ghosh, S.; Moulik, S. P.; Palepu, R., Self-Aggregation of Alkyltrimethylammonium Bromides (C10-, C12-, C14-, and C16TAB) and Their Binary Mixtures in Aqueous Medium: A Critical and Comprehensive Assessment of Interfacial Behavior and Bulk Properties with Reference to Two Types of Micelle Formation. *Langmuir* **2005,** *21* (24), 10958-10967.
48. Cui, X.; Jiang, Y.; Yang, C.; Lu, X.; Chen, H.; Mao, S.; Liu, M.; Yuan, H.; Luo, P.; Du, Y., Mechanism of the Mixed Surfactant Micelle Formation. *The Journal of Physical Chemistry B* **2010,** *114* (23), 7808-7816.
49. Jiang, Y.; Chen, H.; Mao, S.; Luo, P.; Du, Y.; Liu, M., Dynamics of Mixed Surfactants in Aqueous Solutions. *The Journal of Physical Chemistry B* **2011,** *115* (9), 1986-1990.
50. Grillo, I.; Penfold, J., Self-Assembly of Mixed Anionic and Nonionic Surfactants in Aqueous Solution. *Langmuir* **2011,** *27* (12), 7453-7463.
51. López, O.; Cócera, M.; Wehrli, E.; Parra, J. L.; de la Maza, A., Solubilization of Liposomes by Sodium Dodecyl Sulfate: New Mechanism Based on the Direct Formation of Mixed Micelles. *Archives of Biochemistry and Biophysics* **1999,** *367* (2), 153-160.
52. Rosen, M. J.; Murphy, D. S., Synergism in binary mixtures of surfactants: V. Two-phase liquid—liquid systems at low surfactant concentrations. *Journal of Colloid and Interface Science* **1986,** *110* (1), 224-236.
53. Palous, J. L.; Turmine, M.; Letellier, P., Mixtures of Nonionic and Ionic Surfactants: Determination of Mixed Micelle Composition Using Cross-Differentiation Relations. *The Journal of Physical Chemistry B* **1998,** *102* (30), 5886-5890.
54. Rosen, M. J.; Zhu, B. Y., Synergism in binary mixtures of surfactants: III. Betaine-containing systems. *Journal of Colloid and Interface Science* **1984,** *99* (2), 427-434.

Table 1. Critical Micellar Concentrations (*CMC*), surface pressure (π_{cmc}), minimum area per molecule (A_{min}), efficiency of interfacial adsorption (pC_{20}), standard free energy of micellization (ΔG_m^0), standard free energy of interfacial adsorption (ΔG_{ad}^0), surface tension at *CMC* (γ_{CMC}), minimum free energy of the surface with maximum adsorption (ΔG_{min}^S) at 298.15 K.

$\alpha_{Brij-30}$	CMC (exp)	CMC $(ideal)$	π_{CMC} $(mN.m^{-1})$	$10^6\Gamma_{max}$ $(mol\,m^{-2})$	A_{min} $(nm^2$ $/molecule)$	pC_{20}	ΔG_m^0 $(kJ.mol^{-1})$	ΔG_{ads}^0 $(kJ.mol^{-1})$	γ_{cmc} $(\pm 0.2\,mN.m^{-1})$	ΔG_{min}^S $(kJ.mol^{-1})$
Brij-30/ NaC										
0	10.23		24.8	0.80	2.07	0.40	-21.31	-52.29	46.5	58.08
0.2	0.19	0.23	41.8	2.69	0.62	1.59	-31.13	-46.65	29.2	10.84
0.4	0.09	0.11	42.6	3.28	0.50	1.97	-32.99	-45.95	29.2	8.88
0.6	0.07	0.08	41.9	2.51	0.66	2.18	-33.50	-50.18	28.5	11.35
0.8	0.05	0.06	43.7	3.90	0.42	2.19	-34.45	-45.63	28	7.17
1.0	0.04		44.8	3.56	0.47	2.46	-34.59	-47.14	25.7	7.20
Brij-30/ NaDC										
0	4.09		29	0.81	2.05	0.43	-23.58	-59.42	43.4	53.64
0.2	0.43	0.22	40.1	2.10	0.79	1.45	-29.15	-48.17	31.3	14.85
0.4	0.42	0.11	41.2	1.83	0.91	1.76	-29.18	-51.69	30.4	16.61
0.6	0.39	0.07	42.7	3.23	0.51	1.53	-29.34	-42.52	27.6	8.52
0.8	0.06	0.06	41.0	3.29	0.50	2.72	-33.88	-46.33	30.2	9.17
1.0	0.04		44.8	3.56	0.47	2.46	-34.59	-47.14	25.7	7.20

Table 2. Time-Resolved Decay Parameter of Coumarin 153 in Brij-30/ NaC and Brij-30/ NaDC systems.

[Brij-30]$/mM$	$\tau_1(ns)$	a_1	$\tau_2(ns)$	a_2	$\tau_{avg}(ns)$	χ^2
Brij-30 in 1.0 mM NaC						
0.0	1.49	1.0	-	-	1.49	1.06
0.02	1.03	0.09	3.75	0.90	3.00	1.00
0.05	1.99	0.12	4.17	0.88	3.69	1.03
0.14	2.13	0.06	4.00	0.94	3.98	1.05
0.50	2.04	0.02	4.04	0.98	3.95	1.05
0.78	3.42	0.45	3.51	0.54	3.47	1.12
1.00	2.08	0.01	4.05	0.99	4.00	1.08
Brij-30 in 1.0 mM NaDC						
0.0	0.75	0.16	1.71	0.84	1.42	1.12
0.02	3.65	1.00	-	-	3.65	1.08
0.05	3.97	1.00	-	-	3.97	1.05
0.14	4.01	1.00	-	-	4.01	1.09
0.50	4.02	1.00	-	-	4.02	1.08
0.78	4.06	1.00	-	-	4.06	1.09
1.00	4.08	1.00	-	-	4.08	1.11

Summary and conclusions

The first chapter discussed CPZ-assisted aggregate formation from a zwitterionic gemini surfactant using DLS, CLSM, TEM, and time-resolved fluorescence measurements. Increasing mole fraction of CPZ raises the critical micelle concentration, indicating CPZ incorporation into C_{14}Ab micelles. High packing parameters and microscopic techniques confirm large aggregate formation. Mixed micellization is entropy-driven at higher CPZ mole fractions. The free energy of micellization in a nonideal state is more negative than in an ideal state, favoring mixed micelle formation. These results highlight the influence CPZ on micelle formation, aggregate size, and thermodynamics.

From the discussion in the second chapter, it was observed that the decrease in CMC of ionic surfactants (SDS, SDDS, CTAB, CTAT) with increasing TFE is due to reduced micellar charge density as TFE penetrates the surface layer. Constant anisotropy decay values of coumarin 153 confirm that TFE is not in the palisade layer. For non-ionic TX-114, CMC remains constant at low TFE concentrations, but increases at higher concentrations due to conformational changes increasing steric repulsion. Time-resolved fluorescence decay studies show that TFE penetrates the TX-114 micelle's palisade layer via hydrogen bonding and quenching fluorescence lifetime. This study provides novel insights into micelle interactions, aiding in membrane protein stabilization and pharmaceutical applications.

The systemic study in the third chapter explores interactions between TX-114/TX-100 and β-cyclodextrin using various analytical techniques. Increased β-cyclodextrin concentrations result in higher CMC values for both surfactant systems, suggesting a delay in micellization. TX-100 forms more stable complexes compared to TX-114, attributed to its lower hydrophobicity. Incorporation of Triton X into β-cyclodextrin enhances fluorescence intensity from phenyl groups, reflecting changes in microenvironment and hydrophobic interactions. Higher A_{min} values in β-CD/TX-100 indicate compact monomer packing. Negative ΔG_m^0 and ΔG_{ad}^0 values demonstrate thermodynamically stable micellization and adsorption processes, although becoming less spontaneous with increasing β-cyclodextrin concentration. These findings advance our understanding of β-cyclodextrin and Triton X interactions, offering implications for diverse applications and suggesting avenues for further research.

The systematic investigation discussed in the fourth chapter includes TCSPC, tensiometry, and DLS to explore NaC/NaDC bile salt interactions with Brij-30. Increasing bile salt mole fractions raise CMC values, delaying micellization. NaC shows stronger synergistic interaction with Brij-30 due to lower hydrophobicity than NaDC. Brij-30 has higher surface activity than bile salts. Decreasing A_{min} values with increasing concentration of Brij-30 indicate denser packing. More negative ΔG_m^0 for Brij-30/NaC suggests spontaneous micellization. Higher τ_{av} values in Brij-30/NaDC imply a less compact micellar structure, allowing greater probe penetration. These insights into bile salt and Brij-30 interactions inform micellar structure and dynamics.

Appendix

Basic Data

Chapter-I

1.1. Tensiometric data of CPZ/C_{12}DmCB system at various mole fraction of CPZ at 298.15 K.

α_{CPZ}= 0.2		α_{CPZ}= 0.4		α_{CPZ}= 0.6		α_{CPZ}= 0.8	
[Conc]/mM	γ/mNm^{-1}	[Conc]/mM	γ/mNm^{-1}	[Conc]/mM	γ/mNm^{-1}	[Conc]/mM	γ/mNm^{-1}
0.000	70.6	0.000	70.3	0.000	70.8	0.000	70.6
0.014	67.4	0.016	66.8	0.018	63.8	0.045	60
0.072	59.1	0.048	62.6	0.054	62.3	0.134	57.5
0.158	55.2	0.112	60.1	0.126	59.7	0.313	54.2
0.287	52.2	0.239	54.9	0.269	55.4	0.579	51.3
0.472	47.8	0.461	50.6	0.483	52.5	0.977	49.2
0.741	43.2	0.808	45.4	0.803	49.7	1.546	47.9
1.134	39.5	1.306	41	1.225	46.9	2.325	46.6
1.688	35.7	1.982	35.9	1.747	45.6	3.347	45.1
2.435	36.1	2.854	35	2.4	44.3	4.597	44.3
3.494	36.5	3.94	34.6	3.211	43.2	6.1	43.7
4.898	36.7	5.248	34.4	4.204	43.1	7.833	43.6
6.629	37.1	6.753	34.3	5.398	43.4	9.848	43.5
				6.805	43.5	12.143	43.5
				8.463	43.7	14.676	43.5
				10.34	44	17.405	43.4

1.2. Tensiometric data of CPZ/C_{14}AB system at various mole fraction of CPZ at 298.15 K.

α_{CPZ}= 0.2	α_{CPZ}= 0.4	α_{CPZ}= 0.6	α_{CPZ}= 0.8	α_{CPZ}= 0.2	α_{CPZ}= 0.4	α_{CPZ}= 0.6	α_{CPZ}= 0.8
[Conc]/mM	γ/mNm^{-1}	[Conc]/mM	γ/mNm^{-1}	[Conc]/mM	γ/mNm^{-1}	[Conc]/mM	γ/mNm^{-1}
0.0000	71.2	0.000	71.2	0.000	71.3	0.000	70.9
0.0004	66.2	0.001	65.8	0.001	66.5	0.002	69.1
0.0012	65.7	0.002	63.2	0.002	66	0.008	66.9
0.0032	64.4	0.004	62.6	0.006	65.6	0.020	65.7
0.0068	63.4	0.009	62.2	0.012	65.5	0.040	64.8
0.0126	61.4	0.018	61.2	0.024	64.2	0.074	63.3
0.0208	59.1	0.031	60.3	0.043	62.9	0.127	62.8
0.0310	57.1	0.049	59.3	0.071	60.2	0.202	60.8
0.0432	53.7	0.074	54.9	0.108	55.1	0.301	59.1
0.0577	49.6	0.106	49.8	0.152	49.8	0.425	55.2
0.0751	43.1	0.144	40.5	0.200	45.3	0.571	50.1
0.0935	37.9	0.187	37.5	0.252	40.8	0.723	43.4
0.1144	33.9	0.233	36.8	0.307	38.6	0.878	38.9

0.1373	33.9	0.282	36.7	0.363	36.2	1.035	36.8
0.1619	33.9	0.334	36.8	0.421	36.2	1.186	36.8
0.1878	33.9	0.386	36.7	0.481	36.2	1.337	36.7
				0.548	36.2	1.491	36.8

1.3. Tensiometric data of CPZ, C_{12}DmCB and C_{14}AB systems in water at 298.15 K.

CPZ		C_{12}DmCB		C_{14}Ab	
[Conc]/mM	γ/mNm^{-1}	[Conc]/mM	γ/mNm^{-1}	[Conc]/mM	γ/mNm^{-1}
0.000	70.6	0.000	70.5	0.000	70.9
0.028	63.8	0.004	64.5	0.0004	70.8
0.083	62.7	0.012	60.4	0.0013	70.6
0.222	60.6	0.024	54.8	0.0031	69.5
0.498	58.3	0.040	49.9	0.0067	65.9
0.965	55.4	0.060	47.1	0.0138	62.6
1.647	53.6	0.088	44.6	0.0243	58.1
2.723	51.8	0.127	42.4	0.0382	52
4.306	50.7	0.186	38.7	0.0562	44.5
6.486	49.7	0.264	35.9	0.0772	36.9
9.326	48.5	0.361	32.9	0.1011	28.4
12.853	47.6	0.484	30.6	0.1253	27.9
17.053	46.3	0.635	27.4	0.1528	28.1
21.777	45.2	0.821	24.9	0.1833	27.8
26.876	45.5	1.039	23.3	0.2167	27.8
32.372	45.7	1.287	21.8	0.2525	27.8
38.091	45.8	1.597	19.9	0.2921	27.8
43.881	46.0	1.962	19.4	0.3350	27.8
		2.407	19.0		
		2.918	19.0		
		3.482	18.6		
		4.137	18.5		
		4.858	18.5		

1.4. Normalized turbidity of CPZ/C_{14}AB system in water at various mole fraction of CPZ at 298.15 K.

α_{CPZ}	Normalized turbidity
0	0.16
0.1	0.24
0.2	0.33

0.3	0.65
0.4	0.91
0.5	0.95
0.6	1
0.7	0.24
0.8	0.01
0.9	0
1	0

1.5. Hydrodynamic radii (r_h) of CPZ/C_{14}AB system in water at various mole fraction of CPZ at 298.15 K.

α_{CPZ}	r_h (nm)
0	127.5
0.1	307.6
0.2	265.6
0.4	307.6
0.5	553.2
0.6	553.2
0.7	147.7
0.8	127.5
1	0.416

1.6. Steady-state fluorescence anisotropy (r_{ss}) of CPZ/C_{12}DmCB system in water at various mole fraction of CPZ at 298.15 K.

α_{CPZ}	r_{ss}
0	0.024
0.1	0.025
0.2	0.027
0.3	0.028
0.4	0.030
0.5	0.016
0.6	0.033
0.7	0.033
0.8	0.055
1	0.150

1.7. Steady-state fluorescence anisotropy (r_{ss}) of CPZ/C_{14}AB system in water at various mole fraction of CPZ at 298.15 K.

α_{CPZ}	r_{ss}
0	0.297
0.1	0.277
0.2	0.282
0.3	0.2
0.4	0.186
0.5	0.262
0.6	0.593
0.7	0.133
0.8	0.036

1.8. Lifetime (τ) of solubilized acridine orange in water of CPZ/C_{12}DmCB and CPZ/C_{14}Ab systems at different mole fractions of CPZ at 298.15 K.

α_{CPZ}	Systems	
	Life time (τ) of CPZ/C_{12}DmCB (ns)	Life time (τ) of CPZ/C_{14}Ab (ns)
0	1.71	1.71
0.1	1.67	1.63
0.2	1.65	1.62
0.3	1.69	1.66
0.4	1.63	1.61
0.5	1.71	1.60
0.6	1.98	1.19
0.7	2.20	0.93
0.8	2.68	0.78
1	2.81	2.81

1.9. Zeta potential (ζ) of CPZ/C_{12}DmCB and CPZ/C_{14}Ab systems at different mole fractions of CPZ at 298.15 K.

α_{CPZ}	Zeta potential (ζ) of CPZ/C_{12}DmCB (mV)	Zeta potential (ζ) of CPZ/C_{14}AB (mV)
0	-3.79	-4.12
0.1	8.39	0.21
0.2	13.7	0.36

0.3	6.15	2.27
0.4	6.95	4.40
0.5	6.56	4.48
0.6	9.22	8.91
0.7	9.15	8.73
0.8	9.15	6.86

1.10. Specific conductivity (κ) of CPZ/C_{12}DmCB and CPZ/C_{14}Ab systems at different mole fractions of CPZ at 298.15 K.

α_{CPZ}	Specific conductivity (κ) of CPZ/C_{12}DmCB (mS.cm^{-1})	Specific conductivity (κ) of CPZ/C_{14}AB (mS.cm^{-1})
0	2.1	2.4
0.1	2.5	2.5
0.2	3.2	2.8
0.3	2.7	2.7
0.4	2.6	2.7
0.5	2.5	2.8
0.6	2.4	2.8
0.7	2.5	2.9
0.8	2.8	2.9
0.9	2.9	3.0
1	3.1	3.1

Chapter-II

2.1. Tensiometric data of SDS in water and water/TFE mixtures at 298.15 K.

SDS in water		SDS in 5% TFE		SDS in 10% TFE		SDS in 20% TFE	
[Conc]/mM	γ/mNm^{-1}	[Conc]/mM	γ/mNm^{-1}	[Conc]/mM	γ/mNm^{-1}	[Conc]/mM	γ/mNm^{-1}
0.000	70.7	0.000	43.0	0.000	33.5	0.000	26.2
0.048	64	0.040	43.5	0.048	35.3	0.040	26.5
0.096	59.4	0.140	42.4	0.096	36.2	0.120	26.9
0.144	56.2	0.339	36.0	0.192	37.0	0.240	27.1

0.192	54	0.577	31.7	0.335	33.4	0.438	27.2
0.240	51.3	0.854	28.2	0.478	30.4	0.640	25.5
0.335	47.6	1.129	26.1	0.621	27.7	0.834	24.3
0.430	43.8	1.442	24.4	0.763	25.9	1.070	23.7
0.526	41.6	1.754	23.1	0.952	24.3	1.384	24.3
0.622	38.1	2.103	22.1	1.141	23.3	1.696	25.0
0.716	35.9	2.526	21.5	1.376	22.2	2.083	25.6
0.810	34.9	3.006	20.7	1.657	21.6	2.468	25.9
0.905	34	3.583	19.9	1.936	20.9	2.946	26.2
1.047	32.8	4.337	19.5	2.307	20.0		
1.188	31.9	5.259	19.0	2.767	19.4		
1.329	31.3	5.557	20.1	3.405	19.0		
1.517	30.3	6.269	21.0	4.192	18.5		
1.750	28.9	7.215	21.5	4.926	19.6		
1.983	27.7	8.305	22.2	5.446	20.4		
2.214	26.5			6.225	21.1		
2.445	25.4			7.165	21.4		
2.675	24.3						
2.904	23.7						
3.132	22.9						
3.359	22						
3.586	21.6						
3.811	21.3						
4.148	21						
4.593	20.6						
5.035	20.2						
5.474	19.3						
6.126	20.2						
6.771	21						
7.197	21.7						
7.619	22.3						
8.039	22.9						

2.2. Tensiometric data of SDDS in water and water/TFE mixtures at 298.15 K.

SDDS in water		SDDS in 5% TFE		SDDS in 10% TFE		SDDS in 15% TFE	
[Conc]/mM	γ/mNm^{-1}	[Conc]/mM	γ/mNm^{-1}	[Conc]/mM	γ/mNm^{-1}	[Conc]/mM	γ/mNm^{-1}
0.000	70.9	0.000	42.8	0.000	32.4	0.000	28.6
0.075	65.1	0.075	43.8	0.075	33.4	0.075	29.5
0.262	57.2	0.300	44.0	0.300	34.0	0.300	30.5

0.449	52.6	0.673	41.8	0.673	34.9	0.673	31.1
0.710	48.9	1.268	37.7	1.194	33.5	1.268	31.6
1.045	45.7	2.007	33.2	1.933	30.4	2.007	30.0
1.490	41.8	2.814	30.4	2.851	28.0	2.961	28.1
2.044	38.3	3.725	28.0	3.942	25.6	4.051	27.1
2.668	35.8	4.808	26.3	5.202	24.8	5.345	27.7
3.398	32.8	6.093	24.6	6.624	25.5	6.765	28.3
4.304	30.4	7.504	23.4	8.376	26.4	8.376	28.6
5.273	28.2	9.104	23.8	10.271	27.0		
6.341	26.2	10.816	24.6				
7.574	24.6	12.852	24.9				
8.965	23.8	14.687	25.2				
10.510	24.7	16.827	25.6				
12.201	25.6						
14.029	26.3						
15.989	26.6						

2.3. Tensiometric data of CTAB in water and water/TFE mixtures at 298.15 K.

CTAB in water		CTAB in 5% TFE		CTAB in 10% TFE	
[Conc]/mM	γ/mNm^{-1}	[Conc]/mM	γ/mNm^{-1}	[Conc]/mM	γ/mNm^{-1}
0.000	70	0.000	42	0.000	34
0.005	57.5	0.005	42.9	0.002	34.5
0.015	53.4	0.015	41	0.007	32.8
0.030	50.1	0.035	39	0.017	32.2
0.050	46.8	0.065	37.3	0.032	31.9
0.075	44.1	0.114	35.5	0.057	31.6
0.104	41.2	0.188	33.9	0.094	31.4
0.141	39.5	0.272	33	0.139	31.1
0.190	37.4	0.368	31.8	0.188	30.6
0.263	36.1	0.475	31	0.248	30.3
0.359	34.2	0.602	30.4	0.321	30.1
0.477	32.8	0.750	30.5	0.404	30
0.616	31.7	0.907	30.7	0.510	30
0.764	31.2	1.081	30.9	0.625	30.1
0.920	31.4	1.272	30.9	0.750	30.2
1.083	31.7	1.478	30.9	0.885	30.2
1.253	31.8	1.776	30.9	1.038	30.2
1.440	31.9	2.154	30.9	1.230	30.2
				1.438	30.2

2.4. Tensiometric data of CTAT in water and water/TFE mixtures at 298.15 K.

CTAT in water		CTAT in 5% TFE		CTAT in 10% TFE		CTAT in 15% TFE	
[Conc]/mM	γ/mNm^{-1}	[Conc]/mM	γ/mNm^{-1}	[Conc]/mM	γ/mNm^{-1}	[Conc]/mM	γ/mNm^{-1}
0.000	70.6	0.000	43.5	0.000	34.3	0.000	28.1
0.001	67.2	0.001	44.3	0.001	35	0.001	28.8
0.008	61	0.005	45.3	0.005	35.5	0.003	30.1
0.016	58.9	0.011	45	0.011	35.6	0.006	30.4
0.028	54	0.017	44.4	0.017	35.8	0.013	30.6
0.044	50.6	0.027	43	0.027	35.5	0.023	30.4
0.063	46	0.040	41.4	0.040	34.9	0.035	29.9
0.082	43.2	0.056	39.5	0.059	33.2	0.048	29.5
0.104	39.6	0.075	37.2	0.084	31.3	0.064	28.8
0.128	37.1	0.096	34.8	0.115	29.3	0.076	28.5
0.155	34.8	0.118	33.2	0.148	28.3	0.104	27.5
0.185	32.1	0.142	31	0.184	28.2	0.129	27.4
0.217	31	0.169	29.5	0.225	28.2	0.159	27.4
0.252	30.4	0.196	29.2	0.270	28.2	0.195	27.4
0.288	29.9	0.225	29	0.320	28.2	0.235	27.4
0.327	29.9	0.256	29	0.374	28.2		
0.367	29.9	0.290	29				
0.410	29.9	0.329	29				
0.453	29.9	0.372	29				

2.5. Tensiometric data of TX-114 in water and water/TFE mixtures at 298.15 K.

TX-114 in water		TX-114 in 5%		TX-114 in 10%		TX-114 in 15%	
[Conc]/mM	γ/mNm^{-1}	[Conc]/mM	γ/mNm^{-1}	[Conc]/mM	γ/mNm^{-1}	[Conc]/mM	γ/mNm^{-1}
0.000	70.2	0.000	42.7	0.000	34.6	0.000	26.4
0.001	59.7	0.001	43.2	0.001	35.1	0.001	27.4
0.005	53.1	0.003	41.8	0.004	36.2	0.003	27.9
0.010	48.8	0.006	40.6	0.008	35.8	0.006	29.1
0.019	45.3	0.011	38.9	0.014	35.2	0.012	29.5
0.029	42.4	0.019	37.1	0.023	34.4	0.019	30
0.043	38.8	0.029	35.5	0.035	33.5	0.030	30.3
0.059	36.2	0.042	33.5	0.051	32.6	0.045	29.5
0.080	33.7	0.058	31.5	0.069	31.5	0.066	28.8
0.106	31.4	0.077	30.1	0.090	30.2	0.091	28.2
0.139	29.4	0.100	28.1	0.114	29.1	0.120	27.9

0.177	27.8	0.128	26.9	0.140	28.3	0.159	27.5
0.224	26.8	0.161	26	0.172	26.7	0.206	26.5
0.279	26.4	0.200	25.5	0.209	25.6	0.260	25.5
0.344	26.2	0.249	25.2	0.251	25	0.321	24.4
0.419	26.2	0.305	24.8	0.299	24.8	0.388	23.6
0.501	26.2	0.366	24.8	0.357	24.7	0.459	23.4
0.590	26.2	0.433	24.8	0.422	24.7	0.534	23
0.684	26.2			0.495	24.7	0.612	23
				0.574	24.7	0.692	23
						0.773	23
						0.854	23

2.6. Conductometric data for SDS in water and water/TFE mixtures at 298.15 K.

SDS in water		SDS in 5% TFE		SDS in 10% TFE		SDS in 20% TFE	
[Conc]/mM	$\kappa/\mu S\ cm^{-1}$	[Conc]/mM	$\kappa/\mu S\ cm^{-1}$	[Conc]/mM	$\kappa/\mu S\ cm^{-1}$	[Conc]/mM	$\kappa/\mu S\ cm^{-1}$
0	5	0	4	0	6.5	0	4.3
0.171	22	0.074	9	0.342	37	0.342	29
0.342	40	0.184	18	0.682	69	0.682	54
0.512	59	0.295	27	1.020	99	1.020	77
0.682	83	0.405	36	1.356	127	1.356	102
0.851	101	0.588	50	1.690	156	1.690	127
1.020	122	0.770	65	2.022	184	2.022	150
1.188	139	0.952	80	2.353	210	2.353	172
1.356	159	1.134	93	2.682	240	2.682	196
1.523	177	1.315	108	3.008	260	3.008	220
1.690	196	1.495	122	3.333	290	3.333	240
2.022	230	1.675	136	3.657	320	3.657	260
2.353	260	1.854	149	3.978	340	3.978	290
2.682	290	2.033	163	4.298	370	4.298	310
3.008	330	2.211	176	4.615	390	4.615	330
3.333	360	2.388	190	4.932	410	4.932	350
3.657	390	2.565	200	5.246	440	5.246	370
3.978	420	2.742	220	5.559	460	5.559	390
4.298	450	2.918	230	5.870	480	5.870	410
4.615	490	3.094	240	6.179	500	6.179	430
4.932	500	3.443	270	6.486	520	6.486	450
5.246	550	3.790	290	6.792	540	6.792	470
5.559	580	4.135	320	7.097	560	7.097	490
5.870	620	4.479	340	7.399	590	7.399	510

6.179	650	4.820	370	7.701	610	7.701	530
6.486	680	5.159	390	8.000	630	8.000	550
6.792	710	5.496	410	8.298	650	8.298	570
7.097	730	5.831	430	8.594	670	8.594	590
7.399	760	6.165	460	8.889	690	8.889	610
7.701	790	6.496	480	9.182	710	9.182	620
8.000	810	6.825	500	9.474	730	9.474	640
8.298	830	7.153	510	9.764	750	9.764	670
8.594	850	7.640	540	10.052	760	10.052	680
8.889	870	8.124	570	10.339	780	10.339	700
9.182	890	8.603	590	10.625	800	10.625	720
9.474	910	9.079	620	10.909	820	10.909	740
9.764	930	9.550	650	11.192	830	11.192	750
10.052	950	10.017	670	11.473	850	11.473	770
10.339	960	10.480	700	11.753	870	11.753	790
10.625	980	10.940	720	12.031	880	12.031	800
10.909	1000	11.395	740	12.308	900	12.308	820
11.192	1010	11.847	760	12.583	920	12.583	840
11.473	1020	12.592	800	12.857	930	12.857	850
11.753	1040	13.326	840	13.130	950	13.130	870
12.031	1060	14.051	880	13.401	960	13.401	890
12.308	1080	14.765	920	13.671	980	13.671	900
12.583	1090	15.470	950	13.939	1000	13.939	920
12.857	1110	16.166	980	14.207	1010		
13.130	1120	16.853	1020	14.472	1030		
13.401	1140	17.530	1050	14.737	1040		
13.671	1160	18.199	1090	15.000	1060		
		18.859	1120	15.262	1070		
		20.154	1180	15.522	1090		
		21.416	1250				
		22.646	1310				
		23.250	1340				
		23.489	1350				

2.7. Conductometric data for SDDS in water and water/TFE mixtures at 298.15 K.

SDDS in water		SDDS in 5% TFE		SDDS in 10% TFE	
[Conc]/mM	$\kappa/\mu S\ cm^{-1}$	[Conc]/mM	$\kappa/\mu S\ cm^{-1}$	[Conc]/mM	$\kappa/\mu S\ cm^{-1}$
0	3.6	0	3.7	0	2.5
0.641	46	0.321	24	0.321	23

1.278	88	0.641	45	0.641	42
1.912	136	0.960	66	0.960	63
2.542	176	1.278	88	1.278	81
3.169	210	1.596	108	1.596	102
3.792	250	1.912	129	1.912	124
4.412	290	2.228	151	2.228	143
5.028	330	2.542	171	2.542	163
5.641	370	2.856	192	2.856	183
6.250	410	3.169	210	3.169	200
6.856	450	3.481	230	3.792	240
7.459	480	3.792	250	4.412	280
8.058	520	4.412	290	5.028	310
8.654	560	5.028	330	5.641	350
9.247	600	5.641	370	6.250	380
9.836	630	6.250	400	6.856	410
10.422	670	6.856	440	7.459	440
11.005	700	7.459	470	8.058	480
11.585	740	8.058	510	8.654	510
12.162	770	8.654	540	9.247	540
12.736	800	9.247	570	10.130	580
13.306	830	9.836	600	11.005	620
13.874	860	10.422	630	11.874	660
14.439	890	11.005	650	12.736	700
15.000	920	11.585	680	13.591	750
15.559	940	12.162	700	14.439	780
16.114	960	12.736	730	15.280	820
16.667	980	13.306	750	16.114	860
17.216	1000	13.874	770	16.942	900
17.763	1020	14.439	800	17.763	930
18.307	1040	15.000	820	18.848	980
18.848	1060	15.559	840	19.922	1020
19.386	1080	16.114	870	20.984	1070
		16.667	890	22.036	1110
		17.216	910	23.077	1160
		17.763	930	24.107	1190
		18.307	960		
		18.848	980		
		19.386	1000		
		19.922	1020		
		20.455	1040		
		20.984	1060		

		21.512	1080		
		22.036	1110		
		22.558	1130		

2.8. Conductometric data for CTAB in water and water/TFE mixtures at 298.15 K.

CTAB in water		CTAB in 5% TFE		CTAB in 10% TFE	
[Conc]/mM	$\kappa/\mu S\ cm^{-1}$	[Conc]/mM	$\kappa/\mu S\ cm^{-1}$	[Conc]/mM	$\kappa/\mu S\ cm^{-1}$
0	3.3	0	6	0	6.8
0.043	7	0.023	7	0.043	10.6
0.085	11.3	0.069	12	0.085	15.3
0.127	15.5	0.115	17	0.127	19.2
0.169	19.5	0.160	22	0.169	25
0.211	24	0.205	27	0.211	29
0.253	28	0.250	32	0.253	33
0.294	32	0.294	37	0.294	37
0.335	36	0.338	42	0.335	41
0.376	40	0.382	46	0.376	45
0.417	44	0.426	51	0.417	49
0.457	48	0.469	55	0.457	52
0.497	52	0.513	60	0.497	55
0.537	56	0.556	64	0.537	58
0.577	60	0.598	68	0.577	62
0.616	64	0.641	72	0.616	64
0.656	68	0.683	76	0.656	67
0.695	72	0.725	79	0.695	70
0.734	75	0.766	83	0.734	72
0.772	79	0.808	87	0.772	75
0.811	83	0.849	90	0.811	77
0.849	87	0.890	94	0.849	79
0.887	90	0.931	97	0.887	82
0.925	94	0.971	100	0.925	84
0.963	97	1.011	103	0.963	86
1.000	100	1.052	107	1.000	89
1.037	103	1.091	110	1.037	91
1.074	105	1.131	113	1.074	93
1.111	107	1.170	116	1.111	95
1.148	109	1.209	119	1.148	98

1.184	110	1.248	122	1.184	100
1.220	111	1.287	125	1.220	102
1.257	113	1.325	128	1.257	104
1.292	114	1.364	131	1.292	106
1.328	115	1.402	134	1.328	108
1.364	116	1.440	136	1.364	110
1.399	118	1.477	139	1.399	113
1.434	119	1.515	142	1.434	115
1.469	120	1.552	144	1.469	117
1.504	122	1.589	147	1.504	119
		1.626	149	1.538	121
		1.662	152	1.573	123
				1.607	125
				1.641	127
				1.675	130
				1.709	132
				1.742	134

2.9. Conductometric data for CTAT in water and water/TFE mixtures at 298.15 K.

CTAT in water		CTAT in 5% TFE		CTAT in 10% TFE	
[Conc]/ mM	$\kappa/\mu S\ cm^{-1}$	[Conc]/mM	$\kappa/\mu S\ cm^{-1}$	[Conc]/mM	$\kappa/\mu S\ cm^{-1}$
0	3.8	0	3	0	2.8
0.011	4.6	0.011	3.4	0.011	3.1
0.022	5.2	0.022	4.1	0.022	3.7
0.033	5.9	0.033	4.7	0.033	4.3
0.050	7	0.044	5.3	0.044	4.8
0.066	8	0.055	5.9	0.055	5.5
0.082	9	0.066	6.4	0.066	6
0.098	9.9	0.076	7	0.076	6.5
0.114	10.9	0.087	7.6	0.087	7.1
0.129	11.9	0.098	8.1	0.098	7.6
0.145	12.8	0.108	8.7	0.108	8.1
0.160	13.7	0.119	9.2	0.119	8.7
0.176	14.7	0.129	9.6	0.129	9.1
0.191	15.6	0.140	10	0.140	9.6
0.206	16.4	0.150	10.4	0.150	10.1
0.221	17.2	0.160	10.7	0.160	10.5
0.236	17.9	0.170	11	0.170	11
0.250	18.5	0.181	11.3	0.181	11.4

0.265	19.1	0.191	11.6	0.191	11.8
0.279	19.7	0.201	11.9	0.201	12.2
0.308	21	0.211	12.2	0.211	12.6
0.350	22	0.221	12.4	0.221	13
0.391	23	0.231	12.7	0.231	13.4
		0.240	13	0.240	13.7
		0.250	13.3	0.250	14.1
		0.260	13.5	0.260	14.4
		0.270	13.8	0.270	14.8
		0.279	14	0.279	15.1
				0.289	15.4
				0.298	15.8
				0.308	16.1
				0.317	16.4
				0.327	16.8
				0.336	17.1

2.10. Quenching of pyrene by [CPC] at micellar SDS solution in presence of water and water/TFE mixtures at 298.15 K.

SDS in water		SDS in 5 % TFE		SDS in 10% TFE		SDS in 20% TFE	
[CPC]/mM	$\ln(F_0/F)$	[CPC]/mM	$\ln(F_0/F)$	[CPC]/mM	$\ln(F_0/F)$	[CPC]/mM	$\ln(F_0/F)$
0.000	0	0	0	0.098	-0.006	0.045	0
0.005	-0.001	0.005	-0.009	0.136	0.015	0.069	0.006
0.015	0.014	0.020	0.002	0.178	0.038	0.105	0.021
0.030	0.030	0.045	0.022	0.224	0.066	0.153	0.042
0.054	0.059	0.081	0.054	0.274	0.097	0.199	0.066
0.091	0.108	0.129	0.100	0.327	0.132	0.245	0.088
0.139	0.168	0.188	0.156	0.383	0.171	0.294	0.113
0.197	0.244	0.256	0.221	0.442	0.217	0.342	0.141
0.265	0.336	0.334	0.300			0.390	0.166
0.342	0.433	0.419	0.389				
0.428	0.540	0.512	0.489				
0.520	0.668	0.610	0.618				

2.11. Quenching of pyrene by [CPC] at micellar SDDS solution in presence of water and water/TFE mixtures at 298.15 K.

SDDS in water		SDDS in 5% TFE		SDDS in 10% TFE		SDDS in 15% TFE	
[CPC]/mM	$\ln(F_0/F)$	[CPC]/mM	$\ln(F_0/F)$	[CPC]/mM	$\ln(F_0/F)$	[CPC]/mM	$\ln(F_0/F)$
0.012	-0.022	0.224	0.058	0.037	-0.006	0.025	-0.003
0.037	-0.015	0.281	0.084	0.074	0.009	0.037	0.000
0.074	-0.002	0.336	0.109	0.122	0.023	0.062	0.008
0.122	0.022	0.400	0.140	0.192	0.055	0.098	0.021
0.169	0.045	0.467	0.176	0.261	0.081	0.146	0.039
0.215	0.067	0.536	0.211	0.349	0.119	0.204	0.060
0.272	0.096	0.606	0.254	0.434	0.153	0.265	0.087
0.327	0.126			0.536	0.198	0.329	0.114
0.381	0.156			0.633	0.242	0.396	0.143
				0.745	0.296	0.465	0.173
				0.851	0.345	0.536	0.206
				0.960	0.399	0.608	0.239

2.12. Quenching of pyrene by [CPC] at micellar CTAB solution in presence of water and water/TFE mixtures at 298.15 K.

CTAB in water		CTAB in 5% TFE		CTAB in 10% TFE	
[CPC]/mM	$\ln(F_0/F)$	[CPC]/mM	$\ln(F_0/F)$	[CPC]/mM	$\ln(F_0/F)$
0.003	0.0002	0.015	0.026	0.035	0.033
0.010	0.0569	0.022	0.060	0.052	0.080
0.017	0.1177	0.035	0.121	0.074	0.153
0.025	0.1748	0.047	0.183	0.100	0.237
0.032	0.2320	0.059	0.247	0.131	0.348
0.045	0.3228	0.076	0.346	0.167	0.474
0.057	0.4149	0.093	0.435	0.206	0.594
0.069	0.5017	0.110	0.523	0.249	0.732
0.086	0.6193	0.131	0.643	0.296	0.905
		0.153	0.754	0.347	1.085
		0.174	0.855	0.400	1.275
		0.199	0.991		
		0.224	1.115		
		0.249	1.238		

2.13. Quenching of pyrene by [CPC] at micellar CTAT solution in presence of water and water/TFE mixtures at 298.15 K.

CTAT in water		CTAT in 5% TFE		CTAT in 10% TFE		CTAT in 15% TFE	
[CPC]/mM	$\ln(F_0/F)$	[CPC]/mM	$\ln(F_0/F)$	[CPC]/mM	$\ln(F_0/F)$	[CPC]/mM	$\ln(F_0/F)$
0	0	0	0	0.005	0.017	0	0
0.005	0.126	0.005	0.071	0.012	0.099	0.005	0.025
0.015	0.339	0.010	0.165	0.020	0.190	0.010	0.056
0.030	0.684	0.015	0.260	0.027	0.281	0.020	0.125
0.045	0.980	0.022	0.402	0.037	0.393	0.030	0.194
0.059	1.228	0.030	0.535	0.047	0.507	0.042	0.279
		0.037	0.661	0.062	0.673	0.057	0.377
		0.047	0.823	0.079	0.847	0.074	0.496
		0.057	0.964	0.098	1.055	0.093	0.623
						0.117	0.786
						0.146	0.969

2.14. Quenching of pyrene by [CPC] at micellar TX-114 solution in presence of water and water/TFE mixtures at 298.15 K.

TX-114 in water		TX-114 in 5% TFE		TX-114 in 10% TFE		TX-114 in 15% TFE	
[CPC]/mM	$\ln(F_0/F)$	[CPC]/mM	$\ln(F_0/F)$	[CPC]/mM	$\ln(F_0/F)$	[CPC]/mM	$\ln(F_0/F)$
0.012	0.113	0.027	0.200	0.040	0.251	0.040	0.353
0.025	0.243	0.040	0.311	0.059	0.288	0.059	0.405
0.037	0.378	0.052	0.438	0.084	0.336	0.084	0.468
0.052	0.537	0.067	0.599	0.112	0.397	0.112	0.541
0.067	0.685	0.081	0.745	0.146	0.462	0.146	0.628
0.081	0.824	0.100	0.925	0.183	0.534	0.183	0.723
0.098	0.977			0.229	0.632	0.224	0.838
0.115	1.117						
0.131	1.241						

2.15. Calorimetric data of [SDS] in water and water/TFE mixtures at 298.15 K.

SDS in water		SDS in 20% TFE	
[Conc]/mM	ΔH^0_{obs}(kJ.mol^{-1})	[Conc]/mM	ΔH^0_{obs}(kJ.mol^{-1})
0	--	0	--
0.220	3.341	0.220	12.971
1.526	3.667	1.526	--
2.812	3.096	2.812	11.712
4.080	2.842	4.080	--
5.328	2.451	5.328	11.623
6.557	2.483	6.557	8.215
7.766	2.287	7.766	6.889
8.956	2.157	8.956	5.259
10.127	2.023	10.127	4.064
11.279	1.853	11.279	3.165
12.411	1.725	12.411	2.489
13.524	1.598	13.524	1.792
14.617	1.469	14.617	1.385
15.691	--	15.691	--

2.16. Calorimetric data of [SDDS] in water and water/TFE mixtures at 298.15 K.

SDDS in water		SDDS in 15% TFE	
[Conc]/mM	ΔH^0_{obs}(kJ.mol^{-1})	[Conc]/mM	ΔH^0_{obs}(kJ.mol^{-1})
0	-1.738	0	--
0.415	-2.231	0.415	--
2.882	-2.224	2.882	--
5.312	-2.155	5.312	6.463
7.707	-2.009	7.707	8.847
10.064	-1.727	10.064	6.747
12.385	-1.319	12.385	5.931
14.670	-0.819	14.670	5.310
16.918	-0.431	16.918	4.520
19.129	-0.184	19.129	3.739
21.304	-0.055	21.304	3.206
23.443	-0.003	23.443	2.731
25.545	0.009	25.545	2.251
27.610	0.003	27.610	1.883

29.639	--	29.639	--

2.17. Calorimetric data of [CTAB] in water and water/TFE mixtures at 298.15 K.

CTAB in water		CTAB in 10% TFE	
[Conc]/mM	ΔH^0_{obs}(kJ.mol^{-1})	[Conc]/mM	ΔH^0_{obs}(kJ.mol^{-1})
0	--	0	--
0.019	1.607	0.019	7.805
0.131	1.713	0.131	6.303
0.241	1.610	0.241	4.455
0.349	1.373	0.349	4.421
0.456	0.742	0.456	4.083
0.561	0.687	0.561	3.717
0.664	0.502	0.664	3.372
0.766	0.333	0.766	2.579
0.866	0.188	0.866	2.732
0.965	0.079	0.965	2.485
1.062	0.011	1.062	2.204
1.157	-0.069	1.157	1.985
1.251	-0.183	1.251	1.690
1.342	--	1.342	--

2.18. Quenching of fluorescence lifetime of coumarin 153 by TFE in an aqueous solution of TX-114 at 298.15 K.

[TFE]/M	$\frac{\tau_0}{\tau}$
0	1
0.694	1.199
1.388	1.193
2.082	1.219
2.776	1.429

Chapter-III

3.1. Tensiometric data of TX-100 at various mole fraction of β-CD at 298.15 K.

$\alpha_{\beta-CD} = 0$		$\alpha_{\beta-CD} = 0.2$		$\alpha_{\beta-CD} = 0.4$		$\alpha_{\beta-CD} = 0.6$		$\alpha_{\beta-CD} = 0.8$		$\alpha_{\beta-CD} = 1.0$	
[TX-100]/mM	**γ/mNm^{-1}**	**[TX-100]/mM**	**γ/mNm^{-1}**	**[TX-100]/mM**	**γ/mNm^{-1}**	**[TX-100]/mM**	**γ/mNm^{-1}**	**[TX-100]/mM**	**γ/mNm^{-1}**	**[TX-100]/mM**	**γ/mNm^{-1}**
0.000	70.4	0.000	71.4	0.000	71.3	0.000	71.4	0.000	70.4	0.000	71.6
0.002	58.1	0.002	59.9	0.004	59.3	0.004	60.8	0.004	63.3	0.004	66.4
0.006	56.3	0.006	56.7	0.012	57.7	0.012	59.4	0.012	61.4	0.012	64.5
0.012	53.4	0.012	55.5	0.024	54.4	0.024	57.1	0.024	58	0.024	63.9
0.022	49.8	0.022	53.2	0.044	51.9	0.044	55.1	0.044	56	0.040	62.8
0.037	46.6	0.037	50.8	0.073	48.7	0.073	53.3	0.073	54.6	0.060	61
0.056	43	0.061	48	0.122	46.4	0.122	50.5	0.113	52.6	0.089	59.5
0.081	40.3	0.095	45	0.190	43.7	0.190	48.1	0.161	50.5	0.128	58.5
0.110	36.5	0.138	42.3	0.286	41.1	0.286	45.3	0.219	48.9	0.186	57
0.143	33.3	0.190	39.8	0.398	37.3	0.398	43.1	0.286	47.3	0.263	54.4
0.180	31	0.249	37.2	0.525	31.3	0.525	39.2	0.361	46.2	0.357	51.8
0.222	30.2	0.316	34.8	0.666	29.3	0.666	32.9	0.453	43.9	0.467	49
0.267	29.7	0.389	32.5	0.821	29.7	0.821	28.2	0.561	41.9	0.593	45.8
0.316	29.7	0.469	30.2	0.986	29.7	0.986	28.1	0.684	37.4	0.732	41.8
0.368	29.8	0.553	30.4	1.177	30	1.177	28.3	0.821	31.3	0.884	36.7
0.427	29.8	0.642	30.4	1.404	29.8	1.390	28.2	0.970	29	1.047	32.1
0.493	29.8	0.735	30.4	1.690	30	1.621	28.2	1.130	29	1.220	30.2
0.565	29.6	0.831	30.4			1.892	28.3	1.300	29.2	1.402	29.7
0.642	29.6							1.478	28.9	1.590	29.8
								1.662	28.8	1.783	29.8
										1.994	29.6
										2.218	29.7
										2.453	29.4

3.2. Tensiometric data of TX-114 at various mole fraction of β-CD at 298.15 K.

$\alpha_{\beta-CD} = 0$		$\alpha_{\beta-CD} = 0.2$		$\alpha_{\beta-CD} = 0.4$		$\alpha_{\beta-CD} = 0.6$		$\alpha_{\beta-CD} = 0.8$		$\alpha_{\beta-CD} = 1.0$	
[TX-114]/mM	**γ/mNm^{-1}**	**[TX-114]/mM**	**γ/mNm^{-1}**	**[TX-114]/mM**	**γ/mNm^{-1}**	**[TX-114]/mM**	**γ/mNm^{-1}**	**[TX-114]/mM**	**γ/mNm^{-1}**	**[TX-114]/mM**	**γ/mNm^{-1}**
0.000	71.4	0.000	70.5	0.000	71.5	0.000	71.3	0.000	71.6	0.000	71.4
0.001	58.2	0.002	59.9	0.002	63.4	0.004	65.2	0.004	70	0.004	70
0.005	54.0	0.008	58.5	0.008	61.4	0.012	63.4	0.012	67	0.012	67.2
0.010	50.0	0.018	56.4	0.018	60.3	0.032	58.8	0.024	64.6	0.024	64
0.019	45.7	0.033	54.7	0.038	57.3	0.062	54.6	0.040	61.2	0.040	61
0.029	42.5	0.057	52.8	0.067	53.7	0.111	49.4	0.060	58.5	0.060	58.8
0.043	38.9	0.091	49.2	0.106	46.8	0.179	46.0	0.089	54.8	0.089	56.1

0.059	35.6	0.139	44.5	0.153	41.6	0.265	41.5	0.128	50.9	0.138	52.7
0.080	32.2	0.195	37.3	0.209	38.5	0.368	36.7	0.177	47.4	0.206	47.5
0.106	29.0	0.259	33	0.272	34.3	0.487	30.0	0.244	44.3	0.301	43.5
0.139	26.8	0.330	29.7	0.343	30.7	0.621	29.8	0.329	38.2	0.412	40.8
0.177	25.2	0.407	28.9	0.420	28	0.768	29.7	0.431	35.1	0.539	38
0.224	23.3	0.490	28.6	0.502	26.2	0.927	29.5	0.548	31.9	0.698	35.4
0.279	23.4	0.585	28.5	0.589	25.8	1.097	29.3	0.680	30.7	0.868	33.4
0.344	23.2	0.692	28.4	0.681	25.8			0.826	29.3	1.047	31
0.419	23.2	0.807	28.5	0.776	25.8			0.991	28.2	1.236	30.4
0.501	23.2	0.944	28.3	0.873	25.8			1.166	28	1.446	29.8
0.590	23.2							1.349	27.8	1.674	29
0.684	23.2							1.540	27.8	1.916	28.5
								1.736	27.7	2.169	28.5
										2.464	28.5

3.3. Quenching of pyrene by [CPC] in case of TX-100 in various mole fractions of β-CD at 298.15 K.

$\alpha_{\beta-CD}$= 0.2		$\alpha_{\beta-CD}$= 0.4		$\alpha_{\beta-CD}$= 0.5		$\alpha_{\beta-CD}$= 0.8		$\alpha_{\beta-CD}$= 1	
[CPC]/mM	ln(F_0/F)	[CPC]/mM	ln(F_0/F)	[CPC]/mM	ln(F_0/F)	[CPC]/mM	ln(F_0/F)	[CPC]/mM	ln(F_0/F)
0	0	0	0	0	0	0	0	0	0
0.003	0.062	0.003	0.044	0.003	0.025	0.003	0.019	0.003	0.020
0.007	0.129	0.007	0.096	0.007	0.067	0.007	0.049	0.007	0.046
0.015	0.217	0.015	0.171	0.015	0.126	0.015	0.101	0.015	0.080
0.025	0.345	0.025	0.269	0.025	0.194	0.025	0.160	0.025	0.119
0.037	0.477	0.037	0.379	0.037	0.280	0.037	0.227	0.037	0.177
0.052	0.639	0.052	0.512	0.052	0.380	0.052	0.319	0.052	0.236
0.069	0.815	0.069	0.660	0.069	0.500	0.069	0.413	0.069	0.307
0.088	0.992	0.088	0.817	0.088	0.618	0.088	0.523	0.088	0.395
0.110	1.180	0.110	0.979	0.110	0.763	0.110	0.640	0.110	0.469
0.134	1.383	0.134	1.158	0.134	0.907	0.134	0.755	0.134	0.562

3.4. Quenching of pyrene by [CPC] in case of TX-114 in various mole fractions of β-CD at 298.15 K.

$\alpha_{\beta-CD}$= 0.2		$\alpha_{\beta-CD}$= 0.4		$\alpha_{\beta-CD}$= 0.5		$\alpha_{\beta-CD}$= 0.8		$\alpha_{\beta-CD}$= 1	
[CPC]/mM	ln(F_0/F)	[CPC]/mM	ln(F_0/F)	[CPC]/mM	ln(F_0/F)	[CPC]/mM	ln(F_0/F)	[CPC]/mM	ln(F_0/F)
0	0	0	0	0	0	0	0	0	0
0.003	0.035	0.003	0.006	0.003	0.026	0.003	0.006	0.003	0.026
0.007	0.099	0.007	0.005	0.007	0.081	0.007	0.004	0.007	0.042

0.015	0.207	0.015	0.043	0.015	0.152	0.015	0.021	0.015	0.074
0.025	0.350	0.025	0.049	0.025	0.251	0.025	0.083	0.025	0.113
0.037	0.522	0.037	0.167	0.037	0.382	0.037	0.177	0.037	0.187
0.052	0.746	0.052	0.323	0.052	0.536	0.052	0.300	0.052	0.297
0.069	0.959	0.069	0.488	0.069	0.682	0.069	0.437	0.069	0.368
0.088	1.169	0.088	0.664	0.088	0.851	0.088	0.582	0.088	0.432
0.110	1.369	0.110	0.844	0.110	0.908	0.110	0.731	0.110	0.522
0.134	1.566	0.134	1.013	0.134	1.090	0.134	0.896	0.134	0.607
						0.160	1.054	0.160	0.704
						0.188	1.211	0.188	0.818
						0.218	1.356		

3.5. Absorbance of TX-100 with variation of its concentration in water at 298.15 K.

λ/nm	0.00 mM	0.02 mM	0.05 mM	0.07 mM	0.10 mM	0.12 mM	0.17 mM	0.22 mM	0.26 mM	0.31 mM	0.35 mM	0.39 mM	0.43 mM	0.48 mM	0.52 mM	0.56 mM
250	0	-0.003	-0.006	-0.012	-0.005	0.005	0.004	0.002	0.006	0.011	0.039	0.043	0.044	0.051	0.058	0.053
250.5	0.001	-0.002	-0.006	-0.012	-0.005	0.005	0.004	0.003	0.006	0.012	0.041	0.045	0.047	0.054	0.061	0.056
251	0.001	-0.002	-0.005	-0.012	-0.005	0.006	0.005	0.003	0.007	0.013	0.043	0.047	0.049	0.057	0.064	0.06
251.5	0.001	-0.002	-0.005	-0.011	-0.004	0.006	0.005	0.004	0.008	0.014	0.045	0.049	0.052	0.061	0.068	0.063
252	0.001	-0.002	-0.005	-0.011	-0.004	0.006	0.005	0.004	0.009	0.015	0.048	0.052	0.054	0.064	0.072	0.068
252.5	0.001	-0.002	-0.005	-0.011	-0.004	0.007	0.006	0.005	0.01	0.016	0.051	0.055	0.057	0.068	0.076	0.072
253	0.001	-0.002	-0.005	-0.011	-0.003	0.007	0.006	0.005	0.011	0.018	0.053	0.058	0.061	0.072	0.08	0.077
253.5	0.001	-0.002	-0.005	-0.011	-0.003	0.008	0.007	0.006	0.012	0.019	0.056	0.061	0.064	0.076	0.085	0.081
254	0.001	-0.002	-0.005	-0.01	-0.003	0.009	0.008	0.007	0.013	0.021	0.059	0.064	0.068	0.081	0.089	0.087
254.5	0.001	-0.002	-0.005	-0.01	-0.002	0.009	0.009	0.007	0.014	0.022	0.063	0.068	0.071	0.086	0.094	0.092
255	0.001	-0.002	-0.005	-0.01	-0.002	0.01	0.009	0.008	0.015	0.024	0.066	0.071	0.075	0.09	0.1	0.098
255.5	0.001	-0.002	-0.004	-0.01	-0.002	0.01	0.01	0.009	0.016	0.026	0.069	0.075	0.079	0.095	0.105	0.104
256	0.001	-0.001	-0.004	-0.009	-0.001	0.011	0.011	0.01	0.018	0.028	0.073	0.078	0.083	0.101	0.111	0.11
256.5	0.001	-0.001	-0.004	-0.009	-0.001	0.012	0.011	0.01	0.019	0.029	0.077	0.082	0.087	0.106	0.117	0.116
257	0.001	-0.001	-0.004	-0.009	0	0.012	0.012	0.011	0.02	0.031	0.08	0.086	0.091	0.111	0.122	0.122
257.5	0.001	-0.001	-0.004	-0.008	0	0.013	0.013	0.012	0.021	0.033	0.084	0.09	0.096	0.117	0.129	0.129
258	0.001	-0.001	-0.004	-0.008	0.001	0.014	0.014	0.013	0.023	0.035	0.088	0.094	0.101	0.123	0.135	0.136
258.5	0.001	-0.001	-0.003	-0.008	0.001	0.015	0.015	0.014	0.024	0.037	0.093	0.099	0.106	0.13	0.142	0.144
259	0.001	-0.001	-0.003	-0.007	0.002	0.016	0.016	0.015	0.026	0.04	0.098	0.104	0.111	0.137	0.15	0.152
259.5	0.001	-0.001	-0.003	-0.007	0.002	0.016	0.017	0.016	0.028	0.042	0.103	0.109	0.117	0.144	0.158	0.16
260	0.001	0	-0.003	-0.006	0.003	0.017	0.018	0.017	0.03	0.045	0.108	0.115	0.123	0.152	0.166	0.169
260.5	0.001	0	-0.003	-0.006	0.003	0.018	0.019	0.018	0.031	0.047	0.113	0.12	0.129	0.159	0.174	0.178
261	0.001	0	-0.002	-0.005	0.004	0.019	0.02	0.019	0.033	0.05	0.118	0.126	0.135	0.167	0.183	0.187
261.5	0.001	0	-0.002	-0.005	0.005	0.02	0.021	0.021	0.035	0.052	0.124	0.132	0.141	0.176	0.192	0.197
262	0.001	0	-0.002	-0.005	0.005	0.021	0.022	0.022	0.037	0.055	0.129	0.137	0.148	0.184	0.2	0.207

262.5	0.002	0	-0.002	-0.004	0.006	0.022	0.023	0.023	0.039	0.057	0.135	0.143	0.154	0.192	0.209	0.216
263	0.002	0.001	-0.001	-0.004	0.007	0.023	0.025	0.024	0.041	0.06	0.141	0.149	0.161	0.2	0.219	0.226
263.5	0.002	0.001	-0.001	-0.003	0.007	0.025	0.026	0.026	0.043	0.063	0.147	0.156	0.167	0.209	0.228	0.236
264	0.002	0.001	-0.001	-0.003	0.008	0.026	0.027	0.027	0.045	0.066	0.153	0.162	0.175	0.218	0.238	0.247
264.5	0.002	0.001	0	-0.002	0.009	0.027	0.028	0.028	0.047	0.07	0.159	0.169	0.182	0.227	0.247	0.257
265	0.002	0.001	0	-0.001	0.009	0.028	0.03	0.03	0.05	0.073	0.166	0.175	0.189	0.237	0.257	0.268
265.5	0.002	0.002	0	-0.001	0.01	0.029	0.031	0.031	0.052	0.076	0.172	0.182	0.196	0.246	0.268	0.279
266	0.002	0.002	0	0	0.011	0.03	0.033	0.033	0.054	0.079	0.179	0.189	0.204	0.255	0.278	0.29
266.5	0.002	0.002	0.001	0	0.012	0.031	0.034	0.034	0.056	0.082	0.185	0.195	0.211	0.265	0.288	0.302
267	0.002	0.002	0.001	0.001	0.012	0.033	0.035	0.036	0.058	0.085	0.191	0.202	0.218	0.274	0.298	0.313
267.5	0.002	0.002	0.001	0.001	0.013	0.034	0.036	0.037	0.061	0.088	0.198	0.208	0.225	0.283	0.308	0.324
268	0.002	0.003	0.002	0.002	0.014	0.035	0.038	0.038	0.063	0.091	0.203	0.215	0.232	0.292	0.318	0.334
268.5	0.002	0.003	0.002	0.003	0.014	0.036	0.039	0.039	0.065	0.094	0.209	0.221	0.239	0.302	0.328	0.345
269	0.003	0.003	0.002	0.003	0.015	0.037	0.04	0.041	0.067	0.096	0.215	0.226	0.245	0.31	0.337	0.355
269.5	0.003	0.003	0.002	0.003	0.016	0.038	0.041	0.042	0.069	0.099	0.22	0.231	0.25	0.318	0.345	0.364
270	0.003	0.003	0.003	0.004	0.016	0.039	0.042	0.043	0.07	0.101	0.225	0.236	0.256	0.325	0.354	0.373
270.5	0.003	0.003	0.003	0.004	0.016	0.04	0.043	0.044	0.072	0.103	0.229	0.241	0.261	0.332	0.361	0.382
271	0.003	0.004	0.003	0.004	0.017	0.04	0.044	0.045	0.074	0.105	0.234	0.246	0.266	0.339	0.369	0.39
271.5	0.003	0.004	0.003	0.005	0.018	0.041	0.045	0.046	0.075	0.108	0.239	0.251	0.272	0.346	0.376	0.399
272	0.003	0.004	0.003	0.005	0.018	0.042	0.046	0.047	0.077	0.11	0.244	0.256	0.277	0.353	0.384	0.407
272.5	0.003	0.004	0.004	0.006	0.019	0.043	0.047	0.048	0.079	0.112	0.248	0.261	0.282	0.36	0.392	0.415
273	0.003	0.004	0.004	0.006	0.019	0.044	0.048	0.049	0.08	0.115	0.253	0.266	0.287	0.367	0.399	0.423
273.5	0.003	0.004	0.004	0.007	0.02	0.045	0.049	0.05	0.082	0.117	0.258	0.27	0.292	0.374	0.407	0.432
274	0.003	0.005	0.004	0.007	0.02	0.046	0.05	0.051	0.083	0.119	0.262	0.275	0.297	0.38	0.414	0.44
274.5	0.003	0.005	0.004	0.007	0.021	0.046	0.051	0.052	0.085	0.121	0.266	0.278	0.301	0.386	0.421	0.447
275	0.003	0.005	0.005	0.007	0.021	0.047	0.051	0.052	0.086	0.122	0.269	0.281	0.305	0.391	0.426	0.453
275.5	0.003	0.005	0.005	0.008	0.021	0.047	0.052	0.053	0.087	0.123	0.271	0.283	0.307	0.395	0.431	0.458
276	0.003	0.005	0.005	0.008	0.021	0.047	0.052	0.053	0.087	0.123	0.272	0.284	0.308	0.398	0.434	0.461
276.5	0.003	0.005	0.005	0.007	0.021	0.047	0.051	0.052	0.087	0.123	0.272	0.284	0.307	0.4	0.435	0.463
277	0.003	0.005	0.004	0.007	0.021	0.046	0.051	0.052	0.087	0.121	0.271	0.282	0.305	0.399	0.434	0.462
277.5	0.003	0.004	0.004	0.007	0.02	0.045	0.05	0.051	0.086	0.12	0.268	0.279	0.302	0.397	0.431	0.459
278	0.003	0.004	0.004	0.006	0.02	0.045	0.049	0.05	0.084	0.117	0.265	0.274	0.297	0.393	0.427	0.454
278.5	0.003	0.004	0.004	0.006	0.019	0.043	0.048	0.048	0.083	0.115	0.26	0.269	0.292	0.388	0.42	0.447
279	0.003	0.004	0.003	0.005	0.019	0.042	0.046	0.047	0.081	0.112	0.255	0.264	0.286	0.381	0.413	0.439
279.5	0.003	0.004	0.003	0.005	0.018	0.041	0.045	0.046	0.079	0.109	0.25	0.258	0.28	0.374	0.405	0.429
280	0.003	0.004	0.003	0.005	0.017	0.04	0.044	0.045	0.078	0.106	0.245	0.253	0.274	0.366	0.396	0.419
280.5	0.003	0.004	0.003	0.004	0.017	0.039	0.043	0.044	0.076	0.104	0.24	0.248	0.268	0.358	0.388	0.409
281	0.003	0.003	0.003	0.004	0.016	0.039	0.042	0.043	0.074	0.103	0.235	0.244	0.264	0.35	0.38	0.4
281.5	0.003	0.003	0.002	0.004	0.016	0.038	0.042	0.042	0.073	0.101	0.232	0.24	0.26	0.344	0.372	0.392
282	0.003	0.003	0.002	0.003	0.016	0.038	0.041	0.042	0.072	0.1	0.228	0.237	0.256	0.338	0.366	0.385
282.5	0.003	0.003	0.002	0.003	0.015	0.037	0.04	0.041	0.07	0.098	0.225	0.234	0.252	0.333	0.36	0.378

283	0.002	0.003	0.002	0.003	0.015	0.036	0.039	0.04	0.068	0.096	0.22	0.229	0.247	0.328	0.354	0.371
283.5	0.002	0.003	0.002	0.002	0.014	0.035	0.038	0.038	0.067	0.093	0.215	0.223	0.24	0.322	0.347	0.363
284	0.002	0.003	0.001	0.001	0.013	0.033	0.036	0.036	0.064	0.088	0.208	0.214	0.232	0.314	0.338	0.353
284.5	0.002	0.002	0.001	0	0.012	0.031	0.033	0.033	0.061	0.082	0.198	0.203	0.219	0.303	0.326	0.339
285	0.002	0.002	0	-0.001	0.01	0.028	0.03	0.029	0.056	0.075	0.186	0.188	0.204	0.287	0.308	0.32
285.5	0.002	0.001	-0.001	-0.003	0.008	0.025	0.026	0.025	0.051	0.066	0.171	0.172	0.186	0.268	0.287	0.297
286	0.002	0.001	-0.002	-0.004	0.006	0.021	0.022	0.022	0.046	0.058	0.155	0.155	0.167	0.246	0.264	0.271
286.5	0.001	0	-0.003	-0.006	0.004	0.018	0.019	0.018	0.041	0.049	0.138	0.137	0.147	0.221	0.237	0.242
287	0.001	-0.001	-0.003	-0.007	0.002	0.015	0.015	0.014	0.035	0.041	0.12	0.118	0.127	0.193	0.208	0.21
287.5	0.001	-0.001	-0.004	-0.009	0	0.012	0.012	0.01	0.029	0.033	0.102	0.1	0.107	0.165	0.179	0.178
288	0.001	-0.001	-0.005	-0.01	-0.002	0.009	0.009	0.007	0.023	0.026	0.085	0.084	0.089	0.138	0.151	0.147
288.5	0.001	-0.002	-0.005	-0.011	-0.003	0.007	0.006	0.005	0.018	0.019	0.07	0.069	0.072	0.113	0.124	0.119
289	0.001	-0.002	-0.006	-0.012	-0.004	0.005	0.004	0.002	0.013	0.013	0.056	0.055	0.058	0.09	0.1	0.093
289.5	0	-0.002	-0.006	-0.013	-0.005	0.003	0.002	0	0.008	0.008	0.045	0.044	0.045	0.071	0.08	0.072
290	0	-0.003	-0.006	-0.013	-0.006	0.002	0	-0.002	0.005	0.005	0.035	0.035	0.035	0.056	0.063	0.054
290.5	0	-0.003	-0.007	-0.014	-0.007	0.001	-0.001	-0.003	0.002	0.001	0.027	0.028	0.027	0.045	0.049	0.04
291	0	-0.003	-0.007	-0.014	-0.008	0	-0.002	-0.004	0	-0.001	0.021	0.022	0.021	0.043	0.038	0.028
291.5	0	-0.003	-0.007	-0.015	-0.008	-0.001	-0.003	-0.005	-0.002	-0.003	0.016	0.017	0.015	0.042	0.029	0.019
292	0	-0.003	-0.007	-0.015	-0.009	-0.001	-0.004	-0.005	-0.004	-0.005	0.012	0.013	0.011	0.034	0.021	0.011
292.5	0	-0.003	-0.007	-0.015	-0.009	-0.002	-0.004	-0.006	-0.005	-0.006	0.009	0.01	0.008	0.028	0.016	0.006
293	0	-0.003	-0.007	-0.015	-0.009	-0.002	-0.005	-0.006	-0.006	-0.007	0.006	0.008	0.005	0.023	0.011	0.001
293.5	0	-0.003	-0.008	-0.016	-0.009	-0.002	-0.005	-0.007	-0.007	-0.008	0.004	0.006	0.003	0.019	0.008	-0.002
294	0	-0.003	-0.008	-0.016	-0.01	-0.003	-0.005	-0.007	-0.008	-0.009	0.003	0.005	0.001	0.017	0.005	-0.005
294.5	0	-0.003	-0.008	-0.016	-0.01	-0.003	-0.005	-0.007	-0.008	-0.009	0.002	0.004	0	0.014	0.003	-0.007
295	0	-0.003	-0.008	-0.016	-0.01	-0.003	-0.006	-0.008	-0.008	-0.01	0.001	0.003	-0.001	0.013	0.001	-0.009
295.5	0	-0.003	-0.008	-0.016	-0.01	-0.003	-0.006	-0.008	-0.009	-0.01	0	0.002	-0.002	0.011	0	-0.01
296	0	-0.003	-0.008	-0.016	-0.01	-0.003	-0.006	-0.008	-0.009	-0.01	0	0.001	-0.002	0.01	-0.001	-0.011
296.5	0	-0.003	-0.008	-0.016	-0.01	-0.003	-0.006	-0.008	-0.009	-0.01	-0.001	0.001	-0.003	0.009	-0.002	-0.012
297	0	-0.003	-0.008	-0.016	-0.01	-0.003	-0.006	-0.008	-0.009	-0.01	-0.001	0.001	-0.003	0.009	-0.003	-0.013
297.5	0	-0.003	-0.008	-0.016	-0.01	-0.004	-0.006	-0.008	-0.009	-0.011	-0.002	0	-0.004	0.008	-0.003	-0.013
298	0	-0.003	-0.008	-0.016	-0.01	-0.004	-0.006	-0.008	-0.01	-0.011	-0.002	0	-0.004	0.008	-0.003	-0.014
298.5	0	-0.004	-0.008	-0.016	-0.01	-0.004	-0.006	-0.008	-0.01	-0.011	-0.002	0	-0.004	0.007	-0.004	-0.014
299	0	-0.004	-0.008	-0.016	-0.01	-0.004	-0.006	-0.008	-0.01	-0.011	-0.002	0	-0.004	0.007	-0.004	-0.015
299.5	0	-0.003	-0.008	-0.016	-0.01	-0.004	-0.006	-0.008	-0.01	-0.011	-0.002	-0.001	-0.005	0.007	-0.004	-0.015
300	0	-0.003	-0.008	-0.016	-0.01	-0.004	-0.006	-0.008	-0.01	-0.011	-0.002	-0.001	-0.005	0.007	-0.005	-0.015

3.6. Absorbance of TX-114 with variation of its concentration in water at 298.15 K.

λ/nm	0.00 mM	0.02 mM	0.05 mM	0.07 mM	0.10 mM	0.12 mM	0.17 mM	0.22 mM	0.26 mM	0.31 mM	0.35 mM	0.39 mM	0.43 mM	0.48 mM	0.52 mM	0.56 mM
250	0.014	0.019	0.016	0.107	0.082	0.109	0.084	0.08	0.089	0.143	0.124	0.127	0.076	0.104	0.067	0.091
250.5	0.014	0.019	0.016	0.107	0.082	0.109	0.084	0.08	0.09	0.144	0.125	0.128	0.078	0.106	0.069	0.092
251	0.014	0.019	0.016	0.107	0.082	0.109	0.085	0.08	0.091	0.146	0.127	0.13	0.079	0.107	0.07	0.094
251.5	0.014	0.019	0.016	0.107	0.083	0.109	0.085	0.08	0.092	0.147	0.128	0.132	0.081	0.109	0.072	0.096
252	0.014	0.019	0.016	0.107	0.083	0.109	0.085	0.08	0.093	0.149	0.13	0.133	0.083	0.111	0.074	0.098
252.5	0.014	0.019	0.016	0.107	0.083	0.11	0.085	0.081	0.094	0.15	0.131	0.135	0.085	0.113	0.076	0.101
253	0.014	0.019	0.016	0.107	0.083	0.11	0.085	0.081	0.095	0.152	0.133	0.137	0.087	0.115	0.078	0.103
253.5	0.014	0.019	0.016	0.107	0.083	0.11	0.085	0.081	0.097	0.154	0.135	0.14	0.09	0.118	0.081	0.106
254	0.014	0.019	0.016	0.107	0.083	0.11	0.085	0.082	0.098	0.156	0.137	0.142	0.092	0.12	0.083	0.109
254.5	0.014	0.019	0.016	0.108	0.083	0.11	0.086	0.082	0.099	0.158	0.139	0.144	0.095	0.123	0.086	0.112
255	0.014	0.019	0.017	0.108	0.084	0.111	0.086	0.082	0.101	0.161	0.141	0.146	0.097	0.125	0.089	0.115
255.5	0.014	0.019	0.017	0.108	0.084	0.111	0.086	0.083	0.102	0.163	0.143	0.149	0.1	0.128	0.091	0.118
256	0.014	0.019	0.017	0.108	0.084	0.112	0.086	0.083	0.104	0.166	0.145	0.152	0.103	0.131	0.094	0.122
256.5	0.014	0.019	0.017	0.108	0.084	0.112	0.086	0.083	0.106	0.168	0.148	0.154	0.106	0.134	0.098	0.125
257	0.014	0.019	0.017	0.109	0.085	0.112	0.087	0.083	0.107	0.171	0.15	0.157	0.109	0.137	0.101	0.129
257.5	0.014	0.019	0.017	0.109	0.085	0.113	0.087	0.084	0.109	0.174	0.152	0.16	0.112	0.141	0.104	0.132
258	0.014	0.019	0.017	0.109	0.085	0.113	0.087	0.084	0.111	0.177	0.155	0.163	0.115	0.144	0.108	0.136
258.5	0.014	0.019	0.017	0.109	0.085	0.114	0.087	0.085	0.113	0.18	0.158	0.167	0.119	0.148	0.111	0.141
259	0.014	0.019	0.017	0.11	0.086	0.114	0.088	0.085	0.115	0.183	0.161	0.17	0.123	0.152	0.116	0.145
259.5	0.014	0.019	0.017	0.11	0.086	0.115	0.088	0.086	0.117	0.187	0.164	0.174	0.127	0.156	0.12	0.15
260	0.014	0.019	0.018	0.111	0.086	0.115	0.088	0.086	0.12	0.191	0.168	0.178	0.132	0.16	0.124	0.155
260.5	0.014	0.019	0.018	0.111	0.087	0.116	0.089	0.087	0.122	0.194	0.171	0.182	0.136	0.165	0.129	0.16
261	0.014	0.019	0.018	0.112	0.087	0.117	0.089	0.087	0.125	0.198	0.175	0.186	0.14	0.169	0.133	0.165
261.5	0.014	0.019	0.018	0.112	0.087	0.117	0.089	0.088	0.127	0.202	0.178	0.191	0.145	0.174	0.138	0.17
262	0.014	0.019	0.018	0.113	0.088	0.118	0.09	0.088	0.13	0.207	0.182	0.195	0.149	0.178	0.142	0.176
262.5	0.014	0.019	0.018	0.113	0.088	0.119	0.09	0.089	0.132	0.211	0.186	0.199	0.154	0.183	0.147	0.182
263	0.014	0.019	0.018	0.114	0.089	0.119	0.091	0.089	0.135	0.215	0.19	0.204	0.159	0.188	0.152	0.187
263.5	0.014	0.019	0.018	0.114	0.089	0.12	0.091	0.09	0.138	0.22	0.193	0.208	0.164	0.193	0.157	0.193
264	0.014	0.019	0.019	0.115	0.089	0.121	0.091	0.09	0.141	0.224	0.198	0.213	0.169	0.198	0.163	0.199
264.5	0.014	0.019	0.019	0.115	0.09	0.122	0.092	0.091	0.144	0.229	0.202	0.218	0.174	0.204	0.168	0.206
265	0.014	0.019	0.019	0.116	0.09	0.122	0.092	0.092	0.147	0.234	0.206	0.223	0.18	0.21	0.174	0.212
265.5	0.014	0.019	0.019	0.117	0.091	0.123	0.093	0.092	0.15	0.239	0.21	0.228	0.185	0.215	0.18	0.219
266	0.014	0.02	0.019	0.117	0.091	0.124	0.093	0.093	0.153	0.244	0.215	0.233	0.191	0.221	0.185	0.225
266.5	0.014	0.02	0.02	0.118	0.092	0.125	0.094	0.094	0.156	0.248	0.219	0.239	0.196	0.227	0.191	0.232
267	0.015	0.02	0.02	0.118	0.092	0.126	0.094	0.094	0.158	0.253	0.223	0.244	0.202	0.232	0.197	0.238

267.5	0.015	0.02	0.02	0.119	0.093	0.127	0.094	0.095	0.161	0.258	0.228	0.248	0.207	0.237	0.202	0.244
268	0.015	0.02	0.02	0.12	0.093	0.128	0.095	0.096	0.164	0.262	0.232	0.253	0.212	0.243	0.207	0.25
268.5	0.015	0.02	0.02	0.12	0.094	0.129	0.095	0.096	0.167	0.267	0.236	0.258	0.217	0.248	0.213	0.256
269	0.015	0.02	0.02	0.121	0.094	0.129	0.096	0.097	0.169	0.271	0.24	0.262	0.222	0.252	0.217	0.261
269.5	0.015	0.02	0.021	0.122	0.094	0.13	0.096	0.097	0.172	0.275	0.243	0.266	0.226	0.257	0.222	0.267
270	0.015	0.02	0.021	0.122	0.095	0.131	0.097	0.098	0.174	0.279	0.247	0.27	0.23	0.261	0.226	0.271
270.5	0.015	0.02	0.021	0.123	0.095	0.131	0.097	0.098	0.176	0.282	0.25	0.274	0.234	0.265	0.23	0.276
271	0.015	0.02	0.021	0.123	0.095	0.132	0.097	0.099	0.178	0.286	0.253	0.277	0.238	0.269	0.234	0.281
271.5	0.015	0.02	0.021	0.124	0.096	0.133	0.098	0.099	0.181	0.29	0.256	0.281	0.242	0.273	0.239	0.286
272	0.015	0.02	0.021	0.124	0.096	0.133	0.098	0.099	0.183	0.293	0.26	0.285	0.246	0.277	0.243	0.291
272.5	0.015	0.02	0.021	0.125	0.097	0.134	0.098	0.1	0.185	0.297	0.263	0.289	0.25	0.281	0.247	0.296
273	0.015	0.02	0.021	0.125	0.097	0.135	0.099	0.1	0.188	0.3	0.266	0.292	0.254	0.286	0.251	0.301
273.5	0.015	0.02	0.021	0.126	0.097	0.135	0.099	0.101	0.19	0.304	0.269	0.296	0.258	0.29	0.255	0.305
274	0.015	0.02	0.021	0.126	0.098	0.136	0.099	0.101	0.192	0.307	0.272	0.3	0.262	0.293	0.259	0.31
274.5	0.015	0.02	0.021	0.126	0.098	0.137	0.099	0.102	0.193	0.31	0.275	0.303	0.265	0.297	0.263	0.314
275	0.015	0.02	0.021	0.127	0.098	0.137	0.1	0.102	0.195	0.313	0.277	0.305	0.267	0.299	0.266	0.317
275.5	0.015	0.02	0.021	0.127	0.099	0.138	0.1	0.102	0.195	0.314	0.279	0.306	0.269	0.301	0.267	0.319
276	0.015	0.02	0.021	0.127	0.099	0.138	0.1	0.102	0.196	0.315	0.28	0.307	0.27	0.302	0.268	0.32
276.5	0.015	0.02	0.021	0.128	0.099	0.138	0.1	0.102	0.195	0.315	0.28	0.307	0.269	0.301	0.267	0.319
277	0.015	0.02	0.021	0.128	0.099	0.138	0.1	0.102	0.194	0.314	0.279	0.305	0.268	0.299	0.266	0.318
277.5	0.014	0.02	0.021	0.128	0.098	0.138	0.099	0.101	0.192	0.312	0.277	0.302	0.265	0.296	0.263	0.315
278	0.014	0.02	0.021	0.128	0.098	0.138	0.099	0.101	0.19	0.309	0.275	0.299	0.261	0.293	0.259	0.311
278.5	0.014	0.02	0.021	0.128	0.098	0.138	0.099	0.1	0.188	0.306	0.272	0.295	0.257	0.288	0.255	0.306
279	0.014	0.02	0.021	0.127	0.098	0.137	0.098	0.099	0.185	0.302	0.269	0.291	0.252	0.284	0.25	0.301
279.5	0.014	0.02	0.02	0.127	0.097	0.137	0.098	0.099	0.182	0.298	0.265	0.286	0.247	0.279	0.245	0.295
280	0.014	0.02	0.02	0.126	0.097	0.136	0.098	0.098	0.18	0.294	0.262	0.282	0.243	0.274	0.24	0.29
280.5	0.014	0.02	0.02	0.126	0.097	0.135	0.097	0.098	0.178	0.29	0.259	0.279	0.239	0.27	0.236	0.285
281	0.014	0.019	0.02	0.125	0.096	0.134	0.097	0.097	0.176	0.287	0.257	0.275	0.235	0.266	0.233	0.281
281.5	0.014	0.019	0.02	0.125	0.096	0.133	0.096	0.097	0.174	0.284	0.254	0.273	0.232	0.263	0.229	0.277
282	0.013	0.019	0.02	0.124	0.096	0.132	0.096	0.097	0.173	0.281	0.252	0.27	0.23	0.26	0.226	0.273
282.5	0.013	0.019	0.019	0.123	0.095	0.132	0.096	0.096	0.171	0.278	0.25	0.267	0.226	0.257	0.223	0.269
283	0.013	0.019	0.019	0.123	0.095	0.131	0.095	0.096	0.169	0.274	0.247	0.263	0.222	0.253	0.219	0.264
283.5	0.013	0.019	0.019	0.122	0.095	0.13	0.095	0.095	0.166	0.27	0.243	0.258	0.216	0.247	0.213	0.258
284	0.013	0.019	0.018	0.122	0.094	0.13	0.094	0.094	0.161	0.264	0.238	0.251	0.209	0.239	0.205	0.25
284.5	0.013	0.018	0.018	0.122	0.094	0.129	0.093	0.093	0.155	0.256	0.231	0.242	0.199	0.229	0.195	0.239
285	0.013	0.018	0.018	0.121	0.093	0.128	0.092	0.091	0.148	0.246	0.223	0.23	0.186	0.216	0.182	0.225
285.5	0.012	0.018	0.017	0.12	0.092	0.126	0.091	0.09	0.14	0.234	0.213	0.218	0.172	0.202	0.168	0.209
286	0.012	0.018	0.016	0.119	0.091	0.125	0.09	0.088	0.132	0.222	0.202	0.205	0.158	0.188	0.154	0.193
286.5	0.012	0.017	0.016	0.117	0.089	0.122	0.089	0.086	0.124	0.209	0.191	0.191	0.144	0.173	0.139	0.176
287	0.011	0.017	0.015	0.115	0.088	0.12	0.087	0.084	0.116	0.195	0.18	0.177	0.129	0.158	0.123	0.159
287.5	0.011	0.017	0.015	0.113	0.087	0.117	0.086	0.083	0.108	0.182	0.168	0.164	0.115	0.144	0.109	0.142

288	0.011	0.016	0.014	0.111	0.085	0.114	0.085	0.081	0.101	0.17	0.158	0.152	0.102	0.13	0.095	0.126
288.5	0.011	0.016	0.014	0.109	0.084	0.111	0.083	0.079	0.095	0.158	0.148	0.141	0.09	0.119	0.083	0.111
289	0.01	0.016	0.013	0.107	0.083	0.109	0.082	0.078	0.09	0.148	0.139	0.131	0.08	0.108	0.072	0.098
289.5	0.01	0.016	0.013	0.105	0.082	0.107	0.081	0.077	0.085	0.139	0.131	0.123	0.072	0.099	0.063	0.088
290	0.01	0.015	0.013	0.103	0.081	0.105	0.08	0.076	0.081	0.132	0.125	0.117	0.065	0.092	0.056	0.078
290.5	0.01	0.015	0.012	0.102	0.08	0.103	0.08	0.075	0.078	0.126	0.12	0.111	0.059	0.086	0.05	0.071
291	0.01	0.015	0.012	0.101	0.079	0.102	0.079	0.075	0.076	0.121	0.116	0.107	0.054	0.081	0.045	0.065
291.5	0.01	0.015	0.012	0.1	0.079	0.1	0.079	0.074	0.074	0.117	0.112	0.103	0.05	0.077	0.041	0.06
292	0.01	0.015	0.012	0.099	0.079	0.099	0.078	0.074	0.072	0.114	0.109	0.1	0.047	0.074	0.038	0.057
292.5	0.009	0.015	0.012	0.099	0.078	0.099	0.078	0.073	0.071	0.112	0.107	0.098	0.045	0.071	0.035	0.054
293	0.009	0.015	0.012	0.098	0.078	0.098	0.078	0.073	0.07	0.11	0.106	0.096	0.043	0.069	0.033	0.051
293.5	0.009	0.015	0.012	0.098	0.078	0.098	0.078	0.073	0.069	0.108	0.104	0.095	0.042	0.068	0.032	0.049
294	0.009	0.015	0.011	0.097	0.078	0.097	0.077	0.073	0.068	0.107	0.103	0.094	0.04	0.067	0.031	0.048
294.5	0.009	0.014	0.011	0.097	0.078	0.097	0.077	0.072	0.068	0.106	0.102	0.093	0.04	0.066	0.03	0.047
295	0.009	0.014	0.011	0.097	0.078	0.096	0.077	0.072	0.067	0.105	0.101	0.092	0.039	0.065	0.033	0.046
295.5	0.009	0.014	0.011	0.096	0.077	0.096	0.077	0.072	0.067	0.104	0.101	0.092	0.038	0.064	0.038	0.045
296	0.009	0.014	0.011	0.096	0.077	0.096	0.077	0.072	0.067	0.104	0.1	0.091	0.038	0.064	0.039	0.045
296.5	0.009	0.014	0.011	0.096	0.077	0.096	0.077	0.072	0.067	0.103	0.1	0.091	0.037	0.064	0.039	0.044
297	0.009	0.014	0.011	0.096	0.077	0.095	0.077	0.072	0.066	0.103	0.1	0.091	0.037	0.063	0.038	0.044
297.5	0.009	0.014	0.011	0.096	0.077	0.095	0.077	0.072	0.066	0.103	0.099	0.09	0.037	0.063	0.038	0.044
298	0.009	0.014	0.011	0.096	0.077	0.095	0.077	0.072	0.066	0.102	0.099	0.09	0.037	0.063	0.038	0.043
298.5	0.009	0.014	0.011	0.095	0.077	0.095	0.077	0.072	0.066	0.102	0.099	0.09	0.036	0.062	0.038	0.043
299	0.009	0.014	0.011	0.095	0.077	0.095	0.076	0.072	0.066	0.102	0.099	0.09	0.036	0.062	0.037	0.043
299.5	0.009	0.014	0.011	0.095	0.077	0.095	0.076	0.072	0.066	0.102	0.099	0.09	0.036	0.062	0.037	0.043
300	0.009	0.014	0.011	0.095	0.077	0.095	0.076	0.072	0.066	0.102	0.098	0.09	0.036	0.062	0.037	0.043

3.7. Absorbance of TX-100 with variation of concentration of β-CD in water at 298.15 K.

λ/nm	0.0 mM	1.5 mM	2.7 mM	3.7 mM	4.6 mM	5.3 mM	6.0 mM	6.6 mM	7.1 mM	8.0 mM
250	0.140	0.138	0.136	0.135	0.137	0.137	0.136	0.135	0.135	0.135
250.1	0.141	0.139	0.137	0.137	0.138	0.138	0.137	0.136	0.136	0.136
250.2	0.142	0.140	0.138	0.138	0.139	0.140	0.138	0.137	0.137	0.137
250.3	0.144	0.141	0.140	0.139	0.141	0.141	0.140	0.138	0.138	0.138
250.4	0.145	0.143	0.141	0.141	0.142	0.142	0.141	0.140	0.139	0.139
250.5	0.146	0.144	0.143	0.142	0.143	0.144	0.142	0.141	0.140	0.140
250.6	0.148	0.146	0.144	0.144	0.145	0.145	0.144	0.142	0.141	0.141
250.7	0.149	0.147	0.145	0.145	0.146	0.146	0.145	0.143	0.143	0.142
250.8	0.150	0.148	0.147	0.146	0.147	0.148	0.146	0.145	0.144	0.143

250.9	0.152	0.149	0.148	0.147	0.149	0.149	0.147	0.146	0.145	0.144
251	0.153	0.151	0.149	0.149	0.150	0.150	0.149	0.147	0.146	0.145
251.1	0.154	0.152	0.151	0.150	0.151	0.151	0.150	0.148	0.147	0.146
251.2	0.156	0.153	0.152	0.152	0.153	0.153	0.151	0.149	0.148	0.147
251.3	0.157	0.155	0.153	0.153	0.154	0.154	0.153	0.151	0.149	0.148
251.4	0.158	0.156	0.155	0.155	0.156	0.156	0.154	0.152	0.151	0.150
251.5	0.160	0.158	0.157	0.156	0.157	0.157	0.156	0.153	0.152	0.151
251.6	0.161	0.159	0.158	0.158	0.159	0.159	0.157	0.155	0.153	0.152
251.7	0.163	0.161	0.160	0.159	0.160	0.160	0.159	0.156	0.155	0.153
251.8	0.165	0.162	0.161	0.161	0.162	0.162	0.160	0.157	0.156	0.154
251.9	0.166	0.164	0.163	0.162	0.164	0.163	0.161	0.159	0.157	0.155
252	0.168	0.166	0.164	0.164	0.165	0.165	0.163	0.160	0.158	0.157
252.1	0.169	0.167	0.166	0.166	0.167	0.167	0.164	0.162	0.160	0.158
252.2	0.171	0.169	0.168	0.167	0.168	0.168	0.166	0.163	0.161	0.159
252.3	0.173	0.170	0.169	0.169	0.170	0.170	0.168	0.165	0.163	0.160
252.4	0.174	0.172	0.171	0.170	0.172	0.171	0.169	0.166	0.164	0.162
252.5	0.176	0.174	0.172	0.172	0.173	0.173	0.171	0.167	0.165	0.163
252.6	0.177	0.175	0.174	0.173	0.175	0.174	0.172	0.169	0.167	0.164
252.7	0.179	0.177	0.176	0.175	0.176	0.176	0.173	0.170	0.168	0.165
252.8	0.180	0.178	0.177	0.177	0.178	0.177	0.175	0.171	0.169	0.167
252.9	0.182	0.180	0.179	0.178	0.180	0.179	0.176	0.173	0.171	0.168
253	0.184	0.182	0.181	0.180	0.181	0.180	0.178	0.174	0.172	0.169
253.1	0.185	0.184	0.182	0.182	0.183	0.182	0.180	0.176	0.174	0.171
253.2	0.187	0.185	0.184	0.184	0.185	0.184	0.181	0.177	0.175	0.172
253.3	0.189	0.187	0.186	0.185	0.187	0.186	0.183	0.179	0.177	0.173
253.4	0.191	0.189	0.188	0.187	0.188	0.187	0.185	0.181	0.178	0.175
253.5	0.192	0.191	0.190	0.189	0.190	0.189	0.186	0.182	0.180	0.176
253.6	0.194	0.193	0.192	0.191	0.192	0.191	0.188	0.184	0.181	0.178
253.7	0.196	0.195	0.193	0.193	0.194	0.193	0.190	0.185	0.183	0.179
253.8	0.198	0.196	0.195	0.195	0.196	0.194	0.192	0.187	0.184	0.180
253.9	0.200	0.198	0.197	0.197	0.198	0.196	0.194	0.189	0.186	0.182
254	0.202	0.200	0.199	0.199	0.200	0.198	0.195	0.190	0.188	0.183
254.1	0.204	0.202	0.201	0.201	0.202	0.200	0.197	0.192	0.189	0.185
254.2	0.206	0.204	0.203	0.202	0.203	0.201	0.199	0.194	0.191	0.186
254.3	0.207	0.206	0.205	0.204	0.205	0.203	0.201	0.195	0.192	0.188
254.4	0.209	0.208	0.206	0.206	0.207	0.205	0.202	0.197	0.194	0.189
254.5	0.211	0.210	0.208	0.208	0.209	0.206	0.204	0.198	0.195	0.190
254.6	0.213	0.212	0.210	0.210	0.211	0.208	0.206	0.200	0.197	0.192
254.7	0.215	0.214	0.212	0.212	0.213	0.210	0.208	0.202	0.199	0.193
254.8	0.217	0.216	0.214	0.214	0.215	0.212	0.210	0.204	0.200	0.195
254.9	0.219	0.218	0.216	0.216	0.217	0.214	0.212	0.205	0.202	0.197

255	0.221	0.220	0.219	0.218	0.219	0.216	0.214	0.207	0.204	0.198
255.1	0.223	0.222	0.221	0.220	0.221	0.218	0.216	0.209	0.206	0.200
255.2	0.225	0.224	0.223	0.222	0.223	0.220	0.218	0.211	0.208	0.201
255.3	0.228	0.227	0.225	0.225	0.225	0.223	0.220	0.213	0.209	0.203
255.4	0.230	0.229	0.227	0.227	0.228	0.225	0.222	0.215	0.211	0.205
255.5	0.232	0.231	0.230	0.229	0.230	0.227	0.224	0.217	0.213	0.206
255.6	0.235	0.233	0.232	0.231	0.232	0.229	0.226	0.219	0.215	0.208
255.7	0.237	0.236	0.234	0.234	0.235	0.231	0.228	0.221	0.217	0.210
255.8	0.239	0.238	0.236	0.236	0.237	0.233	0.230	0.223	0.219	0.212
255.9	0.242	0.240	0.239	0.238	0.239	0.236	0.232	0.225	0.221	0.213
256	0.244	0.243	0.241	0.240	0.241	0.238	0.234	0.227	0.222	0.215
256.1	0.246	0.245	0.243	0.243	0.243	0.240	0.236	0.229	0.224	0.216
256.2	0.248	0.247	0.245	0.245	0.245	0.242	0.238	0.230	0.226	0.218
256.3	0.250	0.249	0.247	0.247	0.248	0.244	0.240	0.232	0.228	0.220
256.4	0.252	0.251	0.249	0.249	0.250	0.246	0.242	0.234	0.230	0.221
256.5	0.254	0.254	0.252	0.252	0.252	0.248	0.244	0.236	0.232	0.223
256.6	0.257	0.256	0.254	0.254	0.255	0.251	0.247	0.238	0.234	0.225
256.7	0.259	0.259	0.257	0.256	0.257	0.253	0.249	0.241	0.236	0.227
256.8	0.262	0.261	0.259	0.259	0.260	0.256	0.251	0.243	0.238	0.229
256.9	0.264	0.264	0.262	0.262	0.262	0.258	0.254	0.245	0.240	0.231
257	0.267	0.266	0.264	0.264	0.265	0.260	0.256	0.247	0.242	0.233
257.1	0.269	0.269	0.267	0.267	0.267	0.263	0.259	0.250	0.244	0.235
257.2	0.272	0.272	0.269	0.269	0.270	0.266	0.261	0.252	0.247	0.237
257.3	0.275	0.274	0.272	0.272	0.272	0.268	0.264	0.254	0.249	0.239
257.4	0.277	0.277	0.275	0.275	0.275	0.271	0.266	0.257	0.251	0.241
257.5	0.280	0.280	0.277	0.277	0.278	0.273	0.269	0.259	0.253	0.243
257.6	0.283	0.282	0.280	0.280	0.280	0.276	0.271	0.261	0.256	0.245
257.7	0.286	0.285	0.283	0.283	0.283	0.279	0.274	0.264	0.258	0.247
257.8	0.288	0.288	0.286	0.285	0.286	0.282	0.277	0.267	0.261	0.250
257.9	0.291	0.291	0.288	0.288	0.288	0.284	0.279	0.269	0.263	0.252
258	0.294	0.293	0.291	0.290	0.291	0.287	0.282	0.271	0.265	0.254
258.1	0.296	0.296	0.293	0.293	0.293	0.289	0.284	0.274	0.267	0.256
258.2	0.299	0.298	0.296	0.295	0.296	0.292	0.287	0.276	0.269	0.258
258.3	0.301	0.301	0.298	0.298	0.298	0.295	0.289	0.278	0.272	0.260
258.4	0.304	0.304	0.301	0.301	0.301	0.298	0.292	0.281	0.274	0.262
258.5	0.307	0.307	0.304	0.304	0.304	0.301	0.295	0.284	0.277	0.264
258.6	0.310	0.310	0.307	0.306	0.307	0.304	0.298	0.286	0.279	0.267
258.7	0.313	0.313	0.310	0.310	0.310	0.307	0.301	0.289	0.282	0.269
258.8	0.316	0.316	0.313	0.313	0.313	0.310	0.304	0.292	0.284	0.272
258.9	0.319	0.319	0.316	0.316	0.316	0.313	0.307	0.295	0.287	0.274
259	0.322	0.322	0.320	0.319	0.319	0.316	0.310	0.298	0.290	0.277

259.1	0.325	0.325	0.323	0.322	0.322	0.319	0.313	0.300	0.292	0.279
259.2	0.328	0.328	0.326	0.325	0.325	0.322	0.316	0.303	0.295	0.281
259.3	0.331	0.331	0.329	0.328	0.328	0.325	0.319	0.306	0.297	0.284
259.4	0.334	0.334	0.332	0.331	0.331	0.329	0.322	0.309	0.300	0.286
259.5	0.338	0.337	0.336	0.335	0.335	0.332	0.325	0.312	0.303	0.289
259.6	0.341	0.341	0.339	0.338	0.338	0.335	0.328	0.315	0.306	0.291
259.7	0.344	0.344	0.343	0.341	0.341	0.338	0.331	0.318	0.309	0.294
259.8	0.347	0.347	0.346	0.345	0.344	0.342	0.334	0.321	0.311	0.297
259.9	0.351	0.350	0.349	0.348	0.347	0.345	0.337	0.324	0.314	0.299
260	0.354	0.353	0.352	0.351	0.350	0.348	0.340	0.327	0.316	0.301
260.1	0.357	0.357	0.355	0.354	0.353	0.351	0.342	0.329	0.319	0.304
260.2	0.360	0.360	0.358	0.357	0.356	0.354	0.345	0.332	0.322	0.306
260.3	0.363	0.363	0.362	0.361	0.360	0.356	0.348	0.335	0.324	0.308
260.4	0.366	0.366	0.365	0.364	0.363	0.360	0.351	0.338	0.327	0.311
260.5	0.370	0.370	0.368	0.367	0.366	0.363	0.354	0.341	0.330	0.314
260.6	0.373	0.373	0.372	0.371	0.370	0.366	0.357	0.344	0.333	0.316
260.7	0.377	0.377	0.376	0.375	0.373	0.369	0.361	0.347	0.336	0.319
260.8	0.380	0.380	0.379	0.378	0.377	0.373	0.364	0.350	0.339	0.322
260.9	0.384	0.384	0.383	0.382	0.380	0.376	0.367	0.352	0.341	0.324
261	0.387	0.387	0.386	0.385	0.384	0.379	0.370	0.355	0.344	0.327
261.1	0.391	0.391	0.390	0.389	0.387	0.382	0.373	0.358	0.347	0.329
261.2	0.395	0.394	0.394	0.392	0.390	0.386	0.376	0.362	0.350	0.332
261.3	0.398	0.398	0.397	0.396	0.394	0.389	0.380	0.365	0.353	0.335
261.4	0.402	0.402	0.401	0.400	0.398	0.392	0.383	0.368	0.356	0.337
261.5	0.406	0.405	0.405	0.403	0.401	0.396	0.386	0.371	0.359	0.340
261.6	0.410	0.409	0.409	0.407	0.405	0.399	0.389	0.374	0.362	0.343
261.7	0.413	0.413	0.412	0.411	0.408	0.403	0.393	0.377	0.365	0.346
261.8	0.417	0.416	0.416	0.414	0.412	0.406	0.396	0.380	0.368	0.349
261.9	0.421	0.420	0.420	0.418	0.416	0.410	0.399	0.383	0.371	0.351
262	0.424	0.424	0.423	0.422	0.419	0.413	0.403	0.386	0.374	0.354
262.1	0.428	0.427	0.427	0.425	0.422	0.416	0.406	0.389	0.377	0.356
262.2	0.431	0.431	0.430	0.428	0.426	0.419	0.409	0.392	0.380	0.359
262.3	0.435	0.434	0.433	0.432	0.429	0.422	0.412	0.394	0.382	0.361
262.4	0.438	0.437	0.437	0.435	0.432	0.425	0.415	0.397	0.385	0.364
262.5	0.442	0.441	0.440	0.439	0.436	0.429	0.418	0.400	0.388	0.367
262.6	0.446	0.445	0.444	0.443	0.440	0.432	0.422	0.404	0.391	0.369
262.7	0.449	0.448	0.448	0.446	0.443	0.436	0.425	0.407	0.394	0.372
262.8	0.453	0.452	0.452	0.450	0.447	0.440	0.429	0.410	0.397	0.375
262.9	0.457	0.456	0.456	0.454	0.451	0.443	0.432	0.413	0.401	0.378
263	0.461	0.460	0.460	0.458	0.455	0.447	0.436	0.417	0.404	0.381
263.1	0.465	0.464	0.464	0.462	0.459	0.450	0.439	0.420	0.407	0.384

263.2	0.469	0.468	0.468	0.466	0.462	0.454	0.443	0.423	0.410	0.387
263.3	0.472	0.472	0.471	0.470	0.466	0.458	0.447	0.426	0.413	0.390
263.4	0.476	0.476	0.475	0.473	0.470	0.461	0.450	0.430	0.416	0.393
263.5	0.480	0.480	0.479	0.477	0.474	0.465	0.454	0.433	0.419	0.396
263.6	0.484	0.484	0.483	0.481	0.478	0.469	0.458	0.437	0.423	0.399
263.7	0.488	0.488	0.487	0.485	0.482	0.473	0.461	0.440	0.426	0.402
263.8	0.492	0.492	0.491	0.489	0.486	0.477	0.465	0.444	0.429	0.405
263.9	0.496	0.496	0.495	0.493	0.490	0.481	0.469	0.447	0.433	0.408
264	0.500	0.500	0.499	0.498	0.494	0.485	0.473	0.451	0.436	0.411
264.1	0.504	0.504	0.504	0.501	0.498	0.488	0.477	0.454	0.440	0.414
264.2	0.509	0.508	0.508	0.506	0.502	0.492	0.481	0.458	0.443	0.417
264.3	0.513	0.512	0.511	0.510	0.506	0.496	0.484	0.462	0.446	0.420
264.4	0.516	0.516	0.515	0.513	0.510	0.500	0.488	0.465	0.450	0.423
264.5	0.520	0.520	0.519	0.517	0.514	0.504	0.492	0.469	0.453	0.426
264.6	0.524	0.525	0.523	0.521	0.518	0.508	0.495	0.472	0.456	0.429
264.7	0.528	0.529	0.527	0.525	0.522	0.512	0.499	0.476	0.460	0.432
264.8	0.533	0.533	0.531	0.529	0.526	0.515	0.503	0.479	0.463	0.435
264.9	0.537	0.537	0.535	0.533	0.530	0.520	0.507	0.484	0.467	0.439
265	0.542	0.542	0.539	0.538	0.535	0.524	0.512	0.488	0.471	0.442
265.1	0.546	0.546	0.544	0.542	0.539	0.528	0.516	0.492	0.475	0.446
265.2	0.551	0.551	0.548	0.547	0.544	0.533	0.520	0.496	0.479	0.449
265.3	0.556	0.556	0.553	0.551	0.548	0.537	0.524	0.500	0.483	0.453
265.4	0.560	0.560	0.557	0.556	0.552	0.541	0.529	0.504	0.487	0.456
265.5	0.565	0.565	0.561	0.560	0.557	0.546	0.533	0.508	0.491	0.460
265.6	0.569	0.570	0.566	0.565	0.562	0.550	0.537	0.513	0.495	0.464
265.7	0.574	0.574	0.571	0.569	0.566	0.555	0.542	0.517	0.499	0.468
265.8	0.579	0.579	0.575	0.574	0.571	0.559	0.546	0.521	0.503	0.472
265.9	0.584	0.584	0.580	0.579	0.576	0.564	0.551	0.525	0.507	0.475
266	0.588	0.589	0.585	0.583	0.580	0.568	0.555	0.529	0.511	0.479
266.1	0.593	0.594	0.590	0.588	0.585	0.573	0.560	0.534	0.515	0.483
266.2	0.598	0.598	0.594	0.592	0.589	0.577	0.564	0.538	0.519	0.487
266.3	0.603	0.603	0.599	0.597	0.594	0.582	0.568	0.542	0.523	0.490
266.4	0.607	0.608	0.604	0.602	0.599	0.586	0.572	0.546	0.527	0.494
266.5	0.612	0.613	0.609	0.606	0.603	0.591	0.577	0.551	0.531	0.498
266.6	0.617	0.618	0.613	0.611	0.608	0.595	0.581	0.555	0.535	0.502
266.7	0.622	0.623	0.618	0.616	0.613	0.600	0.585	0.559	0.540	0.506
266.8	0.627	0.628	0.623	0.621	0.617	0.604	0.590	0.563	0.544	0.509
266.9	0.632	0.632	0.628	0.625	0.621	0.608	0.594	0.567	0.547	0.513
267	0.636	0.636	0.632	0.629	0.626	0.612	0.598	0.571	0.551	0.517
267.1	0.641	0.641	0.636	0.634	0.630	0.616	0.601	0.575	0.555	0.520
267.2	0.645	0.645	0.641	0.638	0.633	0.620	0.605	0.579	0.558	0.523

267.3	0.649	0.649	0.645	0.642	0.637	0.624	0.609	0.582	0.562	0.527
267.4	0.653	0.653	0.649	0.646	0.641	0.628	0.613	0.586	0.565	0.530
267.5	0.658	0.658	0.654	0.651	0.645	0.632	0.617	0.590	0.569	0.533
267.6	0.662	0.663	0.658	0.655	0.650	0.636	0.621	0.594	0.573	0.537
267.7	0.667	0.667	0.663	0.660	0.654	0.640	0.625	0.598	0.576	0.540
267.8	0.671	0.672	0.668	0.665	0.658	0.644	0.629	0.602	0.580	0.544
267.9	0.676	0.676	0.672	0.669	0.663	0.648	0.633	0.605	0.583	0.547
268	0.680	0.680	0.677	0.674	0.667	0.653	0.636	0.609	0.587	0.550
268.1	0.685	0.685	0.682	0.678	0.671	0.656	0.640	0.613	0.590	0.553
268.2	0.689	0.689	0.686	0.682	0.675	0.660	0.644	0.616	0.593	0.556
268.3	0.693	0.693	0.690	0.687	0.679	0.664	0.647	0.620	0.596	0.559
268.4	0.697	0.698	0.695	0.691	0.683	0.668	0.651	0.623	0.600	0.562
268.5	0.701	0.702	0.699	0.695	0.686	0.672	0.654	0.627	0.603	0.565
268.6	0.706	0.706	0.704	0.699	0.690	0.675	0.657	0.630	0.606	0.568
268.7	0.710	0.710	0.708	0.703	0.694	0.679	0.661	0.633	0.609	0.571
268.8	0.714	0.714	0.712	0.708	0.698	0.682	0.664	0.636	0.612	0.574
268.9	0.718	0.719	0.717	0.712	0.702	0.686	0.667	0.640	0.615	0.576
269	0.722	0.723	0.721	0.716	0.706	0.690	0.671	0.643	0.617	0.579
269.1	0.726	0.727	0.725	0.720	0.709	0.693	0.674	0.646	0.620	0.582
269.2	0.730	0.731	0.729	0.724	0.713	0.697	0.677	0.649	0.623	0.584
269.3	0.734	0.735	0.733	0.728	0.717	0.700	0.680	0.652	0.626	0.587
269.4	0.738	0.739	0.737	0.732	0.721	0.704	0.683	0.655	0.629	0.590
269.5	0.742	0.743	0.741	0.736	0.724	0.707	0.686	0.658	0.632	0.592
269.6	0.746	0.747	0.745	0.740	0.728	0.710	0.689	0.661	0.635	0.595
269.7	0.750	0.751	0.749	0.744	0.732	0.714	0.693	0.663	0.637	0.597
269.8	0.754	0.754	0.753	0.747	0.735	0.717	0.695	0.666	0.640	0.600
269.9	0.757	0.758	0.756	0.751	0.739	0.720	0.698	0.669	0.643	0.602
270	0.761	0.761	0.760	0.754	0.742	0.723	0.701	0.671	0.645	0.604
270.1	0.764	0.765	0.763	0.758	0.745	0.726	0.704	0.674	0.647	0.606
270.2	0.768	0.768	0.767	0.761	0.748	0.729	0.707	0.676	0.650	0.609
270.3	0.771	0.772	0.770	0.765	0.752	0.732	0.710	0.679	0.653	0.611
270.4	0.775	0.775	0.774	0.768	0.755	0.735	0.713	0.682	0.655	0.613
270.5	0.778	0.778	0.778	0.772	0.758	0.738	0.716	0.685	0.658	0.616
270.6	0.782	0.782	0.781	0.775	0.762	0.741	0.719	0.688	0.661	0.618
270.7	0.786	0.785	0.785	0.779	0.765	0.744	0.722	0.691	0.663	0.620
270.8	0.789	0.789	0.788	0.782	0.769	0.748	0.726	0.694	0.666	0.623
270.9	0.793	0.793	0.792	0.786	0.772	0.751	0.729	0.696	0.669	0.625
271	0.796	0.797	0.795	0.789	0.776	0.754	0.732	0.699	0.672	0.628
271.1	0.800	0.800	0.799	0.793	0.779	0.758	0.735	0.702	0.675	0.630
271.2	0.803	0.804	0.803	0.797	0.783	0.761	0.739	0.705	0.677	0.633
271.3	0.807	0.807	0.806	0.800	0.786	0.765	0.742	0.708	0.680	0.636

271.4	0.810	0.811	0.810	0.803	0.790	0.768	0.745	0.711	0.683	0.638
271.5	0.814	0.814	0.813	0.807	0.793	0.771	0.748	0.714	0.686	0.641
271.6	0.817	0.818	0.817	0.811	0.797	0.774	0.752	0.718	0.689	0.644
271.7	0.821	0.822	0.821	0.814	0.801	0.778	0.755	0.721	0.692	0.646
271.8	0.825	0.825	0.824	0.818	0.804	0.781	0.759	0.724	0.695	0.649
271.9	0.828	0.829	0.828	0.822	0.808	0.785	0.762	0.727	0.698	0.652
272	0.832	0.833	0.832	0.826	0.812	0.788	0.766	0.730	0.701	0.655
272.1	0.836	0.836	0.835	0.830	0.815	0.792	0.769	0.734	0.705	0.658
272.2	0.840	0.840	0.839	0.833	0.819	0.795	0.773	0.737	0.708	0.661
272.3	0.843	0.844	0.843	0.837	0.823	0.799	0.776	0.740	0.711	0.664
272.4	0.847	0.848	0.847	0.841	0.826	0.802	0.780	0.744	0.714	0.667
272.5	0.851	0.851	0.850	0.844	0.830	0.806	0.784	0.747	0.717	0.670
272.6	0.855	0.855	0.854	0.848	0.834	0.810	0.787	0.751	0.721	0.673
272.7	0.858	0.859	0.858	0.851	0.838	0.813	0.791	0.754	0.724	0.676
272.8	0.862	0.862	0.862	0.855	0.841	0.817	0.795	0.758	0.728	0.679
272.9	0.865	0.866	0.865	0.859	0.845	0.821	0.798	0.761	0.731	0.682
273	0.869	0.870	0.869	0.862	0.848	0.824	0.802	0.765	0.734	0.685
273.1	0.872	0.873	0.872	0.865	0.852	0.827	0.805	0.768	0.737	0.688
273.2	0.876	0.876	0.875	0.868	0.855	0.831	0.808	0.771	0.740	0.691
273.3	0.879	0.880	0.878	0.871	0.858	0.834	0.811	0.774	0.743	0.694
273.4	0.883	0.883	0.882	0.875	0.861	0.837	0.814	0.777	0.746	0.696
273.5	0.886	0.887	0.885	0.878	0.865	0.840	0.817	0.781	0.749	0.699
273.6	0.890	0.890	0.888	0.882	0.868	0.843	0.820	0.784	0.752	0.702
273.7	0.893	0.894	0.892	0.885	0.871	0.846	0.823	0.787	0.755	0.705
273.8	0.897	0.898	0.895	0.889	0.874	0.849	0.827	0.790	0.759	0.708
273.9	0.901	0.901	0.898	0.892	0.877	0.852	0.830	0.793	0.762	0.711
274	0.904	0.904	0.902	0.895	0.880	0.855	0.833	0.796	0.765	0.714
274.1	0.907	0.908	0.905	0.898	0.883	0.858	0.835	0.799	0.768	0.717
274.2	0.910	0.911	0.908	0.901	0.886	0.860	0.838	0.802	0.771	0.719
274.3	0.914	0.914	0.911	0.904	0.889	0.863	0.841	0.805	0.773	0.722
274.4	0.917	0.918	0.914	0.907	0.891	0.865	0.843	0.808	0.776	0.725
274.5	0.920	0.921	0.917	0.910	0.894	0.867	0.845	0.810	0.778	0.727
274.6	0.923	0.924	0.920	0.912	0.896	0.869	0.847	0.813	0.781	0.729
274.7	0.925	0.926	0.922	0.915	0.898	0.871	0.849	0.815	0.783	0.731
274.8	0.928	0.929	0.925	0.917	0.901	0.873	0.851	0.817	0.785	0.734
274.9	0.931	0.931	0.927	0.920	0.903	0.875	0.852	0.819	0.787	0.736
275	0.933	0.934	0.930	0.922	0.904	0.876	0.854	0.821	0.789	0.738
275.1	0.936	0.936	0.932	0.924	0.906	0.877	0.855	0.823	0.790	0.739
275.2	0.938	0.938	0.934	0.926	0.907	0.878	0.856	0.824	0.792	0.741
275.3	0.940	0.940	0.936	0.928	0.908	0.878	0.857	0.825	0.793	0.743
275.4	0.942	0.942	0.938	0.930	0.909	0.879	0.857	0.826	0.794	0.744

275.5	0.943	0.943	0.939	0.931	0.910	0.879	0.857	0.827	0.795	0.745
275.6	0.945	0.945	0.941	0.932	0.911	0.880	0.858	0.827	0.796	0.745
275.7	0.946	0.946	0.942	0.934	0.911	0.880	0.857	0.828	0.796	0.746
275.8	0.947	0.947	0.943	0.934	0.912	0.879	0.857	0.828	0.797	0.747
275.9	0.948	0.948	0.944	0.935	0.912	0.879	0.856	0.828	0.797	0.747
276	0.949	0.949	0.945	0.936	0.912	0.878	0.856	0.828	0.797	0.747
276.1	0.950	0.950	0.945	0.936	0.912	0.877	0.855	0.827	0.796	0.747
276.2	0.950	0.950	0.946	0.937	0.911	0.876	0.853	0.826	0.795	0.746
276.3	0.951	0.950	0.946	0.936	0.911	0.874	0.852	0.826	0.794	0.746
276.4	0.951	0.950	0.946	0.936	0.910	0.873	0.850	0.824	0.793	0.745
276.5	0.951	0.950	0.946	0.936	0.909	0.871	0.848	0.823	0.792	0.744
276.6	0.950	0.950	0.946	0.935	0.908	0.869	0.846	0.821	0.790	0.743
276.7	0.950	0.950	0.946	0.934	0.906	0.867	0.844	0.819	0.789	0.741
276.8	0.949	0.949	0.945	0.933	0.905	0.865	0.841	0.817	0.787	0.740
276.9	0.948	0.948	0.944	0.933	0.903	0.862	0.838	0.814	0.784	0.738
277	0.947	0.947	0.943	0.931	0.901	0.859	0.835	0.811	0.782	0.735
277.1	0.946	0.945	0.942	0.930	0.899	0.856	0.832	0.808	0.779	0.733
277.2	0.944	0.944	0.940	0.928	0.896	0.853	0.828	0.805	0.776	0.730
277.3	0.943	0.942	0.939	0.926	0.893	0.850	0.824	0.801	0.773	0.727
277.4	0.941	0.940	0.937	0.924	0.891	0.846	0.820	0.797	0.770	0.723
277.5	0.939	0.938	0.935	0.921	0.888	0.842	0.816	0.793	0.766	0.720
277.6	0.937	0.935	0.932	0.919	0.884	0.838	0.812	0.789	0.762	0.716
277.7	0.934	0.933	0.930	0.916	0.881	0.834	0.807	0.785	0.758	0.712
277.8	0.931	0.930	0.927	0.913	0.877	0.830	0.803	0.781	0.753	0.708
277.9	0.928	0.927	0.924	0.910	0.874	0.825	0.799	0.776	0.749	0.704
278	0.925	0.923	0.920	0.906	0.870	0.821	0.794	0.772	0.744	0.700
278.1	0.921	0.920	0.917	0.903	0.866	0.817	0.790	0.767	0.739	0.695
278.2	0.918	0.916	0.913	0.899	0.862	0.813	0.785	0.762	0.734	0.690
278.3	0.914	0.912	0.909	0.895	0.857	0.808	0.781	0.758	0.729	0.686
278.4	0.910	0.908	0.905	0.891	0.853	0.804	0.776	0.753	0.724	0.681
278.5	0.906	0.904	0.901	0.887	0.849	0.800	0.772	0.748	0.719	0.676
278.6	0.902	0.899	0.896	0.883	0.844	0.795	0.767	0.743	0.714	0.671
278.7	0.897	0.895	0.891	0.878	0.840	0.791	0.763	0.739	0.710	0.666
278.8	0.892	0.890	0.887	0.873	0.836	0.787	0.759	0.734	0.705	0.661
278.9	0.888	0.886	0.882	0.869	0.831	0.783	0.754	0.729	0.699	0.656
279	0.883	0.881	0.877	0.864	0.827	0.778	0.750	0.724	0.695	0.651
279.1	0.878	0.876	0.872	0.859	0.822	0.774	0.746	0.719	0.690	0.647
279.2	0.872	0.871	0.866	0.854	0.818	0.771	0.742	0.715	0.685	0.642
279.3	0.867	0.865	0.861	0.849	0.813	0.767	0.738	0.711	0.680	0.637
279.4	0.862	0.860	0.856	0.844	0.809	0.763	0.734	0.706	0.676	0.633
279.5	0.857	0.855	0.851	0.839	0.804	0.760	0.731	0.702	0.672	0.629

279.6	0.852	0.850	0.845	0.834	0.800	0.756	0.727	0.698	0.668	0.625
279.7	0.847	0.846	0.841	0.830	0.796	0.753	0.724	0.695	0.665	0.621
279.8	0.843	0.841	0.836	0.825	0.793	0.750	0.722	0.692	0.661	0.618
279.9	0.838	0.837	0.831	0.821	0.789	0.748	0.719	0.689	0.659	0.614
280	0.833	0.832	0.827	0.817	0.785	0.745	0.717	0.686	0.656	0.612
280.1	0.829	0.828	0.822	0.812	0.782	0.743	0.715	0.684	0.653	0.609
280.2	0.824	0.824	0.818	0.808	0.779	0.740	0.713	0.682	0.651	0.607
280.3	0.819	0.819	0.814	0.804	0.775	0.738	0.711	0.680	0.649	0.604
280.4	0.815	0.815	0.809	0.800	0.772	0.736	0.710	0.678	0.647	0.602
280.5	0.811	0.811	0.805	0.796	0.769	0.734	0.708	0.676	0.645	0.600
280.6	0.807	0.807	0.801	0.792	0.767	0.732	0.707	0.675	0.644	0.599
280.7	0.803	0.803	0.797	0.789	0.764	0.730	0.706	0.674	0.643	0.598
280.8	0.799	0.799	0.794	0.785	0.762	0.729	0.705	0.673	0.642	0.597
280.9	0.796	0.795	0.790	0.782	0.759	0.728	0.704	0.672	0.641	0.596
281	0.792	0.792	0.787	0.779	0.757	0.726	0.703	0.672	0.641	0.596
281.1	0.789	0.789	0.784	0.776	0.755	0.725	0.703	0.671	0.641	0.596
281.2	0.786	0.786	0.781	0.774	0.753	0.724	0.702	0.671	0.641	0.596
281.3	0.783	0.783	0.778	0.771	0.751	0.723	0.702	0.671	0.641	0.596
281.4	0.780	0.780	0.776	0.769	0.749	0.722	0.702	0.672	0.641	0.596
281.5	0.778	0.778	0.773	0.767	0.748	0.721	0.702	0.672	0.642	0.597
281.6	0.776	0.776	0.771	0.765	0.746	0.720	0.701	0.672	0.643	0.598
281.7	0.774	0.774	0.769	0.763	0.745	0.719	0.701	0.672	0.643	0.599
281.8	0.772	0.772	0.768	0.761	0.743	0.718	0.701	0.673	0.644	0.600
281.9	0.770	0.770	0.766	0.760	0.742	0.717	0.700	0.673	0.645	0.602
282	0.769	0.768	0.765	0.758	0.740	0.716	0.700	0.674	0.646	0.603
282.1	0.768	0.767	0.763	0.757	0.739	0.715	0.699	0.674	0.647	0.604
282.2	0.766	0.766	0.762	0.756	0.738	0.714	0.699	0.675	0.647	0.605
282.3	0.766	0.765	0.762	0.755	0.736	0.712	0.698	0.675	0.648	0.606
282.4	0.765	0.764	0.761	0.754	0.735	0.710	0.697	0.675	0.648	0.607
282.5	0.764	0.763	0.760	0.752	0.733	0.708	0.695	0.675	0.649	0.608
282.6	0.763	0.762	0.759	0.751	0.732	0.706	0.693	0.674	0.649	0.609
282.7	0.762	0.762	0.758	0.750	0.730	0.704	0.691	0.674	0.648	0.609
282.8	0.761	0.761	0.757	0.749	0.728	0.701	0.689	0.672	0.648	0.609
282.9	0.760	0.760	0.757	0.748	0.726	0.699	0.686	0.671	0.647	0.609
283	0.759	0.759	0.756	0.747	0.724	0.696	0.684	0.670	0.646	0.609
283.1	0.759	0.758	0.755	0.746	0.722	0.693	0.681	0.668	0.645	0.608
283.2	0.758	0.757	0.754	0.744	0.719	0.689	0.677	0.666	0.643	0.607
283.3	0.756	0.755	0.752	0.742	0.717	0.685	0.673	0.663	0.641	0.606
283.4	0.755	0.754	0.751	0.740	0.713	0.680	0.669	0.660	0.638	0.604
283.5	0.753	0.752	0.749	0.738	0.710	0.676	0.664	0.656	0.635	0.601
283.6	0.751	0.750	0.747	0.736	0.706	0.670	0.658	0.652	0.631	0.598

283.7	0.749	0.748	0.745	0.733	0.702	0.665	0.652	0.647	0.627	0.595
283.8	0.747	0.746	0.742	0.730	0.697	0.659	0.646	0.642	0.622	0.591
283.9	0.744	0.743	0.739	0.726	0.692	0.652	0.639	0.635	0.616	0.586
284	0.740	0.739	0.736	0.722	0.687	0.645	0.631	0.629	0.610	0.581
284.1	0.736	0.735	0.732	0.718	0.681	0.637	0.623	0.622	0.603	0.575
284.2	0.732	0.731	0.728	0.713	0.675	0.629	0.615	0.614	0.596	0.569
284.3	0.727	0.727	0.723	0.708	0.669	0.621	0.606	0.606	0.589	0.562
284.4	0.722	0.722	0.718	0.702	0.661	0.612	0.597	0.598	0.581	0.555
284.5	0.716	0.716	0.712	0.695	0.654	0.603	0.587	0.589	0.572	0.547
284.6	0.710	0.710	0.706	0.689	0.646	0.593	0.577	0.580	0.563	0.539
284.7	0.703	0.703	0.699	0.681	0.638	0.584	0.567	0.571	0.554	0.530
284.8	0.695	0.696	0.691	0.673	0.629	0.574	0.556	0.560	0.544	0.521
284.9	0.687	0.688	0.684	0.665	0.620	0.563	0.545	0.550	0.534	0.511
285	0.679	0.679	0.675	0.656	0.611	0.552	0.534	0.539	0.523	0.501
285.1	0.670	0.670	0.666	0.647	0.601	0.541	0.523	0.527	0.512	0.490
285.2	0.660	0.661	0.656	0.637	0.590	0.530	0.511	0.516	0.501	0.480
285.3	0.650	0.650	0.646	0.626	0.580	0.518	0.499	0.504	0.489	0.469
285.4	0.639	0.640	0.636	0.616	0.569	0.507	0.487	0.492	0.478	0.458
285.5	0.628	0.629	0.625	0.605	0.558	0.495	0.475	0.480	0.466	0.447
285.6	0.617	0.618	0.614	0.593	0.546	0.483	0.463	0.468	0.454	0.435
285.7	0.605	0.606	0.602	0.581	0.534	0.471	0.451	0.456	0.442	0.424
285.8	0.594	0.594	0.590	0.570	0.523	0.460	0.440	0.444	0.430	0.413
285.9	0.583	0.583	0.579	0.558	0.512	0.449	0.429	0.433	0.419	0.402
286	0.571	0.571	0.567	0.547	0.500	0.437	0.417	0.421	0.408	0.392
286.1	0.559	0.558	0.555	0.535	0.488	0.426	0.406	0.410	0.397	0.381
286.2	0.547	0.546	0.543	0.523	0.477	0.415	0.395	0.399	0.385	0.370
286.3	0.535	0.533	0.531	0.510	0.465	0.404	0.384	0.387	0.374	0.360
286.4	0.521	0.520	0.517	0.497	0.452	0.392	0.372	0.375	0.362	0.348
286.5	0.507	0.506	0.504	0.484	0.440	0.380	0.360	0.363	0.350	0.337
286.6	0.493	0.492	0.490	0.470	0.427	0.368	0.349	0.351	0.339	0.325
286.7	0.479	0.477	0.476	0.457	0.414	0.356	0.337	0.339	0.327	0.314
286.8	0.465	0.463	0.462	0.443	0.401	0.345	0.326	0.327	0.316	0.303
286.9	0.450	0.448	0.448	0.430	0.389	0.333	0.315	0.315	0.304	0.293
287	0.436	0.434	0.434	0.416	0.376	0.321	0.304	0.304	0.293	0.282
287.1	0.422	0.420	0.420	0.402	0.363	0.310	0.293	0.293	0.282	0.272
287.2	0.408	0.406	0.406	0.389	0.351	0.299	0.282	0.282	0.272	0.262
287.3	0.393	0.392	0.392	0.376	0.339	0.288	0.272	0.271	0.262	0.252
287.4	0.380	0.378	0.378	0.363	0.327	0.278	0.262	0.261	0.252	0.242
287.5	0.366	0.365	0.364	0.350	0.315	0.268	0.253	0.251	0.242	0.234
287.6	0.353	0.352	0.351	0.338	0.304	0.258	0.243	0.242	0.233	0.225
287.7	0.341	0.339	0.338	0.325	0.293	0.249	0.234	0.233	0.224	0.216

287.8	0.328	0.326	0.326	0.313	0.282	0.240	0.225	0.224	0.215	0.208
287.9	0.315	0.313	0.313	0.302	0.271	0.231	0.217	0.215	0.207	0.200
288	0.303	0.301	0.301	0.290	0.260	0.222	0.208	0.207	0.199	0.193
288.1	0.291	0.289	0.289	0.279	0.250	0.213	0.200	0.199	0.191	0.185
288.2	0.280	0.277	0.277	0.268	0.240	0.205	0.192	0.191	0.184	0.178
288.3	0.269	0.266	0.265	0.257	0.231	0.197	0.184	0.183	0.177	0.171
288.4	0.258	0.255	0.254	0.246	0.221	0.189	0.177	0.176	0.170	0.165
288.5	0.248	0.246	0.244	0.237	0.213	0.182	0.170	0.169	0.163	0.159
288.6	0.238	0.236	0.235	0.228	0.205	0.176	0.164	0.163	0.157	0.154
288.7	0.229	0.228	0.226	0.219	0.197	0.169	0.158	0.157	0.152	0.148
288.8	0.220	0.219	0.217	0.211	0.189	0.163	0.153	0.152	0.146	0.143
288.9	0.212	0.211	0.209	0.203	0.182	0.157	0.147	0.146	0.141	0.139
289	0.204	0.203	0.200	0.195	0.175	0.151	0.142	0.141	0.136	0.134
289.1	0.195	0.194	0.192	0.186	0.167	0.145	0.136	0.135	0.131	0.129
289.2	0.186	0.186	0.183	0.178	0.160	0.139	0.130	0.130	0.126	0.124
289.3	0.178	0.178	0.175	0.170	0.153	0.133	0.125	0.125	0.121	0.120
289.4	0.171	0.170	0.167	0.163	0.146	0.128	0.120	0.120	0.117	0.116
289.5	0.163	0.163	0.160	0.156	0.140	0.122	0.115	0.116	0.113	0.112
289.6	0.156	0.156	0.153	0.149	0.134	0.118	0.111	0.111	0.108	0.108
289.7	0.150	0.149	0.146	0.142	0.128	0.113	0.106	0.107	0.105	0.104
289.8	0.144	0.143	0.140	0.136	0.123	0.108	0.102	0.103	0.101	0.101
289.9	0.138	0.136	0.133	0.130	0.118	0.104	0.098	0.099	0.097	0.098
290	0.132	0.131	0.127	0.124	0.112	0.100	0.094	0.095	0.094	0.094
290.1	0.126	0.125	0.122	0.119	0.108	0.095	0.091	0.092	0.091	0.091
290.2	0.121	0.120	0.116	0.114	0.103	0.092	0.087	0.089	0.087	0.089
290.3	0.116	0.114	0.111	0.109	0.098	0.088	0.084	0.086	0.084	0.086
290.4	0.111	0.109	0.106	0.104	0.094	0.084	0.081	0.083	0.082	0.083
290.5	0.106	0.105	0.102	0.100	0.090	0.081	0.078	0.080	0.079	0.081
290.6	0.102	0.100	0.098	0.095	0.087	0.078	0.075	0.077	0.076	0.078
290.7	0.098	0.096	0.094	0.091	0.083	0.075	0.072	0.074	0.074	0.076
290.8	0.094	0.092	0.090	0.088	0.080	0.072	0.069	0.072	0.072	0.074
290.9	0.090	0.088	0.086	0.084	0.077	0.069	0.067	0.069	0.070	0.072
291	0.086	0.085	0.083	0.081	0.074	0.067	0.065	0.067	0.068	0.070
291.1	0.083	0.082	0.079	0.078	0.071	0.065	0.063	0.065	0.066	0.069
291.2	0.080	0.079	0.076	0.075	0.069	0.063	0.061	0.063	0.064	0.067
291.3	0.077	0.076	0.074	0.072	0.066	0.060	0.059	0.062	0.062	0.066
291.4	0.074	0.073	0.071	0.069	0.064	0.058	0.057	0.060	0.061	0.064
291.5	0.072	0.071	0.068	0.067	0.062	0.057	0.055	0.058	0.059	0.063
291.6	0.069	0.068	0.066	0.064	0.059	0.055	0.054	0.057	0.058	0.061
291.7	0.066	0.066	0.063	0.062	0.057	0.053	0.052	0.055	0.056	0.060
291.8	0.064	0.063	0.061	0.059	0.055	0.051	0.050	0.053	0.055	0.059

291.9	0.062	0.061	0.059	0.057	0.053	0.049	0.049	0.052	0.053	0.057
292	0.059	0.059	0.057	0.055	0.051	0.048	0.047	0.050	0.052	0.056
292.1	0.057	0.057	0.055	0.053	0.050	0.046	0.046	0.049	0.051	0.055
292.2	0.055	0.055	0.053	0.051	0.048	0.044	0.044	0.048	0.050	0.054
292.3	0.053	0.053	0.051	0.049	0.046	0.043	0.043	0.047	0.048	0.053
292.4	0.052	0.051	0.049	0.048	0.045	0.042	0.042	0.046	0.047	0.052
292.5	0.050	0.049	0.048	0.046	0.044	0.040	0.041	0.044	0.046	0.051
292.6	0.048	0.048	0.046	0.045	0.042	0.039	0.040	0.043	0.045	0.050
292.7	0.047	0.046	0.045	0.043	0.041	0.038	0.039	0.042	0.045	0.049
292.8	0.045	0.045	0.043	0.042	0.040	0.037	0.038	0.041	0.044	0.048
292.9	0.044	0.043	0.042	0.040	0.039	0.036	0.037	0.041	0.043	0.048
293	0.043	0.042	0.041	0.039	0.038	0.035	0.036	0.040	0.042	0.047
293.1	0.041	0.041	0.039	0.038	0.036	0.034	0.035	0.039	0.041	0.046
293.2	0.040	0.040	0.038	0.037	0.035	0.033	0.034	0.038	0.041	0.045
293.3	0.039	0.039	0.037	0.036	0.035	0.032	0.033	0.037	0.040	0.045
293.4	0.038	0.038	0.036	0.035	0.034	0.032	0.033	0.037	0.039	0.044
293.5	0.037	0.037	0.035	0.034	0.033	0.031	0.032	0.036	0.039	0.044
293.6	0.036	0.036	0.034	0.033	0.032	0.030	0.031	0.036	0.038	0.043
293.7	0.035	0.035	0.034	0.032	0.031	0.030	0.031	0.035	0.038	0.043
293.8	0.034	0.034	0.033	0.031	0.031	0.029	0.030	0.034	0.037	0.042
293.9	0.034	0.033	0.032	0.031	0.030	0.028	0.030	0.034	0.037	0.042
294	0.033	0.032	0.031	0.030	0.029	0.028	0.029	0.033	0.036	0.041
294.1	0.032	0.032	0.030	0.029	0.029	0.027	0.029	0.033	0.036	0.041
294.2	0.031	0.031	0.030	0.028	0.028	0.026	0.028	0.032	0.035	0.040
294.3	0.031	0.030	0.029	0.028	0.027	0.026	0.028	0.032	0.035	0.040
294.4	0.030	0.029	0.028	0.027	0.027	0.025	0.027	0.031	0.034	0.040
294.5	0.029	0.029	0.028	0.027	0.026	0.025	0.027	0.031	0.034	0.039
294.6	0.029	0.028	0.027	0.026	0.026	0.024	0.026	0.031	0.033	0.039
294.7	0.028	0.028	0.026	0.025	0.025	0.024	0.026	0.030	0.033	0.038
294.8	0.027	0.027	0.026	0.025	0.025	0.024	0.025	0.030	0.033	0.038
294.9	0.027	0.026	0.025	0.024	0.024	0.023	0.025	0.029	0.032	0.038
295	0.026	0.026	0.025	0.024	0.024	0.023	0.025	0.029	0.032	0.038
295.1	0.026	0.025	0.024	0.023	0.024	0.022	0.024	0.029	0.032	0.037
295.2	0.026	0.025	0.024	0.023	0.023	0.022	0.024	0.028	0.031	0.037
295.3	0.025	0.024	0.023	0.023	0.023	0.022	0.024	0.028	0.031	0.037
295.4	0.025	0.024	0.023	0.022	0.022	0.021	0.023	0.028	0.031	0.036
295.5	0.024	0.024	0.023	0.022	0.022	0.021	0.023	0.028	0.031	0.036
295.6	0.024	0.023	0.022	0.022	0.022	0.021	0.023	0.027	0.030	0.036
295.7	0.023	0.023	0.022	0.021	0.021	0.021	0.022	0.027	0.030	0.036
295.8	0.023	0.023	0.022	0.021	0.021	0.020	0.022	0.027	0.030	0.035
295.9	0.023	0.022	0.021	0.021	0.021	0.020	0.022	0.027	0.030	0.035

296	0.023	0.022	0.021	0.020	0.021	0.020	0.022	0.026	0.030	0.035
296.1	0.022	0.022	0.021	0.020	0.020	0.020	0.022	0.026	0.029	0.035
296.2	0.022	0.021	0.020	0.020	0.020	0.020	0.022	0.026	0.029	0.035
296.3	0.022	0.021	0.020	0.020	0.020	0.019	0.021	0.026	0.029	0.034
296.4	0.021	0.021	0.020	0.019	0.020	0.019	0.021	0.026	0.029	0.034
296.5	0.021	0.021	0.020	0.019	0.019	0.019	0.021	0.025	0.029	0.034
296.6	0.021	0.020	0.019	0.019	0.019	0.019	0.021	0.025	0.028	0.034
296.7	0.021	0.020	0.019	0.018	0.019	0.018	0.021	0.025	0.028	0.034
296.8	0.020	0.020	0.019	0.018	0.019	0.018	0.020	0.025	0.028	0.034
296.9	0.020	0.020	0.019	0.018	0.019	0.018	0.020	0.025	0.028	0.034
297	0.020	0.020	0.018	0.018	0.018	0.018	0.020	0.025	0.028	0.034
297.1	0.020	0.019	0.018	0.018	0.018	0.018	0.020	0.025	0.028	0.033
297.2	0.020	0.019	0.018	0.018	0.018	0.018	0.020	0.024	0.028	0.033
297.3	0.019	0.019	0.018	0.017	0.018	0.018	0.020	0.024	0.027	0.033
297.4	0.019	0.019	0.018	0.017	0.018	0.018	0.020	0.024	0.027	0.033
297.5	0.019	0.019	0.018	0.017	0.018	0.017	0.020	0.024	0.027	0.033
297.6	0.019	0.018	0.017	0.017	0.018	0.017	0.020	0.024	0.027	0.033
297.7	0.019	0.018	0.017	0.017	0.017	0.017	0.019	0.024	0.027	0.033
297.8	0.019	0.018	0.017	0.017	0.017	0.017	0.019	0.024	0.027	0.033
297.9	0.019	0.018	0.017	0.017	0.017	0.017	0.019	0.024	0.027	0.032
298	0.018	0.018	0.017	0.016	0.017	0.017	0.019	0.024	0.027	0.032
298.1	0.018	0.018	0.017	0.016	0.017	0.017	0.019	0.024	0.027	0.032
298.2	0.018	0.018	0.017	0.016	0.017	0.017	0.019	0.023	0.027	0.032
298.3	0.018	0.018	0.017	0.016	0.017	0.017	0.019	0.023	0.027	0.032
298.4	0.018	0.017	0.017	0.016	0.017	0.017	0.019	0.023	0.026	0.032
298.5	0.018	0.017	0.016	0.016	0.017	0.016	0.019	0.023	0.026	0.032
298.6	0.018	0.017	0.016	0.016	0.017	0.016	0.019	0.023	0.026	0.032
298.7	0.018	0.017	0.016	0.016	0.017	0.016	0.019	0.023	0.026	0.032
298.8	0.018	0.017	0.016	0.016	0.016	0.016	0.019	0.023	0.026	0.032
298.9	0.018	0.017	0.016	0.016	0.016	0.016	0.019	0.023	0.026	0.032
299	0.017	0.017	0.016	0.016	0.016	0.016	0.018	0.023	0.026	0.032
299.1	0.017	0.017	0.016	0.016	0.016	0.016	0.018	0.023	0.026	0.032
299.2	0.017	0.017	0.016	0.015	0.016	0.016	0.018	0.023	0.026	0.032
299.3	0.017	0.017	0.016	0.015	0.016	0.016	0.018	0.023	0.026	0.032
299.4	0.017	0.017	0.016	0.015	0.016	0.016	0.018	0.023	0.026	0.032
299.5	0.017	0.017	0.016	0.015	0.016	0.016	0.018	0.023	0.026	0.031
299.6	0.017	0.017	0.015	0.015	0.016	0.016	0.018	0.023	0.026	0.031
299.7	0.017	0.017	0.015	0.015	0.016	0.016	0.018	0.022	0.026	0.031
299.8	0.017	0.016	0.015	0.015	0.016	0.016	0.018	0.022	0.026	0.031
299.9	0.017	0.016	0.015	0.015	0.016	0.016	0.018	0.022	0.026	0.031
300	0.017	0.016	0.015	0.015	0.016	0.016	0.018	0.022	0.026	0.031

3.8. Absorbance of TX-114 with variation of concentration of β-CD in water at 298.15 K.

λ/nm	0.0 mM	1.5 mM	1.7 mM	2.0 mM	2.7 mM	3.7 mM	4.6 mM	5.3 mM	6.0 mM	6.6 mM	7.1 mM	7.3 mM	7.5 mM	7.8 mM	8.0 mM
250	0.586	0.385	0.214	0.189	0.174	0.155	0.148	0.141	0.140	0.139	0.138	0.137	0.137	0.137	0.137
250.1	0.586	0.385	0.215	0.190	0.175	0.156	0.149	0.142	0.141	0.140	0.139	0.138	0.137	0.137	0.138
250.2	0.585	0.385	0.216	0.191	0.176	0.157	0.150	0.143	0.142	0.141	0.140	0.139	0.138	0.138	0.139
250.3	0.585	0.386	0.217	0.192	0.177	0.158	0.151	0.144	0.143	0.142	0.141	0.140	0.139	0.139	0.140
250.4	0.585	0.386	0.217	0.193	0.178	0.159	0.152	0.145	0.144	0.143	0.142	0.141	0.140	0.139	0.140
250.5	0.585	0.387	0.218	0.193	0.179	0.160	0.153	0.146	0.145	0.143	0.143	0.142	0.141	0.140	0.141
250.6	0.585	0.387	0.219	0.194	0.180	0.161	0.154	0.147	0.145	0.144	0.143	0.143	0.142	0.141	0.142
250.7	0.585	0.388	0.220	0.195	0.181	0.162	0.155	0.148	0.146	0.145	0.144	0.143	0.142	0.142	0.142
250.8	0.585	0.388	0.221	0.196	0.181	0.163	0.156	0.149	0.147	0.146	0.145	0.144	0.143	0.142	0.143
250.9	0.585	0.388	0.222	0.197	0.182	0.164	0.156	0.150	0.148	0.147	0.146	0.145	0.144	0.143	0.144
251	0.585	0.389	0.222	0.198	0.183	0.165	0.157	0.150	0.149	0.148	0.147	0.146	0.145	0.144	0.144
251.1	0.585	0.389	0.223	0.199	0.184	0.166	0.158	0.151	0.150	0.149	0.148	0.147	0.146	0.145	0.145
251.2	0.585	0.390	0.224	0.199	0.185	0.167	0.159	0.152	0.151	0.150	0.149	0.148	0.147	0.145	0.146
251.3	0.585	0.390	0.225	0.200	0.186	0.168	0.160	0.153	0.152	0.151	0.150	0.149	0.148	0.146	0.147
251.4	0.585	0.391	0.226	0.201	0.187	0.169	0.161	0.155	0.153	0.152	0.151	0.150	0.149	0.147	0.147
251.5	0.585	0.392	0.227	0.202	0.188	0.170	0.163	0.156	0.154	0.153	0.152	0.151	0.150	0.148	0.148
251.6	0.585	0.392	0.228	0.203	0.189	0.171	0.164	0.157	0.155	0.154	0.153	0.152	0.151	0.149	0.149
251.7	0.585	0.393	0.229	0.204	0.190	0.172	0.165	0.158	0.156	0.155	0.154	0.153	0.152	0.150	0.150
251.8	0.586	0.393	0.230	0.205	0.191	0.173	0.166	0.159	0.157	0.156	0.155	0.154	0.153	0.151	0.151
251.9	0.586	0.394	0.231	0.207	0.192	0.174	0.167	0.160	0.158	0.157	0.156	0.155	0.153	0.152	0.151
252	0.586	0.394	0.232	0.208	0.193	0.176	0.168	0.161	0.159	0.158	0.157	0.156	0.154	0.152	0.152
252.1	0.586	0.395	0.233	0.209	0.194	0.177	0.169	0.162	0.161	0.159	0.158	0.157	0.155	0.153	0.153
252.2	0.586	0.396	0.234	0.210	0.196	0.178	0.171	0.163	0.162	0.161	0.159	0.158	0.156	0.154	0.154
252.3	0.587	0.397	0.235	0.211	0.197	0.179	0.172	0.164	0.163	0.162	0.160	0.159	0.157	0.155	0.155
252.4	0.587	0.397	0.236	0.212	0.198	0.180	0.173	0.166	0.164	0.163	0.161	0.160	0.158	0.156	0.156
252.5	0.587	0.398	0.237	0.213	0.199	0.181	0.174	0.167	0.165	0.164	0.162	0.161	0.159	0.157	0.156
252.6	0.587	0.399	0.238	0.214	0.200	0.182	0.175	0.168	0.166	0.165	0.163	0.162	0.160	0.158	0.157
252.7	0.587	0.399	0.239	0.215	0.201	0.184	0.176	0.169	0.167	0.166	0.164	0.163	0.161	0.159	0.158
252.8	0.588	0.400	0.240	0.216	0.202	0.185	0.177	0.170	0.168	0.167	0.165	0.164	0.162	0.160	0.159
252.9	0.588	0.401	0.242	0.217	0.203	0.186	0.179	0.171	0.169	0.168	0.167	0.165	0.163	0.161	0.160
253	0.588	0.402	0.243	0.219	0.205	0.187	0.180	0.172	0.171	0.169	0.168	0.166	0.164	0.162	0.161
253.1	0.589	0.402	0.244	0.220	0.206	0.188	0.181	0.174	0.172	0.171	0.169	0.167	0.166	0.163	0.162
253.2	0.589	0.403	0.245	0.221	0.207	0.190	0.183	0.175	0.173	0.172	0.170	0.168	0.167	0.164	0.163
253.3	0.590	0.404	0.246	0.222	0.208	0.191	0.184	0.176	0.174	0.173	0.171	0.170	0.168	0.165	0.164
253.4	0.590	0.405	0.248	0.224	0.210	0.192	0.185	0.177	0.176	0.174	0.173	0.171	0.169	0.166	0.164
253.5	0.591	0.406	0.249	0.225	0.211	0.194	0.186	0.179	0.177	0.175	0.174	0.172	0.170	0.167	0.165
253.6	0.591	0.407	0.250	0.226	0.212	0.195	0.188	0.180	0.178	0.177	0.175	0.173	0.171	0.168	0.166

253.7	0.592	0.408	0.251	0.227	0.214	0.196	0.189	0.181	0.180	0.178	0.176	0.174	0.172	0.169	0.167
253.8	0.592	0.409	0.253	0.229	0.215	0.198	0.190	0.183	0.181	0.179	0.177	0.176	0.174	0.170	0.168
253.9	0.593	0.410	0.254	0.230	0.216	0.199	0.192	0.184	0.182	0.181	0.179	0.177	0.175	0.171	0.169
254	0.593	0.411	0.255	0.231	0.218	0.200	0.193	0.185	0.183	0.182	0.180	0.178	0.176	0.172	0.170
254.1	0.594	0.411	0.256	0.233	0.219	0.202	0.194	0.186	0.185	0.183	0.181	0.179	0.177	0.173	0.171
254.2	0.594	0.412	0.258	0.234	0.220	0.203	0.196	0.188	0.186	0.184	0.182	0.180	0.178	0.174	0.172
254.3	0.595	0.413	0.259	0.235	0.222	0.204	0.197	0.189	0.187	0.185	0.183	0.182	0.179	0.175	0.173
254.4	0.595	0.414	0.260	0.236	0.223	0.206	0.198	0.190	0.188	0.187	0.185	0.183	0.180	0.176	0.174
254.5	0.596	0.415	0.261	0.238	0.224	0.207	0.200	0.191	0.190	0.188	0.186	0.184	0.181	0.177	0.175
254.6	0.597	0.416	0.263	0.239	0.225	0.208	0.201	0.193	0.191	0.189	0.187	0.185	0.183	0.178	0.176
254.7	0.597	0.417	0.264	0.240	0.227	0.210	0.202	0.194	0.192	0.191	0.188	0.186	0.184	0.179	0.177
254.8	0.598	0.418	0.266	0.242	0.228	0.211	0.204	0.196	0.194	0.192	0.190	0.188	0.185	0.180	0.178
254.9	0.598	0.419	0.267	0.243	0.230	0.213	0.205	0.197	0.195	0.193	0.191	0.189	0.186	0.181	0.179
255	0.599	0.420	0.269	0.245	0.231	0.214	0.207	0.199	0.197	0.195	0.192	0.190	0.188	0.183	0.180
255.1	0.600	0.422	0.270	0.246	0.233	0.216	0.208	0.200	0.198	0.196	0.194	0.192	0.189	0.184	0.181
255.2	0.600	0.423	0.271	0.248	0.234	0.217	0.210	0.202	0.199	0.198	0.195	0.193	0.190	0.185	0.182
255.3	0.601	0.424	0.273	0.249	0.236	0.219	0.212	0.203	0.201	0.199	0.197	0.194	0.192	0.186	0.184
255.4	0.602	0.425	0.274	0.251	0.238	0.221	0.213	0.205	0.203	0.201	0.198	0.196	0.193	0.188	0.185
255.5	0.603	0.426	0.276	0.253	0.239	0.222	0.215	0.206	0.204	0.202	0.200	0.197	0.194	0.189	0.186
255.6	0.604	0.428	0.278	0.254	0.241	0.224	0.216	0.208	0.206	0.204	0.201	0.199	0.196	0.190	0.187
255.7	0.605	0.429	0.279	0.256	0.243	0.226	0.218	0.209	0.207	0.205	0.203	0.200	0.197	0.191	0.188
255.8	0.606	0.430	0.281	0.258	0.244	0.227	0.220	0.211	0.209	0.207	0.204	0.202	0.199	0.193	0.189
255.9	0.607	0.432	0.282	0.259	0.246	0.229	0.221	0.213	0.210	0.208	0.205	0.203	0.200	0.194	0.191
256	0.607	0.433	0.284	0.261	0.247	0.230	0.223	0.214	0.212	0.210	0.207	0.204	0.201	0.195	0.192
256.1	0.608	0.434	0.285	0.262	0.249	0.232	0.224	0.216	0.213	0.211	0.208	0.206	0.203	0.196	0.193
256.2	0.609	0.435	0.287	0.264	0.250	0.233	0.226	0.217	0.215	0.212	0.210	0.207	0.204	0.197	0.194
256.3	0.610	0.436	0.288	0.265	0.252	0.235	0.227	0.218	0.216	0.214	0.211	0.208	0.205	0.198	0.195
256.4	0.611	0.438	0.290	0.267	0.253	0.237	0.229	0.220	0.217	0.215	0.212	0.210	0.206	0.200	0.196
256.5	0.612	0.439	0.292	0.268	0.255	0.238	0.231	0.222	0.219	0.217	0.214	0.211	0.208	0.201	0.197
256.6	0.613	0.440	0.293	0.270	0.257	0.240	0.232	0.223	0.221	0.219	0.215	0.213	0.209	0.202	0.198
256.7	0.614	0.442	0.295	0.272	0.259	0.242	0.234	0.225	0.222	0.220	0.217	0.214	0.211	0.204	0.200
256.8	0.615	0.443	0.297	0.274	0.260	0.244	0.236	0.227	0.224	0.222	0.219	0.216	0.212	0.205	0.201
256.9	0.616	0.445	0.299	0.275	0.262	0.246	0.238	0.229	0.226	0.224	0.220	0.218	0.214	0.206	0.202
257	0.617	0.446	0.301	0.277	0.264	0.247	0.240	0.230	0.228	0.225	0.222	0.219	0.216	0.208	0.204
257.1	0.618	0.447	0.302	0.279	0.266	0.249	0.241	0.232	0.230	0.227	0.224	0.221	0.217	0.209	0.205
257.2	0.619	0.449	0.304	0.281	0.268	0.251	0.243	0.234	0.231	0.229	0.225	0.223	0.219	0.210	0.206
257.3	0.621	0.451	0.306	0.283	0.270	0.253	0.245	0.236	0.233	0.231	0.227	0.224	0.220	0.212	0.207
257.4	0.622	0.452	0.308	0.285	0.272	0.255	0.247	0.238	0.235	0.232	0.229	0.226	0.222	0.213	0.209
257.5	0.623	0.454	0.310	0.287	0.274	0.257	0.249	0.240	0.237	0.234	0.231	0.228	0.224	0.215	0.210
257.6	0.624	0.456	0.312	0.289	0.276	0.259	0.251	0.242	0.239	0.236	0.232	0.229	0.225	0.216	0.212
257.7	0.626	0.457	0.314	0.291	0.278	0.261	0.253	0.243	0.241	0.238	0.234	0.231	0.227	0.218	0.213

257.8	0.627	0.459	0.316	0.293	0.280	0.263	0.255	0.245	0.242	0.240	0.236	0.233	0.229	0.220	0.214
257.9	0.628	0.461	0.318	0.295	0.282	0.265	0.257	0.247	0.244	0.242	0.238	0.234	0.230	0.221	0.216
258	0.629	0.462	0.320	0.297	0.284	0.267	0.259	0.249	0.246	0.243	0.239	0.236	0.232	0.222	0.217
258.1	0.631	0.464	0.322	0.299	0.286	0.269	0.261	0.251	0.248	0.245	0.241	0.238	0.233	0.224	0.218
258.2	0.632	0.465	0.324	0.301	0.288	0.271	0.263	0.253	0.249	0.247	0.243	0.239	0.235	0.225	0.220
258.3	0.633	0.467	0.326	0.303	0.290	0.273	0.265	0.254	0.251	0.248	0.244	0.241	0.236	0.227	0.221
258.4	0.635	0.468	0.328	0.305	0.292	0.275	0.267	0.256	0.253	0.250	0.246	0.243	0.238	0.228	0.222
258.5	0.636	0.470	0.330	0.307	0.294	0.277	0.269	0.258	0.255	0.252	0.248	0.244	0.240	0.230	0.224
258.6	0.638	0.472	0.332	0.309	0.296	0.279	0.271	0.260	0.257	0.254	0.250	0.246	0.241	0.231	0.226
258.7	0.639	0.474	0.334	0.311	0.298	0.282	0.273	0.262	0.259	0.256	0.252	0.248	0.243	0.233	0.227
258.8	0.640	0.476	0.336	0.313	0.300	0.284	0.275	0.264	0.261	0.258	0.254	0.250	0.245	0.235	0.229
258.9	0.642	0.478	0.339	0.316	0.303	0.286	0.277	0.267	0.263	0.260	0.256	0.252	0.247	0.236	0.230
259	0.644	0.480	0.341	0.318	0.305	0.288	0.280	0.269	0.265	0.262	0.258	0.254	0.249	0.238	0.232
259.1	0.645	0.481	0.343	0.320	0.307	0.290	0.282	0.271	0.267	0.264	0.260	0.256	0.251	0.240	0.234
259.2	0.647	0.483	0.345	0.322	0.309	0.293	0.284	0.273	0.269	0.266	0.262	0.258	0.253	0.242	0.235
259.3	0.649	0.485	0.348	0.324	0.312	0.295	0.286	0.275	0.272	0.269	0.264	0.260	0.255	0.244	0.237
259.4	0.650	0.487	0.350	0.327	0.314	0.297	0.289	0.277	0.274	0.271	0.266	0.262	0.257	0.245	0.239
259.5	0.652	0.489	0.352	0.329	0.316	0.300	0.291	0.280	0.276	0.273	0.268	0.265	0.259	0.247	0.241
259.6	0.654	0.491	0.354	0.331	0.319	0.302	0.293	0.282	0.278	0.275	0.271	0.267	0.261	0.249	0.242
259.7	0.656	0.493	0.357	0.334	0.321	0.304	0.296	0.284	0.281	0.278	0.273	0.269	0.263	0.251	0.244
259.8	0.657	0.495	0.359	0.336	0.324	0.307	0.298	0.287	0.283	0.280	0.275	0.271	0.265	0.253	0.246
259.9	0.659	0.497	0.361	0.338	0.326	0.309	0.300	0.289	0.285	0.282	0.277	0.273	0.267	0.255	0.248
260	0.661	0.499	0.363	0.340	0.328	0.311	0.303	0.291	0.287	0.284	0.279	0.275	0.269	0.257	0.249
260.1	0.662	0.501	0.365	0.343	0.330	0.313	0.305	0.293	0.289	0.286	0.281	0.277	0.271	0.259	0.251
260.2	0.664	0.503	0.368	0.345	0.332	0.316	0.307	0.295	0.292	0.288	0.283	0.279	0.273	0.260	0.253
260.3	0.666	0.505	0.370	0.347	0.334	0.318	0.309	0.297	0.294	0.290	0.285	0.281	0.275	0.262	0.254
260.4	0.667	0.507	0.372	0.349	0.336	0.320	0.311	0.300	0.296	0.293	0.287	0.283	0.277	0.264	0.256
260.5	0.669	0.509	0.374	0.352	0.339	0.322	0.314	0.302	0.298	0.295	0.290	0.285	0.279	0.266	0.258
260.6	0.671	0.511	0.377	0.354	0.341	0.325	0.316	0.304	0.300	0.297	0.292	0.288	0.281	0.268	0.260
260.7	0.673	0.513	0.379	0.356	0.344	0.327	0.319	0.307	0.303	0.299	0.294	0.290	0.284	0.270	0.261
260.8	0.675	0.516	0.382	0.359	0.346	0.330	0.321	0.309	0.305	0.302	0.296	0.292	0.286	0.272	0.263
260.9	0.677	0.518	0.384	0.361	0.349	0.332	0.324	0.312	0.308	0.304	0.299	0.294	0.288	0.274	0.265
261	0.679	0.520	0.387	0.364	0.351	0.335	0.326	0.314	0.310	0.306	0.301	0.297	0.290	0.276	0.267
261.1	0.681	0.522	0.389	0.366	0.354	0.337	0.329	0.316	0.312	0.309	0.303	0.299	0.292	0.278	0.269
261.2	0.683	0.525	0.392	0.369	0.356	0.340	0.331	0.319	0.315	0.311	0.305	0.301	0.294	0.280	0.271
261.3	0.685	0.527	0.394	0.371	0.359	0.342	0.334	0.321	0.317	0.313	0.308	0.303	0.296	0.282	0.272
261.4	0.687	0.529	0.397	0.374	0.361	0.345	0.336	0.324	0.319	0.316	0.310	0.306	0.298	0.284	0.274
261.5	0.689	0.532	0.400	0.377	0.364	0.348	0.339	0.326	0.322	0.318	0.312	0.308	0.301	0.286	0.276
261.6	0.691	0.534	0.402	0.379	0.366	0.350	0.341	0.329	0.324	0.320	0.315	0.310	0.303	0.288	0.278
261.7	0.693	0.537	0.405	0.382	0.369	0.353	0.344	0.331	0.327	0.323	0.317	0.312	0.305	0.290	0.280
261.8	0.696	0.539	0.408	0.384	0.372	0.355	0.346	0.334	0.329	0.325	0.319	0.315	0.307	0.292	0.282

261.9	0.698	0.542	0.410	0.387	0.374	0.358	0.349	0.336	0.332	0.328	0.322	0.317	0.310	0.294	0.284
262	0.700	0.544	0.413	0.390	0.377	0.361	0.352	0.339	0.334	0.330	0.324	0.319	0.312	0.296	0.285
262.1	0.702	0.546	0.415	0.392	0.379	0.363	0.354	0.341	0.336	0.332	0.326	0.321	0.314	0.298	0.287
262.2	0.704	0.548	0.418	0.394	0.382	0.365	0.356	0.343	0.339	0.335	0.328	0.323	0.316	0.299	0.289
262.3	0.706	0.551	0.420	0.397	0.384	0.368	0.359	0.346	0.341	0.337	0.330	0.325	0.318	0.301	0.290
262.4	0.708	0.553	0.423	0.399	0.387	0.370	0.361	0.348	0.343	0.339	0.333	0.328	0.320	0.303	0.292
262.5	0.710	0.555	0.425	0.402	0.389	0.373	0.364	0.350	0.346	0.341	0.335	0.330	0.322	0.305	0.294
262.6	0.713	0.558	0.428	0.405	0.392	0.375	0.366	0.353	0.348	0.344	0.337	0.332	0.324	0.307	0.296
262.7	0.715	0.560	0.431	0.407	0.394	0.378	0.369	0.356	0.351	0.347	0.340	0.334	0.327	0.309	0.298
262.8	0.717	0.562	0.433	0.410	0.397	0.381	0.372	0.358	0.353	0.349	0.342	0.337	0.329	0.311	0.300
262.9	0.720	0.565	0.436	0.413	0.400	0.384	0.374	0.361	0.356	0.352	0.345	0.339	0.331	0.313	0.302
263	0.722	0.568	0.439	0.416	0.403	0.387	0.377	0.364	0.359	0.354	0.347	0.342	0.333	0.315	0.304
263.1	0.724	0.570	0.442	0.418	0.405	0.389	0.380	0.366	0.361	0.357	0.350	0.344	0.336	0.318	0.306
263.2	0.727	0.573	0.445	0.421	0.408	0.392	0.383	0.369	0.364	0.359	0.352	0.346	0.338	0.320	0.308
263.3	0.729	0.575	0.448	0.424	0.411	0.395	0.386	0.372	0.366	0.362	0.354	0.349	0.340	0.322	0.310
263.4	0.731	0.578	0.450	0.427	0.414	0.398	0.388	0.374	0.369	0.364	0.357	0.351	0.343	0.324	0.311
263.5	0.734	0.581	0.453	0.430	0.417	0.401	0.391	0.377	0.372	0.367	0.360	0.354	0.345	0.326	0.313
263.6	0.736	0.583	0.456	0.432	0.420	0.403	0.394	0.380	0.374	0.370	0.362	0.356	0.348	0.328	0.315
263.7	0.739	0.586	0.459	0.435	0.423	0.406	0.397	0.382	0.377	0.373	0.365	0.359	0.350	0.330	0.317
263.8	0.741	0.589	0.462	0.438	0.426	0.409	0.400	0.385	0.380	0.375	0.367	0.361	0.352	0.333	0.320
263.9	0.744	0.591	0.465	0.441	0.429	0.412	0.403	0.388	0.383	0.378	0.370	0.364	0.355	0.335	0.322
264	0.746	0.594	0.468	0.444	0.432	0.415	0.406	0.391	0.385	0.381	0.373	0.366	0.357	0.337	0.324
264.1	0.749	0.597	0.471	0.447	0.435	0.418	0.409	0.394	0.388	0.383	0.375	0.369	0.360	0.339	0.326
264.2	0.751	0.600	0.474	0.450	0.438	0.421	0.412	0.397	0.391	0.386	0.378	0.372	0.362	0.342	0.328
264.3	0.754	0.602	0.477	0.453	0.441	0.424	0.415	0.399	0.394	0.389	0.380	0.374	0.365	0.344	0.330
264.4	0.756	0.605	0.480	0.456	0.444	0.427	0.417	0.402	0.396	0.391	0.383	0.377	0.367	0.346	0.332
264.5	0.758	0.608	0.483	0.459	0.446	0.430	0.420	0.405	0.399	0.394	0.386	0.379	0.370	0.348	0.334
264.6	0.761	0.610	0.486	0.462	0.449	0.433	0.423	0.408	0.402	0.397	0.388	0.382	0.372	0.351	0.336
264.7	0.764	0.613	0.489	0.465	0.453	0.436	0.426	0.410	0.405	0.399	0.391	0.384	0.374	0.353	0.338
264.8	0.766	0.616	0.492	0.468	0.456	0.439	0.429	0.413	0.407	0.402	0.393	0.387	0.377	0.355	0.340
264.9	0.769	0.619	0.495	0.472	0.459	0.443	0.433	0.417	0.411	0.405	0.396	0.390	0.380	0.358	0.342
265	0.772	0.622	0.498	0.475	0.462	0.446	0.436	0.420	0.414	0.408	0.399	0.393	0.382	0.360	0.345
265.1	0.775	0.625	0.502	0.478	0.466	0.449	0.439	0.423	0.417	0.411	0.402	0.395	0.385	0.363	0.347
265.2	0.778	0.628	0.505	0.482	0.469	0.453	0.442	0.426	0.420	0.414	0.405	0.398	0.388	0.365	0.349
265.3	0.781	0.631	0.508	0.485	0.472	0.456	0.446	0.429	0.423	0.418	0.408	0.401	0.391	0.368	0.352
265.4	0.784	0.635	0.512	0.488	0.476	0.459	0.449	0.433	0.426	0.421	0.411	0.404	0.394	0.370	0.354
265.5	0.787	0.638	0.515	0.492	0.479	0.463	0.452	0.436	0.429	0.424	0.414	0.407	0.397	0.373	0.357
265.6	0.790	0.641	0.519	0.495	0.483	0.466	0.456	0.439	0.433	0.427	0.417	0.410	0.399	0.376	0.359
265.7	0.793	0.644	0.522	0.499	0.486	0.469	0.459	0.442	0.436	0.430	0.420	0.413	0.402	0.378	0.362
265.8	0.796	0.647	0.526	0.502	0.490	0.473	0.463	0.446	0.439	0.434	0.424	0.417	0.405	0.381	0.364
265.9	0.799	0.651	0.529	0.505	0.493	0.477	0.466	0.449	0.443	0.437	0.427	0.420	0.408	0.384	0.367

266	0.802	0.654	0.533	0.509	0.496	0.480	0.470	0.452	0.446	0.440	0.430	0.423	0.411	0.386	0.369
266.1	0.805	0.657	0.536	0.512	0.500	0.483	0.473	0.456	0.449	0.443	0.433	0.426	0.414	0.389	0.372
266.2	0.808	0.660	0.540	0.516	0.503	0.487	0.476	0.459	0.452	0.446	0.436	0.429	0.417	0.392	0.374
266.3	0.811	0.664	0.543	0.519	0.507	0.490	0.480	0.462	0.456	0.450	0.439	0.432	0.420	0.394	0.377
266.4	0.814	0.667	0.546	0.523	0.510	0.494	0.483	0.466	0.459	0.453	0.443	0.435	0.423	0.397	0.379
266.5	0.818	0.670	0.550	0.526	0.514	0.497	0.487	0.469	0.462	0.456	0.446	0.438	0.426	0.400	0.382
266.6	0.821	0.674	0.553	0.530	0.517	0.500	0.490	0.472	0.465	0.459	0.449	0.441	0.429	0.403	0.385
266.7	0.824	0.677	0.557	0.533	0.521	0.504	0.494	0.476	0.469	0.463	0.452	0.444	0.432	0.405	0.387
266.8	0.827	0.680	0.560	0.537	0.524	0.507	0.497	0.479	0.472	0.466	0.455	0.447	0.435	0.408	0.390
266.9	0.830	0.684	0.564	0.540	0.528	0.511	0.500	0.482	0.475	0.469	0.458	0.450	0.438	0.411	0.392
267	0.833	0.686	0.567	0.543	0.531	0.514	0.503	0.485	0.478	0.472	0.461	0.453	0.440	0.413	0.395
267.1	0.836	0.689	0.570	0.546	0.534	0.517	0.506	0.488	0.481	0.474	0.464	0.455	0.443	0.416	0.397
267.2	0.838	0.692	0.573	0.549	0.537	0.520	0.509	0.491	0.483	0.477	0.466	0.458	0.445	0.418	0.399
267.3	0.841	0.695	0.576	0.552	0.539	0.522	0.512	0.494	0.486	0.480	0.469	0.461	0.448	0.420	0.401
267.4	0.844	0.698	0.579	0.555	0.542	0.525	0.515	0.496	0.489	0.482	0.471	0.463	0.450	0.423	0.403
267.5	0.847	0.701	0.582	0.558	0.546	0.528	0.518	0.499	0.492	0.485	0.474	0.466	0.453	0.425	0.406
267.6	0.850	0.704	0.585	0.561	0.549	0.531	0.521	0.502	0.495	0.488	0.477	0.469	0.456	0.428	0.408
267.7	0.854	0.708	0.588	0.564	0.552	0.534	0.523	0.505	0.498	0.491	0.480	0.472	0.459	0.430	0.411
267.8	0.857	0.711	0.592	0.567	0.555	0.537	0.526	0.508	0.501	0.494	0.483	0.474	0.461	0.433	0.413
267.9	0.860	0.714	0.595	0.570	0.557	0.540	0.529	0.511	0.503	0.497	0.485	0.477	0.464	0.435	0.416
268	0.863	0.717	0.598	0.573	0.560	0.543	0.532	0.514	0.506	0.499	0.488	0.480	0.467	0.438	0.418
268.1	0.866	0.720	0.601	0.576	0.563	0.546	0.535	0.516	0.509	0.502	0.491	0.482	0.469	0.440	0.420
268.2	0.869	0.723	0.604	0.579	0.566	0.549	0.538	0.519	0.512	0.505	0.493	0.485	0.472	0.442	0.423
268.3	0.871	0.725	0.606	0.582	0.569	0.552	0.540	0.522	0.514	0.507	0.496	0.487	0.474	0.445	0.425
268.4	0.874	0.728	0.609	0.584	0.571	0.554	0.543	0.524	0.517	0.510	0.498	0.490	0.477	0.447	0.427
268.5	0.877	0.731	0.612	0.587	0.574	0.557	0.546	0.527	0.519	0.513	0.501	0.492	0.479	0.449	0.429
268.6	0.880	0.734	0.615	0.590	0.577	0.559	0.548	0.529	0.522	0.515	0.503	0.495	0.481	0.452	0.431
268.7	0.883	0.737	0.618	0.593	0.580	0.562	0.551	0.532	0.524	0.518	0.506	0.497	0.484	0.454	0.433
268.8	0.886	0.739	0.620	0.595	0.582	0.565	0.554	0.535	0.527	0.520	0.508	0.500	0.486	0.456	0.435
268.9	0.889	0.742	0.623	0.598	0.585	0.567	0.556	0.537	0.530	0.523	0.511	0.502	0.489	0.458	0.437
269	0.891	0.745	0.626	0.601	0.588	0.570	0.559	0.540	0.532	0.525	0.513	0.505	0.491	0.460	0.439
269.1	0.894	0.748	0.629	0.603	0.590	0.573	0.562	0.542	0.535	0.528	0.516	0.507	0.493	0.462	0.441
269.2	0.897	0.750	0.631	0.606	0.593	0.575	0.564	0.545	0.537	0.530	0.518	0.509	0.495	0.464	0.443
269.3	0.899	0.753	0.634	0.609	0.595	0.578	0.567	0.547	0.539	0.533	0.520	0.511	0.497	0.466	0.445
269.4	0.902	0.756	0.637	0.611	0.598	0.580	0.569	0.550	0.542	0.535	0.523	0.514	0.500	0.468	0.447
269.5	0.905	0.758	0.640	0.614	0.600	0.583	0.572	0.552	0.544	0.537	0.525	0.516	0.502	0.470	0.449
269.6	0.907	0.761	0.642	0.616	0.603	0.585	0.574	0.555	0.547	0.540	0.527	0.518	0.504	0.472	0.450
269.7	0.910	0.764	0.645	0.619	0.606	0.588	0.577	0.557	0.549	0.542	0.529	0.520	0.506	0.474	0.452
269.8	0.913	0.766	0.647	0.622	0.608	0.590	0.579	0.559	0.551	0.544	0.532	0.522	0.508	0.476	0.454
269.9	0.915	0.768	0.650	0.624	0.610	0.592	0.582	0.561	0.553	0.546	0.533	0.524	0.510	0.478	0.456
270	0.917	0.771	0.652	0.626	0.612	0.595	0.584	0.563	0.555	0.548	0.535	0.526	0.512	0.479	0.457

270.1	0.920	0.773	0.654	0.628	0.615	0.597	0.586	0.566	0.558	0.550	0.537	0.528	0.513	0.481	0.459
270.2	0.922	0.776	0.657	0.631	0.617	0.599	0.588	0.568	0.560	0.552	0.539	0.530	0.515	0.483	0.460
270.3	0.924	0.778	0.660	0.633	0.619	0.602	0.591	0.570	0.562	0.555	0.541	0.532	0.517	0.484	0.462
270.4	0.927	0.781	0.662	0.636	0.622	0.604	0.593	0.572	0.564	0.557	0.543	0.534	0.519	0.486	0.463
270.5	0.929	0.783	0.665	0.638	0.624	0.606	0.595	0.575	0.566	0.559	0.545	0.536	0.521	0.488	0.465
270.6	0.932	0.786	0.667	0.641	0.626	0.609	0.598	0.577	0.568	0.561	0.548	0.538	0.523	0.489	0.467
270.7	0.934	0.788	0.670	0.643	0.629	0.611	0.600	0.579	0.571	0.563	0.550	0.540	0.525	0.491	0.468
270.8	0.937	0.791	0.672	0.646	0.631	0.614	0.603	0.581	0.573	0.565	0.552	0.542	0.527	0.493	0.470
270.9	0.939	0.793	0.675	0.648	0.634	0.616	0.605	0.584	0.575	0.568	0.554	0.544	0.529	0.495	0.472
271	0.942	0.796	0.678	0.651	0.637	0.619	0.608	0.586	0.578	0.570	0.556	0.546	0.531	0.497	0.474
271.1	0.944	0.798	0.681	0.654	0.639	0.621	0.610	0.588	0.580	0.572	0.558	0.548	0.533	0.498	0.475
271.2	0.947	0.801	0.683	0.656	0.642	0.624	0.613	0.591	0.583	0.575	0.561	0.551	0.535	0.500	0.477
271.3	0.950	0.804	0.686	0.659	0.644	0.626	0.615	0.593	0.585	0.577	0.563	0.553	0.537	0.502	0.479
271.4	0.952	0.806	0.688	0.661	0.647	0.629	0.618	0.596	0.587	0.579	0.565	0.555	0.539	0.504	0.480
271.5	0.955	0.808	0.691	0.664	0.649	0.632	0.621	0.598	0.589	0.582	0.567	0.557	0.541	0.506	0.482
271.6	0.957	0.811	0.694	0.666	0.652	0.634	0.623	0.601	0.592	0.584	0.570	0.559	0.544	0.508	0.484
271.7	0.959	0.814	0.696	0.669	0.655	0.637	0.626	0.603	0.594	0.587	0.572	0.562	0.546	0.510	0.486
271.8	0.961	0.816	0.699	0.672	0.657	0.640	0.628	0.606	0.597	0.589	0.574	0.564	0.548	0.512	0.488
271.9	0.964	0.819	0.702	0.675	0.660	0.642	0.631	0.608	0.600	0.592	0.577	0.566	0.550	0.514	0.490
272	0.966	0.821	0.705	0.677	0.663	0.645	0.634	0.611	0.602	0.594	0.579	0.569	0.552	0.516	0.492
272.1	0.969	0.824	0.707	0.680	0.666	0.648	0.637	0.614	0.605	0.597	0.582	0.571	0.555	0.518	0.494
272.2	0.971	0.827	0.710	0.683	0.668	0.651	0.639	0.616	0.607	0.599	0.584	0.574	0.557	0.520	0.496
272.3	0.974	0.830	0.713	0.685	0.671	0.653	0.642	0.619	0.610	0.602	0.587	0.576	0.559	0.522	0.498
272.4	0.977	0.832	0.715	0.688	0.674	0.656	0.645	0.622	0.613	0.604	0.589	0.579	0.562	0.524	0.500
272.5	0.979	0.835	0.718	0.691	0.677	0.659	0.648	0.624	0.615	0.607	0.592	0.581	0.564	0.526	0.502
272.6	0.982	0.838	0.721	0.694	0.680	0.662	0.650	0.627	0.618	0.610	0.594	0.584	0.566	0.529	0.504
272.7	0.985	0.840	0.724	0.696	0.682	0.664	0.653	0.630	0.621	0.612	0.597	0.586	0.569	0.531	0.506
272.8	0.987	0.843	0.727	0.699	0.685	0.667	0.656	0.633	0.623	0.615	0.600	0.589	0.571	0.533	0.508
272.9	0.990	0.846	0.729	0.702	0.688	0.670	0.659	0.635	0.626	0.618	0.602	0.591	0.574	0.535	0.511
273	0.992	0.848	0.732	0.704	0.690	0.672	0.661	0.638	0.628	0.620	0.604	0.593	0.576	0.537	0.513
273.1	0.994	0.850	0.734	0.707	0.693	0.675	0.664	0.640	0.631	0.622	0.607	0.596	0.578	0.540	0.514
273.2	0.996	0.853	0.737	0.709	0.695	0.677	0.666	0.643	0.633	0.625	0.609	0.598	0.580	0.541	0.516
273.3	0.999	0.855	0.739	0.712	0.698	0.680	0.669	0.645	0.636	0.627	0.611	0.600	0.582	0.543	0.518
273.4	1.001	0.857	0.741	0.714	0.700	0.682	0.671	0.647	0.638	0.629	0.614	0.602	0.585	0.545	0.520
273.5	1.003	0.860	0.744	0.716	0.702	0.685	0.674	0.650	0.640	0.632	0.616	0.605	0.587	0.548	0.522
273.6	1.006	0.862	0.746	0.719	0.705	0.687	0.676	0.652	0.643	0.634	0.618	0.607	0.589	0.550	0.524
273.7	1.008	0.865	0.749	0.722	0.707	0.690	0.679	0.655	0.645	0.637	0.621	0.609	0.592	0.552	0.526
273.8	1.010	0.867	0.751	0.724	0.710	0.692	0.681	0.657	0.648	0.639	0.623	0.612	0.594	0.554	0.528
273.9	1.013	0.869	0.753	0.726	0.712	0.695	0.684	0.659	0.650	0.641	0.626	0.614	0.596	0.556	0.530
274	1.015	0.871	0.756	0.728	0.715	0.697	0.686	0.662	0.653	0.643	0.628	0.616	0.598	0.558	0.532
274.1	1.017	0.874	0.758	0.731	0.717	0.699	0.688	0.664	0.655	0.646	0.630	0.619	0.600	0.560	0.534

274.2	1.019	0.876	0.760	0.733	0.719	0.701	0.690	0.666	0.657	0.648	0.632	0.621	0.603	0.562	0.536
274.3	1.021	0.878	0.762	0.735	0.721	0.703	0.692	0.668	0.659	0.650	0.634	0.623	0.604	0.564	0.538
274.4	1.023	0.880	0.764	0.737	0.723	0.705	0.694	0.671	0.661	0.652	0.636	0.625	0.606	0.566	0.540
274.5	1.025	0.882	0.766	0.739	0.725	0.707	0.696	0.672	0.663	0.654	0.638	0.626	0.608	0.568	0.542
274.6	1.027	0.884	0.768	0.740	0.727	0.708	0.698	0.674	0.665	0.656	0.640	0.628	0.610	0.569	0.543
274.7	1.030	0.886	0.770	0.742	0.728	0.710	0.699	0.676	0.666	0.658	0.641	0.630	0.611	0.571	0.545
274.8	1.031	0.887	0.771	0.743	0.730	0.711	0.701	0.677	0.668	0.659	0.643	0.631	0.613	0.572	0.546
274.9	1.033	0.889	0.773	0.745	0.731	0.713	0.702	0.679	0.669	0.660	0.644	0.633	0.614	0.574	0.548
275	1.035	0.891	0.774	0.746	0.732	0.714	0.703	0.680	0.671	0.662	0.646	0.634	0.616	0.575	0.549
275.1	1.037	0.892	0.775	0.747	0.734	0.715	0.705	0.681	0.672	0.663	0.647	0.636	0.617	0.577	0.550
275.2	1.039	0.893	0.776	0.748	0.734	0.716	0.705	0.682	0.673	0.664	0.648	0.637	0.618	0.578	0.552
275.3	1.040	0.894	0.777	0.749	0.735	0.717	0.706	0.683	0.674	0.665	0.649	0.638	0.619	0.578	0.553
275.4	1.041	0.895	0.778	0.750	0.735	0.717	0.707	0.683	0.675	0.666	0.650	0.638	0.620	0.579	0.554
275.5	1.043	0.896	0.779	0.750	0.736	0.717	0.707	0.684	0.675	0.666	0.650	0.639	0.621	0.580	0.555
275.6	1.044	0.897	0.779	0.750	0.736	0.718	0.707	0.684	0.676	0.667	0.651	0.640	0.621	0.581	0.555
275.7	1.045	0.897	0.779	0.750	0.736	0.718	0.707	0.685	0.676	0.667	0.651	0.640	0.622	0.581	0.556
275.8	1.046	0.898	0.779	0.750	0.736	0.718	0.707	0.685	0.676	0.667	0.651	0.640	0.622	0.582	0.557
275.9	1.046	0.898	0.779	0.750	0.736	0.717	0.707	0.685	0.676	0.667	0.651	0.641	0.622	0.582	0.557
276	1.047	0.898	0.779	0.750	0.735	0.717	0.706	0.684	0.676	0.667	0.651	0.641	0.622	0.582	0.557
276.1	1.048	0.898	0.779	0.750	0.735	0.716	0.706	0.684	0.675	0.667	0.651	0.640	0.622	0.582	0.557
276.2	1.048	0.898	0.778	0.749	0.734	0.715	0.705	0.683	0.675	0.666	0.651	0.640	0.622	0.582	0.557
276.3	1.048	0.898	0.778	0.748	0.733	0.714	0.704	0.682	0.674	0.666	0.650	0.640	0.622	0.582	0.557
276.4	1.048	0.897	0.777	0.747	0.732	0.713	0.703	0.681	0.673	0.665	0.650	0.639	0.621	0.582	0.557
276.5	1.048	0.897	0.776	0.746	0.731	0.712	0.702	0.680	0.672	0.664	0.649	0.638	0.620	0.581	0.557
276.6	1.048	0.896	0.775	0.745	0.729	0.710	0.701	0.679	0.671	0.663	0.648	0.637	0.620	0.580	0.556
276.7	1.048	0.896	0.774	0.743	0.728	0.709	0.699	0.677	0.670	0.662	0.647	0.636	0.618	0.580	0.555
276.8	1.047	0.895	0.773	0.742	0.726	0.707	0.698	0.676	0.668	0.660	0.645	0.635	0.617	0.578	0.554
276.9	1.047	0.894	0.771	0.740	0.724	0.705	0.696	0.674	0.666	0.658	0.643	0.633	0.615	0.577	0.553
277	1.046	0.893	0.770	0.738	0.722	0.703	0.693	0.672	0.664	0.656	0.642	0.631	0.614	0.575	0.552
277.1	1.046	0.892	0.768	0.736	0.719	0.700	0.691	0.670	0.662	0.654	0.639	0.629	0.612	0.574	0.550
277.2	1.045	0.890	0.766	0.734	0.717	0.698	0.688	0.667	0.659	0.651	0.637	0.627	0.609	0.572	0.548
277.3	1.044	0.888	0.764	0.731	0.714	0.695	0.685	0.664	0.657	0.649	0.634	0.624	0.607	0.569	0.546
277.4	1.043	0.886	0.761	0.729	0.712	0.692	0.683	0.662	0.654	0.646	0.632	0.622	0.605	0.567	0.544
277.5	1.041	0.884	0.759	0.726	0.709	0.689	0.680	0.659	0.651	0.643	0.629	0.619	0.602	0.565	0.542
277.6	1.040	0.882	0.757	0.724	0.706	0.686	0.676	0.656	0.648	0.640	0.626	0.616	0.599	0.562	0.539
277.7	1.038	0.880	0.754	0.721	0.703	0.683	0.673	0.652	0.644	0.637	0.622	0.612	0.596	0.559	0.536
277.8	1.036	0.878	0.751	0.718	0.700	0.679	0.670	0.649	0.641	0.633	0.619	0.609	0.592	0.556	0.533
277.9	1.034	0.876	0.749	0.715	0.696	0.676	0.666	0.645	0.637	0.630	0.615	0.606	0.589	0.553	0.530
278	1.032	0.874	0.746	0.712	0.693	0.673	0.663	0.641	0.634	0.626	0.612	0.602	0.586	0.549	0.527
278.1	1.030	0.871	0.743	0.709	0.690	0.669	0.659	0.638	0.630	0.622	0.608	0.598	0.582	0.546	0.524
278.2	1.028	0.868	0.740	0.705	0.686	0.665	0.655	0.634	0.626	0.618	0.604	0.595	0.578	0.542	0.520

278.3	1.026	0.866	0.737	0.702	0.683	0.662	0.652	0.630	0.622	0.615	0.601	0.591	0.574	0.538	0.517
278.4	1.023	0.863	0.734	0.699	0.679	0.658	0.648	0.626	0.618	0.611	0.597	0.587	0.570	0.535	0.514
278.5	1.020	0.859	0.731	0.695	0.676	0.655	0.644	0.622	0.614	0.607	0.593	0.583	0.567	0.531	0.510
278.6	1.017	0.856	0.727	0.692	0.672	0.651	0.641	0.618	0.610	0.603	0.589	0.579	0.563	0.527	0.506
278.7	1.014	0.853	0.724	0.689	0.669	0.647	0.637	0.614	0.606	0.599	0.585	0.575	0.559	0.523	0.503
278.8	1.011	0.849	0.721	0.685	0.665	0.644	0.633	0.610	0.603	0.595	0.581	0.571	0.555	0.520	0.499
278.9	1.008	0.846	0.718	0.682	0.662	0.640	0.630	0.607	0.599	0.591	0.577	0.567	0.551	0.516	0.495
279	1.004	0.842	0.714	0.678	0.658	0.637	0.626	0.603	0.595	0.587	0.573	0.563	0.547	0.512	0.491
279.1	1.001	0.839	0.711	0.675	0.655	0.633	0.623	0.599	0.591	0.583	0.570	0.559	0.543	0.508	0.488
279.2	0.997	0.835	0.708	0.671	0.651	0.630	0.619	0.596	0.588	0.580	0.566	0.556	0.540	0.505	0.484
279.3	0.993	0.832	0.704	0.668	0.648	0.626	0.616	0.593	0.584	0.576	0.562	0.552	0.536	0.501	0.481
279.4	0.990	0.828	0.701	0.665	0.645	0.623	0.613	0.589	0.581	0.573	0.559	0.549	0.533	0.498	0.477
279.5	0.986	0.825	0.698	0.662	0.642	0.620	0.610	0.586	0.578	0.570	0.556	0.545	0.529	0.494	0.474
279.6	0.982	0.821	0.695	0.659	0.639	0.617	0.607	0.583	0.575	0.567	0.552	0.542	0.526	0.491	0.471
279.7	0.978	0.818	0.692	0.657	0.637	0.615	0.605	0.581	0.572	0.564	0.550	0.540	0.523	0.488	0.468
279.8	0.975	0.814	0.689	0.654	0.634	0.613	0.602	0.578	0.570	0.561	0.547	0.537	0.520	0.485	0.466
279.9	0.971	0.811	0.687	0.652	0.632	0.610	0.600	0.576	0.567	0.559	0.545	0.534	0.518	0.483	0.463
280	0.967	0.808	0.684	0.649	0.630	0.609	0.598	0.574	0.565	0.557	0.543	0.532	0.516	0.481	0.461
280.1	0.964	0.805	0.682	0.647	0.628	0.607	0.596	0.572	0.563	0.555	0.541	0.530	0.514	0.479	0.459
280.2	0.960	0.802	0.680	0.645	0.626	0.605	0.595	0.570	0.561	0.553	0.538	0.528	0.511	0.476	0.457
280.3	0.956	0.799	0.677	0.643	0.624	0.603	0.593	0.569	0.559	0.551	0.537	0.526	0.510	0.475	0.455
280.4	0.952	0.796	0.675	0.641	0.622	0.602	0.591	0.567	0.558	0.549	0.535	0.524	0.508	0.473	0.453
280.5	0.949	0.793	0.673	0.639	0.621	0.600	0.590	0.566	0.556	0.548	0.534	0.523	0.507	0.471	0.452
280.6	0.945	0.791	0.670	0.637	0.619	0.599	0.589	0.564	0.555	0.547	0.532	0.522	0.505	0.470	0.451
280.7	0.942	0.788	0.668	0.635	0.618	0.598	0.588	0.563	0.554	0.546	0.531	0.521	0.504	0.469	0.450
280.8	0.938	0.785	0.666	0.634	0.617	0.597	0.587	0.562	0.553	0.545	0.531	0.520	0.503	0.468	0.449
280.9	0.935	0.783	0.665	0.632	0.616	0.596	0.586	0.562	0.552	0.544	0.530	0.519	0.503	0.467	0.448
281	0.932	0.780	0.663	0.631	0.615	0.595	0.585	0.561	0.552	0.544	0.529	0.519	0.502	0.467	0.448
281.1	0.929	0.778	0.661	0.630	0.614	0.594	0.584	0.561	0.552	0.543	0.529	0.519	0.502	0.467	0.447
281.2	0.926	0.775	0.660	0.628	0.613	0.594	0.584	0.561	0.552	0.543	0.529	0.518	0.502	0.467	0.448
281.3	0.923	0.773	0.658	0.627	0.612	0.593	0.583	0.560	0.551	0.543	0.529	0.518	0.502	0.467	0.448
281.4	0.920	0.771	0.657	0.626	0.612	0.593	0.583	0.560	0.552	0.543	0.529	0.519	0.502	0.467	0.448
281.5	0.918	0.769	0.656	0.625	0.611	0.592	0.583	0.560	0.552	0.544	0.529	0.519	0.503	0.468	0.449
281.6	0.916	0.767	0.654	0.624	0.610	0.592	0.582	0.560	0.552	0.544	0.530	0.519	0.503	0.468	0.449
281.7	0.914	0.766	0.653	0.623	0.610	0.592	0.582	0.560	0.552	0.544	0.530	0.520	0.504	0.469	0.450
281.8	0.912	0.764	0.652	0.622	0.609	0.591	0.582	0.561	0.552	0.544	0.531	0.521	0.505	0.470	0.451
281.9	0.910	0.762	0.651	0.621	0.609	0.591	0.581	0.561	0.553	0.545	0.531	0.521	0.505	0.471	0.452
282	0.908	0.761	0.649	0.620	0.608	0.590	0.581	0.561	0.553	0.545	0.532	0.522	0.506	0.472	0.453
282.1	0.906	0.759	0.648	0.619	0.607	0.590	0.581	0.561	0.553	0.545	0.532	0.522	0.507	0.472	0.454
282.2	0.905	0.757	0.647	0.618	0.606	0.589	0.580	0.561	0.553	0.545	0.532	0.523	0.507	0.473	0.455
282.3	0.903	0.756	0.646	0.617	0.606	0.588	0.580	0.560	0.553	0.545	0.533	0.523	0.508	0.474	0.456

282.4	0.902	0.755	0.644	0.616	0.604	0.587	0.579	0.560	0.553	0.545	0.533	0.523	0.508	0.475	0.457
282.5	0.901	0.753	0.643	0.615	0.603	0.586	0.578	0.559	0.553	0.545	0.533	0.523	0.509	0.475	0.458
282.6	0.899	0.752	0.642	0.613	0.602	0.585	0.577	0.559	0.552	0.545	0.533	0.523	0.509	0.476	0.458
282.7	0.898	0.751	0.640	0.612	0.600	0.583	0.576	0.558	0.551	0.544	0.532	0.523	0.509	0.476	0.459
282.8	0.897	0.749	0.638	0.610	0.598	0.581	0.574	0.556	0.550	0.543	0.531	0.523	0.509	0.476	0.459
282.9	0.896	0.747	0.637	0.608	0.597	0.580	0.572	0.555	0.549	0.543	0.531	0.522	0.508	0.476	0.459
283	0.895	0.746	0.635	0.606	0.595	0.578	0.570	0.553	0.548	0.541	0.530	0.521	0.508	0.476	0.459
283.1	0.894	0.744	0.633	0.604	0.593	0.575	0.568	0.552	0.546	0.540	0.528	0.520	0.507	0.476	0.459
283.2	0.893	0.743	0.631	0.602	0.590	0.573	0.565	0.550	0.544	0.538	0.527	0.519	0.506	0.476	0.459
283.3	0.892	0.741	0.629	0.599	0.588	0.570	0.563	0.547	0.542	0.536	0.525	0.518	0.504	0.475	0.458
283.4	0.891	0.739	0.626	0.596	0.584	0.567	0.559	0.544	0.539	0.534	0.523	0.516	0.503	0.473	0.457
283.5	0.890	0.737	0.623	0.593	0.581	0.563	0.556	0.541	0.536	0.531	0.521	0.513	0.501	0.472	0.456
283.6	0.889	0.734	0.620	0.590	0.577	0.559	0.552	0.538	0.533	0.528	0.518	0.511	0.499	0.470	0.455
283.7	0.887	0.731	0.616	0.586	0.573	0.555	0.548	0.534	0.529	0.524	0.515	0.508	0.496	0.468	0.453
283.8	0.885	0.728	0.612	0.582	0.568	0.550	0.543	0.530	0.525	0.520	0.511	0.504	0.493	0.465	0.450
283.9	0.883	0.725	0.608	0.577	0.563	0.545	0.538	0.525	0.521	0.516	0.507	0.500	0.489	0.462	0.448
284	0.881	0.721	0.604	0.572	0.558	0.539	0.533	0.520	0.516	0.511	0.503	0.496	0.485	0.459	0.444
284.1	0.878	0.717	0.599	0.567	0.553	0.533	0.527	0.514	0.510	0.506	0.498	0.492	0.480	0.455	0.441
284.2	0.875	0.713	0.594	0.561	0.547	0.527	0.521	0.508	0.505	0.501	0.492	0.487	0.475	0.450	0.437
284.3	0.872	0.709	0.589	0.556	0.541	0.521	0.514	0.502	0.499	0.495	0.487	0.481	0.470	0.446	0.432
284.4	0.868	0.704	0.583	0.550	0.534	0.514	0.508	0.496	0.492	0.488	0.481	0.475	0.465	0.441	0.427
284.5	0.864	0.699	0.578	0.543	0.527	0.507	0.501	0.489	0.486	0.482	0.474	0.469	0.459	0.435	0.422
284.6	0.860	0.693	0.571	0.536	0.520	0.500	0.494	0.482	0.479	0.475	0.468	0.462	0.452	0.429	0.417
284.7	0.856	0.687	0.565	0.530	0.513	0.492	0.486	0.475	0.472	0.468	0.461	0.455	0.446	0.423	0.411
284.8	0.851	0.681	0.558	0.522	0.505	0.484	0.478	0.467	0.464	0.460	0.453	0.448	0.438	0.416	0.405
284.9	0.845	0.675	0.551	0.515	0.497	0.476	0.470	0.459	0.456	0.452	0.445	0.440	0.431	0.409	0.398
285	0.839	0.668	0.543	0.507	0.489	0.468	0.462	0.451	0.448	0.444	0.437	0.432	0.423	0.402	0.391
285.1	0.833	0.660	0.536	0.498	0.481	0.459	0.454	0.442	0.439	0.435	0.429	0.424	0.415	0.395	0.384
285.2	0.826	0.653	0.527	0.490	0.472	0.450	0.445	0.433	0.430	0.426	0.420	0.415	0.407	0.387	0.376
285.3	0.819	0.645	0.519	0.481	0.463	0.441	0.436	0.424	0.421	0.417	0.411	0.406	0.398	0.379	0.369
285.4	0.812	0.637	0.511	0.473	0.454	0.432	0.427	0.415	0.412	0.408	0.402	0.397	0.389	0.371	0.361
285.5	0.804	0.628	0.502	0.464	0.445	0.423	0.418	0.405	0.402	0.399	0.393	0.388	0.381	0.362	0.353
285.6	0.796	0.620	0.494	0.455	0.436	0.414	0.408	0.396	0.393	0.390	0.384	0.379	0.372	0.354	0.345
285.7	0.788	0.611	0.485	0.446	0.427	0.404	0.399	0.386	0.384	0.380	0.375	0.370	0.363	0.345	0.337
285.8	0.779	0.602	0.476	0.437	0.418	0.395	0.390	0.377	0.374	0.371	0.366	0.361	0.354	0.337	0.329
285.9	0.771	0.593	0.468	0.429	0.409	0.387	0.381	0.368	0.366	0.362	0.357	0.353	0.346	0.329	0.321
286	0.763	0.585	0.459	0.420	0.400	0.378	0.372	0.360	0.357	0.353	0.348	0.344	0.337	0.321	0.314
286.1	0.754	0.576	0.450	0.411	0.391	0.369	0.363	0.351	0.348	0.344	0.339	0.335	0.329	0.313	0.306
286.2	0.745	0.567	0.442	0.402	0.382	0.360	0.354	0.342	0.339	0.336	0.331	0.327	0.320	0.305	0.298
286.3	0.736	0.558	0.433	0.393	0.373	0.351	0.345	0.333	0.330	0.327	0.322	0.318	0.312	0.297	0.290
286.4	0.726	0.548	0.423	0.384	0.364	0.342	0.335	0.323	0.320	0.317	0.313	0.309	0.302	0.289	0.282

286.5	0.716	0.538	0.414	0.374	0.354	0.332	0.326	0.314	0.311	0.308	0.303	0.299	0.293	0.280	0.274
286.6	0.705	0.528	0.404	0.365	0.345	0.323	0.317	0.304	0.302	0.299	0.294	0.290	0.285	0.272	0.266
286.7	0.695	0.517	0.394	0.355	0.336	0.313	0.307	0.295	0.292	0.289	0.285	0.281	0.276	0.263	0.258
286.8	0.684	0.507	0.385	0.346	0.326	0.304	0.298	0.286	0.283	0.280	0.276	0.272	0.267	0.255	0.251
286.9	0.673	0.497	0.375	0.336	0.317	0.295	0.289	0.277	0.274	0.271	0.267	0.263	0.259	0.247	0.243
287	0.662	0.486	0.365	0.327	0.308	0.286	0.280	0.268	0.265	0.262	0.258	0.255	0.250	0.239	0.235
287.1	0.651	0.476	0.356	0.317	0.298	0.277	0.271	0.259	0.256	0.254	0.250	0.246	0.242	0.232	0.228
287.2	0.640	0.465	0.346	0.308	0.290	0.268	0.262	0.250	0.248	0.245	0.241	0.238	0.234	0.224	0.221
287.3	0.629	0.455	0.337	0.299	0.281	0.260	0.254	0.242	0.239	0.237	0.233	0.230	0.226	0.217	0.214
287.4	0.618	0.445	0.328	0.291	0.272	0.251	0.245	0.233	0.231	0.229	0.225	0.222	0.219	0.210	0.207
287.5	0.608	0.435	0.319	0.282	0.264	0.243	0.237	0.226	0.224	0.221	0.218	0.215	0.211	0.203	0.200
287.6	0.597	0.426	0.310	0.274	0.256	0.236	0.230	0.218	0.216	0.214	0.211	0.208	0.204	0.197	0.194
287.7	0.587	0.417	0.302	0.266	0.249	0.228	0.222	0.211	0.209	0.207	0.204	0.201	0.198	0.191	0.188
287.8	0.577	0.407	0.294	0.258	0.241	0.221	0.215	0.204	0.202	0.200	0.197	0.195	0.191	0.184	0.182
287.9	0.567	0.398	0.286	0.250	0.234	0.213	0.208	0.197	0.195	0.193	0.190	0.188	0.185	0.178	0.177
288	0.557	0.389	0.278	0.242	0.226	0.206	0.201	0.190	0.188	0.186	0.184	0.182	0.179	0.173	0.171
288.1	0.548	0.381	0.270	0.235	0.219	0.200	0.194	0.184	0.182	0.180	0.177	0.176	0.173	0.167	0.166
288.2	0.538	0.372	0.262	0.228	0.213	0.193	0.187	0.177	0.176	0.174	0.171	0.170	0.167	0.162	0.161
288.3	0.529	0.364	0.255	0.221	0.206	0.187	0.181	0.171	0.170	0.168	0.166	0.164	0.162	0.157	0.156
288.4	0.520	0.356	0.248	0.214	0.200	0.181	0.175	0.166	0.164	0.162	0.160	0.159	0.156	0.152	0.151
288.5	0.512	0.348	0.241	0.208	0.194	0.175	0.170	0.161	0.159	0.157	0.155	0.154	0.152	0.147	0.147
288.6	0.504	0.341	0.235	0.203	0.189	0.170	0.165	0.156	0.154	0.153	0.151	0.149	0.147	0.143	0.143
288.7	0.496	0.335	0.230	0.197	0.184	0.165	0.160	0.151	0.150	0.148	0.146	0.145	0.143	0.139	0.139
288.8	0.489	0.328	0.224	0.192	0.179	0.160	0.155	0.147	0.145	0.143	0.142	0.141	0.139	0.136	0.135
288.9	0.482	0.322	0.219	0.187	0.174	0.156	0.151	0.142	0.141	0.139	0.138	0.137	0.135	0.132	0.132
289	0.475	0.316	0.213	0.182	0.169	0.151	0.146	0.138	0.137	0.135	0.134	0.133	0.131	0.128	0.128
289.1	0.468	0.309	0.208	0.177	0.164	0.146	0.142	0.133	0.132	0.131	0.129	0.128	0.127	0.125	0.125
289.2	0.460	0.303	0.202	0.172	0.160	0.142	0.137	0.129	0.128	0.126	0.125	0.124	0.123	0.121	0.121
289.3	0.453	0.297	0.197	0.167	0.155	0.138	0.133	0.125	0.124	0.122	0.121	0.120	0.119	0.118	0.118
289.4	0.447	0.291	0.192	0.162	0.151	0.133	0.129	0.121	0.120	0.118	0.117	0.117	0.116	0.114	0.115
289.5	0.440	0.285	0.187	0.158	0.147	0.129	0.125	0.117	0.116	0.115	0.114	0.113	0.112	0.111	0.112
289.6	0.434	0.280	0.183	0.154	0.143	0.126	0.121	0.113	0.112	0.111	0.110	0.110	0.109	0.108	0.109
289.7	0.428	0.275	0.179	0.150	0.139	0.122	0.117	0.110	0.109	0.108	0.107	0.107	0.106	0.105	0.107
289.8	0.422	0.270	0.174	0.146	0.135	0.119	0.114	0.107	0.106	0.104	0.104	0.104	0.103	0.103	0.104
289.9	0.417	0.265	0.171	0.142	0.132	0.115	0.110	0.104	0.103	0.101	0.101	0.101	0.100	0.100	0.102
290	0.412	0.261	0.167	0.138	0.128	0.112	0.107	0.100	0.100	0.098	0.098	0.098	0.097	0.098	0.099
290.1	0.407	0.256	0.163	0.135	0.125	0.109	0.104	0.098	0.097	0.096	0.095	0.096	0.095	0.095	0.097
290.2	0.402	0.252	0.159	0.132	0.122	0.106	0.101	0.095	0.094	0.093	0.093	0.093	0.093	0.093	0.095
290.3	0.397	0.248	0.156	0.128	0.119	0.103	0.098	0.092	0.091	0.090	0.090	0.091	0.090	0.091	0.093
290.4	0.393	0.244	0.153	0.125	0.116	0.100	0.096	0.090	0.089	0.088	0.088	0.088	0.088	0.089	0.091
290.5	0.388	0.240	0.150	0.122	0.113	0.097	0.093	0.087	0.087	0.086	0.086	0.086	0.086	0.087	0.089

290.6	0.384	0.237	0.147	0.120	0.111	0.095	0.091	0.085	0.085	0.084	0.084	0.084	0.084	0.085	0.088
290.7	0.380	0.234	0.144	0.117	0.108	0.093	0.088	0.083	0.082	0.082	0.082	0.082	0.082	0.084	0.086
290.8	0.376	0.230	0.141	0.115	0.106	0.090	0.086	0.081	0.080	0.080	0.080	0.080	0.080	0.082	0.085
290.9	0.373	0.227	0.138	0.112	0.104	0.088	0.084	0.079	0.079	0.078	0.078	0.079	0.079	0.081	0.083
291	0.369	0.224	0.136	0.110	0.102	0.087	0.082	0.077	0.077	0.076	0.076	0.077	0.077	0.079	0.082
291.1	0.366	0.222	0.134	0.108	0.100	0.085	0.081	0.076	0.075	0.074	0.075	0.076	0.076	0.078	0.080
291.2	0.363	0.219	0.132	0.106	0.098	0.083	0.079	0.074	0.074	0.073	0.073	0.074	0.074	0.077	0.079
291.3	0.360	0.216	0.130	0.104	0.096	0.081	0.077	0.073	0.072	0.072	0.072	0.073	0.073	0.075	0.078
291.4	0.358	0.214	0.128	0.103	0.095	0.080	0.076	0.071	0.071	0.070	0.071	0.072	0.072	0.074	0.077
291.5	0.355	0.212	0.126	0.101	0.093	0.078	0.074	0.070	0.070	0.069	0.070	0.070	0.071	0.073	0.076
291.6	0.352	0.210	0.124	0.099	0.092	0.077	0.073	0.069	0.068	0.068	0.068	0.069	0.070	0.072	0.075
291.7	0.350	0.207	0.122	0.098	0.090	0.075	0.072	0.067	0.067	0.066	0.067	0.068	0.068	0.071	0.074
291.8	0.347	0.205	0.121	0.096	0.089	0.074	0.070	0.066	0.066	0.065	0.066	0.067	0.067	0.070	0.073
291.9	0.344	0.203	0.119	0.094	0.087	0.073	0.069	0.065	0.065	0.064	0.065	0.066	0.066	0.069	0.072
292	0.342	0.201	0.118	0.093	0.086	0.071	0.068	0.064	0.063	0.063	0.064	0.065	0.065	0.068	0.071
292.1	0.340	0.199	0.116	0.092	0.085	0.070	0.067	0.063	0.062	0.062	0.063	0.064	0.064	0.067	0.070
292.2	0.338	0.197	0.115	0.090	0.083	0.069	0.066	0.061	0.061	0.061	0.062	0.063	0.063	0.066	0.069
292.3	0.336	0.196	0.113	0.089	0.082	0.068	0.064	0.060	0.060	0.060	0.061	0.062	0.063	0.066	0.069
292.4	0.334	0.194	0.112	0.088	0.081	0.067	0.063	0.059	0.059	0.059	0.060	0.061	0.062	0.065	0.068
292.5	0.332	0.192	0.111	0.087	0.080	0.066	0.063	0.059	0.059	0.058	0.059	0.060	0.061	0.064	0.067
292.6	0.330	0.191	0.110	0.086	0.079	0.065	0.062	0.058	0.058	0.057	0.058	0.059	0.060	0.063	0.067
292.7	0.328	0.189	0.109	0.085	0.078	0.064	0.061	0.057	0.057	0.056	0.057	0.059	0.059	0.063	0.066
292.8	0.326	0.188	0.108	0.084	0.077	0.063	0.060	0.056	0.056	0.056	0.057	0.058	0.059	0.062	0.065
292.9	0.325	0.186	0.107	0.083	0.077	0.063	0.059	0.056	0.056	0.055	0.056	0.057	0.058	0.062	0.065
293	0.323	0.185	0.106	0.082	0.076	0.062	0.058	0.055	0.055	0.054	0.055	0.057	0.057	0.061	0.064
293.1	0.322	0.184	0.105	0.081	0.075	0.061	0.058	0.054	0.054	0.054	0.055	0.056	0.057	0.060	0.064
293.2	0.320	0.182	0.104	0.080	0.074	0.061	0.057	0.054	0.054	0.053	0.054	0.056	0.056	0.060	0.063
293.3	0.319	0.181	0.103	0.079	0.074	0.060	0.057	0.053	0.053	0.052	0.054	0.055	0.056	0.059	0.063
293.4	0.318	0.180	0.102	0.079	0.073	0.059	0.056	0.052	0.052	0.052	0.053	0.055	0.055	0.059	0.062
293.5	0.316	0.179	0.102	0.078	0.072	0.059	0.055	0.052	0.052	0.051	0.053	0.054	0.055	0.058	0.062
293.6	0.315	0.178	0.101	0.077	0.072	0.058	0.055	0.051	0.051	0.051	0.052	0.054	0.054	0.058	0.062
293.7	0.314	0.177	0.100	0.077	0.071	0.058	0.054	0.051	0.051	0.050	0.052	0.053	0.054	0.058	0.061
293.8	0.313	0.176	0.100	0.076	0.071	0.057	0.054	0.051	0.050	0.050	0.051	0.053	0.054	0.057	0.061
293.9	0.312	0.175	0.099	0.076	0.070	0.057	0.053	0.050	0.050	0.050	0.051	0.052	0.053	0.057	0.061
294	0.311	0.174	0.098	0.075	0.070	0.056	0.053	0.050	0.050	0.049	0.050	0.052	0.053	0.056	0.060
294.1	0.310	0.173	0.098	0.075	0.069	0.056	0.052	0.049	0.049	0.049	0.050	0.051	0.052	0.056	0.060
294.2	0.308	0.173	0.097	0.074	0.069	0.055	0.052	0.049	0.049	0.048	0.050	0.051	0.052	0.056	0.060
294.3	0.307	0.172	0.096	0.074	0.068	0.055	0.051	0.048	0.048	0.048	0.049	0.051	0.052	0.055	0.059
294.4	0.306	0.171	0.096	0.073	0.068	0.054	0.051	0.048	0.048	0.048	0.049	0.050	0.051	0.055	0.059
294.5	0.305	0.170	0.095	0.073	0.067	0.054	0.051	0.048	0.048	0.047	0.048	0.050	0.051	0.055	0.059
294.6	0.304	0.169	0.095	0.072	0.067	0.053	0.050	0.047	0.047	0.047	0.048	0.050	0.051	0.054	0.058

294.7	0.303	0.168	0.094	0.072	0.067	0.053	0.050	0.047	0.047	0.047	0.048	0.049	0.050	0.054	0.058
294.8	0.302	0.168	0.094	0.071	0.066	0.053	0.050	0.047	0.047	0.046	0.047	0.049	0.050	0.054	0.058
294.9	0.302	0.167	0.093	0.071	0.066	0.052	0.049	0.046	0.046	0.046	0.047	0.049	0.050	0.054	0.057
295	0.301	0.166	0.093	0.070	0.065	0.052	0.049	0.046	0.046	0.046	0.047	0.048	0.049	0.053	0.057
295.1	0.300	0.166	0.093	0.070	0.065	0.052	0.049	0.046	0.046	0.045	0.047	0.048	0.049	0.053	0.057
295.2	0.299	0.165	0.092	0.070	0.065	0.051	0.048	0.045	0.046	0.045	0.046	0.048	0.049	0.053	0.057
295.3	0.298	0.164	0.092	0.069	0.064	0.051	0.048	0.045	0.045	0.045	0.046	0.048	0.049	0.053	0.056
295.4	0.297	0.164	0.091	0.069	0.064	0.051	0.048	0.045	0.045	0.045	0.046	0.047	0.048	0.052	0.056
295.5	0.297	0.163	0.091	0.069	0.064	0.051	0.048	0.045	0.045	0.044	0.046	0.047	0.048	0.052	0.056
295.6	0.296	0.162	0.091	0.068	0.064	0.050	0.047	0.045	0.044	0.044	0.045	0.047	0.048	0.052	0.056
295.7	0.295	0.162	0.090	0.068	0.063	0.050	0.047	0.044	0.044	0.044	0.045	0.047	0.048	0.052	0.056
295.8	0.295	0.161	0.090	0.068	0.063	0.050	0.047	0.044	0.044	0.044	0.045	0.047	0.048	0.052	0.055
295.9	0.294	0.161	0.090	0.068	0.063	0.050	0.047	0.044	0.044	0.044	0.045	0.046	0.048	0.052	0.055
296	0.293	0.160	0.089	0.067	0.063	0.050	0.047	0.044	0.044	0.043	0.045	0.046	0.047	0.051	0.055
296.1	0.293	0.160	0.089	0.067	0.062	0.049	0.046	0.044	0.043	0.043	0.044	0.046	0.047	0.051	0.055
296.2	0.292	0.159	0.089	0.067	0.062	0.049	0.046	0.043	0.043	0.043	0.044	0.046	0.047	0.051	0.055
296.3	0.292	0.159	0.088	0.067	0.062	0.049	0.046	0.043	0.043	0.043	0.044	0.046	0.047	0.051	0.055
296.4	0.291	0.158	0.088	0.066	0.062	0.049	0.046	0.043	0.043	0.043	0.044	0.045	0.047	0.051	0.055
296.5	0.290	0.158	0.088	0.066	0.062	0.049	0.046	0.043	0.043	0.043	0.044	0.045	0.047	0.051	0.055
296.6	0.290	0.157	0.088	0.066	0.062	0.048	0.045	0.043	0.043	0.042	0.044	0.045	0.046	0.050	0.054
296.7	0.289	0.157	0.087	0.066	0.061	0.048	0.045	0.042	0.043	0.042	0.043	0.045	0.046	0.050	0.054
296.8	0.288	0.156	0.087	0.065	0.061	0.048	0.045	0.042	0.042	0.042	0.043	0.045	0.046	0.050	0.054
296.9	0.288	0.156	0.087	0.065	0.061	0.048	0.045	0.042	0.042	0.042	0.043	0.045	0.046	0.050	0.054
297	0.287	0.156	0.087	0.065	0.061	0.048	0.045	0.042	0.042	0.042	0.043	0.045	0.046	0.050	0.054
297.1	0.287	0.155	0.086	0.065	0.061	0.048	0.045	0.042	0.042	0.042	0.043	0.045	0.046	0.050	0.054
297.2	0.286	0.155	0.086	0.065	0.061	0.048	0.045	0.042	0.042	0.042	0.043	0.044	0.046	0.050	0.054
297.3	0.286	0.154	0.086	0.065	0.060	0.048	0.044	0.042	0.042	0.042	0.043	0.044	0.046	0.050	0.054
297.4	0.285	0.154	0.086	0.065	0.060	0.047	0.044	0.042	0.042	0.041	0.043	0.044	0.045	0.050	0.054
297.5	0.285	0.153	0.086	0.064	0.060	0.047	0.044	0.042	0.042	0.041	0.043	0.044	0.045	0.049	0.053
297.6	0.284	0.153	0.085	0.064	0.060	0.047	0.044	0.042	0.042	0.041	0.042	0.044	0.045	0.049	0.053
297.7	0.284	0.153	0.085	0.064	0.060	0.047	0.044	0.041	0.041	0.041	0.042	0.044	0.045	0.049	0.053
297.8	0.283	0.152	0.085	0.064	0.060	0.047	0.044	0.041	0.041	0.041	0.042	0.044	0.045	0.049	0.053
297.9	0.283	0.152	0.085	0.064	0.060	0.047	0.044	0.041	0.041	0.041	0.042	0.044	0.045	0.049	0.053
298	0.282	0.152	0.085	0.064	0.060	0.047	0.044	0.041	0.041	0.041	0.042	0.044	0.045	0.049	0.053
298.1	0.282	0.151	0.085	0.063	0.060	0.047	0.044	0.041	0.041	0.041	0.042	0.044	0.045	0.049	0.053
298.2	0.281	0.151	0.084	0.063	0.060	0.047	0.044	0.041	0.041	0.041	0.042	0.043	0.045	0.049	0.053
298.3	0.281	0.151	0.084	0.063	0.060	0.046	0.044	0.041	0.041	0.041	0.042	0.043	0.045	0.049	0.053
298.4	0.280	0.151	0.084	0.063	0.059	0.046	0.043	0.041	0.041	0.041	0.042	0.043	0.045	0.049	0.053
298.5	0.280	0.150	0.084	0.063	0.059	0.046	0.043	0.041	0.041	0.040	0.042	0.043	0.045	0.048	0.053
298.6	0.280	0.150	0.084	0.063	0.059	0.046	0.043	0.041	0.041	0.040	0.042	0.043	0.045	0.048	0.053
298.7	0.279	0.150	0.084	0.063	0.059	0.046	0.043	0.041	0.041	0.040	0.042	0.043	0.045	0.048	0.053

298.8	0.279	0.149	0.083	0.063	0.059	0.046	0.043	0.041	0.041	0.040	0.041	0.043	0.044	0.048	0.053
298.9	0.278	0.149	0.083	0.063	0.059	0.046	0.043	0.041	0.040	0.040	0.041	0.043	0.044	0.048	0.053
299	0.278	0.149	0.083	0.062	0.059	0.046	0.043	0.041	0.040	0.040	0.041	0.043	0.044	0.048	0.052
299.1	0.277	0.149	0.083	0.062	0.059	0.046	0.043	0.041	0.040	0.040	0.041	0.043	0.044	0.048	0.052
299.2	0.277	0.148	0.083	0.062	0.059	0.046	0.043	0.040	0.040	0.040	0.041	0.043	0.044	0.048	0.052
299.3	0.277	0.148	0.083	0.062	0.059	0.046	0.043	0.040	0.040	0.040	0.041	0.043	0.044	0.048	0.052
299.4	0.276	0.148	0.083	0.062	0.059	0.046	0.043	0.040	0.040	0.040	0.041	0.043	0.044	0.048	0.052
299.5	0.276	0.147	0.082	0.062	0.059	0.046	0.043	0.040	0.040	0.040	0.041	0.042	0.044	0.048	0.052
299.6	0.275	0.147	0.082	0.062	0.058	0.046	0.042	0.040	0.040	0.040	0.041	0.042	0.044	0.047	0.052
299.7	0.275	0.147	0.082	0.062	0.058	0.046	0.042	0.040	0.040	0.040	0.041	0.042	0.044	0.047	0.052
299.8	0.275	0.147	0.082	0.062	0.058	0.045	0.042	0.040	0.040	0.040	0.041	0.042	0.044	0.047	0.052
299.9	0.274	0.146	0.082	0.062	0.058	0.045	0.042	0.040	0.040	0.039	0.041	0.042	0.044	0.047	0.052
300	0.274	0.146	0.082	0.061	0.058	0.045	0.042	0.040	0.040	0.039	0.041	0.042	0.044	0.047	0.052

3.9. Fluorescence intensity of TX-100 with variation of concentration of β-CD in water at 298.15 K.

λ/nm	0 mM	0.5 mM	1.0 mM	1.7 mM	2.4 mM	3.0 mM	3.2 mM	3.5 mM	3.7 mM	3.9 mM	4.0 mm	4.2 mM	4.6 mM	5.0 mM	5.7 mM	6.4 mM	7 mM
290.0	4.032	6.281	7.836	9.967	9.316	11.045	14.746	14.361	13.959	17.819	19.203	21.278	22.666	24.687	23.827	26.743	28.557
290.5	6.789	8.665	11.217	13.811	14.714	16.374	19.648	20.265	21.776	24.387	26.356	28.140	30.375	32.014	33.279	35.650	37.841
291.0	9.507	11.532	15.100	18.084	19.966	22.015	25.310	26.609	29.443	31.480	33.975	35.584	38.434	40.321	42.760	44.761	47.365
291.5	12.611	15.304	19.602	23.054	25.935	28.460	31.938	33.764	37.523	39.482	42.701	43.862	47.523	49.792	52.991	55.021	57.681
292.0	16.258	19.798	24.616	28.659	32.407	35.681	39.431	41.945	46.135	48.356	52.299	53.094	57.557	60.588	64.115	66.271	69.207
292.5	20.718	25.111	30.343	34.946	39.312	43.575	47.874	50.844	55.404	58.373	62.623	63.459	68.601	72.537	75.714	78.587	82.069
293.0	25.823	31.055	36.605	41.994	46.965	52.090	56.710	60.411	65.760	69.322	73.830	74.799	80.559	84.945	88.262	91.986	95.707
293.5	31.762	37.547	43.416	49.922	55.589	61.192	66.153	70.803	76.947	81.103	85.670	86.848	93.266	98.198	101.478	106.245	110.105
294.0	37.939	44.406	50.850	58.381	64.477	70.640	76.094	81.530	88.182	93.363	97.744	99.652	106.240	111.996	115.088	120.508	124.832
294.5	44.450	51.877	58.810	67.014	73.915	80.559	86.666	92.466	99.883	105.956	110.120	112.860	119.673	125.992	129.344	135.193	139.548
295.0	51.138	59.103	66.703	75.722	83.475	90.626	97.340	103.974	111.504	118.318	122.295	126.162	133.025	140.210	143.916	149.760	154.419
295.5	58.403	66.135	74.500	84.504	92.950	101.152	108.824	115.454	123.044	130.237	134.305	139.279	146.265	154.160	158.225	164.464	169.587
296.0	65.576	73.148	81.951	93.109	102.091	111.316	119.856	126.563	134.421	141.644	146.212	151.920	159.347	167.383	172.282	178.718	184.465
296.5	73.015	80.163	89.069	101.819	111.316	121.114	130.569	137.519	145.696	152.569	158.755	164.057	172.204	180.328	186.207	192.756	199.189
297.0	80.024	87.052	96.421	110.645	119.936	130.459	140.654	147.848	156.076	162.870	171.698	175.850	184.560	192.807	199.852	205.949	213.506
297.5	86.629	94.180	104.233	118.977	128.074	139.366	150.019	157.409	166.609	173.070	184.516	187.613	196.589	205.042	213.074	218.958	227.262
298.0	92.545	101.300	112.015	126.722	135.894	147.791	158.084	167.040	176.761	183.525	196.400	198.971	208.169	217.148	226.128	231.197	240.293
298.5	98.510	107.883	119.603	134.175	143.528	156.243	165.951	176.312	186.781	193.848	207.139	209.914	218.942	228.496	237.903	243.074	252.531
299.0	103.724	114.048	126.383	140.880	151.061	164.265	173.138	185.017	196.283	204.067	215.543	219.903	229.052	238.856	248.665	253.788	263.533
299.5	108.920	119.718	132.141	146.792	158.635	172.102	180.441	193.505	205.449	214.194	222.781	228.696	238.159	248.242	258.538	263.674	272.950
300.0	113.887	124.440	136.979	152.598	165.569	179.480	187.658	201.278	212.739	222.932	229.778	236.106	245.993	256.289	267.321	272.382	281.637
300.5	118.601	128.500	141.471	157.954	171.462	185.901	194.673	207.936	219.206	230.138	236.439	243.234	252.998	263.900	275.098	280.445	289.759
301.0	122.864	132.438	145.619	162.781	176.448	191.275	200.231	214.040	224.389	236.010	242.847	249.429	259.184	271.318	282.602	288.069	297.429
301.5	126.901	136.056	149.656	167.683	179.869	195.819	205.033	219.332	229.169	240.650	249.562	255.175	264.310	278.127	289.013	295.984	304.181
302.0	130.223	139.454	153.421	172.256	183.474	199.458	208.670	223.945	233.661	244.891	254.994	261.111	269.026	284.639	294.780	303.086	310.306

302.5	133.242	142.871	157.284	175.786	187.169	202.591	212.557	228.028	238.670	249.605	259.392	266.439	273.703	290.612	300.214	309.772	315.244
303.0	135.890	145.955	160.662	178.763	191.140	205.988	216.696	231.645	242.419	254.031	263.682	270.777	278.662	295.284	305.061	315.058	320.056
303.5	138.090	148.680	163.956	181.299	195.301	209.382	221.312	234.345	245.578	258.689	267.623	275.251	284.149	298.904	309.103	318.962	324.731
304.0	139.864	150.910	166.782	183.545	199.306	212.582	225.443	236.502	248.330	262.622	270.995	279.060	289.461	301.959	312.745	321.924	329.317
304.5	141.307	153.166	168.864	185.649	201.350	215.208	229.082	237.798	250.423	266.090	274.557	281.831	294.176	304.270	315.754	325.114	333.020
305.0	142.251	154.873	169.830	188.202	202.948	217.175	230.997	238.822	252.214	268.877	277.493	284.654	297.953	306.505	318.410	327.328	336.838
305.5	143.221	156.395	171.019	190.049	203.773	218.614	232.111	240.195	254.972	271.034	279.774	286.866	300.123	309.125	320.444	329.366	339.345
306.0	144.419	157.045	171.942	191.712	204.171	220.012	232.630	242.125	257.425	271.996	282.017	288.234	301.530	311.891	321.966	330.772	341.804
306.5	145.761	157.694	173.095	193.098	205.033	221.093	233.263	244.493	259.344	272.557	283.849	288.745	302.520	313.553	323.330	331.325	343.086
307.0	147.055	157.492	174.152	194.289	206.447	221.865	233.371	247.100	260.558	272.205	284.906	288.714	302.815	314.296	323.980	331.204	343.447
307.5	147.858	157.530	174.798	194.307	207.179	222.482	233.928	248.779	260.691	271.867	284.954	287.881	303.066	313.640	324.306	331.178	342.508
308.0	147.657	157.069	174.140	194.307	207.738	222.641	234.420	249.304	259.915	271.955	283.712	286.872	303.423	312.091	324.585	330.799	341.787
308.5	147.184	157.001	173.103	193.643	207.567	222.363	234.293	248.654	258.783	271.712	281.735	285.812	302.545	310.392	324.005	330.693	340.574
309.0	146.608	156.506	171.703	192.484	206.699	221.871	233.522	246.873	257.155	270.429	279.630	284.952	301.346	309.477	322.691	330.007	340.066
309.5	146.277	156.378	170.717	190.968	205.557	220.680	231.964	244.273	255.125	268.459	277.724	283.397	299.821	307.947	320.819	328.224	339.221
310.0	145.945	155.625	169.962	189.838	203.983	218.704	229.360	241.701	252.830	265.341	275.795	281.422	296.971	305.870	317.904	325.627	336.959
310.5	145.317	155.081	169.734	187.978	201.803	216.788	226.357	238.933	250.103	261.692	273.550	279.285	293.485	302.692	314.368	322.325	332.760
311.0	143.657	153.585	168.731	185.755	199.517	214.282	224.047	236.149	247.182	258.599	270.200	276.354	290.497	298.702	310.847	318.227	328.003
311.5	141.601	151.956	167.328	183.434	197.181	211.534	221.863	233.074	244.332	256.009	266.427	273.377	286.922	294.713	306.515	314.117	322.535
312.0	139.375	149.875	164.993	180.766	194.972	208.632	219.570	229.940	241.580	253.017	262.504	270.298	283.151	290.719	302.014	309.375	317.459
312.5	137.427	147.870	162.319	178.111	192.686	205.408	216.975	226.719	239.171	249.724	258.915	266.958	279.419	286.524	297.038	303.891	312.826
313.0	135.779	145.573	159.433	175.728	190.024	201.629	213.337	223.868	236.641	245.998	255.686	263.428	274.925	281.908	291.709	298.322	307.941
313.5	134.015	143.463	157.165	173.430	186.564	198.232	208.487	220.978	233.384	241.538	253.158	259.758	269.390	277.022	286.361	293.376	303.066
314.0	131.559	140.831	154.758	170.396	183.132	195.032	203.923	218.135	229.324	236.974	249.922	255.272	264.281	271.618	281.097	288.429	298.174
314.5	128.684	137.721	152.486	167.021	179.447	192.241	200.172	214.265	225.092	233.044	245.869	250.470	259.437	267.000	275.664	284.038	293.497
315.0	125.734	134.493	149.718	163.143	176.353	189.559	197.446	209.897	220.672	229.073	240.578	245.174	254.590	262.298	271.032	279.780	288.871
315.5	122.847	131.510	146.498	159.445	173.414	186.715	195.289	204.818	216.446	225.148	235.112	239.525	250.452	257.550	266.741	275.318	283.876
316.0	120.253	128.849	142.948	156.109	170.345	183.255	193.041	200.130	212.889	221.634	229.280	234.236	246.626	252.296	262.113	270.060	278.216
316.5	117.977	126.669	139.700	153.623	167.023	179.718	189.509	195.849	209.301	217.827	224.264	229.510	241.531	246.802	257.097	264.526	272.728
317.0	115.631	125.142	136.748	151.415	163.634	175.522	185.074	192.102	205.074	213.348	219.598	225.106	236.463	241.149	251.680	258.353	266.526

317.5	113.077	123.240	134.223	149.071	159.800	171.215	179.917	188.651	200.382	208.345	215.215	220.641	231.185	236.069	245.809	251.581	259.957
318.0	110.841	120.873	131.775	145.911	156.242	166.815	175.097	185.184	195.042	202.978	210.302	216.020	225.319	231.303	240.311	244.770	253.880
318.5	108.685	117.996	129.414	142.448	152.730	162.620	170.824	180.929	189.570	197.371	205.047	211.148	219.588	226.366	235.010	238.522	247.730
319.0	106.482	114.836	126.712	138.699	148.559	158.444	167.095	176.644	184.488	192.375	199.261	206.276	214.614	221.084	229.911	232.839	241.124
319.5	104.381	111.797	123.559	135.028	144.748	154.880	163.403	172.339	179.320	188.291	193.814	201.669	208.482	215.457	224.825	227.697	235.488
320.0	102.222	109.092	120.510	131.567	141.225	151.231	159.682	167.892	174.757	184.669	188.778	197.704	202.724	210.043	219.094	222.936	230.128
320.5	99.671	106.514	117.402	128.382	137.924	147.740	155.365	163.873	171.039	180.886	184.386	193.607	197.209	205.055	213.090	217.582	224.494
321.0	97.024	103.871	114.230	125.042	134.971	144.223	151.369	160.377	167.359	176.553	180.145	189.001	191.942	200.608	207.196	211.945	219.254
321.5	94.309	100.990	111.516	121.788	132.392	140.996	147.311	156.587	164.032	171.389	176.034	184.034	186.915	196.133	201.614	206.362	213.829
322.0	91.536	97.851	108.739	118.797	129.070	137.574	143.166	152.745	160.350	165.586	171.938	178.417	182.932	191.482	196.626	201.239	207.496
322.5	89.029	95.040	105.847	115.933	126.037	134.122	139.047	148.763	155.461	160.168	168.024	172.646	178.493	185.904	191.845	196.112	201.276
323.0	86.801	92.559	103.240	113.106	122.477	130.070	135.245	144.326	149.890	155.508	163.908	167.350	174.203	180.046	187.172	191.087	195.435
323.5	84.876	90.603	100.639	110.477	118.895	126.094	131.490	140.076	144.564	151.600	159.794	162.939	169.573	174.307	182.526	185.848	189.739
324.0	83.204	89.076	97.606	107.518	115.192	121.917	128.089	136.336	139.606	148.043	155.868	158.843	165.021	169.220	178.092	180.727	184.809
324.5	81.460	87.585	95.033	104.299	111.783	118.113	125.136	132.861	135.777	144.578	151.834	155.214	160.415	164.820	173.665	175.905	180.298
325.0	79.817	85.764	92.355	101.135	108.388	114.867	122.273	129.951	132.690	140.470	147.722	151.490	156.100	161.154	169.247	171.205	175.899
325.5	78.242	83.863	89.907	98.065	105.670	112.030	119.379	126.772	130.037	136.290	143.787	147.801	152.201	157.708	164.632	166.558	171.480
326.0	76.505	81.588	87.650	94.966	102.978	109.262	116.280	123.462	127.061	132.281	139.725	143.913	148.411	154.100	160.107	161.726	167.239
326.5	74.648	79.317	85.498	92.345	100.559	106.745	113.266	119.918	124.162	128.776	135.277	140.101	144.418	150.376	155.695	156.973	162.913
327.0	72.909	77.308	82.933	89.936	97.961	103.895	110.193	116.278	121.095	125.664	131.006	136.050	140.878	146.243	151.329	152.838	158.451
327.5	71.133	75.457	80.479	87.812	95.336	101.043	107.253	112.326	118.338	122.964	126.646	131.936	137.246	142.230	147.060	149.375	153.830
328.0	69.507	73.837	78.116	85.756	92.675	98.346	104.426	109.103	115.008	120.045	122.448	127.778	133.334	138.232	142.839	145.975	149.202
328.5	68.123	72.124	76.333	83.915	90.129	95.919	101.655	106.307	111.828	116.878	119.307	124.120	129.625	134.543	138.506	142.764	144.466
329.0	66.905	70.082	74.890	81.805	87.514	93.581	98.701	103.712	108.403	113.505	116.969	121.040	125.825	130.880	134.537	139.238	140.366
329.5	65.556	67.954	73.625	79.567	85.294	91.688	96.098	101.419	104.987	110.347	114.801	118.458	121.809	127.394	131.150	135.078	136.873
330.0	63.986	65.850	72.030	76.996	83.183	89.466	93.482	99.355	101.649	107.546	112.731	115.970	118.035	123.883	127.882	130.916	133.699
330.5	62.284	64.107	70.100	74.974	81.035	87.140	90.884	96.638	99.091	104.905	110.304	113.460	114.219	120.727	124.670	127.407	130.742
331.0	60.710	62.891	67.953	72.925	79.067	84.461	88.014	93.887	96.504	101.949	106.837	110.548	110.590	117.541	121.406	123.655	127.767
331.5	59.224	62.007	66.224	71.382	77.133	81.904	85.305	91.391	94.220	99.090	103.237	107.142	107.591	114.854	117.759	120.168	124.489
332.0	58.095	61.177	64.679	69.856	74.929	79.442	82.466	88.701	91.995	96.045	99.486	103.738	104.975	112.013	114.203	117.134	121.294

332.5	57.076	60.296	63.251	68.530	73.064	77.494	79.914	86.024	89.895	93.136	95.887	100.479	102.340	109.106	111.205	113.894	118.072
333.0	55.785	59.126	61.695	66.747	71.463	75.724	77.592	83.961	87.436	90.690	92.923	97.496	99.901	105.634	108.318	110.636	114.731
333.5	54.341	57.649	59.966	65.016	69.763	74.136	75.693	81.759	85.122	88.698	90.604	94.555	97.360	102.373	105.563	108.026	111.598
334.0	53.049	55.980	58.145	62.894	67.940	72.065	73.858	79.375	82.818	86.666	88.390	91.967	94.726	99.098	103.154	105.639	108.440
334.5	51.795	54.199	56.583	61.005	66.278	69.970	72.406	77.362	80.573	84.598	86.605	89.279	92.433	96.644	100.498	103.090	105.437
335.0	50.721	52.425	55.271	59.160	64.248	67.739	71.134	75.491	78.270	82.387	84.736	86.832	90.572	94.362	97.824	100.783	102.766
335.5	49.784	51.049	54.128	57.713	62.240	65.663	70.039	73.654	76.367	80.029	82.721	84.571	89.018	92.342	95.288	98.287	100.155
336.0	48.837	50.104	52.851	56.286	60.651	63.723	68.964	72.172	74.381	77.850	80.514	82.704	87.270	90.212	92.700	95.454	97.809
336.5	47.763	49.419	51.399	55.086	59.292	62.172	67.752	70.575	72.521	76.012	77.993	80.817	85.350	87.888	90.011	92.646	95.532
337.0	46.701	48.909	49.796	53.701	57.723	60.741	66.125	68.792	70.632	74.167	75.505	78.940	82.892	85.370	87.408	90.226	93.021
337.5	45.743	48.530	48.129	52.409	56.478	59.421	64.051	67.003	68.705	72.135	73.229	76.826	80.058	83.195	85.040	87.874	90.370
338.0	45.127	47.835	46.732	50.906	55.062	58.167	61.804	65.179	66.624	69.879	71.153	74.586	77.222	80.968	83.091	85.514	87.665
338.5	44.376	46.835	45.536	49.593	53.541	56.931	59.467	63.039	64.873	67.874	69.230	72.214	74.677	78.866	81.156	83.103	84.938
339.0	43.644	45.776	44.444	48.285	52.141	55.655	57.473	61.249	63.193	65.996	67.838	70.132	72.213	76.777	79.272	80.733	82.544
339.5	42.831	44.481	43.343	47.178	50.935	54.408	55.752	59.470	61.831	64.252	66.371	68.262	70.295	74.485	77.257	77.986	80.398
340.0	41.864	43.081	42.292	46.069	49.359	53.051	54.380	57.854	60.459	62.866	65.035	66.709	68.677	72.001	74.624	75.559	78.503
340.5	40.753	42.054	41.085	45.079	47.885	51.605	53.019	56.222	58.917	61.284	63.564	65.167	67.177	69.660	71.945	73.611	76.592
341.0	39.872	40.932	40.100	44.072	46.347	50.039	51.811	54.772	57.424	59.280	61.745	63.503	65.609	67.344	69.637	71.857	74.594
341.5	38.888	39.881	39.353	43.193	44.852	48.429	50.419	53.157	56.081	57.538	59.705	61.750	63.872	65.277	67.693	70.108	72.572
342.0	38.135	38.930	38.687	41.939	43.540	46.944	48.999	51.710	54.569	56.112	57.955	59.787	61.787	63.833	66.162	68.561	70.685
342.5	37.584	37.968	38.153	40.624	42.550	45.566	47.582	50.219	53.269	54.665	56.329	57.849	59.995	62.524	64.877	66.791	68.789
343.0	37.046	37.012	37.710	39.267	41.669	44.313	46.353	48.774	51.782	53.478	55.022	56.114	58.457	61.272	63.349	64.863	67.107
343.5	36.274	36.321	36.902	37.956	40.793	43.212	45.011	47.140	49.671	52.367	53.946	54.635	56.996	59.764	61.540	63.226	65.384
344.0	35.550	35.733	35.848	36.717	39.645	42.156	43.851	45.521	47.833	50.681	52.712	53.414	55.863	57.874	59.572	61.571	63.517
344.5	34.710	35.378	34.785	35.692	38.463	41.000	42.782	43.934	46.306	49.058	51.184	52.450	54.837	55.767	57.546	59.802	61.661
345.0	33.897	34.989	33.515	34.550	37.253	39.696	41.581	42.449	45.035	47.732	49.503	51.457	53.281	53.776	55.870	58.006	59.848
345.5	33.286	34.456	32.308	33.426	36.114	38.369	40.365	41.125	44.296	46.349	47.884	50.379	51.757	51.942	54.347	56.246	57.960
346.0	32.775	33.712	31.366	32.216	35.212	37.018	39.187	40.289	43.648	45.029	46.452	49.079	50.304	50.539	52.956	54.315	56.168
346.5	32.238	32.831	30.460	31.096	34.412	35.804	37.878	39.431	42.514	44.003	45.198	47.450	48.618	49.323	51.749	52.577	54.364

3.10. Fluorescence intensity of TX-114 with variation of concentration of β-CD in water at 298.15 K.

λ/nm	0 mM	0.6 mM	1.2 mM	1.8 mM	2.4 mM	3.0 mM	3.1 mM	3.2 mM	3.4 mM	3.5 mM	4.0 mM	4.5 mM	5.0 mM	5.5 mM	6.0 mM	6.1 mM	6.3 mM	6.4 mM	6.8 mM	7.0 mM
290	4.373	5.219	5.276	6.084	6.199	7.598	10.148	12.508	12.489	13.289	15.977	16.094	16.973	19.970	22.064	23.584	23.430	24.378	27.144	29.818
290.5	6.972	7.272	7.477	8.594	10.105	12.126	14.488	16.380	17.643	19.289	21.373	22.859	24.300	26.179	28.668	30.763	32.071	33.210	35.911	37.451
291	10.058	9.819	10.105	11.498	14.057	16.732	19.144	21.193	23.261	25.381	27.461	29.769	31.573	33.309	36.081	38.508	41.037	42.182	44.931	46.037
291.5	14.114	13.317	13.608	15.052	18.797	21.787	24.580	27.211	29.621	32.035	34.350	37.388	39.540	41.707	44.420	47.428	50.482	52.023	54.891	56.478
292	19.114	17.754	18.042	19.499	23.994	27.385	30.779	34.265	36.881	39.622	42.416	45.704	48.337	51.171	54.081	57.405	60.495	62.698	65.893	68.605
292.5	25.293	23.356	23.334	25.068	29.708	33.727	37.809	42.288	45.140	48.369	51.823	55.000	58.126	62.013	64.757	68.393	71.691	74.449	78.514	82.154
293	32.598	29.845	29.505	31.630	36.202	40.985	45.806	50.840	54.028	58.097	61.987	65.466	69.105	73.643	76.156	80.389	83.886	87.052	92.191	96.460
293.5	41.412	37.668	36.632	38.849	43.386	49.112	54.482	59.401	63.646	68.682	73.004	77.077	81.310	85.673	88.355	93.643	97.279	100.919	107.053	111.168
294	51.240	46.481	44.562	46.641	51.099	57.808	63.526	68.341	73.813	79.529	84.484	89.140	93.692	98.175	101.163	107.740	111.535	115.251	122.044	125.883
294.5	62.323	56.115	53.112	54.958	59.589	66.822	73.192	77.794	84.178	90.254	95.820	101.457	106.161	111.197	114.097	122.061	126.432	129.578	137.210	140.830
295	73.945	65.894	61.974	63.283	68.254	75.869	82.874	87.611	94.872	100.962	107.177	113.461	118.291	123.975	127.435	136.370	140.819	143.218	151.591	155.536
295.5	85.918	75.804	70.736	71.817	76.687	85.051	92.413	97.735	105.728	112.033	118.314	125.103	130.285	136.685	141.002	150.066	154.760	156.772	165.634	169.890
296	97.529	84.984	79.566	80.525	84.798	94.078	101.683	107.901	116.190	123.036	129.056	136.152	141.886	148.864	154.297	162.914	167.723	169.880	179.126	183.747
296.5	109.139	94.131	88.326	89.212	92.770	103.064	110.634	117.894	126.378	134.051	139.979	147.380	153.934	160.589	167.541	175.453	180.355	182.942	192.882	197.338
297	120.481	103.370	97.043	97.559	100.528	112.178	119.142	127.631	136.458	145.053	150.827	158.516	165.636	171.617	180.123	188.051	192.608	196.138	206.255	210.208
297.5	131.843	112.651	105.722	105.667	108.524	120.814	127.731	137.087	145.769	155.640	161.231	169.416	176.686	182.895	191.786	199.673	204.679	209.039	219.570	222.851
298	142.839	121.813	113.710	113.138	116.471	128.664	136.149	146.417	155.046	165.335	171.259	179.792	186.752	193.870	202.534	210.770	216.030	220.977	231.667	235.081
298.5	153.695	131.013	120.590	120.081	123.953	136.013	144.329	155.153	164.203	174.763	180.365	189.311	196.336	204.940	212.785	221.259	227.028	232.191	242.748	246.586
299	163.739	139.595	126.651	126.421	130.602	142.664	152.055	163.323	172.441	183.203	188.898	197.459	205.201	215.121	221.914	230.629	237.052	242.162	252.589	257.533
299.5	172.457	147.367	132.162	132.873	136.628	148.769	159.292	170.653	180.145	190.829	197.093	205.340	214.089	224.980	230.950	239.380	246.355	251.200	262.255	267.819
300	180.116	154.461	137.582	139.068	141.827	154.786	165.584	177.032	187.417	197.537	204.732	212.883	222.909	233.714	239.276	248.463	254.968	259.831	271.021	276.746
300.5	187.198	160.545	143.418	144.824	146.828	160.209	171.361	182.393	193.744	203.365	211.868	220.148	230.886	241.549	247.232	256.521	263.149	268.038	279.538	285.027
301	193.357	166.009	149.477	149.978	151.900	164.923	176.250	187.703	199.368	208.310	218.374	227.377	237.841	248.303	254.587	263.738	271.169	276.501	287.241	292.589
301.5	198.957	171.077	154.922	154.293	156.973	169.817	180.899	192.881	205.106	213.261	223.472	234.021	243.470	253.889	261.407	271.032	278.804	284.989	294.209	299.221
302	204.326	175.972	159.561	157.190	161.870	174.262	185.448	197.792	209.627	217.378	227.620	239.113	247.967	258.127	267.105	277.352	285.549	292.972	299.637	306.114

302.5	208.350	180.708	163.747	159.799	166.421	178.364	190.080	202.648	213.400	221.988	231.566	243.594	251.524	262.499	272.409	282.928	291.318	299.978	305.502	312.830
303	211.321	184.905	167.072	162.406	169.858	182.102	194.251	206.896	216.807	226.338	235.004	247.380	254.979	266.880	276.786	288.612	295.922	305.699	311.240	318.305
303.5	214.265	188.211	169.672	164.944	172.592	185.056	198.161	210.019	220.171	230.351	239.067	250.894	258.560	271.544	280.236	293.363	299.587	309.553	317.038	323.093
304	217.341	190.924	171.797	167.578	174.635	186.620	200.869	212.807	222.752	233.897	242.880	254.328	262.466	276.179	283.563	296.592	303.019	312.601	322.551	327.027
304.5	220.349	193.109	173.186	170.223	176.219	188.102	202.319	214.998	225.870	237.629	246.324	257.901	266.085	279.649	286.574	299.582	305.895	314.923	327.339	330.151
305	223.586	195.172	173.478	172.142	177.579	189.470	203.294	216.614	228.074	239.539	248.926	260.259	269.903	281.582	289.031	301.670	308.379	316.301	329.840	333.614
305.5	226.033	197.757	174.197	173.673	178.810	191.252	204.227	218.344	229.859	241.330	251.291	262.269	273.101	282.710	291.532	303.245	310.504	317.357	331.794	337.040
306	227.388	200.215	175.283	175.079	179.578	192.871	205.429	219.576	231.003	242.848	253.065	263.914	274.907	283.336	293.751	305.236	311.806	318.125	332.964	339.836
306.5	228.190	202.062	176.500	175.988	179.891	194.216	207.186	220.028	232.423	243.880	255.075	265.203	275.651	284.251	294.881	307.169	312.767	318.655	333.553	341.646
307	228.894	202.916	178.085	176.313	179.850	194.225	208.822	220.376	233.279	244.746	255.588	265.503	275.806	286.077	295.602	308.172	313.852	319.570	333.967	341.390
307.5	229.563	203.018	179.393	176.620	179.409	194.178	209.694	220.601	233.872	246.340	255.678	266.275	274.861	287.047	295.675	308.457	314.953	320.605	334.434	340.098
308	230.003	201.681	179.556	176.588	179.446	193.884	210.311	220.281	233.620	246.369	254.705	266.203	273.695	286.700	294.980	307.644	315.644	320.935	334.049	338.867
308.5	229.667	199.985	179.498	176.117	179.432	193.973	209.880	219.914	232.677	245.386	252.994	265.285	272.998	285.352	293.657	305.849	315.352	321.385	333.080	337.303
309	228.670	198.521	179.088	175.583	179.393	193.524	208.474	219.361	230.729	243.521	250.780	264.061	271.301	282.511	292.676	303.949	313.284	320.629	331.343	336.060
309.5	226.845	197.380	177.959	174.643	178.787	192.928	206.349	218.144	228.627	241.048	249.205	262.630	269.380	279.093	290.618	302.174	310.530	319.094	328.912	335.158
310	224.786	196.417	176.582	173.193	178.033	191.276	204.082	216.531	226.445	238.695	246.860	259.558	267.513	276.046	287.618	300.558	307.250	316.686	325.733	332.868
310.5	222.949	195.811	174.947	171.762	176.086	189.335	201.575	214.411	224.165	237.452	244.901	256.451	265.308	273.391	284.321	298.956	304.002	313.836	322.367	330.355
311	220.998	194.515	172.644	170.240	174.030	187.396	199.949	211.994	221.840	235.867	242.842	253.092	262.346	271.207	280.884	296.654	300.950	309.619	318.768	327.447
311.5	218.766	192.222	170.140	168.308	171.512	185.900	198.315	209.120	219.621	233.803	240.827	249.111	260.041	269.170	276.664	293.928	298.157	305.604	315.144	323.407
312	216.517	189.313	167.910	166.094	169.167	183.931	196.565	206.200	217.012	230.961	238.260	245.898	256.867	266.356	273.363	290.513	294.580	301.450	311.009	318.928
312.5	213.756	186.391	165.418	163.551	166.586	181.491	193.854	203.033	214.455	226.892	235.648	243.553	253.313	263.065	269.796	285.957	290.567	297.392	306.622	314.579
313	211.035	183.451	162.807	160.944	164.915	178.375	190.718	199.674	211.553	222.497	232.175	240.275	249.243	259.246	265.922	280.701	286.097	293.421	301.282	309.310
313.5	208.339	181.085	160.252	158.468	162.983	174.806	186.751	196.060	208.294	218.602	228.462	237.150	245.119	255.173	262.137	275.146	281.070	289.027	296.156	304.275
314	205.069	178.957	157.678	156.395	161.434	171.779	183.131	193.323	204.951	214.764	224.706	234.007	240.432	251.300	258.658	269.239	275.792	283.775	291.326	299.268
314.5	201.364	176.545	155.224	154.748	159.361	169.385	180.114	190.677	201.668	211.370	221.276	230.031	236.337	247.020	254.207	263.796	270.607	277.691	286.951	293.306
315	197.581	173.435	153.043	152.632	156.841	167.311	177.315	188.486	197.674	208.415	217.443	225.773	231.723	242.313	250.250	259.023	265.310	271.747	282.539	287.305
315.5	193.466	170.427	150.875	149.914	153.328	165.016	174.363	186.216	193.768	204.810	213.180	221.568	227.083	237.971	245.738	254.349	260.246	266.246	278.154	280.884
316	189.854	167.426	148.264	147.030	149.659	162.296	171.341	183.365	189.681	200.799	208.701	216.533	221.662	233.062	240.729	249.525	255.190	261.734	272.532	274.004
316.5	186.693	164.648	145.402	143.467	145.900	158.293	167.745	179.403	185.362	196.532	204.106	211.506	216.504	227.730	235.674	244.807	249.942	257.355	266.536	267.816
317	183.182	161.929	142.422	139.703	142.798	153.865	163.881	175.444	181.267	191.529	199.826	206.831	211.627	222.793	230.651	239.587	244.630	253.207	260.572	262.477

317.5	179.493	159.496	139.469	136.646	140.154	149.480	160.215	171.127	177.854	186.649	195.947	202.114	207.606	217.090	225.255	233.877	239.412	247.577	254.594	257.198
318	175.314	156.240	136.397	133.627	137.955	145.640	156.563	167.001	174.285	182.510	192.007	197.786	203.819	210.990	219.957	228.508	233.619	241.518	248.597	252.726
318.5	170.610	152.815	133.584	130.540	135.695	142.447	152.808	163.168	170.776	178.650	187.157	193.988	200.148	205.975	214.701	223.138	228.050	235.314	243.123	248.140
319	166.429	149.195	130.530	127.953	133.186	139.833	149.181	159.548	167.382	174.985	182.226	189.770	195.541	201.452	209.537	217.592	222.377	229.858	237.398	242.845
319.5	162.995	145.673	126.999	125.110	129.997	137.116	145.473	155.740	163.676	171.410	176.788	184.869	190.147	197.644	204.877	212.582	216.989	225.059	231.630	237.100
320	160.261	141.901	123.445	122.178	126.757	134.134	141.874	152.231	159.872	167.448	172.029	180.022	184.838	194.515	200.251	207.991	211.996	221.143	226.488	231.076
320.5	157.970	138.446	120.601	119.870	123.538	131.129	138.802	148.521	156.277	163.267	167.826	175.414	179.923	190.632	195.741	203.212	207.794	216.561	221.330	225.012
321	155.438	135.076	118.116	117.741	120.453	127.816	135.897	144.703	152.736	159.248	164.835	171.061	175.429	185.813	191.144	198.406	203.358	211.343	215.999	219.697
321.5	152.352	132.140	116.247	115.409	117.459	124.966	133.253	140.844	148.946	155.292	161.725	167.171	171.438	181.113	186.098	193.480	199.146	205.601	210.813	214.954
322	148.980	129.755	114.638	113.181	114.649	122.282	130.596	136.837	145.097	151.277	158.781	163.641	167.349	176.131	180.778	188.032	194.293	199.754	205.121	209.869
322.5	145.234	127.963	112.571	110.490	111.727	119.933	127.334	133.026	141.056	147.298	155.274	159.697	162.912	171.641	175.990	182.859	189.475	194.031	199.259	204.875
323	141.552	125.981	109.971	107.692	108.694	117.073	123.915	129.631	137.046	143.228	151.445	155.358	159.023	167.429	171.209	178.001	184.451	188.922	193.670	199.550
323.5	138.304	124.115	107.443	105.243	105.593	114.297	120.192	126.518	133.008	139.082	146.928	150.696	155.577	163.405	166.397	173.524	179.750	183.885	188.200	193.957
324	135.489	121.957	105.035	103.224	102.864	111.114	116.679	123.636	129.537	135.440	142.632	145.857	151.951	158.967	161.896	169.180	175.107	179.009	183.299	188.616
324.5	133.160	119.924	103.037	101.156	100.263	108.084	113.452	120.850	126.468	132.372	138.216	141.373	148.363	154.694	157.272	165.222	170.543	174.517	178.900	183.778
325	131.471	117.922	101.498	99.344	97.777	104.790	110.602	117.759	123.381	129.648	134.387	137.895	144.631	150.294	152.556	160.963	165.569	170.449	174.365	178.205
325.5	129.492	116.014	100.140	97.281	95.572	102.161	107.592	114.777	120.167	126.976	130.731	135.007	140.582	146.484	148.558	156.800	160.782	166.228	170.073	172.749
326	127.649	114.084	98.381	95.452	93.395	99.230	104.732	111.935	116.783	124.088	127.477	132.043	136.615	142.506	145.184	152.441	156.176	161.863	165.694	167.786
326.5	125.618	112.205	96.810	93.939	91.158	96.457	101.850	109.154	113.200	120.293	124.217	129.050	133.026	138.758	141.726	148.472	151.909	157.425	161.393	163.371
327	123.547	110.224	95.337	92.495	89.108	93.703	99.071	106.423	109.992	116.416	121.180	125.768	129.198	134.795	138.518	144.399	147.701	152.546	157.249	159.609
327.5	121.471	108.848	94.035	90.745	87.296	91.267	96.563	103.716	107.137	112.701	117.857	121.797	125.456	131.123	135.269	140.955	144.096	147.876	153.176	156.378
328	120.209	107.596	92.691	88.778	85.486	88.361	94.345	100.599	104.656	109.264	114.830	118.047	121.715	127.342	131.536	137.444	140.930	143.951	148.981	152.394
328.5	119.227	106.598	91.576	86.512	84.146	86.171	92.118	97.405	102.116	106.471	111.694	114.740	118.281	124.153	127.859	133.940	137.968	140.084	144.900	147.798
329	118.708	105.587	90.096	84.502	82.919	84.105	89.860	94.471	99.424	104.039	108.458	111.677	115.204	120.893	124.757	130.311	134.930	136.210	140.562	143.347
329.5	117.875	104.334	88.803	82.864	81.307	82.077	87.333	91.926	96.755	101.272	105.062	108.912	112.605	117.677	121.742	126.765	131.904	132.470	136.418	139.319
330	117.242	102.859	87.841	81.722	79.383	80.014	84.945	89.551	94.312	98.600	102.050	106.498	110.154	114.349	118.673	122.769	128.273	128.353	132.505	135.576
330.5	116.233	102.054	86.989	80.933	77.475	78.476	82.838	87.616	91.874	96.087	98.870	103.571	107.744	111.292	115.447	119.303	124.649	124.733	128.705	132.322
331	115.324	101.286	86.173	80.232	75.463	76.512	80.886	85.616	89.771	93.736	96.394	100.780	105.146	108.217	112.026	115.977	120.984	121.669	124.980	128.718
331.5	114.295	100.720	85.492	79.455	73.636	74.887	79.071	83.523	87.301	91.694	94.355	98.064	102.546	105.567	108.672	112.915	117.622	118.943	121.249	124.736
332	113.820	100.416	84.393	78.643	71.965	73.208	77.140	81.388	84.437	89.735	92.589	95.388	99.539	103.088	105.737	110.110	114.420	116.414	117.530	120.837

332.5	113.182	99.821	83.169	77.751	70.557	71.488	75.106	79.357	81.505	87.342	90.540	92.676	96.301	100.295	103.099	107.409	111.700	113.872	114.215	117.614
333	112.849	98.920	82.260	76.951	69.072	69.553	73.204	77.171	78.765	84.707	88.572	90.363	92.958	97.628	100.855	104.490	108.683	110.982	111.237	114.799
333.5	112.228	98.329	81.462	76.084	68.047	67.985	71.428	75.079	76.297	81.997	85.847	88.054	90.020	94.875	98.472	101.615	105.683	108.171	108.817	112.546
334	111.473	97.634	80.894	75.175	67.156	66.411	69.800	72.821	74.717	79.605	82.781	85.845	87.593	92.263	96.139	98.576	102.532	105.202	106.836	110.493
334.5	110.335	96.916	80.694	74.280	66.157	65.105	68.310	70.571	73.537	77.425	79.730	83.490	86.123	90.059	93.774	95.690	99.608	102.106	104.729	107.833
335	109.195	96.139	80.720	73.509	64.962	63.590	66.688	68.567	72.472	75.501	77.331	81.187	84.877	88.077	91.460	93.265	96.700	99.118	102.574	105.038
335.5	107.894	95.165	80.395	72.640	63.744	62.109	64.905	67.045	71.544	73.645	75.233	78.795	83.559	85.979	89.205	91.121	94.168	96.127	100.540	102.314
336	106.754	93.859	79.916	71.871	62.061	60.627	63.238	65.772	70.470	71.603	73.920	76.511	81.651	83.957	87.186	89.146	91.853	93.339	98.207	99.494
336.5	105.493	92.668	78.898	70.760	60.599	59.194	61.539	64.940	68.951	69.408	72.620	74.667	79.474	81.651	84.704	87.386	89.687	91.094	95.675	96.682
337	104.401	91.777	77.886	69.655	59.442	57.720	59.978	63.820	67.039	67.559	71.035	73.432	76.788	79.416	82.166	85.397	87.411	89.161	93.381	94.311
337.5	103.272	91.156	76.703	68.567	58.323	56.662	58.675	62.331	65.007	66.097	68.933	72.081	74.707	77.419	79.616	83.025	85.219	87.416	90.719	91.587
338	102.174	90.578	75.836	67.660	57.149	55.308	57.302	60.689	62.870	64.901	66.722	70.649	72.747	75.400	77.109	80.628	82.846	85.613	87.923	89.036
338.5	101.452	90.244	75.072	66.808	56.138	53.666	55.999	58.710	60.943	64.087	64.447	69.050	70.992	73.518	74.703	78.208	80.513	83.387	85.517	86.780
339	101.030	89.946	74.372	66.420	54.862	52.079	54.876	56.833	59.180	63.050	62.874	67.160	69.009	71.642	72.594	75.839	78.403	81.031	83.144	84.818
339.5	100.422	89.672	73.482	65.882	53.610	50.405	53.593	55.600	57.675	61.588	61.640	64.888	67.334	69.533	70.474	73.809	76.199	78.669	80.772	82.666
340	99.954	89.280	72.981	65.344	52.430	48.947	52.266	54.485	56.045	59.866	60.551	63.107	65.520	67.472	68.420	72.161	74.162	76.480	78.753	80.956
340.5	99.501	88.763	72.236	64.540	51.079	47.856	50.877	53.109	54.501	58.072	59.439	61.394	63.920	65.706	66.542	70.525	72.268	74.430	76.790	78.714
341	98.849	87.709	71.778	63.597	49.862	47.020	49.384	51.906	53.129	56.089	57.937	59.872	62.324	64.002	64.903	69.119	70.570	72.505	74.836	76.349
341.5	98.551	86.649	71.387	62.431	48.927	46.332	47.996	50.191	51.740	54.457	56.147	58.543	60.713	62.570	63.546	67.785	68.887	70.389	73.108	74.217
342	98.553	85.678	70.932	61.367	48.271	45.736	46.615	48.214	50.339	53.176	54.568	57.479	58.747	61.124	62.389	66.241	67.266	68.451	71.187	72.447
342.5	98.484	85.206	70.247	60.526	47.901	44.880	45.318	46.680	49.325	51.990	53.091	56.014	56.892	59.414	61.209	64.526	65.206	66.743	69.094	70.585
343	98.404	84.918	69.790	60.202	47.452	43.835	44.177	45.495	48.144	50.796	51.785	54.570	55.194	57.654	59.729	62.807	63.223	65.257	67.190	68.918
343.5	98.281	85.167	69.218	60.064	46.706	42.621	42.991	44.319	46.941	49.577	50.759	52.847	53.648	55.864	58.147	60.837	61.221	63.683	65.219	67.115
344	97.530	85.322	68.894	60.087	45.798	41.466	41.869	43.705	45.871	48.094	49.659	50.953	52.104	54.146	56.468	59.005	59.402	61.978	63.431	65.084
344.5	96.833	85.162	68.756	59.881	44.607	40.388	41.059	42.941	44.818	46.639	48.321	49.095	50.805	52.495	54.837	57.295	57.690	59.901	61.965	63.217
345	96.097	84.711	68.405	59.420	43.353	39.484	40.259	41.829	43.462	45.423	46.915	47.794	49.521	50.910	53.199	55.631	56.103	57.702	60.309	61.406
345.5	95.450	84.100	68.361	58.844	42.471	38.678	39.277	40.630	42.105	44.313	45.671	46.784	48.273	49.323	51.624	54.254	54.220	55.750	58.612	59.807
346	95.018	83.365	68.489	58.276	41.673	37.827	38.293	39.519	40.655	43.301	44.363	46.080	47.217	47.856	49.961	52.935	52.405	54.162	56.867	58.319
346.5	94.815	82.858	68.435	57.405	41.022	36.952	37.121	38.302	39.273	42.173	43.179	45.339	46.150	46.489	48.316	51.183	50.765	52.773	54.980	56.898

Chapter-IV

4.1. Tensiometric data of Brij-30/NaC system at various mole fraction of Brij-30 at 298.15 K.

α_{Brij}= 0.2		α_{Brij}= 0.4		α_{Brij}= 0.6		α_{Brij}= 0.8		α_{Brij}= 1	
log [Conc]	γ/mNm^{-1}	log [Conc]	γ/mNm^{-1}	log [Conc]	γ/mNm^{-1}	log [Conc]	γ/mNm^{-1}	log [Conc]	γ/mNm^{-1}
--	73.7	--	71.8	--	70.4	--	71.7	--	70.5
-2.921	72.1	-3.222	66.1	-3.398	62.3	-3.398	71.3	-3.369	58
-2.319	69.6	-2.745	63.7	-2.921	58.7	-2.797	61.3	-2.892	57.3
-1.923	57.5	-2.445	60.8	-2.621	54.3	-2.445	57.3	-2.525	51.7
-1.645	52.4	-2.202	56.1	-2.358	51.4	-2.183	51.8	-2.257	47
-1.408	45.8	-1.970	51.9	-2.134	48.4	-1.963	45	-2.030	41.6
-1.206	40.0	-1.764	46.8	-1.933	42.9	-1.777	39.1	-1.843	35.3
-1.029	36.0	-1.586	41.6	-1.757	41.5	-1.613	34.8	-1.678	32.6
-0.878	31.9	-1.427	37.4	-1.583	37.5	-1.459	31.2	-1.529	29.6
-0.742	30.2	-1.276	33.7	-1.417	33.4	-1.322	29.8	-1.398	27.6
-0.614	29.2	-1.133	31.2	-1.262	31.0	-1.196	28	-1.280	26.9
-0.496	28.8	-0.999	29.2	-1.121	29.4	-1.079	27.9	-1.171	26.3
-0.390	28.7	-0.875	29.0	-0.994	28.5	-0.970	27.9	-1.074	25.7
-0.297	28.4	-0.764	29.0	-0.878	28.2	-0.872	27.9	-0.987	25.7
		-0.663	29.0					-0.908	25.5
								-0.837	25.5

4.2. Tensiometric data of Brij-30/NaDC system at various mole fraction of Brij-30 at 298.15 K.

α_{Brij}= 0.2		α_{Brij}= 0.4		α_{Brij}= 0.6		α_{Brij}= 0.8		α_{Brij}= 1	
log [Conc]	γ/mNm^{-1}	log [Conc]	γ/mNm^{-1}	log [Conc]	γ/mNm^{-1}	log [Conc]	γ/mNm^{-1}	log [Conc]	γ/mNm^{-1}
--	71.4	--	71.6	--	70.3	--	71.2	--	70.4
-2.699	72.8	-2.699	61.4	-2.699	65.5	-3.553	58	-3.369	58
-2.222	67.2	-2.222	57.1	-2.222	60.4	-3.076	54.7	-2.892	57.3
-1.921	61.6	-1.854	53.3	-1.921	57.9	-2.776	51.6	-2.525	51.7
-1.699	58.0	-1.585	48.0	-1.699	53.3	-2.555	49.9	-2.257	47
-1.523	53.7	-1.357	43.9	-1.523	50.5	-2.379	48.4	-2.030	41.6
-1.377	49.4	-1.161	40.0	-1.377	46.5	-2.205	45.8	-1.843	35.3
-1.244	46.5	-0.996	37.9	-1.244	44.5	-2.047	42.5	-1.678	32.6
-1.114	43.1	-0.851	34.3	-1.114	40.8	-1.907	41.9	-1.529	29.6
-0.991	39.3	-0.719	32.8	-0.991	38.4	-1.768	38.3	-1.398	27.6
-0.879	36.8	-0.592	31.0	-0.873	35.3	-1.638	35.6	-1.280	26.9
-0.764	35.0	-0.467	30.5	-0.754	32.3	-1.515	32.2	-1.171	26.3

-0.654	33.4	-0.346	29.9	-0.636	30.2	-1.405	30.4	-1.074	25.7
-0.550	32.6	-0.228	29.7	-0.521	28	-1.303	30.3	-0.987	25.7
-0.453	31.5	-0.113	29.3	-0.408	27.3	-1.210	29.8	-0.908	25.5
-0.365	30.9	-0.013	29.1	-0.296	26.5	-1.123	29.1	-0.837	25.5
-0.282	30.7	0.087	29.0	-0.190	26.5	-1.038	28.8		
-0.206	30.5			-0.094	26.5	-0.951	28.5		
-0.112	30.4					-0.867	28.2		
-0.012	30.1					-0.791	28.2		
0.104	29.7								

4.3. Hydrodynamic diameter data vs. Mean Intensity for Brij-30/NaDC system at 0.2 mole fraction of Brij-30 at 298.15 K.

Size	Mean	Size	Mean	Size	Mean	Size	Mean
d (nm)	Intensity %	d (nm)	Intensity %	d (nm)	Intensity %	d (nm)	Intensity %
0.4	0	5.615	0	78.82	0	1106	12.1
0.4632	0	6.503	0	91.28	0	1281	28.6
0.5365	0	7.531	0	105.7	0	1484	32.5
0.6213	0	8.721	0	122.4	0	1718	21
0.7195	0	10.1	0	141.8	0	1990	5.8
0.8332	0	11.7	0	164.2	0	2305	0
0.9649	0	13.54	0	190.1	0	2669	0
1.117	0	15.69	0	220.2	0	3091	0
1.294	0	18.17	0	255	0	3580	0
1.499	0	21.04	0	295.3	0	4145	0
1.736	0	24.36	0	342	0	4801	0
2.01	0	28.21	0	396.1	0	5560	0
2.328	0	32.67	0	458.7	0	6439	0
2.696	0	37.84	0	531.2	0	7456	0
3.122	0	43.82	0	615.1	0	8635	0
3.615	0	50.75	0	712.4	0	1.00E+04	0
4.187	0	58.77	0	825	0		
4.849	0	68.06	0	955.4	0		

4.4. Hydrodynamic diameter data vs. Mean Intensity for Brij-30/NaDC system at 0.4 mole fraction of Brij-30 at 298.15 K.

Size	Mean	Size	Mean	Size	Mean	Size	Mean
d (nm)	Intensity %	d (nm)	Intensity %	d (nm)	Intensity %	d (nm)	Intensity %
0.4	0	5.615	0	78.82	0	1106	26.2
0.4632	0	6.503	0	91.28	0	1281	0
0.5365	0	7.531	0	105.7	0	1484	0
0.6213	0	8.721	0	122.4	0	1718	0
0.7195	0	10.1	0	141.8	0	1990	0
0.8332	0	11.7	0	164.2	0	2305	0
0.9649	0	13.54	0	190.1	0	2669	0
1.117	0	15.69	0	220.2	0	3091	0
1.294	0	18.17	0	255	0	3580	0
1.499	0	21.04	0	295.3	0	4145	0
1.736	0	24.36	0	342	0	4801	0
2.01	0	28.21	0	396.1	0	5560	0
2.328	0	32.67	0	458.7	0	6439	0
2.696	0	37.84	0	531.2	0	7456	0
3.122	0	43.82	0	615.1	0	8635	0
3.615	0	50.75	0	712.4	0	1.00E+04	0
4.187	0	58.77	0	825	25.7		
4.849	0	68.06	0	955.4	48.1		

4.5. Hydrodynamic diameter data vs. Mean Intensity for Brij-30/NaDC system at 0.6 mole fraction of Brij-30 at 298.15 K.

Size	Mean	Size	Mean	Size	Mean	Size	Mean
d (nm)	Intensity %	d (nm)	Intensity %	d (nm)	Intensity %	d (nm)	Intensity %
0.4	0	5.615	0	78.82	0	1106	0
0.4632	0	6.503	0	91.28	0	1281	0
0.5365	0	7.531	0	105.7	0	1484	0
0.6213	0	8.721	0	122.4	0	1718	0
0.7195	0	10.1	0	141.8	0	1990	0
0.8332	0	11.7	0	164.2	0	2305	0
0.9649	0	13.54	0	190.1	0	2669	0
1.117	0	15.69	0	220.2	0	3091	0
1.294	0	18.17	0	255	0	3580	0
1.499	0	21.04	0	295.3	0	4145	0

1.736	0	24.36	0	342	0	4801	0
2.01	0	28.21	0	396.1	0	5560	0
2.328	0	32.67	0	458.7	9.4	6439	0
2.696	0	37.84	0	531.2	56.4	7456	0
3.122	0	43.82	0	615.1	34.2	8635	0
3.615	0	50.75	0	712.4	0	1.00E+04	0
4.187	0	58.77	0	825	0		
4.849	0	68.06	0	955.4	0		

4.6. Hydrodynamic diameter data vs. Mean Intensity for Brij-30/NaDC system at 0.8 mole fraction of Brij-30 at 298.15 K.

Size	Mean	Size	Mean	Size	Mean	Size	Mean
d (nm)	Intensity %	d (nm)	Intensity %	d (nm)	Intensity %	d (nm)	Intensity %
0.4	0	5.615	0	78.82	1	1106	0.5
0.4632	0	6.503	0	91.28	1.3	1281	0
0.5365	0	7.531	0	105.7	1.4	1484	0
0.6213	0	8.721	0	122.4	1.5	1718	0
0.7195	0	10.1	0	141.8	1.7	1990	0
0.8332	0	11.7	0	164.2	2.1	2305	0
0.9649	0	13.54	0	190.1	3.1	2669	0
1.117	0	15.69	0	220.2	4.5	3091	0
1.294	0	18.17	0	255	6.4	3580	0
1.499	0	21.04	0	295.3	8.3	4145	0.4
1.736	0	24.36	0	342	10	4801	1.4
2.01	0	28.21	0	396.1	11.1	5560	2.5
2.328	0	32.67	0	458.7	11.2	6439	0
2.696	0	37.84	0	531.2	10.3	7456	0
3.122	0	43.82	0	615.1	8.6	8635	0
3.615	0	50.75	0	712.4	6.3	1.00E+04	0
4.187	0	58.77	0.2	825	3.8		
4.849	0	68.06	0.6	955.4	1.8		

4.7. Hydrodynamic diameter data vs. Mean Intensity for Brij-30/NaC system at 0.2 mole fraction of Brij-30 at 298.15 K.

Size	Mean	Size	Mean	Size	Mean	Size	Mean
d (nm)	Intensity %	d (nm)	Intensity %	d (nm)	Intensity %	d (nm)	Intensity %
0.4	0	5.615	0	78.82	0	1106	0
0.4632	0	6.503	0	91.28	0	1281	0
0.5365	0	7.531	0	105.7	0	1484	0
0.6213	0	8.721	0	122.4	0	1718	0
0.7195	0	10.1	0	141.8	0	1990	0
0.8332	0	11.7	0	164.2	0	2305	0
0.9649	0	13.54	0	190.1	0	2669	0
1.117	0	15.69	0	220.2	0	3091	0
1.294	0	18.17	0	255	0	3580	0
1.499	0	21.04	0	295.3	8.5	4145	0
1.736	0	24.36	0	342	27.5	4801	0
2.01	0	28.21	0	396.1	35.8	5560	0
2.328	0	32.67	0	458.7	23.7	6439	0
2.696	0	37.84	0	531.2	4.6	7456	0
3.122	0	43.82	0	615.1	0	8635	0
3.615	0	50.75	0	712.4	0	1.00E+04	0
4.187	0	58.77	0	825	0		
4.849	0	68.06	0	955.4	0		

4.8. Hydrodynamic diameter data vs. Mean Intensity for Brij-30/NaC system at 0.4 mole fraction of Brij-30 at 298.15 K.

Size	Mean	Size	Mean	Size	Mean	Size	Mean
d (nm)	Intensity %	d (nm)	Intensity %	d (nm)	Intensity %	d (nm)	Intensity %
0.4	0	5.615	0	78.82	1.7	1106	0
0.4632	0	6.503	0	91.28	2.5	1281	0
0.5365	0	7.531	0	105.7	2.9	1484	0
0.6213	0	8.721	0	122.4	2.8	1718	0
0.7195	0	10.1	0	141.8	2.8	1990	0
0.8332	0	11.7	0	164.2	3.1	2305	0
0.9649	0	13.54	0	190.1	3.9	2669	0
1.117	0	15.69	0	220.2	5.4	3091	0
1.294	0	18.17	0	255	7.2	3580	0.4
1.499	0	21.04	0	295.3	8.9	4145	1.2

1.736	0	24.36	0	342	10.1	4801	2.2
2.01	0	28.21	0	396.1	10.4	5560	3.2
2.328	0	32.67	0	458.7	9.8	6439	0
2.696	0	37.84	0	531.2	8.3	7456	0
3.122	0	43.82	0	615.1	6.2	8635	0
3.615	0	50.75	0	712.4	3.9	1.00E+04	0
4.187	0	58.77	0	825	1.9		
4.849	0	68.06	0.7	955.4	0.6		

4.9. Hydrodynamic diameter data vs. Mean Intensity for Brij-30/NaC system at 0.6 mole fraction of Brij-30 at 298.15 K.

Size	Mean	Size	Mean	Size	Mean	Size	Mean
d (nm)	Intensity %	d (nm)	Intensity %	d (nm)	Intensity %	d (nm)	Intensity %
0.4	0	5.615	0	78.82	1.6	1106	2.9
0.4632	0	6.503	0	91.28	1.6	1281	1.5
0.5365	0	7.531	0	105.7	1.6	1484	0.5
0.6213	0	8.721	0	122.4	1.5	1718	0.1
0.7195	0	10.1	0	141.8	1.5	1990	0
0.8332	0	11.7	0	164.2	1.7	2305	0
0.9649	0	13.54	0	190.1	2.1	2669	0
1.117	0	15.69	0	220.2	2.9	3091	0
1.294	0	18.17	0	255	4	3580	0.3
1.499	0	21.04	0	295.3	5.4	4145	0.7
1.736	0	24.36	0	342	6.8	4801	1.4
2.01	0	28.21	0.2	396.1	8	5560	2
2.328	0	32.67	0.4	458.7	8.9	6439	0
2.696	0	37.84	0.7	531.2	9.2	7456	0
3.122	0	43.82	1	615.1	8.8	8635	0
3.615	0	50.75	1.2	712.4	7.8	1.00E+04	0
4.187	0	58.77	1.4	825	6.3		
4.849	0	68.06	1.5	955.4	4.6		

4.10. Hydrodynamic diameter data vs. Mean Intensity for Brij-30/NaC system at 0.8 mole fraction of Brij-30 at 298.15 K.

Size	Mean	Size	Mean	Size	Mean	Size	Mean
d (nm)	Intensity %	d (nm)	Intensity %	d (nm)	Intensity %	d (nm)	Intensity %
0.4	0	5.615	0	78.82	1.5	1106	3.5
0.4632	0	6.503	0	91.28	2	1281	2.5
0.5365	0	7.531	0	105.7	2.5	1484	1.6
0.6213	0	8.721	0	122.4	3.1	1718	0.8
0.7195	0	10.1	0	141.8	3.6	1990	0.3
0.8332	0	11.7	0	164.2	4	2305	0
0.9649	0	13.54	0	190.1	4.3	2669	0
1.117	0	15.69	0	220.2	4.5	3091	0.3
1.294	0	18.17	0	255	4.7	3580	0.8
1.499	0	21.04	0	295.3	4.9	4145	1.3
1.736	0	24.36	0.1	342	5.2	4801	1.7
2.01	0	28.21	0.3	396.1	5.5	5560	2
2.328	0	32.67	0.6	458.7	5.8	6439	0
2.696	0	37.84	0.8	531.2	6	7456	0
3.122	0	43.82	1	615.1	6	8635	0
3.615	0	50.75	1	712.4	5.8	1.00E+04	0
4.187	0	58.77	1	825	5.2		
4.849	0	68.06	1.2	955.4	4.5		

4.11. Hydrodynamic diameter (d_h in nm) vs mole fraction of Brij-30 data for Brij-30/NaC and Brij-30/NaDC systems.

α_{Brij}	d_h(nm) for Brij-30/NaC	d_h(nm) for Brij-30/NaDC
0.2	396.1	1484.0
0.4	396.1	955.4
0.6	531.2	531.2
0.8	712.0	458.7

List of Publications and Reprints

For Thesis:

1. Comparative studies on the aggregate formation of synthesized zwitterionic gemini and monomeric surfactants in the presence of the amphiphilic antipsychotic drug chlorpromazine hydrochloride in aqueous solution: an experimental and theoretical approach; **R. Banik**, S. Das, A. Ghosh and S. Ghosh; ***Soft Matter***, **2023**, 19 (41), 7995-8010.

2. Comparative Study of the Aggregation Behavior of Some Ionic Surfactants with Nonionic Triton X-114 in Water and a Water/2, 2, 2-Trifluoroethanol Mixture; **R. Banik**, B. B. Mondal, R. Sardar and S. Ghosh; ***Industrial & Engineering Chemistry Research***, **2024**, 63 (7), 3057-3071.

Other Publications:

3. Exploration of the impact of graphene oxide, acetylenic gemini, and CTAT on the photophysical and aggregation properties of dipolar coumarin 153; R. Sardar, S. Das, **R. Banik**, S. Bhunia, and S. Ghosh; ***Physical Chemistry Chemical Physics***, **2024**, 26 (11), 8900−8918.

4. Impact of 2, 2, 2-trifluoroethanol (TFE) on hydrophobicity enhancement in the aggregation of sodium N-dodecanoyl sarcosinate (SDDS) with nonionic hydroxyethyl cellulose; B. B. Mondal, **R. Banik**, S. Ghosh; ***Colloids and Surfaces A: Physicochemical and Engineering Aspects***, **2024**, 681, 132781.

5. Detailed physicochemical study and thermodynamic aspects of the interaction between nonionic cellulose derivative hydroxyethyl cellulose and anionic surfactant sodium N-dodecanoyl sarcosinate in aqueous media; B. B. Mondal, **R. Banik**, S. Ghosh; ***Journal of the Taiwan Institute of Chemical Engineers***, **2023**, 149, 104982.

6. Temperature Comparative Studies on Self-Assembly of Sodium Dodecyl Sulphate and Didodecyl Dimethyl Ammonium Bromide in Aqueous, Brine, and Trifluoroethanol Media; A. Dey, **R. Banik**, S. Ghosh; ***Journal of Surfactants and Detergents***, **2021**, 24 (3), 459-472.

Poster Presentation:

- **Presented a poster** at the 19th National Conference on Surfactants, Emulsions and Biocolloids (NATCOSEB-XIX) on 18-20th October, 2019, Amity University, Kolkata. (**Topic: Micellar and interfacial properties of antipsychotic drug-zwitterionic surfactant mixed system**)

- **Presented a poster** at the National Seminar on Current Developments in Chemical Sciences (CDCS-2018) on March 7, 2018 under CAS II program organized by Department of Chemistry, Jadavpur University. (**Topic: Aggregation behavior of ionic and non-ionic surfactants in presence of 2, 2, 2-trifluoroethanol (TFE)**).